

**Effect of Cellulose Nanocrystal Particles on Rheology, Transport and Mechanical  
Properties of Oil Well Cement Systems**

by

Mohammad Reza Dousti

A thesis submitted in partial fulfillment of the requirements for the degree of

Doctor of Philosophy

in

Structural Engineering

Department of Civil and Environmental Engineering  
University of Alberta

© Mohammad Reza Dousti, 2018

## **ABSTRACT**

The increase in oil consumption during the past few decades, coupled with oil/gas extraction from shale in the recent years has increased drilling and cementing demands. Well cementing operation is one of the most crucial and important steps in any well completion. However, since it takes place at the end of the drilling process (each segment), a satisfying and acceptable job is rarely done. In the cementing process, cement is used to fill in the annular space between the casing string and the ground formation within the drilled hole. The cementitious system placed in an oil well has exclusive functions to perform. These include restricting the movement of hydrocarbons and/or water in between the permeable zones, providing a suitable mechanical support for the casing string, protecting the casing from any sort of physical damage including corrosion, and supporting the well-bore walls in order to prevent the collapse of the formation.

The prepared paste has to be satisfactorily pumpable and flowable. However, on the other hand, the viscosity and yield stress associated with the paste should be appropriately tailored in order to reduce the risk of lost circulation. Therefore, the rheological behavior of an oil well cement paste should be assessed carefully. Also, the fluid loss (filtration) rate of the prepared cement paste is of great importance since it directly impacts various characteristics of the hardened cement sheath. High filtration and fluid loss rate lead to a change in the water-to-cement ratio of the matrix, influencing not only the flowability of paste while still fresh but also the microstructure of the hardened cement paste. Furthermore, the hardened oil well cement sheath placed in a wellbore should demonstrate adequate mechanical properties. Therefore, while designing the slurry, the strength development rate along with the ultimate compressive and tensile strength of the hardened

paste should be taken into consideration. Moreover, understanding and improving the transport properties of oil well cement paste is essential. The aggression of any type of destructive and detrimental agents through the hardened paste will eventually degrade the cementitious system. Thus, the permeability and pore structure of the hardened oil well cement paste placed in the annulus is extremely critical.

This study was primarily associated with the material behavior of oil well cement paste in the presence of cellulose nanocrystals. The main goal of this research was to develop an oil well cement system and address the associated durability concerns mentioned above. Firstly, the workability and the rheological properties of CNC-dosed fresh oil well cement paste were assessed, followed by static filtration tests to evaluate fluid loss. It was found that adding CNC to oil well cement paste leads to shear thinning which manifests as lower slump for the cement based slurry. Also, based on the experimental results, the presence of CNC increased the time required to collect a given amount of filtrate. Furthermore, the effect of cellulose nanocrystal (CNC) particles on the dynamic mechanical properties of oil well cement paste was studied. Using oscillatory rheology, the linear viscoelastic range of CNC-dosed oil well cement paste was determined and the frequency sweep test was performed at the critical strain. According to the results obtained, the presence of CNC enhanced the complex viscosity, rigidity, hydration rate and solidification of oil well cement paste.

Moreover, the effect of cellulose nanocrystal (CNC) particles on the pore structure and porosity of hardened oil well cement paste was investigated using the gas sorption technique. The strength development (compressive and tensile) of CNC-dosed oil well cement paste was also measured at different ages in order to recognize the impact of this

nanomaterial on the mechanical properties of hardened oil well cement paste. Test results revealed that CNC particles reduced the porosity and surface area of hardened oil well cement paste and enhanced the mechanical properties. Finally, the mass flow rate of early aged hollow cylindrical specimens dosed with CNC was measured by using a pressurized permeability cell and the water permeability of the specimens was evaluated using Darcy's law for laminar flow. The water permeability of oil well cement paste was reduced with the addition of cellulose nanocrystal (CNC) particles.

## PREFACE

This thesis is an original work by Mohammad Reza Dousti. The results reported in Chapter 3 have been previously presented at the ConMAT '15 conference (*Dousti, M. R., Boluk, Y., & Bindiganavile, V. The influence of cellulose nanocrystals on the fresh properties of oil well cement paste. Proc. CONMAT, 15.*). The outcome of Chapter 6 has also been previously presented at the ICBBM EcoGRAFI conference (*Dousti, M. R., Boluk, Y., & Bindiganavile, V. The effect of cellulose nanocrystal (CNC) on the water permeability of early aged oil well cement. Proc. ICBBM 2017, 2nd International Conference on Bio-Based Building Materials. RILEM.*

*To my lovely parents ...*

## ACKNOWLEDGMENTS

First and foremost, I would like to praise the Lord, for providing me this opportunity and granting me the wisdom, capability and strength to proceed.

I would like to express my sincere appreciation and profound gratitude to my research supervisors Dr. Yaman Boluk and Dr. Vivek Bindiganavile for their continuous support all through my study period at the University of Alberta. Their invaluable guidance and inspiration helped me grow confidence and develop both academically and personally. Without their patience, warm encouragements and critical comments this project would not have been materialized. I am forever grateful to them.

As experimental work formed a significant part of this research program, I am also deeply indebted to the technicians who were involved in this study. In particular, my thanks go to Mr. Rizaldy Mariano at the Civil Engineering laboratory, Mr. Greg Miller and Mr. Cameron West at the I. F. Morison Structural Laboratory, Dr. Nancy Zhang at the University of Alberta Fabrication and Characterization Centre (nanoFAB), and Dr. Baki Ozum at the Apex Engineering Inc. Laboratory (Edmonton Research Park) for their technical assistance. Special thanks are also due to all faculty members, staff and personnel in the Department of Civil and Environmental Engineering at the University of Alberta, for their kind support and contribution during my stay.

I would also like to express my deep appreciation to Dr. Rick Chalaturnyk, who has been on my supervisory committee, for his positive feedbacks and recommendations. In addition, I am also thankful to Dr. Alireza Nouri, Dr. Wei Victor Liu, and Dr. Jeffrey Youngblood (Purdue University) for their constructive comments. I have immensely benefited from my association with many graduate students and research associates in my

years at the University of Alberta. I particularly acknowledge my pleasant association with Mr. Pooya Shariaty for sharing his experience and providing intellectual input during this research program.

The authors are grateful to Alberta Innovates – Bio Solution for providing the financial support for this research program. Thanks are also due to Alberta Innovates Technology Futures (AITF) and Alberta Pacific Forest Industries (Alpac) for supplying CNC samples, and to Lafarge Canada for providing the oil well cement employed in this study.

I would like to convey special appreciation and gratitude to my beloved family for their unconditional love, precious prayers, encouragement and moral support throughout my academic trajectory, without which this achievement could not have been possible.

## TABLE OF CONTENTS

Abstract	ii
Preface	v
Acknowledgments	vii
Table of Contents	ix
List of Tables	xvi
List of Figures	xviii

### Chapter I

<b><i>Introduction</i></b>	<b><i>1</i></b>
1. Problem Statement	2
2. Research Objectives and Scope	5
3. Structure of Dissertation	8
4. Significance of the Study	12
<i>References</i>	<i>13</i>

### Chapter II

<b><i>Literature Review</i></b>	<b><i>16</i></b>
1. Oil Well Cement	17
1.1. Introduction	17
1.1.1. Background	17
1.1.2. Failure of Cement Sheath	20
1.2. Hydration	24
1.3. Vital Slurry Characteristics	27
1.3.1. Flow Behavior	27
1.3.2. Density	27
1.3.3. Setting Time	28

1.3.4.	Thickening Time	29
1.4.	Additives	30
1.4.1.	Significance in Oil Well Cement Industry	30
1.4.2.	Common Types of Additives	30
2.	Rheological Behavior and Workability	36
2.1.	Steady Shear Rheology	36
2.1.1.	Introduction	36
2.1.2.	Influencing Factors and Common Rheology Modifying Agents	39
2.2.	Oscillatory Rheology and Dynamic Mechanical Properties	48
2.2.1.	Theory and Background	48
2.2.2.	Dynamic Mechanical Properties of Cementitious Systems	51
3.	Durability Concerns	56
3.1.	Porosity and Pore Structure	56
3.1.1.	Theoretical Background	56
3.1.2.	Porosity of Cementitious Systems	57
3.1.3.	Surface Area and Gas Sorption Technique	60
3.2.	Permeability	69
3.2.1.	Theoretical Background	69
3.2.2.	Permeability of Cementitious Systems	71
3.3.	Mechanical Properties and Strength Development	75
3.3.1.	Significance	75
3.3.2.	Common Strength Enhancing Parameters and Agents	75
4.	Cellulose and Cellulosic Derivatives	82
4.1.	Cellulosic Nanomaterials	82
4.1.1.	Structure of Cellulose	82
4.1.2.	Different Types of Cellulose Nanoparticles	84
4.1.3.	Properties of Cellulose Nanoparticles	85
4.2.	Cellulose in Cement	87
4.2.1.	Application	87

4.2.2.	Hydration of Cement in Presence of Cellulosic Derivatives	91
4.2.3.	Cellulosic Additives: From Fibers to Microcrystals	93
4.3.	Cellulose Nanocrystal (CNC)	96
4.3.1.	From Fibers and Microcrystals to Nanocrystals	96
4.3.2.	Preparation of Cellulose Nanocrystals	97
4.3.3.	Morphology and Dimension of Cellulose Nanocrystal	99
4.3.4.	Properties of Cellulose Nanocrystal Based Composites	100
4.4.	Cellulose Nanocrystal (CNC) Particles in Cementitious Systems	102
4.4.1.	Application	102
4.4.2.	Effect of CNC on the Degree of Hydration	103
4.4.3.	Interaction between CNC and Cement Particles	104
4.4.4.	Influence of CNC on the Microstructure and Strength	108
	<i>References</i>	<i>109</i>

### Chapter III

	<b><i>The Influence of Cellulose Nanocrystal (CNC) Particles on Steady Shear Rheology, Workability and Fluid Loss Properties of Oil Well Cement Paste</i></b>	<b>136</b>
1.	Introduction	137
2.	Experimental Details	142
2.1.	Materials	142
2.1.1.	Oil Well Cement Type G	142
2.1.2.	Cellulose Nanocrystal (CNC)	143
2.1.3.	Bentonite	144
2.1.4.	Carboxymethyl Cellulose (CMC)	144
2.2.	Preparation	145
2.2.1.	Colloidal Suspensions	145
2.2.2.	Cementitious System (Slurry)	147
2.3.	Test Methods	149
2.3.1.	Steady Shear Rheological Parameters	149

2.3.2.	Workability of Fresh Cement Paste	150
2.3.3.	Static Filtration	151
3.	Results and Discussion	152
3.1.	Colloidal Suspensions	152
3.2.	Fresh Cementitious Paste	153
3.2.1.	Steady Shear Rheology of Fresh Cement Paste	154
3.2.2.	Workability of Fresh Cement Paste	155
3.2.3.	Filtration of Fresh Cement Paste	159
4.	Concluding Remarks	162
	<i>References</i>	<i>164</i>

#### **Chapter IV**

	<b><i>Dynamic Mechanical Properties of Oil Well Cement Paste Dosed with Cellulose Nanocrystal (CNC) Particles</i></b>	<b>169</b>
1.	Introduction	170
1.1.	Oil Well Cement	170
1.2.	Oscillatory (Dynamic Mode) Rheology	170
1.3.	Objectives of Study	171
2.	Experimental Details	172
2.1.	Materials	172
2.1.1.	Oil Well Cement Type G	172
2.1.2.	Cellulose Nanocrystal (CNC)	173
2.1.3.	Bentonite	174
2.2.	Slurry Preparation	175
2.3.	Test Methods	177
2.3.1.	Part (I): Strain Amplitude Sweep Test	177
2.3.2.	Part (II): Frequency Sweep Test	178
3.	Results and Discussion	178
3.1.	Strain Amplitude Sweep Test Results	179

3.1.1. Linear Viscoelastic Domain (Range) and Critical Strain $\gamma_c$	179
3.1.2. Effect of CNC on Storage Modulus ( $G'$ ) and Loss Modulus ( $G''$ )	182
3.2. Frequency Sweep Test Results	183
3.2.1. Evolution of Storage Modulus ( $G'$ ) and Loss Modulus ( $G''$ )	183
3.2.2. Complex Shear Modulus ( $G^*$ ) and Complex Viscosity ( $\eta^*$ )	188
3.2.3. Damping factor ( $\tan\delta$ )	191
4. Concluding Remarks	192
<i>References</i>	<i>194</i>

## Chapter V

### ***The Effect of Cellulose Nanocrystal (CNC) Particles on the Porosity and Strength Development of Hardened Oil Well Cement Paste*** 197

1. Introduction	198
1.1. Oil Well Cement	198
1.2. Porosity	199
1.2.1. Theoretical Background	199
1.2.2. Different Measuring Techniques	201
1.2.3. Previous Studies on the Pore Structure of Cementitious Systems	204
1.2.4. The Effect of Additives on Porosity	205
1.3. Mechanical Properties of Oil Well Cement Paste	206
1.3.1. Importance of Strength in Oil Wells	206
1.3.2. Common Additives to Enhance Mechanical Properties	206
1.4. Objectives of Study	208
2. Experimental Details	208
2.1. Materials	208
2.1.1. Oil Well Cement Type G	208
2.1.2. Cellulose Nanocrystal (CNC)	210
2.2. Specimen Preparation	211

2.3.	Test Methods	213
2.3.1.	Porosity Assessment	213
2.3.2.	Investigation of the Mechanical Properties	214
3.	Results and Discussion	215
3.1.	Porosity	216
3.1.1.	Influence of CNC on the Surface Area of Oil Well Cement Paste	217
3.1.2.	Influence of CNC on Pore Volume and Pore Size Distribution	218
3.2.	Mechanical Properties	226
3.2.1.	Impact of CNC on Strength Development of Oil Well Cement Paste	226
3.2.2.	Effect of CNC on the Stress-Strain Profile of Oil Well Cement	229
4.	Concluding Remarks	231
	<i>References</i>	233

## Chapter VI

	<b><i>Permeability of Early Aged Oil Well Cement Paste Dosed with Cellulose Nanocrystal (CNC) Particles</i></b>	<b>239</b>
1.	Introduction	240
1.1.	Oil Well Cement	240
1.2.	Permeability of Oil Well Cement	241
1.3.	Objectives of Study	246
2.	Experimental Details	246
2.1.	Materials	246
2.1.1.	Oil Well Cement Type G	246
2.1.2.	Cellulose Nanocrystal (CNC)	247
2.2.	Specimen Preparation	248
2.3.	Test Method	251
3.	Results and Discussion	252
3.1.	Mass Flow Rate	252

3.2. Water Permeability	256
4. Concluding Remarks	263
<i>References</i>	264

## **Chapter VII**

<i>Summary and Conclusions</i>	267
1. Overview of the Dissertation	268
2. Overall Concluding Remarks	269
3. Recommendations for Future Research	274
<i>References</i>	275
<b>Bibliography</b>	277

## LIST OF TABLES

<b>Table 2.1.</b>	Physical properties of Type G cement (prepared by Lafarge Canada, December 8 <sup>th</sup> , 2015)	18
<b>Table 2.2.</b>	Chemical composition of Type G cement (prepared by Lafarge Canada, December 8 <sup>th</sup> , 2015)	18
<b>Table 2.3.</b>	Short-term and long-term properties required of cement	22
<b>Table 2.4.</b>	Classification of pores within cement, by Mindess and Young	61
<b>Table 2.5.</b>	Different types of cellulose nanocrystal (CNC) particles	109
<b>Table 3.1.</b>	Physical properties of Type G cement (prepared by Lafarge Canada, December 8 <sup>th</sup> , 2015)	142
<b>Table 3.2.</b>	Chemical composition of Type G cement (prepared by Lafarge Canada, December 8 <sup>th</sup> , 2015)	143
<b>Table 3.3.</b>	Mix design (sample) for preparation of colloidal suspensions	146
<b>Table 3.4.</b>	Mix design (sample) for preparation of cement paste	148
<b>Table 3.5.</b>	Cement paste rheology results	155
<b>Table 3.6.</b>	Yield shear stress computed using the equation employed by Hoyos et al.	156
<b>Table 3.7.</b>	Flow table spread diameters after 2 blows	158
<b>Table 3.8.</b>	Flow table spread diameters after 25 blows	158
<b>Table 3.9.</b>	Flow table height of residual paste (spread) after 2 blows	159
<b>Table 4.1.</b>	Physical properties of Type G cement (prepared by Lafarge Canada, December 8 <sup>th</sup> , 2015)	172
<b>Table 4.2.</b>	Chemical composition of Type G cement (prepared by Lafarge Canada, December 8 <sup>th</sup> , 2015)	173
<b>Table 4.3.</b>	Formulation and designation of the samples prepared	175

<b>Table 4.4.</b>	Mix design (sample) for preparation of cement paste	176
<b>Table 5.1.</b>	Physical properties of Type G cement (prepared by Lafarge Canada, December 8 <sup>th</sup> , 2015)	209
<b>Table 5.2.</b>	Chemical composition of Type G cement (prepared by Lafarge Canada, December 8 <sup>th</sup> , 2015)	209
<b>Table 5.3.</b>	Mix design (sample) for preparation of cement paste	212
<b>Table 5.4.</b>	The surface area of neat and CNC-dosed oil well cement paste samples obtained using different models	218
<b>Table 5.5.</b>	Cumulative pore volume of hardened oil well cement pastes	221
<b>Table 6.1.</b>	Physical properties of Type G cement (prepared by Lafarge Canada, December 8 <sup>th</sup> , 2015)	246
<b>Table 6.2.</b>	Chemical composition of Type G cement (prepared by Lafarge Canada, December 8 <sup>th</sup> , 2015)	246
<b>Table 6.3.</b>	The prepared and tested specimens (for permeability measurement)	250
<b>Table 6.4.</b>	Mix design (sample) for preparation of cement paste	250
<b>Table 6.5.</b>	The effect of CNC particles on the flow rate of cementitious samples	255
<b>Table 6.6.</b>	The effect of CNC particles on the coefficient of water permeability of oil well cementitious samples	257
<b>Table 6.7.</b>	The surface area of neat and CNC-dosed oil well cement paste samples obtained using different techniques	260
<b>Table 7.1.</b>	The effect of cellulose nanocrystal (CNC) particles as an additive, on the critical parameters associated with oil well cement paste	272

## LIST OF FIGURES

<b>Figure 1.1.</b>	Major contributing parameters leading to failure in oil well cementing described by Schlumberger in 1996	4
<b>Figure 1.2.</b>	Flowchart (work plan) of the project	11
<b>Figure 2.1.</b>	Two-plates model for oscillatory shear testing	49
<b>Figure 2.2.</b>	Schematic diagram of a permeameter	70
<b>Figure 3.1.</b>	A schematic view of a section of an oil well	137
<b>Figure 3.2.</b>	A schematic demonstration of CNC hierarchy	141
<b>Figure 3.3.</b>	Scanning electron micrograph of the cellulose nanocrystal (CNC) particles used in this study	144
<b>Figure 3.4.</b>	Homogenizing the CNC into a colloidal suspension (left) and prepared suspensions containing variously, CNC, CMC and Bentonite (right)	146
<b>Figure 3.5.</b>	High shear mixer (left) and the prepared cementitious slurry samples (right)	147
<b>Figure 3.6.</b>	Dynamic shear rheometer utilized for steady shear rheology assessment (left) and the schematic showing cone and plate geometry (right)	149
<b>Figure 3.7.</b>	Prepared sample for rheological measurements	149
<b>Figure 3.8.</b>	Flow table (left) and mini slump cone (right) employed to investigate the workability of prepared cement paste.	151
<b>Figure 3.9.</b>	The static filtration test setup	152
<b>Figure 3.10.</b>	Variation in yield shear stress across different suspensions (in the presence of cellulose nanocrystal particles)	152
<b>Figure 3.11.</b>	Variation in viscosity across different suspensions (in the presence of cellulose nanocrystal particles)	153

<b>Figure 3.12.</b>	Effect of mixture composition on rheological behavior of fresh oil well cement paste (1): shear stress profile	154
<b>Figure 3.13.</b>	Effect of mixture composition on rheological behavior of fresh oil well cement paste (2): viscosity profile	154
<b>Figure 3.14.</b>	Results from mini slump test: spread diameter (top) and residual height measured from the base (bottom)	156
<b>Figure 3.15.</b>	Flow table test results: spread diameter after 2 blows (top) and spread diameter after 25 blows (bottom)	157
<b>Figure 3.16.</b>	Static filtration test results; a) Time required to collect 100ml of filtrate volume; b) Time required to collect 150ml of filtrate volume; c) Total amount of filtrate volume after 30 minutes of static filtration	160
<b>Figure 4.1.</b>	Mixers used to prepare bentonite/CNC suspensions (left) and oil well cement slurry (right)	175
<b>Figure 4.2.</b>	Strain amplitude sweep test result demonstrating the linear viscoelastic range associated with sample 1 (C+W)	180
<b>Figure 4.3.</b>	Strain amplitude sweep test result demonstrating the linear viscoelastic range associated with sample 2 (C+W+B)	180
<b>Figure 4.4.</b>	Strain amplitude sweep test result demonstrating the linear viscoelastic range associated with sample 3 (C+W+CNC)	181
<b>Figure 4.5.</b>	Strain amplitude sweep test result demonstrating the linear viscoelastic range associated with sample 4 (C+W+B+CNC)	181
<b>Figure 4.6.</b>	Strain amplitude sweep test result demonstrating the change in storage modulus ( $G'$ ), in the viscoelastic domain for all samples	182
<b>Figure 4.7.</b>	Strain amplitude sweep test result demonstrating the change in loss modulus ( $G''$ ), in the viscoelastic domain for all samples	183
<b>Figure 4.8.</b>	Variation in storage modulus ( $G'$ ) and loss modulus ( $G''$ ) of sample 1 (C+W) with respect to angular frequency	184
<b>Figure 4.9.</b>	Variation in storage modulus ( $G'$ ) and loss modulus ( $G''$ ) of sample 2 (C+W+B) with respect to angular frequency	185
<b>Figure 4.10.</b>	Variation in storage modulus ( $G'$ ) and loss modulus ( $G''$ ) of sample 3 (C+W+CNC) with respect to angular frequency	185

<b>Figure 4.11.</b>	Variation in storage modulus ( $G'$ ) and loss modulus ( $G''$ ) of sample 4 (C+W+B+CNC) with respect to angular frequency	186
<b>Figure 4.12.</b>	Change in storage modulus ( $G'$ ) with respect to angular frequency for all cementitious samples	187
<b>Figure 4.13.</b>	Change in loss modulus ( $G''$ ) with respect to angular frequency for all cementitious samples	187
<b>Figure 4.14.</b>	a) Relationship between storage modulus ( $G'$ ), loss modulus ( $G''$ ) and the resulting complex shear modulus ( $G^*$ ); b) Schematic demonstration of a preset shear strain function ( $\gamma$ ) and the resulting shear stress function ( $\tau$ ) with a phase shift angle ( $\delta$ )	188
<b>Figure 4.15.</b>	Change in complex shear modulus ( $G^*$ ) with respect to angular frequency for all cementitious samples	189
<b>Figure 4.16.</b>	Change in complex viscosity ( $\eta^*$ ) with respect to angular frequency for all cementitious samples compared to the change in shear viscosity ( $\eta$ ) with respect to shear strain (obtained from Chapter 3)	190
<b>Figure 4.17.</b>	Change in damping factor ( $\tan\delta$ ) with respect to angular velocity	192
<b>Figure 5.1.</b>	Compression test setup	215
<b>Figure 5.2.</b>	Nitrogen isotherm associated with neat and CNC-dosed cementitious samples	216
<b>Figure 5.3.</b>	Visual comparison of surface area obtained from different models	217
<b>Figure 5.4.</b>	The effect of cellulose nanocrystal (CNC) particles on the cumulative pore volume of hardened oil well cement paste, obtained using the BJH method	219
<b>Figure 5.5.</b>	The effect of cellulose nanocrystal (CNC) particles on the cumulative pore volume of hardened oil well cement paste, obtained using the DFT method	221
<b>Figure 5.6.</b>	The effect of cellulose nanocrystal (CNC) particles on the pore size distribution of hardened oil well cement paste, obtained using the BJH method	222

<b>Figure 5.7.</b>	The effect of cellulose nanocrystal (CNC) particles on the pore size distribution of hardened oil well cement paste, obtained using the DFT method	222
<b>Figure 5.8.</b>	Porosity profile of neat hardened oil well cement paste obtained using the BJH method	224
<b>Figure 5.9.</b>	Porosity profile of CNC-dosed hardened oil well cement paste obtained using the BJH method	224
<b>Figure 5.10.</b>	Porosity profile of neat hardened oil well cement paste obtained using the DFT method	225
<b>Figure 5.11.</b>	Porosity profile of CNC-dosed hardened oil well cement paste obtained using the DFT method	225
<b>Figure 5.12.</b>	Influence of CNC on the compressive strength development of class G oil well cement paste	226
<b>Figure 5.13.</b>	Influence of CNC on the tensile strength development of class G oil well cement paste	228
<b>Figure 5.14.</b>	Stress-strain diagram of neat and CNC-dosed class G oil well cement paste after 28 days	229
<b>Figure 5.15.</b>	Schematic demonstration of adsorbed CNC particles on a cement grain (seeding agents) and free CNC particles in the matrix	230
<b>Figure 5.16.</b>	Compressive strength vs cumulative pore volume (the impact of CNC)	230
<b>Figure 6.1.</b>	EIRICH high shear mixer (left) and the prepared cementitious paste (right)	249
<b>Figure 6.2.</b>	Hollow cylindrical samples prepared for the permeability test	249
<b>Figure 6.3.</b>	A schematic diagram of the permeability test setup employed	252
<b>Figure 6.4.</b>	The mass flow rate profile of hardened oil well cement paste samples after 1 day of curing time	253
<b>Figure 6.5.</b>	The mass flow rate profile of hardened oil well cement paste samples after 7 days of curing time	253
<b>Figure 6.6.</b>	Flow rate comparison of cementitious systems at steady state condition with and without cellulose nanocrystals (CNC) after 1 day of curing time	254

- Figure 6.7.** Flow rate comparison of cementitious systems at steady state condition with and without cellulose nanocrystals (CNC) after 7 days of curing time 254
- Figure 6.8.** Coefficient of water permeability ( $k_w$ ) in early aged oil well cement pastes with and without cellulose nanocrystal (CNC) particles, after 1 day of curing 257
- Figure 6.9.** Coefficient of water permeability ( $k_w$ ) in early aged oil well cement pastes with and without cellulose nanocrystal (CNC) particles, after 7 days of curing 258
- Figure 6.10.** A visual comparison of surface area obtained from different models 260
- Figure 6.11.** The effect of cellulose nanocrystal (CNC) particles on the cumulative pore volume of hardened oil well cement paste, obtained using the BJH method 261
- Figure 6.12.** The effect of cellulose nanocrystal (CNC) particles on the cumulative pore volume of hardened oil well cement paste, obtained using the DFT method 262

# Chapter I

## *Introduction*

### **ABSTRACT**

This chapter provides an introduction to the presented dissertation. Firstly, the overall concern has been described. Following the problem statement, the main goal of the research is clarified and the objectives to reach the ultimate goal have been defined. Furthermore, the structure of the dissertation and significance of the study have been elaborated.

*Keywords: Oil Well Cement, Cellulose Nanocrystal, Additive, Durability*

## 1. PROBLEM STATEMENT

During the past few decades, oil consumption has increased significantly, particularly from 1964 to 2008 [1]. This is mainly attributed to the fact that today, modern technology and culture are extremely dependent on oil and oil-related products, although alternative renewable energy sources have propagated their way into human lives. The limited amount of oil present on earth has gradually forced everyone to extract, place and consume it properly, with the least time, energy and money wasted on this path. Thus, a large amount of money has been used in the oil industry to introduce and invent appropriate, suitable and advanced technologies to the address this issue [2]. Furthermore, oil/gas extraction from shale in the recent years has also introduced new drilling and cementing demands.

In order to adequately design an oil well, different aspects, dimensions and parameters should be considered and addressed within the design process. A poorly designed oil well might lead to incidents such as oil spill or other environmental disasters (due to toxic substances) [2]. Well cementing is one of the most crucial and important steps in any well completion. However, since it takes place at the end of the drilling process (each segment), a satisfying and acceptable job is rarely done. Hence, a large and significant amount of time and energy is then spent in order to do the required corrections, remedial cementing or retrofitting the well [3, 4].

In the cementing process, cement is used to fill in the annular space between the casing string and the ground formation within the drilled hole. The cement used in an oil well has exclusive functions to perform. These include restricting the movement of hydrocarbons and/or water in between the permeable zones, providing a suitable mechanical support for the casing string, protecting the casing from any sort of physical damage including

corrosion, and supporting the well-bore walls in order to prevent the collapse of formation. Following the functions listed above, the purpose of this operation (oil well cementing) could be summarized in three general points: a) zone isolation, b) corrosion control of the casing, and c) formation stability and pipe strength development [5].

Note that the difference between construction cement and oil well cement is that there is no aggregate added to oil well cement and also a large volume of water is used in oil well cement, in order to make the slurry pumpable. In oil well cementing, analysis and technical measures may be performed from two different points of view: (1) material design and (2) cementing process. The first approach is the study of the cement mixture and its corresponding components, whereas the latter is related to the placing of designed cement paste inside the annulus and the proposed advanced techniques linked with it.

An oil well cement paste needs to fulfill all the requirements mentioned earlier, whether in fresh state or as a hardened sheath around the casing. The prepared paste has to be satisfactorily pumpable and flowable. However, on the other hand, the viscosity and yield stress associated with the paste should be appropriately tailored in order to reduce the risk of lost circulation. Therefore, the rheological behavior of an oil well cement paste should be assessed carefully. Also, the fluid loss (filtration) rate of the prepared cement paste is of great importance since it directly impacts various characteristics of the hardened cement sheath. High filtration and fluid loss rate lead to a change in the water-to-cement ratio of the matrix, influencing not only the flowability of paste while still fresh but also the microstructure of the hardened cement paste.

Furthermore, the hardened oil well cement sheath placed in a wellbore should demonstrate adequate mechanical properties. Therefore, while designing the slurry, the strength

development rate along with the ultimate compressive and tensile strength of the hardened paste should be taken into consideration. Moreover, understanding and improving the transport properties of oil well cement paste is essential. The cement sheath in the annular space between the ground formation and casing may deteriorate for a variety of reasons. The aggression of any type of destructive and detrimental agents through the hardened paste will eventually degrade the cementitious system. This degradation can ultimately influence the zonal isolation and the formation stability provided by the oil well cement paste and also lead towards the corrosion of the casing in the wellbore. Thus, the permeability and pore structure of the hardened oil well cement paste placed in the annulus is extremely critical.

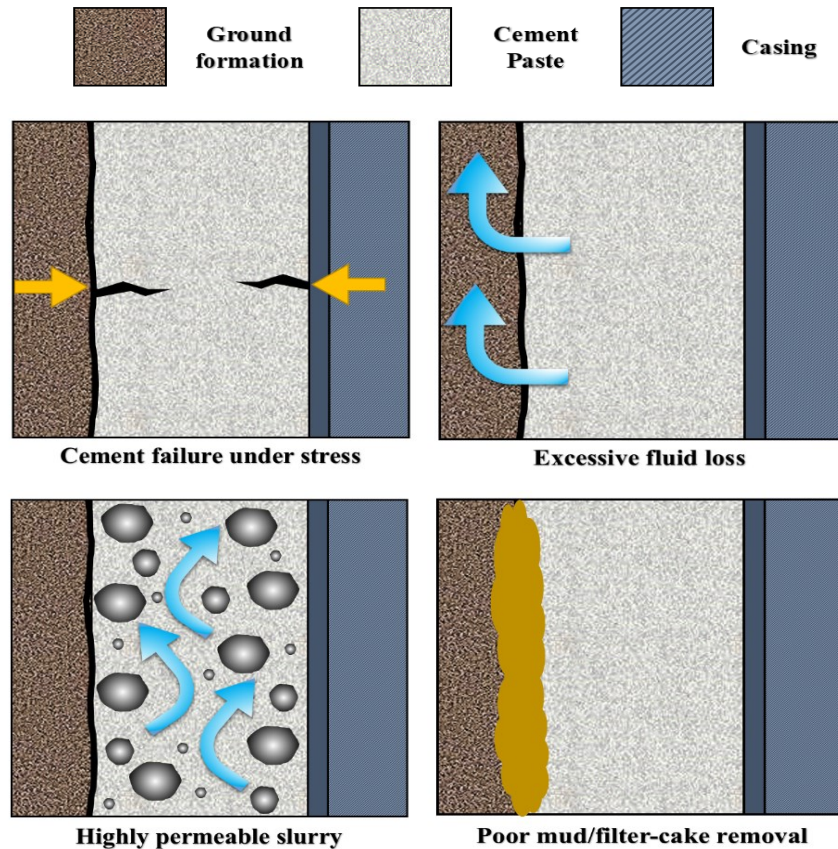


**Figure 1.1.** Major contributing parameters leading to failure in oil well cementing described by Schlumberger in 1996 [6]

Figure 1.1 provides a schematic diagram of the major contributing parameters causing cement failure in an oil well [6]. Based on the discussed criteria in this section and the contributing parameters illustrated, while designing an oil well cement slurry, the following are of great importance and must be assessed: (1) rheology and flowability of paste while fresh, (2) fluid loss rate associated with the paste while fresh, (3) porosity of the hardened cement sheath, (4) strength and (5) permeability. All of these parameters have been addressed in this experimental study.

## **2. RESEARCH OBJECTIVES AND SCOPE**

Durability is one of the main concerns when dealing with any kind of cementitious material or specimen. In structural applications of cementitious materials, maximum load and strength limits are rarely witnessed, therefore durability of the concrete and the reinforcement within the concrete plays a significant role in the failure of structures. Stressed or unstressed, cracks will be observed on any cementitious member. Transport and penetration of different types of harmful fluids into the cementitious member will eventually lead to the failure of the member. Therefore, as mentioned earlier, the permeability of any cementitious material, is also one of the key factors affecting its durability. Permeability itself is a function of porosity and pore structure. Thus, when investigating the permeability of any substance, the associated porosity should be studied and understood.

A similar condition is witnessed in oil well cement systems. While pumped into the annular space between the casing and the ground formation, oil well cement has to isolate and protect the casing from any kind of damage. Therefore, the durability of the cement paste

utilized in oil well cementing is extremely important to any individual involved in the oil industry. In the absence of aggregates, concerns arise both in the short term performance including fluid loss (filtration) and flowability, and in the long term as in strength development and permeability of the cementitious slurry. Thus, aside from being adequately flowable and pumpable, fluid loss, as one of the main concerns, should be controlled to prevent short term and long term deteriorations. Furthermore, the transport properties and strength development of an oil well cement paste should also be taken into consideration.

This study is primarily associated with the material behavior of oil well cement paste in the presence of a proposed additive. Depending on the desired functions and also environmental conditions, different mix designs are used in different cementing operations worldwide. Oil well cement pastes (slurries) are usually designed based on the specifications provided by the American Petroleum Institute [7]. The API specifications have introduced different classes and types of oil well cement. Although Portland cement is the main constituent material in all of these classifications, the chemical composition of these oil well cements is different from the ordinary Portland cement used for general purposes. The composition of API oil well cements is basically different, in order to withstand the conditions associated with the bore-hole (such as high pressure or high temperature). In this research, oil well cement Type G was employed.

A vast number of additives are nowadays available to meet and achieve any kind of desired characteristics. However, when utilizing any kind of additive in a cement mix design, the influence of that additive on the characteristics and properties of the cementitious system must be studied and understood in order to employ the additive wisely and move towards an

acceptable cementing operation [2]. Although the water-to-cement ratio (w/c) has proved to be one of the main parameters affecting the characteristics of a cement paste [5], the API standard [7] specifies the appropriate water-to-cement ratio for each type/class of cement. Therefore, the required and desired changes in the properties and characteristics are achieved by employing sufficient dosages of suitable additives [5, 7]. In the past few decades, different chemical admixtures have been released such as accelerators, retarders, viscosity modifying admixtures, plasticizers, superplasticizers, etc. Utilizing the right amount (dosage) of these additives (if needed) will lead to a durable and well-performed cement sheath in the annulus of the wellbore.

The main goal of this research is to develop an oil well cement system and address the associated durability concerns mentioned above. This study proposes and examines the use of an innovative, non-toxic cellulose-based nanomaterial known as cellulose nanocrystal (CNC) on the properties of oil well cement paste. During the course of the study, the oil well cement system dosed with the proposed additive is assessed at both fresh and hardened states. The cementitious slurry developed in this research is composed of water, Type G oil well cement and cellulose nanocrystals (CNC). However, while investigating the fresh properties of oil well cement paste dosed with CNC, bentonite is also introduced to the mix design. Aside from being a weighting agent, bentonite contamination is inevitable while pumping and placing the cement slurry due to the remaining drilling mud present in the wellbore. In order to achieve the main goal defined above, a multi-scale investigation was carried out, with the following objectives:

- Understanding the influence of cellulose nanocrystal (CNC) particles on the rheological and flow behavior of Type G oil well cement;

- Recognizing the impact of cellulose nanocrystal (CNC) particles on the workability of fresh oil well cement slurry;
- Learning the effect of cellulose nanocrystal (CNC) particles on solidification and hydration of oil well cement paste;
- Observing the change in strength development rate, ultimate compressive and tensile strength associated with oil well cement paste in the presence of cellulose nanocrystal (CNC) particles;
- Identifying the consequences of cellulose nanocrystal (CNC) addition, on the air-void network and pore structure of oil well cement paste;
- Determining the influence of cellulose nanocrystal (CNC) particles on the mass flow rate and water permeability of oil well cement paste.
- Engineering the experimental procedures and providing guidelines (measuring techniques), in order to ease the cementing process and predict the behavior of the placed oil well cement sheath.

### **3. STRUCTURE OF DISSERTATION**

This dissertation is organized and divided into seven chapters.

Chapter 1 provides a general introduction to the research study performed. This chapter defines the problem and states the main goal. Furthermore, the objectives to reach the main goal are elaborated and the significance of the study is described.

In Chapter 2, a comprehensive literature review is presented where the basic concepts related and involved in this study are discussed and elaborated one by one. This chapter contains an introduction to oil well cement and the consequences of cement sheath failure.

The hydration of oil well cement is also discussed along with the main slurry characteristics influencing the well cementing operations. Moreover, the importance of additives is discussed and the most common additives utilized in oil well cement industry are introduced. Furthermore, the rheological behavior and workability of oil well cement pastes are discussed by introducing and exploring steady shear rheology and oscillatory rheology (dynamic mechanical properties). Since the main durability concerns addressed in this study are strength, porosity and permeability, they have been discussed in Chapter 2 thoroughly. Finally, a detailed review on a variety of cellulosic additives, precisely cellulose nanocrystal (CNC) particles is presented in this chapter. This review includes a description on the properties of cellulose, the application of cellulosic additives in cement industry, the preparation process of CNC, the morphology of CNC, and also the influence of CNC particles on cementitious systems.

Chapters 3 and 4 of this dissertation are associated with the impact of cellulose nanocrystal (CNC) particles on fresh oil well cement paste. In Chapter 3, the influence of cellulose nanocrystal (CNC) particles on the flow properties and filtration rate of oil well cement is presented. To meet the first objective of this study, the rheological behavior of CNC-dosed oil well cement was investigated. Even though, shear rheology measurements provide sufficient data regarding the effect of CNC on rheological parameters such viscosity and yield shear stress of cement paste, conventional workability measurements (such as mini slump and flow table) are also performed and reported in this chapter. Furthermore, by utilizing the static filtration test method, the influence of CNC particles on fluid loss (filtration) of oil well cement paste is also determined and described in this chapter. In Chapter 4, the oscillatory rheology (also known as dynamic mode rheology) test method

employed in this study, is explained. This technique and test method are utilized to observe the influence of CNC particles on the solidification and dynamic mechanical properties associated with oil well cement paste.

In this dissertation, Chapters 5 and 6 report the behavior of hardened oil well cement paste dosed with cellulose nanocrystal (CNC). Chapter 5 demonstrates the results of experimental programs employed in understanding the effect of this innovative nanomaterial on the microstructure of oil well cement paste. After understanding the impact of CNC particles on the solidification and hydration of cement paste (Chapter 4), in Chapter 5, the gas sorption technique used for studying the pore structure of the specimens is explained and the influence of CNC on parameters such as surface area and cumulative pore volume of hardened oil well cement paste is illustrated. Furthermore, the compressive and tensile strength of different specimens is reported at different ages along with a stress-strain profile obtained using a load frame after 28 days of curing. Chapter 6 presents the experimental approach utilized to measure the water permeability of hardened oil well cement paste, after witnessing the effect of CNC particles on the pore structure of hardened oil well cement paste and its strength development. Porosity and strength play key roles in determining the permeability of a cementitious system. Thus, investigating them and understanding the pore structure of the specimens prior to measuring permeability is essential. The complete work plan is summarized in Figure 1.2.

Finally, Chapter 7 summarizes the major findings of this study and lists the concluding remarks along with some recommendation for future research.

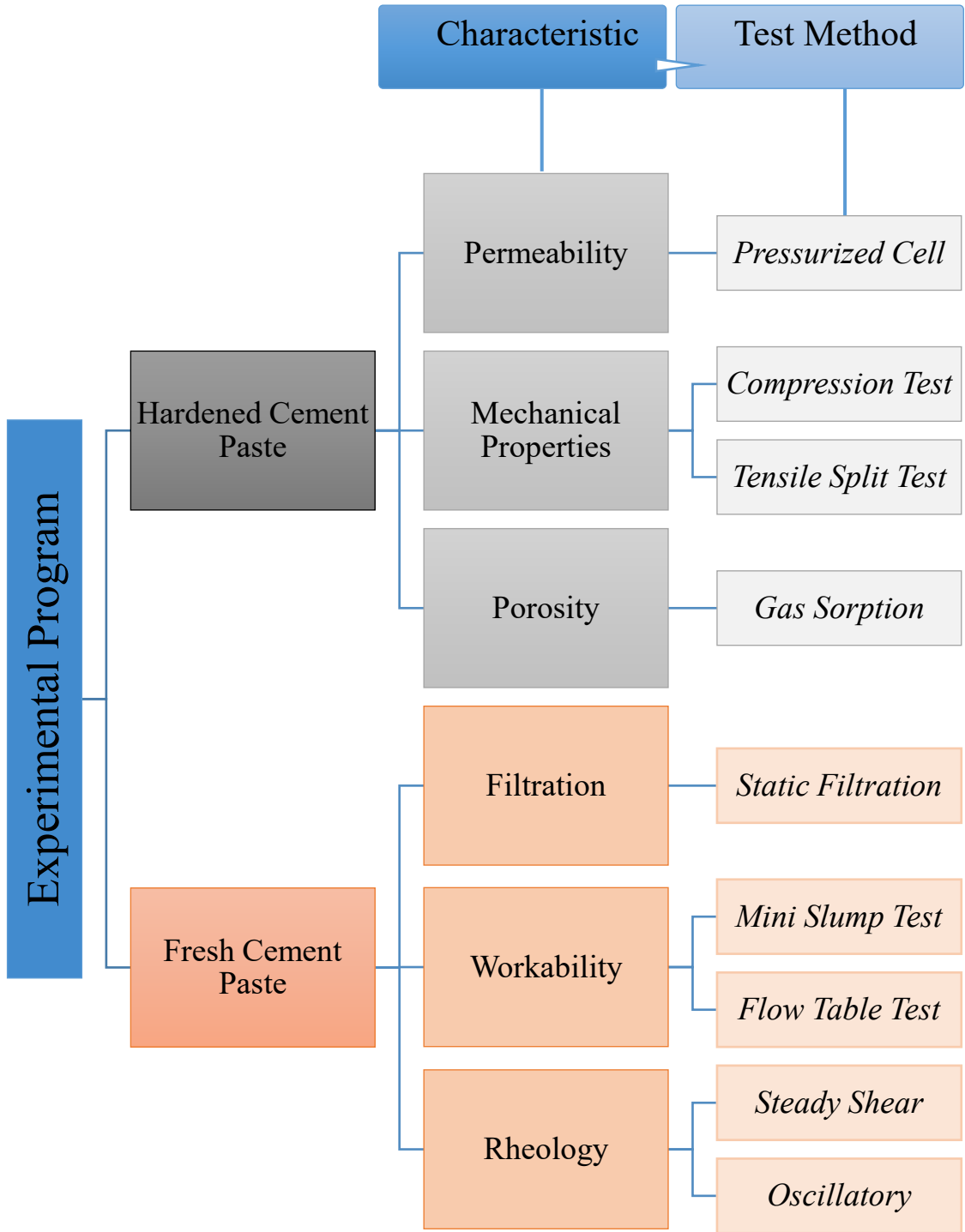


**Figure 1.2.** Flowchart (work plan) of the project

#### **4. SIGNIFICANCE OF THE STUDY**

Cementing is one of the most critical steps in well completion and plays a key role in the integrity of oil wells. Therefore, improving the behavior and properties associated with oil well cement paste has always attracted a significant amount of attention. In order to enhance the oil well cement properties, a wide range of additives have been introduced and employed. However, most of these additives are chemical additives and only address a certain concern. Therefore, when designing the slurry, engineers generally utilize more than one additive to achieve the desired characteristics. Due to their abundance and inherent properties, cellulosic additives have been widely utilized in different industries. Previously, cellulose fibers or cellulose microcrystals have been used in cement [8-11]. One of the most recent cellulosic derivatives produced and employed in many industries is cellulose nanocrystal (CNC) [12, 13].

Cellulose nanocrystal (CNC) particles are extremely smaller than previous conventional (macroscopic) cellulosic additives. Even though CNC particles have been recently used in general cement for strength improvement, they have never been implemented in oil well cement slurries. This dissertation provides a comprehensive study which examines the influence of cellulose nanocrystal (CNC) particles on the performance of oil well cement paste. With the information available from past studies regarding the effect of other cellulosic additives on cementitious systems [8-11], and with recognizing the influence of CNC on a variety of host materials (composites) [12, 13], this study aims to explore the impact of this nanoscale additive on the overall performance of oil well cement paste and shed more light on how this innovative additive could address a number of concerns.

Current literature labels cellulose nanocrystal (CNC) as an ideal additive to enhance the compressive strength of cement paste [14-16]. The contribution of this study is to take a step further and develop a much more reliable oil well cementitious system by utilizing this renewable green additive in oil well cement industry for the first time. By realizing the potential in cellulose nanocrystal (CNC) particles [12, 13], this study targets the production of an enhanced oil well cement system with not only strength development, but also a noticeable improvement in other durability aspects.

## REFERENCES

- [1] Yahaba, N. (2010). *How Does A Decrease In Oil Production Affect The World Economy?*. Australia-Japan Research Centre.
- [2] Shahriar, A. (2011). *Investigation on rheology of oil well cement slurries* (Doctoral dissertation, The University of Western Ontario).
- [3] Harris, K. L., & Johnson, B. J. (1992, January). Successful remedial operations using ultrafine cement. In *SPE Mid-Continent Gas Symposium*. Society of Petroleum Engineers.
- [4] Marca, C. (1990). 13 Remedial Cementing. *Developments in Petroleum Science*, 28, 13-1.
- [5] Nelson, E. B. (Ed.). (1990). Well cementing (Vol. 28). Newnes.
- [6] Bonett, A., & Pafitis, D. (1996). Getting to the root of gas migration. *Oilfield Review*, 8(1), 36-49.
- [7] Specification, A. P. I. (2010). 10A. *Cements and Materials for Well Cementing*.

- [8] Ardanuy, M., Claramunt, J., & Toledo Filho, R. D. (2015). Cellulosic fiber reinforced cement-based composites: a review of recent research. *Construction and building materials*, 79, 115-128.
- [9] Tonoli, G. H. D., Santos, S. F., Savastano, H., Delvasto, S., de Gutiérrez, R. M., & de Murphy, M. D. M. L. (2011). Effects of natural weathering on microstructure and mineral composition of cementitious roofing tiles reinforced with fique fibre. *Cement and Concrete Composites*, 33(2), 225-232.
- [10] Hoyos, C. G., Cristia, E., & Vázquez, A. (2013). Effect of cellulose microcrystalline particles on properties of cement based composites. *Materials & Design*, 51, 810-818.
- [11] Ridi, F., Fratini, E., Mannelli, F., & Baglioni, P. (2005). Hydration process of cement in the presence of a cellulosic additive. A calorimetric investigation. *The Journal of Physical Chemistry B*, 109(30), 14727-14734.
- [12] Habibi, Y., Lucia, L. A., & Rojas, O. J. (2010). Cellulose nanocrystals: chemistry, self-assembly, and applications. *Chemical reviews*, 110(6), 3479-3500.
- [13] Moon, R. J., Martini, A., Nairn, J., Simonsen, J., & Youngblood, J. (2011). Cellulose nanomaterials review: structure, properties and nanocomposites. *Chemical Society Reviews*, 40(7), 3941-3994.
- [14] Cao, Y., Zavaterra, P., Youngblood, J., Moon, R., & Weiss, J. (2015). The influence of cellulose nanocrystal additions on the performance of cement paste. *Cement and Concrete Composites*, 56, 73-83.

- [15] Cao, Y., Zavattieri, P., Youngblood, J., Moon, R., & Weiss, J. (2016). The relationship between cellulose nanocrystal dispersion and strength. *Construction and Building Materials*, 119, 71-79.
- [16] Cao, Y., Tian, N., Bahr, D., Zavattieri, P. D., Youngblood, J., Moon, R. J., & Weiss, J. (2016). The influence of cellulose nanocrystals on the microstructure of cement paste. *Cement and Concrete Composites*, 74, 164-173.

## Chapter II

# *Literature Review*

### **ABSTRACT**

This chapter provides a comprehensive review of the major contributing factors and parameters addressed during the course of this study. At first, a background on oil well cement is provided along with the functions associated with that. Moreover, the hydration process of oil well cement paste is explored and the most common types of additives utilized in well cementing operations are described. Furthermore, the durability concerns regarding oil well cement systems are identified and relevant test methods to investigate the durability of oil well cementitious systems are discussed. Since the intent of this study is to propose cellulose nanocrystal as a suitable additive, a broad review on different cellulosic additives is also presented in this chapter.

*Keywords: Oil Well Cement, Additive, Durability, Rheology, Porosity, Permeability, Mechanical Properties, Cellulose, Cellulose Nanocrystal*

## 1. OIL WELL CEMENT

### 1.1. Introduction

#### *1.1.1. Background*

Oil well cement slurry is generally composed of hydraulic cements and water. However, the type of the cement powder used in oil and gas wells are different from construction cementing on the ground [1]. American Petroleum Institute (API) Specification for Cements and Materials for Well Cementing [2] defines different classes of oil well cement according to downhole condition (pressure and temperature) and desired properties. Moreover, the API standard describes the associated requirements for each individual class. Currently, oil well cement is classified as A, B, C, D, G and H. Also, they are divided into three grades based on the amount of Tricalcium Aluminate ( $C_3A$ ) content: ordinary (O), moderate sulfate-resistance (MSR) and high sulfate resistance (HSR) cements [2]. As mentioned earlier, each of these classes/grades are applicable and suitable for a certain condition and well depth.

Initially, there were only 1-2 types of cement utilized in oil and gas wells [1]. However, as oil and gas wells became deeper and their associated environmental situation was variable, advancements and developments in cement industry were witnessed, with a goal of producing suitable cements to meet specific requirements in different wellbore conditions [3]. Oil well cement classes are basically categorized according to their chemical composition. Nowadays, API classes G and H are the most common classes of cement used in well cementing operations. The chemical composition of class G and class H is similar, but their surface area is not. Class H cement is coarser than class G, therefore it will have

a lower water demand. API specification 10A defines a required water-to-cement ratio of 0.38 for class H cement, whereas the required water-to-cement ratio of class G cement is 0.44 [2, 4]. The oil well cement powder used in this experimental study was a Type G oil well cement provided by Lafarge Canada. The chemical composition and the physical properties of Type G cement are demonstrated in Table 2.1 and Table 2.2.

**Table 2.1.** Physical properties of Type G cement (prepared by Lafarge Canada, December 8<sup>th</sup>, 2015)

<b>Physical Analysis</b>	
Thickening Time (Schedule 5)	99 minutes
Maximum Consistency 15-20 minutes	23 Bc
Fineness 45 $\mu\text{m}$ sieve	93.9%
Blaine	311 $\text{m}^2/\text{kg}$
Free Fluid	4.4%

**Table 2.2.** Chemical composition of Type G cement (prepared by Lafarge Canada, December 8<sup>th</sup>, 2015)

<b>Chemical Analysis</b>	
Silica ( $\text{SiO}_2$ )	20.9%
Alumina ( $\text{Al}_2\text{O}_3$ )	3.8%
Iron Oxide ( $\text{Fe}_2\text{O}_3$ )	4.7%
Calcium Oxide, Total (TCaO)	62.9%
Magnesium Oxide (MgO)	4.5%
Sulphur Trioxide ( $\text{SO}_3$ )	2.6%
Loss on Ignition	0.66%
Insoluble Residue	0.13%
Equivalent Alkali (as $\text{Na}_2\text{O}$ )	0.48%
$\text{C}_3\text{S}$	57.9%

C <sub>2</sub> S	16.1%
C <sub>3</sub> A	2.0%
C <sub>4</sub> AF	14.3%
C <sub>4</sub> AF + 2X C <sub>3</sub> A	18.3%

---

As mentioned by Shahriar, extremely fine cement powders are not desirable in oil well cement industry, since it will not develop or gain the required compressive strength to hold the casing in downhole conditions. Moreover, such micro-fine cements do not exhibit adequate sulfate resistance, hence, not suitable for primary cementing [1]. However, for remedial or repair cementing jobs, these micro-fine cements are a decent option, since they have a smaller particle size compared to a typical oil well cement. As a result, they will be able to penetrate into small cracks easier than normal oil well cement [5].

When designing an oil well cement system, one faces a number of challenges which are rarely a concern in cementing works above ground. For instance, oil well cement slurries will be pumped into extremely deep wells with a temperature higher than 205°C [1]. In such cases, the temperature is reduced by a cooler drilling mud [6]. Also, the increase in pressure (up to 200 MPa) in wellbores can cause severe damage to the integrity of the cement sheath in place [7]. In addition to the challenges mentioned, the oil well cement slurry must be able to cope with porous formations. In order to address all the required and desired characteristics, a wide range of additives have been introduced and employed in the oil well cement industry. Some of these additives change the physical and mechanical properties of the oil well cement slurry whereas some other change the chemical properties.

Shahriar claims [1] that the productivity of an oil or gas well is reliant on the quality of cement sheath in between the casing and the ground formation. Oil well cement needs to

be perfectly pumpable and flowable while fresh (before setting), however, lost circulation should also be taken into account while tuning the rheological behavior of the paste. Basically, the quality of the oil well cement slurry depends on the formulation and composition of the slurry (mix design).

### *1.1.2. Failure of Cement Sheath*

The oil well cement sheath surrounding the pipe within an oil well could fail due to the presence of excessive annular pressure [8]. This pressure can be developed by high temperature changes or simply an internal casing pressure [8]. In 1992 Goodwin and Crook investigated different parameters which were able to cause cement sheath failure. Their main concentration was on the long term problems being experienced by the cementitious system, particularly during the time in which a well begins producing. As stated in their technical paper, these type of (long term) problems basically occur after a certain amount of time whereas the cement system has set and gained some strength [8]. It is usually understood that long term annular influx is actually caused by 2 main reasons: (1) cement sheath failure, or (2) hydrostatic pressure loss. The study by Goodwin and Crook [8] emphasized on the fact that stiff cement sheaths (hardened cement pastes with a higher Young's modulus) are more likely to get damaged by pressure and temperature changes.

Goodwin and Crook eventually concluded that radial cracks will develop within the cementitious system in an oil well, due to the expansion of casing [8]. This expansion can be created by the excessive internal casing pressure. It was observed that these radial cracks were more or less developed in the lower parts of the well, leading to a lack of zonal isolation. Furthermore, they explained that cement systems with a lower compressive strength (up to 1000 psi  $\approx$  6.89 MPa) can withstand the pressure cycle much better than

cementitious systems with a relatively higher compressive strength. An interesting fact mentioned in their technical report was that cement systems with a compressive strength of higher than 82.74 MPa ( $\approx 12000$  psi) can also resist the pressure cycles and no radial cracks were witnessed in them. Aside from the damage caused by the pressure cycle, the change in temperature was also a key factor in developing cracks within the cement sheath. However, unlike the radial cracks caused by the pressure cycle, the cracks developed due to change of temperature were identified in the upper one-third of the well [8].

In another study, Cooke et al. clarify that the cement sheath present in the annulus shows full hydrostatic pressure while it is still in the fresh (liquid) state [9]. However, when the cementitious system starts to set (within the oil well), the cement column pressure changes. According to their experimental findings, this value varies from approximately  $240 \text{ kg/m}^3$  ( $\approx 2 \text{ lbm/gal}$ ) to an equivalent formation pore pressure covered by the column [9]. On the other hand, based on the literature present, scientist have concluded that the cement sheath hydrostatic pressure could be as low as 0 Pa. Carter [10] had the same experience as Burkowsky et al. [11] while investigating the behavior of cement sheath in the wellbore. They identified that these low pressure values can only be observed in circumstances where the cement paste has started to set, but there is no pore pressure or excessive water available for more cement hydration reaction.

Failure in the oil well cement sheath may lead to remedial cementing [1, 4, 8]. This means more financial investment is needed, aside from the extra work required. Therefore, errors leading to failure or economic crisis, are less tolerated in the oil or gas industry [1]. Therefore, as stated by Shahriar, the oil well cementitious system has to be designed appropriately in order address all the desired characteristics [1]. Thus, elements such as

thickening time, fluid loss, viscosity, consistency, strength and durability should be taken into consideration. However, since a neat oil well cement is composed of cement powder and water, most of the required or demanding characteristics are developed by implementing suitable additives or admixtures. Note that the preparation and curing techniques will also be effective and important as well as the presence of additives [1, 4].

Ravi et al. [12] discuss the fact that even though the oil well cement sheath needs to maintain its integrity during the lifespan of the well, but most of the current designs and on-going research are associated with the slurry properties and not the mechanical properties of the hardened cement paste present in the annulus. They were able to propose a design procedure to estimate the risk of cement failure based on a finite element analysis. Debonding, cracking and plastic deformation were among the failure modes investigated in their study. According to the technical paper published by them in 2002 [12], Ravi et al. claim that the main purpose of primary cementing is to provide an adequate cement sheath around the casing so that oil (or gas) can be produced safely and economically. For this objective, the oil well cement sheath needs to fulfill both short-term and long-term duties. Also, the drilling mud employed in the earlier stages of the operation should be completely removed from the annular space and cement paste should replace it. Ravi et al. have listed the short-term and long-term (required) properties of oil well cement in their technical report as following (Table 2.3):

**Table 2.3.** Short-term and long-term properties required of cement [12]

<b>Short-term (cement slurry)</b>	<b>Long-term (cement sheath)</b>
Environmentally acceptable	Thermally stable in HPHT conditions

Desired density	Resists downhole chemicals
Mixable at surface	Withstand stresses
Non-settling under static/dynamic conditions	Providing zonal isolation
Zero free water	
Desired thickening time	
Desired fluid loss	
Desired strength development	
100% placement in annulus	
Resists fluid influx	

---

As mentioned by Ravi et al. [12] nowadays, most of the focus and concentration is associated with the slurry. In other words, the short term properties have been the center of attention in recent years. However, it is crucial to address the long-term properties, if we are aiming for a more durable cementitious system. Therefore, aside from mechanical resistance, the cement sheath should resist chemical attack as well. Hence, permeability and porosity play major roles. Based on the literature [1, 4, 12] a cement slurry could be identified suitable if there is no liquid moving to the formation surface immediately after the cement has been placed. This means the fluid loss (filtration) of the cement slurry designed is low. A low fluid loss will eventually lead to a better strength development and a more reliable cement sheath. Nevertheless, the cement sheath (hardened paste) could lose its integrity anytime during the production operation, project completion or pressure testing [12]. In such cases, the cementitious system in the annulus will not be able to provide zonal isolation desirably. Therefore, such a failure will allow the formation fluids to enter the annular space. In these circumstances, a remedial cementing job needs to take place. Ravi et al. describe the failure of cement sheath as a defeat in the objective of producing hydrocarbons economically.

## 1.2. Hydration

It is believed that the main functions of an oil well cement paste present in a wellbore, is to restrict the movement of the fluids between formations and to protect and support the casing from any kind of damage [3, 4]. As mentioned by Zhang et al. [13] oil well cement paste is pumped inside the wellbore through the casing, but since the entire well is not cemented in a single operation and pumping could take several hours, different types of additives (retarders, dispersants, etc.) are utilized to keep the cement paste pumpable, and prevent the cementitious system from premature hardening. Therefore, understanding the behavior of oil well cement paste and the effect of each individual additive introduced to the cementing industry is of great importance.

On the other hand, understanding the hydration process of oil well cement paste is also crucial. The engineers involved must be aware of the setting time of the cement system used, so the drilling process can be scheduled appropriately. As Zhang et al. [13] describe the primary cementing job, after pumping the cement, the drilling should stop until the cement paste has set. Also, one who designs and formulates the oil well cement system should know that the cement paste needs to set shortly after it has been placed. Time is essential. Taylor identifies the water-to-cement ratio a primary factor affecting the setting time of an oil well cement system [14]. However, other parameters such as the presence of additives, cement composition, particle size distribution, temperature and pressure are also extremely important and effective. Thus, the setting time of a cementitious system is a function of all the parameters and factors mentioned above, and one should address them according to desire.

Zhang et al. explored the behavior and hydration of oil well cement paste with different measuring techniques [13]. In the study performed by them, the chemical shrinkage of oil well cementitious systems was measured at different temperatures, in order to investigate the associated rate of hydration. Furthermore, an ultrasonic transmission measurement also took place in their research scheme along with analyzing the degree of cement hydration at setting time by thermogravimetric analysis (TGA). It was eventually concluded that an increase in temperature and introducing additives such as calcium chloride accelerates the rate of hydration, whereas adding hydroxyethyl cellulose delays the cement hydration and the cement paste sets later than reference mix (with no additive) [13].

However, these are not the only measuring techniques concrete scientists are familiar with. According to the literature, the early hydration of cement paste has been investigated with many different techniques [13-17]. For instance, some scientists have witnessed the rate of the hydration reaction during their experimental studies whereas some others test their cementitious samples and evaluate the properties at different time intervals [15, 16]. Another approach employed to understand the real-time hydration of oil well cement was introduced by Jupe et al. in 2005 [17], where they used synchrotron X-ray diffraction at high temperatures and pressures.

The setting and hardening process of oil well cement is a result of reactions between water and cement [1]. In 1989, Vidick revealed the influence of the chemical composition of cement and additives on the form of hydration products [18]. Although, different types of cement powders demonstrate different behavior when additives are introduced [19]. Later in 1995, it was discovered by Justnes and colleagues that temperature is also effective on the structure of the hydration products [20, 21]. Furthermore, after investigating and

studying the microstructure of class G oil well cement, Vlachou and Piau concluded that the form of the hydration products depends on the experimental and mixing conditions (stirring) [22]. It was understood that the slurry which is under stirring, provides constant viscosity and acceptable flowability for several hours. This could have been due to the production of small spherical hydration products that had no bond between themselves and were able to move freely. However, after the development of more hydrated crystals, the slurry will eventually thicken. Vlachou and Piau describe this as the start of the hardening process in their class G oil well cement system [22].

Moreover, it was concluded that when the slurry is at rest (no stirring or mixing involved), aluminate hydrate crystals are formed in colloidal size [22]. These crystals will then cover the surface of cement grains and consequently, the hydration process slows down. In 2008, Zhang et al investigated the effect of curing temperature on the microstructure of hardened cement paste [23]. They realized that when the curing temperature increases, the microstructure of the calcium silicate hydrate (C-S-H) changes from a three dimension fiber network to a mass block [23]. This was further interpreted as densification or grain size refinement. Zhang et al. also report that this increase in the curing temperature will change the major hydration products to a variety of calcium silicate hydrates [23].

Justnes et al. claim that for cement slurry with a water-to-cement ratio of 0.5 made from Type G oil well cement, only 10% of hydration is required to take place so that the slurry can retain its shape and demonstrate sufficient yield strength at atmospheric pressure [20, 21]. In 2005 Jupe also investigated the relationship between pumping time and temperature. Based on the results obtained [20, 21], Jupe claimed that majority of the change in pumping time occurs in the state where ettringite or monosulphate decomposes

and hydro garnet starts to form in crystals. However, Jupe was not able to correlate the change in pumping time to the hydration of tricalcium silicate ( $C_3S$ ). In another research and experimental study [24], it was identified that a change in curing and preparation temperature not only affects the cement hydration chemistry but also alters the shrinkage of the hardened cement paste. Backe et al. emphasize on the fact that curing the cement paste in any temperature above  $50^\circ C$  leads to an uneven distribution of hydrated products. Thus, densified C-S-H will form around the unhydrated cement grains and eventually the hydration rate slows down [24].

### **1.3. Vital Slurry Characteristics**

#### *1.3.1. Flow Behavior*

Since the oil well cement paste needs to be pumped inside the wellbore (during the placement and cementing process), the flow behavior and pumpability of the slurry is of great importance [1, 4]. In order to understand and predict the flowability of a cementitious matrix prepared for a well cementing operation, rheological measurements take place and vital parameters such as viscosity and yield stress associated with the cement paste are assessed. Certain additives are nowadays produced and employed to alter the rheology of cement paste [4]. Rheological assessment of oil well cement is further explained in section 2 of this chapter.

#### *1.3.2. Density*

The density of a neat oil well cement paste (contains no additive) may be any number between  $1773 \text{ kg/m}^3$  and  $1965 \text{ kg/m}^3$  while still fresh [1]. However, it could change with a change in the water-to-cement ratio. Also, the type of the API cement used plays a major

role in defining the value of density [2]. Basically, in some circumstances, a cement paste with a higher density is required in a wellbore, in order to withstand the bottom-hole formation pressure and to reduce the diffusion of drilling muds or well fluids into the slurry. Whereas in other situations, a low density cementitious system may be required to reduce lost circulation during the cementing operation. [1, 25]. In order to achieve the desired density based on the operation and environmental condition, density modifying additives such as bentonite have been attracting attention. Therefore, one could employ weighting agents for a cement system with a higher density, or include extenders in the mix design to achieve a slurry with a lower density. The topic of additives is comprehensively described and explored in this dissertation. The most common types of weighting agents increase the water demand slightly while increasing the density [4].

### *1.3.3. Setting Time*

The setting time of an oil well cement system placed in the annular space around the casing is of extreme importance [4]. Both premature and very long setting times influence the production of the oil well negatively. It may even lead to significant financial losses [1]. The setting time of a cementitious system can be altered by changing the chemical composition (reducing the amount of  $C_3A$ ), or simply by adding additives such as retarders or accelerators to the mix [4]. Moreover, the literature suggests that during the cementing operation in an oil well, it is essential to maintain the cement setting time over the temperature range of 60°C to 104°C [25]. It is important to know that the setting time of an oil well cement is measured differently from a conventional cement and it is described in terms of change in viscosity [1].

#### 1.3.4. Thickening Time

The API specification defines the thickening time of an oil well cement system as the duration in which the oil well cement slurry remains pumpable [2]. In other words, it determines the length of time that cement slurry can be pumped inside the wellbore. It is perhaps one of the most crucial properties in the displacement progress and is measured using a cement consistometer. Thickening time is influenced by the fineness of the clinker, cement composition, pumping rate, additives, etc. [4]. These additives may be either accelerators or retarders as described earlier. The simple equation below helps one to estimate the appropriate thickening time based on the situation

$$\text{Thickening Time} = \text{Mixing and pumping time} + \text{Displacement time} + \text{Plug release time} + \text{Extra margin (time)}$$

Where mixing and pumping time = volume of cement slurry / mixing rate; displacement time = displacement volume / displacement rate; extra margin time = 30~60 minutes (normally).

The Thickening time is also altered by introducing additives (retarders) to the mix. For instance, Bentz et al. realized that by adding sucrose, they were able to increase the thickening time dramatically [26]. In another research, Bermudez revealed that presence of sugar in low dosage would extend the thickening time, however it was later discovered that if sugar is added in a high concentration it will act as an accelerator in the cement system [27].

## 1.4. Additives

### *1.4.1. Significance in Oil Well Cement Industry*

Nowadays, a vast number of additives and admixtures are available to enhance the behavior of the oil well cement systems [4]. Based on the desired characteristics, the cementitious slurry can be tuned appropriately, so that it could be placed inside the annular space between the pipe and the ground formation adequately. Additives implemented in oil well cement industry have different benefits and each will address a certain issue. Some additives may be employed for rheological purposes so that the cement slurry flows easily inside the wellbore. Hence, certain additives will be added to the mix design to alter the shear viscosity and shear yield stress of the cement system while still fresh. Furthermore, one can utilize other additives, admixtures or supplementary cementitious materials (SCMs) to address mechanical properties and enhance the strength development of the cementitious system designed [1].

### *1.4.2. Common Types of Additives*

As mentioned by Nelson [4], the degree of influence of each individual additive depends on certain parameters such as the chemical composition and particle size distribution of the cement powder, total sulphate content, free alkali content, surface area of the hydration products, dosage of the additive or admixture used, preparation of the paste, water-to-cement ratio, curing, temperature, etc. Basically, Nelson [4] categorizes oil well cementing additives into eight groups: (1) Additives, (2) Retarders, (3) Extenders, (4) Weighting agents, (5) Dispersants, (6) Fluid loss control agents, (7) Lost-circulation control agents and (8) Specialty additives. Researchers around the globe have identified and industrialized

suitable additives for improving the behavior of cement. Using these additives will eventually lead to a more durable cement sheath.

For instance, accelerators shorten the setting time of the oil well cement paste. In other words, they are utilized to accelerate the hardening process, after being placed in the annulus. Based on the observations, these additives also increase the rate of compressive strength development. Some of the most common accelerators currently used in the oil well cement industry are chloride salts, calcium chloride ( $\text{CaCl}_2$ ), sodium chloride ( $\text{NaCl}$ ), sodium hydroxide ( $\text{NaOH}$ ), potassium hydroxide ( $\text{KOH}$ ), etc. However, in order to prevent or minimize the corrosion of the pipes, chloride free accelerators have been developed to use in the oil well cement industry. Note that the concentration of these additives used in the mix design is not similar. Calcium chloride will be most efficient at a dosage of 2-4% by weight of the cement, whereas sodium chloride is usually employed in a dosage of up to 20% by weight of the cement [4].

Each individual additive has a mechanism of action (to alter the behavior of the cement paste). Calcium chloride, for example, effects the hydration rate of the cement. Furthermore, it will cause a morphological change in the C-S-H structure. Thus, after introducing this material as an additive to the cementitious system, the C-S-H gel becomes more permeable. This phenomenon enhances the diffusion and therefore accelerates the hydration process. In this case, the heat of hydration also increases (during the first number of hours after mixing). On the other hand, some additives may demonstrate secondary effects as well. For instance, calcium chloride not only accelerates the hydration process as discussed above but also increases the rate of compressive strength development during the early days after placement. Volumetric shrinkage (10% to 50%) is also a possibility in

such scenarios, as a side effect due to the increase in the degree of hydration. One should also be aware of the fact that the microstructure of an oil well cement paste will be more permeable due to the addition of calcium chloride, hence, the resistance to aggressive sulfate solutions will eventually decrease [4].

Another frequently used group of additives are the retarders. According to Nelson [4], the actual mechanism of action is related to both, chemical nature of the additive, and the chemical nature of the cement phase (silicate and aluminate). To elaborate more, it is understood that the retarder (agent) either adsorbs onto the surface of the hydration products (inhibiting contact with water), or reacts with ions (calcium or hydroxyl or both) in the aqueous phase to form an impermeable layer around the cement particle (grain), or adsorbs onto the nuclei of hydration products to prevent their growth, or simply chelate with the chloride ions and basically prevent the formation of nuclei. The most common classes of retarders could be summarized as lignosulfonates (polymers derived and developed from sulfite pulp by-products), hydroxycarboxylic acids (extremely powerful retarders), organophosphonates (phosphonic acids and their salts which are insensitive to the cement composition) and cellulose derivatives (polysaccharides derived from wood). Each of the mentioned classes has their associated mechanism of action which could be one or a combination of two of the mechanisms described earlier [4].

Extenders have also been widely used as an additive in oil well cement systems. They are mainly employed to decrease the density of the cement slurry in order to prevent scenarios such as lost circulation or to increase the yield. The latter effect will result in a reduction in the cement powder quantity, hence there is an economic benefit to it as well. These additives are classified as either (1) water extenders (such as clay which allow the designer

to use more water in order to obtain a more homogenous mix), (2) low-density aggregates (reducing the slurry density because of the presence of materials with a lower density compared to Portland cement) or (3) gaseous extenders (nitrogen and air employed to develop foamed cements with a lower density). The most common types of extenders are known to be clays, sodium silicates, pozzolans and lightweight particles [4].

These types of additives (accelerators, retarders and extenders) have been elaborated in this chapter because of the materials involved in this experimental study. Although the main objective of this study is to investigate the influence of cellulose nanocrystals on the behavior of oil well cement paste, this comprehensive study also demonstrates the effect of bentonite (a type of clay). Accelerators have been elaborated since they alter the microstructure of the cement paste along with the permeability, retarders have been described since cellulose derivatives have always been a major type of retarding agents, and extenders have been taken into consideration because of clays.

In a recent review article [28], Broni-Bediako et al. investigated the most common additives (calcium chloride, hydroxyethyl cellulose, bentonite, etc.) that have been employed in oil well cementing in order to enhance the overall behavior of the cement sheath around the casing. As explained thoroughly, it is claimed that once the desired characteristic is aimed at, it can be achieved by utilizing a suitable additive in an appropriate dosage. Broni-Bediako et al. describe how additives play a major role in the development of enhanced oil well cement systems. As Magarini et al. claim [29], the circumstance (varying pressure and temperature) in which oil well cement will be designed for, is different from cementing jobs on ground construction, the presence of additives becomes a necessity.

The American Petroleum Institute recommended Practice 10B [30] defines additives as materials which are added to the cement slurry in order to enhance and improve the desired characteristics and properties. According to Bett [31], choosing the correct additive for a cementitious system in a cementing operation is an essential part of well design and integrity. Cowan and Eoff [32] also state the fact that additives are included in the mix design to address placement and durability concerns such as setting time, filtration loss, etc. Each individual additive is added to the mix design to address a certain issue. Generally, in oil well cementing operations, concerns arise regarding issues such as the high formation pressure present, fluid loss and filtration, lost circulation, cement permeability, compressive strength, etc. [28].

In order to accommodate the high formation pressure and restrain it, some heavy weight additives are usually employed with densities greater than  $2037 \text{ kg/m}^3$  ( $\approx 17 \text{ lb/gal}$ ) so that dispersants and/or silica are not effective. The most common heavy weight agents nowadays used in oil well cement industry are Hematite ( $\text{Fe}_2\text{O}_3$ ) [33, 34] which contains more than 70% iron, Ilmenite ( $\text{FeO TiO}_2$ ) which is also known as iron titanium oxide with a submetallic luster containing almost 37% iron [33] and also Barite ( $\text{BaSO}_4$ ), however, the latter is not usually utilized as a weighting agent anymore since it will increase the water demand due to its high surface area [28].

To address fluid loss (filtration) and permeability concerns in oil well cementing operations, a wide range of additives have been introduced and employed. These additives are generally categorized into two groups: (1) water-insoluble and (2) water soluble [28]. Because of the presence of differential pressure, some of the water may be forced out of the cementitious system into the geological (ground) formation. This filtrate loss will

eventually alter the water-to-cement ratio of the cement paste and consequently change the corresponding rheology, flow behavior and mechanical properties. The fluid loss additives utilized in oil well cementing will deposit a very low-permeability filter cake on the formation face in order to restrict or limit the quantity of fluid loss [35]. Hence, minimize the change in water-to-cement ratio and eventually develop a much more durable cement sheath around the pipe. On the other hand, fluid loss agents will reduce the formation damage by reducing the filtrate volume [36].

A secondary effect caused by adding fluid loss agents to the oil well cementitious system is known to be a reduction in gas migration [37]. When the quantity of filtrate is large, there will be free space provided within the cement paste, therefore gas will migrate into the paste and occupy that free space [36, 38]. Even though polyvinyl alcohol, polyalkanolamines, liquid latex (such as styrene butadiene latex) and polymers of polyacrylamides have been widely used to reduce fluid loss of cement paste, Adams and Charrier claim that cellulose derivatives such as hydroxyethyl cellulose (HEC) [39] are the most common and suitable fluid loss additives when used in a dosage of 0.3 to 3.0% by weight of the cement [36]. Since fluid loss additives also increase the viscosity of the cement slurry, using an inappropriate dosage might lead to difficulties during the cementing operation while pumping the paste inside the wellbore [36].

Another common problem faced during an oil well cementing operation is believed to be lost circulation. Lost circulation refers to the cement paste lost into the ground formation during the cementing operation [28]. Broni-Bediako et al. claim that the organic lost circulation materials employed in drilling fluids should not be utilized in oil well cement, because they will evidently increase the porosity and therefore provide a path for the

possible corrosive formation fluids to propagate into the cement sheath [31]. According to the literature, ground coal, ground Gilsonite and ground walnut hull are found to be the most common additives to address lost circulation. Based on the results published by Slagle and Carter in 1958 [40], Gilsonite proved to be an excellent additive in order to combat lost circulation in areas of incompetent formations. Results showed that when Gilsonite was present in the cement mix, fill-up of up to 90% was possible to obtain, whereas only 50-60% fill-up was observed with other types of cement pastes (with no Gilsonite) [40].

Gilsonite can be classified as an asphaltite. It is a naturally occurring carbonaceous material known to be a relatively pure hydrocarbon [41]. Broni-Bediako et al. argue that the presence of Gilsonite could also have a negative influence on thin slurries or slurries with dispersants [28]. In other words, Gilsonite could get separated in such slurries due to its low specific gravity. However, this phenomenon could be disallowed by introducing approximately 2% bentonite to the cementitious slurry. Bentonite will prevent the separation of Gilsonite [28].

## **2. RHEOLOGICAL BEHAVIOR AND WORKABILITY**

### **2.1. Steady Shear Rheology**

#### *2.1.1. Introduction*

As discussed earlier, the rheology and flowability of the oil well cement paste are of great importance, since it needs to be pumped inside the wellbore. Rheological measurements have been a significant part of fresh cement paste assessments in cement and concrete research around the globe. Different types of additives are utilized in order to tune the

rheological and flow behavior of cementitious systems. These additives or admixtures will eventually alter the viscosity and yield shear stress of the cementitious system, hence a change in the flow behavior of the system is observed. In this section, the influence of different additives and admixtures on the rheological behavior of different cementitious systems is explored.

Even though conventional workability tests executed on cement paste and concrete are useful in order to understand and monitor the quality of the final product, concrete engineers have identified the need for a more quantitative measurement of the workability of cementitious systems [42, 43]. Therefore, it has been decades that fresh cementitious systems are treated as multiphase fluids and fluid rheological measuring techniques have been applied to them, to describe their flow behavior [42-44]. Generally, cementitious systems are assumed to behave like a Bingham fluid [45]. Therefore, the two most important parameters defining the rheological behavior of a cementitious system are yield stress and plastic viscosity. Laskar and Talukdar describe the yield stress of a cementitious system, as the quantitative measure of the initial resistance to flow, whereas plastic viscosity controls the flow after it is initiated [45]. According to recent studies, the yield stress of cementitious systems is associated with its slump and the plastic viscosity is linked to parameters such as pumpability, place-ability, segregation and stickiness [46-48].

In their comprehensive study, Laskar and Talukdar investigated the influence of fly ash / pulverized fuel ash (PFA), condensed silica fume (CSF) and rice husk ash (RHA) on the rheological properties of concrete [45]. PFA was used as a mass replacement for cement at rates of 10%, 20%, 30% and 50%. According to the results obtained by Laskar and Talukdar [45], the addition of PFA led to a decrease in yield stress. However, the effect of

PFA addition on plastic viscosity was different. The plastic viscosity increased when PFA replaced cement at a rate of 10%. Furthermore, viscosity gradually decreased when the PFA content increased from 10% to 30%. Finally, change in viscosity was found to be insignificant after a PFA replacement of above 30% [45].

Condensed silica fume (CSF) was also utilized as a mass replacement for cement at the rates of 5%, 10%, 15% and 20%. Rheological results reported and published by Laskar and Talukdar showed that the yield stress was reduced when CSF replaced cement at any rate below 10%, whereas when the replacement rate was more than 10%, a growth in yield stress was also identified [45]. On the other hand, the plastic viscosity of concrete increased dramatically with CSF replacement rate of up to 10%, following a gradual decrease after that [45].

At the final stage of their experimental study, Laskar and Talukdar replaced cement with rice husk ash at rates of 5%, 10%, 15% and 20% (on a mass basis) [45]. The outcome of the experimental approach verified that yield stress of concrete decreases linearly when RHA is present at a rate of 10% or less. Some of the samples tested demonstrated a decrease in yield stress when RHA content was above 10% whereas some other specimens showed no significant change after that. The rheological data obtained from testing specimens containing RHA proved that the plastic viscosity of concrete will increase with an increase in RHA content. According to the findings of Laskar and Talukdar, when the RHA content went beyond 10%, the plastic viscosity of concrete increased dramatically [45]. Laskar and Talukdar conclude that the impact of mineral admixtures on the rheology of concrete is reliant on factors such as surface activity, particle size distribution, specific surface area, shape, surface features, etc. [45].

### *2.1.2. Influencing Factors and Common Rheology Modifying Agents*

Hanehara and Yamada [49] claim that the rheological properties of a cementitious system are basically affected by the ingredients, preparation condition and also the environment where the concrete or cement paste is surrounded with. Furthermore, it is believed that the rheology of cement or concrete also depends on the interactions between the ingredients used, particularly the interaction between the cement particles and the admixture utilized in the mix design [49]. In other words, the compatibility of the cement particles and the admixture used is critical. This compatibility is usually judged by the fluidity associated with the prepared cementitious system [49].

Hanehara and Yamada also explain that the compatibility between cement and admixtures not only leave an impact on the fluidity of the cementitious system but also affect parameters such as setting time and stiffness [49]. According to the experimental studies, Hanehara and Yamada concluded that any interaction problem related to admixtures in cementitious systems, may be categorized in two groups: (1) problems triggered due to the influence of the admixture on the hydration of cement and (2) problems emerged due to the adsorption of the admixture onto the surface of cement particles [49]. In their experimental study, they investigated the effect of different admixtures on the rheological properties of cementitious systems. The admixtures selected in their experimental approach were lignin sulfonic acid-based admixture,  $\beta$ -naphthalene sulfonic acid-based admixture and polycarboxylic acid-based admixture [49].

Hanehara and Yamada realized that when lignin sulfonic acid-based admixture was employed in their cementitious system, the hydration of interstitial phase was affected. This hydration was influenced by the concentration of  $\text{Ca}^{2+}$ ,  $\text{OH}^-$  and  $\text{SO}_4^{2-}$  in the mixing water

[49]. It was observed that in this case, large amounts of ettringite were produced during the hydration of interstitial phases which takes place in the first hour after the mixing process. Consequently, this caused an increase in stiffness and lead to pseudo-setting [49, 50]. According to the results published by Hanehara and Yamada, samples including lignin sulfonic acid-based admixture had a lower  $\text{Ca}(\text{OH})_2$  saturated ratio compared to the reference samples with no additive (during the first 30 minutes) [49, 51].

It was concluded that the loss of slump and stiffness is basically due to the fact that lignin sulfonic acid-based admixture consumes the  $\text{Ca}^{2+}$  in the mixing water. The same experiment was repeated with the presence of fly ash. The results showed an even lower  $\text{Ca}(\text{OH})_2$  saturated ratio when both fly ash and lignin sulfonic acid-based admixture were present in the mix design [49]. According to Hanehara and Yamada, this phenomenon occurred not only because the  $\text{Ca}^{2+}$  in the mixing water was taken by the admixture, but also because of the fixation of  $\text{Ca}^{2+}$  by fly ash [49].

Moreover, the influence of addition time of admixture on the rheological behavior of cementitious systems was investigated by Hanehara and Yamada [49] using other chemical admixtures such as  $\beta$ -naphthalene sulfonic acid-based admixture and polycarboxylic acid-based admixture. According to the results obtained, Hanehara and Yamada claim that delayed addition of the admixture (such as the two-stage mixing process), could be an effective method to reduce the water-to-cement ratio of concrete and increase the strength associated with it [49, 52]. However, it was also mentioned that the effect caused by the delayed addition, depends on the type of the admixture used in the mix design.

For instance, studies prove that the impact of the delayed addition of the naphthalene sulfonic and amino sulfonic acid-based admixtures on the fluidity of cementitious systems

is larger than the effect of delayed addition of lignin sulfonic and polycarboxylic acid-based admixture [49, 52]. The adsorption of the admixture on the surface of the interstitial phase is reduced as a result of the movement of Ca from the interstitial phase towards the mixing water, and the deposition of ettringite (due to the reaction of the interstitial phase with sulfate ions on its surface). Consequently, the admixture is adsorbed on the cement particles. Hence, the cement particles are repelled by each other and therefore the fluidity is improved [49].

Experimental studies show that the newly developed polycarboxylic acid-based admixtures enhance the fluidity of cementitious systems and reduce their viscosity, even if utilized in low dosages in cementitious systems with a low water-to-cement ratio [49, 53]. In cementitious systems containing polycarboxylic acid-based admixtures, the side chains of polyethylene oxide extend on the surface of cement particles and the cement particles are dispersed because of the steric hindrance of the side chains [49]. Hanehara and Yamada claim that the interaction problem of the polycarboxylic acid-based admixtures is reliant on the amount of the admixture added to the mix design, as well as the type of the cement used [49]. Yamaguchi et al investigated the relationship between the type of cement and the rheological properties associated with it, in the presence of polycarboxylic acid-based admixtures [49]. They evaluated 18 different types of cement in their study and realized the correlation between soluble alkali in cement and the fluidity of that cement paste [49]. Matsuhisa and Yamada et al. also performed a detailed analysis on cement pastes prepared with polycarboxylic acid-based admixtures and concluded that 80% of the variation of the fluidity of these pastes dosed with polycarboxylic acid-based admixtures depends on the content of the alkali sulfate which is one of the soluble alkalies in cement [49, 54].

Furthermore, Yamamoto et al. also studied the rheological behavior of cement pastes by measuring the associated viscosity of pastes prepared by adding alkali sulfate and realized that by increasing the amount of alkali sulfate, the fluidity of the cement paste decreases significantly [49, 55]. Hanehara and Yamada further explain this phenomenon by emphasizing on the fact that any reduction in the fluidity of cement paste due to the addition of alkali sulfate, is mainly because of the reduced amount of admixtures adsorbed on cement particles as a result of increasing the sulfate ions in the mix [49].

A common type of additive utilized in cement paste and concrete is polysaccharide gums [56]. Polysaccharide gums (PSG) are long chain carbohydrate polymers used to alter the rheological behavior of cementitious systems. Ghio et al. claim that PSG's are anti-bleeding agents which have several practical applications in the concrete industry. Aside from their impact on the rheological and flow behavior, these polymers have been generally used to improve the bond between concrete (cement paste) and steel [56]. In an experimental study in 1993, Ghio et al. utilized polysaccharide gum to observe its influence on the rheological properties of fresh cement paste [56]. In their approach, Ghio et al. mixed the cement paste in a blender for three minutes, before pausing for a minute to add the additive. Furthermore, the paste was mixed for another three minutes and eventually poured into a concentric cylinder viscometer and high sheared (512 rpm) for a period of two minutes. After the high shear mixing, the specimen was rested for another two minutes in order to reach equilibrium prior to starting the test [56].

Ghio et al. [56] took two measurements only. The first set of data were recorded at a shear rate of 256 rpm whereas the other set was measured at a low shear rate of 8 rpm. According to the results presented by Ghio and colleagues, the addition of polysaccharide gums

increased the apparent viscosity of the cementitious samples. However, the increase in viscosity was more significant when the data were recorded at a low shear rate (8 rpm). Therefore, Ghio et al. concluded that the presence of polysaccharide gums results in a larger increase in the apparent viscosity for low shear rates than higher shear rates.

In their investigation, they also employed water reducing agents and combined it with PSG to study the effect on rheology when both agents are present. Based on the results obtained, the coupled effect of polysaccharide gum and water reducing agents was significant. Samples containing both demonstrated a noticeably higher viscosity compared to the reference samples or samples which only contained polysaccharide gums [56]. Interestingly, an increase in the dosage of the water reducing agent did not further increase the viscosity at a lower shear rate. Ghio et al. also identified a reduction in viscosity when water reducing agents were added alone (without PSG) [56].

In another study in 2014, Poinot et al. investigated the influence of different addition methods of polysaccharide on the rheological behavior of cementitious systems [57]. Therefore, in their experimental approach, polysaccharide was introduced to the cementitious system either in the form of powder or as a solute in the mixing water. According to Poinot et al., polysaccharides alter the rheological behavior of the cementitious system to their thickening properties [57, 58]. The behavior of cementitious systems in the presence of polysaccharides have been studied by many researchers [59-65]. The outcome of all of these experimental investigations proves that the presence of polysaccharide leads to an increase in the apparent viscosity in low shear rates. This will prevent sedimentation. On the other hand, polysaccharides enhance and maintain the fluidity of the cementitious system due to their low viscosity in high shear rates [59-65].

Poinot and colleagues [57] were aware of the potential influence of polysaccharides, however, the main question was the impact of addition methods. Different specimens were prepared with different addition methods (of polysaccharides). Rheological measurements took place using a Vane-cylinder geometry rheometer. Furthermore, Poinot et al. characterized the rheological behavior of the specimens using the Herschel-Bulkley model. According to the results obtained, when pre-dissolved polysaccharides were added to the cement, a higher yield stress was witnessed, compared to the samples where polysaccharides were added in the form of a powder [57]. Poinot et al. claim that this is mainly due to a polymer difference in the pore solution [57]. Based on their experimental findings, a larger quantity of polysaccharide was identified in solution when the polymer was pre-dissolved in the mixing water rather than when the polymer was added to the cementitious system in the form of a powder [57].

Cellulose derivatives are widely used in the concrete and cement industry as additives in order to achieve certain desired characteristics. One of the most common groups of cellulosic additives is cellulose ethers (CE). Brumaud et al. [66] studied the influence of cellulose ethers on the behavior of cement paste. Like other cellulosic derivatives utilized globally, cellulose ethers are also expected to alter the flow and rheological behavior of cementitious systems [66]. Cellulose ethers are also polysaccharides belonging to the cellulose family [66]. Based on the previous research and the present literature, the most common types of cellulose ethers used in mortars are known to be hydroxyethoxy methoxy cellulose (HEMC) and hydroxypropoxy methoxy cellulose (HPMC) [66].

In an experimental study, Brumaud et al. examined the effect of different HEMC and HPMC additives on the properties of cement paste. In order to understand the impact of

such cellulosic derivatives on the flow behavior of cementitious systems, a typical rheological assessment was carried out [66]. In their investigation, Brumaud et al. utilized a stress-controlled rheometer which was equipped with a Vane geometry (containing 4 blades) [66]. The scientific team involved in this study identified that cellulose ethers slow down the nucleation of calcium silicates. Furthermore, it was concluded that the presence of such cellulosic derivative, increases the yield stress of the cement paste compared to the reference mix (with no cellulosic derivative involved) [66].

Cellulose ethers (CE) are able to enhance the fresh properties of cementitious systems such as workability and water retention [67]. Patural et al. investigated the impact of CE on the rheological behavior of cement-based mortars [67]. It is believed that cellulose derivatives are ideal additives to enhance the workability of fresh cementitious systems [68]. However, according to the current literature, one of the main drawbacks of utilizing cellulosic derivatives is the cement hydration delay caused by them [58, 69, 70]. Based on the experimental study performed by Pourchez et al. in 2006, the cement hydration delay caused by CE molecules are reliant on the chemical structure of the molecule itself and also on the dosage of the cellulosic additive used in the mix design [71, 72]. Ferraris and Martys [73] claim that the rheological properties of fresh concrete are linked to the cement hydration and also the chemical interactions in the cementitious system.

In their experimental study, Patural et al. measured rheological parameters of their cementitious samples using a rheometer equipped with vane geometry [67]. Vane geometry has been proved to be adequate and suitable for characterizing cementitious systems [74]. In order to evaluate the rheological properties of the tested cementitious system, Patural et al. applied a pre-selected shear rate and measured the resulting shear stress [67]. For

mixtures with a high water-to-cement ratio, Patural et al. utilized a helical geometry to prevent the impact of bleed water on the outcome of the experiment [67]. For both sets of geometries employed in their experimental approach, Patural et al. selected a minimum gap size of approximately 5 mm. In the measuring technique applied by Patural et al. the cement-based mortar was placed into a cylindrical vessel (within the rheometer) at first. The cylinder was then rotated and the viscous resistance of the cement-based mortar generated a torque. The torque was then registered continuously and utilized in rheological calculations [67]. The researchers began their rheological measurements 5 minutes after the mixing process. The samples were initially pre-sheared prior to testing in order to create uniform conditions and minimize the effect of sedimentation. The studied shear rate was applied for 10 seconds prior to recording the corresponding shear stress generated [67].

Many scientists and researchers working on the rheological measurement of cementitious systems, such as Nehdi and Rahman [75] or Yahia and Khayat [76] have proved that the rheology of a cementitious system prepared, is a function of material composition and also experimental conditions. Depending on the criteria mentioned above, different models such as Bingham, Herschel-Bulkley, Casson or Power-law are utilized to express and compute the rheological parameters of cementitious systems [67].

In the study performed by Patural et al., different types of CE additives were added to cement-based mortars. Eventually, Patural and colleagues plotted shear stress vs shear rate of the tested specimens and concluded that the molecular weight of the CE additive employed, plays a crucial role in determining the rheological and fresh properties of cement-based mortars. According to the experimental findings, as the molecular weight was increased, the yield stress decreased, the consistency increased and the water retention

of the mix was enhanced [67]. Patural et al. also identified that the rheological properties of mortars are among the key characteristics controlling the water retention mechanisms [67].

Hoyos et al. investigated the effect of cellulose microcrystalline (MCC) on the properties and performance of cement based composites [77]. Since Nilsson and Sargenius [78] had already reported the influence of cellulose microfibrils on the rheological and mechanical behavior of cementitious systems (rheology enhancement and slight increase in strength), Hoyos and colleagues decided to explore the impact of cellulosic additives in a finer size and aspect ratio, thus MCC was utilized in their experimental study [77]. By performing a mini-slump test, Hoyos et al. identified a decrease in the spread diameter, when MCC was present in the mix design [77]. Using the spread diameter obtained from the mini slump test, they were able to calculate the yield stress based on the equation presented below:

$$\tau_0 = \frac{225 \cdot \rho g V^2}{128 \cdot \pi^2 R^5}$$

Where V is the tested samples volume and R is the spread diameter measured. According to the authors, the free –OH groups in MCC will result in an interaction between them and the hydration products through hydrogen bonds [77]. This was known to be a consequence of the hydrophilic nature of the cellulosic derivative utilized.

Another well-known cellulosic derivative utilized in the cement and concrete industry is cellulose nanofiber (CNF). Similar to cellulose nanocrystal (CNC) particles, cellulose nanofibers are also manufactured through acid hydrolysis [79]. CNF particles are also employed in oil well cement systems to enhance the overall behavior of the paste placed in the annular space between the ground formation and casing [79]. Sun et al. claim that

among various types of reinforcing agents available for oil well cement systems, cellulosic derivatives such as CNF demonstrate distinctive advantages due to their high modulus of elasticity, large aspect ratio and low coefficient of thermal expansion [80]. However, reinforcement is not the only reason such cellulosic nanomaterials are introduced to cementitious systems.

As stated and emphasized earlier in this report, the rheological properties of oil well cement systems are critical and play a significant role to ensure a successful cementing job [79]. Although, the rheological behavior of an oil well cement system is affected by different parameters such as water-to-cement ratio, Sun et al. claim that the presence of cellulosic additives such as CNF influences the flowability of the matrix noticeably. In an experimental study, Sun et al. prepared different specimens using oil well cement type H, cellulose nanofibers and graphene nano-platelets. Aside from an increase in the degree of hydration, Sun et al. reported an increase in the yield shear stress and also the viscosity of oil well cement pastes hosting cellulose nanofibers. However, the viscosity-shear rate plots illustrate lower viscosity at higher shear rate values [79].

## **2.2. Oscillatory Rheology and Dynamic Mechanical Properties**

### *2.2.1. Theory and Background*

Rheological characterization of materials is performed by utilizing different controlled methods such as steady shear method, stress relaxation method, oscillatory method, etc. Furthermore, the obtained results and findings are quantified and assessed using material functions such as viscosity, storage and loss modulus, creep, etc. [81]. These measurements

are generally used for two purposes: (1) to predict the behavior of cement mix flow, and (2) to understand the structure (or structure development) of the cement mix.

In this section, oscillatory shear rheology is described, which is also referred to as dynamic mechanical analysis (DMA) [82]. The most common technique used to study the rheological behavior of nonlinear viscoelastic materials is known to be the steady shear measurement technique. In this case, a steady stress response of the material is measured at different strain rates applied. Therefore, one is able to differentiate different types of behavior (such as shear thinning or shear thickening behavior). On the other hand, the most common technique employed to study the rheological behavior of a linear viscoelastic material is the oscillatory shear measurement [81, 83, 84].

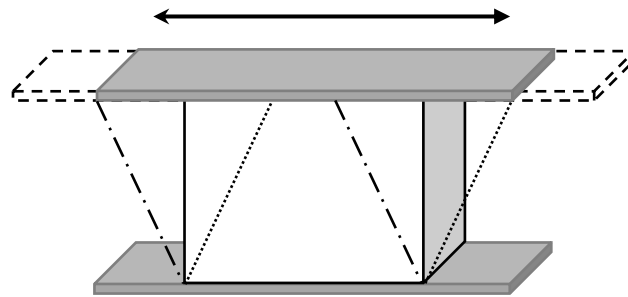


**Figure 2.1.** Two-plates model for oscillatory shear testing

Dynamic mechanical analysis of any (viscoelastic) material is examined by conducting a set of oscillatory tests. These tests or experiments are usually referred to as dynamic mechanical analysis [82]. Eisenschitz and Philippoff were the first people to introduce these set of measurements in 1933 [82]. However a few years later, different apparatuses were designed by scientists such as Roelig, Aleksandrov and Lazurkin [82] in order to carry out such measurements. These new apparatuses presented oscillatory mechanical forces by

combining a pre-stressed spring and an eccentrically rotating mass to investigate and evaluate the resulting deformation amplitude by an optical system [82, 85-87].

Nowadays, modern and well-designed rheometers are utilized to carry out such investigations. As mentioned by Mezger in the “Rheology Handbook”, these modern rheometers measure the torque and also the deflection angle is determined by an opto-electronic incremental position sensor [82]. In this study, parameters such as the storage modulus ( $G'$ ) and the loss modulus ( $G''$ ) associated with Type G oil well cement pastes, are investigated. Although these parameters are well and comprehensively defined in many textbooks and articles, they are briefly described below.

When a material undergoes a shear process and deforms, a deformation energy is stored in it. The storage modulus ( $G'$ ) of a material is basically a measure of the stored energy [82]. This energy is available after unloading the sample or the specimen and will unveil itself as a driving force in order to partially or completely compensate the deformation developed in the structure of the material. Hence, it may be concluded that the storage modulus ( $G'$ ) illustrates the elastic behavior of the material under examination and it is usually represented in Pa (as its unit) [82]. This parameter is associated with the stiffness of the material [82].

On the other hand, the loss modulus ( $G''$ ) of a material is a measure of the deformation energy used by the material (sample) during the shear process where the change in material's structure is occurring. It is understood that the loss modulus ( $G''$ ) represents the viscous behavior of a material [82]. Furthermore, if  $G' > G''$ , the material demonstrates a solid-like behavior, whereas if  $G' < G''$ , the material is believed to exhibit a liquid-like behavior [82, 88].

### 2.2.2. *Dynamic Mechanical Properties of Cementitious Systems*

Nachbaur studied the evolution of the rheological properties of cement pastes using dynamic mode rheology [88]. Majority of the rheological studies on cementitious systems are steady shear rheological assessments [43, 89], which only provide information about the workability and flowability of the cementitious system [88]. Nevertheless, steady shear rheology analysis does not deliver fundamental information regarding the evolution of the structure of the paste and the forces responsible for its associated mechanical properties [88]. Therefore, for such information, dynamic mode rheology (oscillatory rheology) is utilized as an ideal technique [88]. However, as stated by Schultz and Struble [90], dynamic mechanical analysis or oscillatory rheology would only be acceptable if it is performed in the linear viscoelastic domain of the material. Hence, the shear strain value selected for such measurements needs to be below the critical strain and in the linear region.

In an experimental study, Nachbaur et al. investigated the dynamic mechanical properties of two different systems: (1) silica-rich Portland cement and (2) pure tricalcium silicate [88]. In their study, measurements were made using a controlled strain rheometer. Therefore, samples were subjected to a sinusoidal strain and eventually, the resulting stress was recorded [88]. However, it is further explained that the samples are actually submitted to a sinusoidal angular displacement which will cause a torque. The resulted torque is then measured and classical rheological parameters are calculated from that [88]. Nachbaur and colleagues performed the experiment and recorded all the data at room temperature (25°C). In the test method employed by them, the first step was to conduct a strain sweep in which the samples were subjected to an increasing strain. The moduli are basically independent of the strain only at low strain values. However, this independence is only observed until

reaching the critical strain. This is known to be the end of the linear viscoelastic range or domain [88]. Therefore, strain sweep is generally performed in order to identify the linear viscoelastic range and also the associated critical strain value of the sample (material) being tested.

Furthermore, at the second stage of this experimental study, Nachbaur et al. performed the frequency sweep test [88]. The frequency sweep test was performed with an increasing or decreasing frequency in a strain value within the linear viscoelastic domain, which was less than the critical strain observed previously during the strain sweep test. Based on the reported results by Nachbaur et al. the critical strain of the tested samples were found to be approximately 0.03% (end of the linear viscoelastic domain). Hence, the dynamic mode measurements were conducted in strain values below 0.03% [88]. Finally, in the last stage of their dynamic mechanical analysis, Nachbaur et al. conducted a time sweep test on the prepared specimens. During the time sweep test, the samples are subjected to a strain with constant frequency and a magnitude below the critical strain, in order to study the evolution of the mechanical properties of the tested samples with respect to time [88].

According to the results and findings published by Nachbaur and colleagues, the evolution of both type of samples (cement and pure tricalcium silicate pastes), were found to be similar and interestingly, the water-to-cement ratio had no significant influence on the trend of the evolution [88]. Additionally, the authors claim that the main evolution of the structure of the cementitious systems prepared took place within the first few minutes after the mixing process [88]. This is further clarified by emphasizing the fact that the structure of the paste is formed within the very first minutes after the mixing, due to the spontaneous coagulation of the particles. The plotted results also showed that  $G' > G''$  in all of the

cementitious samples tested by Nachbaur et al. hence proving the solid-like behavior of the material [88]. Moreover, the critical strain value identified (end of the viscoelastic domain) was extremely small (0.03%) which indicated that the particles were held together by a powerful short-range force [88].

In 2007, Betioli et al. started to study the effect of hydroxymethyl ethylcellulose (HMEC) on the consolidation of cement pastes. Thus, dynamic mode rheology was performed (as a non-destructive measuring technique) using oscillatory rheometry in order to understand the influence of the above mentioned additive [91]. Betioli et al. utilized a parallel plate rheometer in their study and all the measurements were performed at 25°C [91]. Betioli and colleagues describe the dynamic mode rheology as a common test method to understand the properties of fresh cement pastes.

As explained by the scientific team involved, during a dynamic mode rheology test, small deformation ( $\gamma$ ) or in some cases low tension ( $\tau$ ) is applied to the material without causing rupture [91]. The ratio between tension and deformation is called complex modulus ( $G^*$ ) and it has two components: (1)  $G'$  (storage modulus), which is the elastic component, and (2)  $G''$  (loss modulus), which is the viscous component. Betioli et al. only investigated the elastic modulus ( $G'$ ), since the goal of their study was to analyze the influence of HMEC on the consolidation of cement pastes [91].

Betioli and colleagues also performed the measurements in the linear viscoelastic domain after identifying the critical strain value using the strain sweep curves, since  $G'$  does not rely on the applied deformation in this region [88, 90-94]. The authors found the critical strain to be approximately 0.01% [91]. Betioli et al. also estimated the yield stress value ( $\tau_y$ ) using the proposed equation by Chen and Zukoski [93]:

$$\tau_y = \gamma_c \cdot G'$$

Where  $G'$  is the storage modulus and  $\gamma_c$  is the critical strain value obtained from the strain sweep test [91]. According to the results reported, the addition of the cellulosic additive in this study (HMEC) led to an increase in the storage modulus ( $G'$ ). Additionally, the yield stress of cement samples containing HMEC was found to be slightly greater than the neat samples with no cellulosic additive [91]. Yongliang et al. also studied the dynamic mechanical properties of cement-asphalt binders, using oscillatory rheology [95]. Based on the reported results, an increase in the asphalt-to-cement ratio (A/C) led to a decrease in the dynamic modulus. Also, the authors concluded that the mechanical properties of such binders depend on temperature and loading rate. Furthermore, it was identified that the higher the A/C, the more reliant the mechanical properties are to temperature and loading rate [95].

In another experimental study, Zhang et al. analyzed the dynamic mechanical properties of low amount polymer-modified cement paste at the early age [96]. The polymer (additive) used in their study was ethylene-vinyl acetate copolymer (EVA). After performing the dynamic mechanical analysis (DMA) on neat and EVA-dosed cementitious samples, their storage modulus, loss modulus and loss tangent were compared. Zhang et al. clarify that the elastic properties of a cementitious system can be described by the storage modulus ( $G'$ ), which are relevant to the stiffness of the system [96].

Zhang et al. prepared different types of specimens for their experimental approach. Thus, aside from the neat samples (with no additive), a group of samples was prepared with 1% EVA (BWOC or mass fraction of cement), whereas the second and third group of samples contained 3% and 5% EVA, respectively. The water-to-cement ratio selected was 0.3 and

the EVA powder was added to the water initially [96]. They performed the dynamic mechanical analysis at a constant temperature ( $20 \pm 2^\circ\text{C}$ ) but at various frequencies [96]. The authors emphasize that the polymer-to-cement (P/C) ratio plays an important role in determining the dynamic mechanical properties of a cementitious system, however, since the polymer is the dispersed phase, therefore cement plays the dominant role in defining the dynamic mechanical properties of such polymer-modified cementitious systems [96].

According to the results published by Zhang et al. as the dosage of the EVA polymer increased (from 1% to 5%), the storage modulus decreased. In other words, the larger the value of P/C, the lower the storage modulus will be [96]. Nevertheless, the results verify the fact that in a certain specimen (with a certain EVA dosage), an increase in the storage modulus was observed when the frequency was increased gradually. Therefore, Zhang et al. concluded that an increase in frequency eventually increases the stiffness of the polymer-based cementitious system. They also identified that the storage modulus of a cementitious system (neat or dosed with EVA) is influenced by cement hydration. Evidently, it was witnessed that the greater the hydration, the larger the storage modulus value corresponding to the specimen will be [96].

Furthermore, Zhang and colleagues utilized the terms phase angle ( $\delta$ ) and loss tangent ( $\tan\delta$ ) to compare the cementitious samples. The phase angle ( $\delta$ ) determines the viscoelasticity of a material. According to Zhang et al. [96], a material with a larger value of phase angle shows more viscoelasticity. In dynamic mechanical analysis, loss tangent  $\tan\delta$  (sometimes referred to as loss or damping factor) is computed to reveal the ratio between the viscous and elastic portion of the viscoelastic deformation ( $\tan\delta = G''/G'$ ) [82]. The value of  $\tan\delta$  should be less than 1 for a viscoelastic gel or solid (such as cement paste)

which also verifies that  $G'$  (storage modulus)  $>$   $G''$  (loss modulus) [82]. Zhang et al. identified that with the presence of EVA polymer within the cementitious system, the loss tangent ( $\tan\delta$ ) decreased when the hydration increased [96].

### 3. DURABILITY CONCERNS

#### 3.1. Porosity and Pore Structure

##### 3.1.1. Theoretical Background

A fluid is able to undergo different transport mechanisms within concrete such as permeation, migration and diffusion. All of the named mechanisms are significantly influenced by the effective porosity of the concrete. The effective porosity may be defined as the degree of continuity of the pore system. In other words, transport of any fluid within concrete is highly related to the inherent micro-cracks and the interconnected pore network within the concrete core [97]. In mathematical terms, porosity can be written as [98]:

$$\varphi = \frac{V_p}{V_b}$$

Where

$\varphi$  = Porosity

$V_p$  = Pore volume

$V_b$  = Bulk volume

Based on the definition and the mathematical expression above, the porosity of a porous media (material) varies based on certain influencing factors. One of the most important factors is the particle or grain size of the material. A material with smaller particles will

demonstrate a lower porosity compared to the one with larger grains. Another well-known parameter affecting the porosity magnitude of a substance is the degree of cementation (also referred to as consolidation). As this increases, the porosity tends to decrease and a lower value is obtained. In any porous material, some pores are interconnected whereas some other are completely isolated. Therefore, this affects the measuring value of the porosity of a material. As a result, different porosity values may be obtained from one material, depending on which pore spaces have been analyzed. This phenomenon introduces two categories of porosity measurements: (1) Absolute or total porosity and (2) effective porosity. Absolute porosity is basically the ratio of the total void space to the bulk volume of the sample, as described above mathematically. Effective porosity, on the other hand, is influenced by many factors such as heterogeneity of grain sizes, packing of the grains, pore channels, etc. These factors should be taken into account while measuring effective porosity [98].

### *3.1.2. Porosity of Cementitious Systems*

It should be understood and highlighted that the porosity and the pore structure of a hydrated concrete specimen are different from that of a hydrated cement paste specimen. Since there is no aggregates included in an oil well cement paste, the porosity of the material is basically a function of the paste pore structure, whereas in concrete the aggregate-paste interface has a significant effect on the pore size distribution. This is mainly due to the fact that the aggregates have higher porosity and larger pores.

In a research conducted by Halamickova et al., the effect of pore structure on the transport properties (such as water permeability) of cement mortars were investigated. In their study, the pore structure of different mortars with different water-to-cement ratios was measured

using mercury intrusion porosimetry (MIP). [99] After determining the critical radius using the Katz-Thompson method (inflection point on the volume intrusion measured versus the radius curve), it was reported that higher pore sizes lead to higher degree of hydration. Based on the Katz-Thompson theory, the critical radius is the radius of the smallest pore (that are subsets of a larger pore) that can create a connected path through the sample [99].

Concrete is basically a heterogeneous and porous media. It has pores with different shapes and sizes which affect the physical properties of the concrete. Zhang investigated the effect of nanoparticle addition to concrete porosity and permeability. Based on the experimental work presented, it was understood that some nanoparticles refine the pore structure of concrete [100] whereas some other alter porosity without changing the pore size distribution significantly [100]. In another experimental study performed by Goto and Roy in 1981, the effect of water-to-cement ratio and curing temperature on permeability and pore size distribution of different cement pastes were investigated [101]. They came up with an equation to measure the porosity of their samples based on the weight of the dried samples.

$$\text{Porosity} = (\text{Weight of water saturated sample in air} - \text{Weight of vacuum-oven dried sample}) / (\text{Weight of water saturated sample in air} - \text{Weight of water saturated sample in water})$$

The pore size distribution of the samples was also evaluated using a mercury intrusion porosimetry. Their work demonstrated the fact that as the water-to-cement ratio of the cement paste sample increases, the porosity of it also increases, however, a decrease in the porosity was observed when the samples were cured in a higher temperature [101]. Page and colleagues also investigate the chloride penetration in cement pastes and relate their

results to the porosity of the specimens and their pore sizes. Based on the work published and presented by them, as the water-to-cement ratio (w/c) increases, the porosity increases, and also an increase in the penetration volume is observed [102].

In a research performed on cement paste in 2006, the nanoporosity of different samples was investigated by Jennings et al. by utilizing different techniques [103]. Based on the results, it was understood that the samples hydrated at 20°C produce a low density calcium-silicate-hydrate (C-S-H) gel structure whereas drying the samples in a higher temperature (60°C) will result in to a denser morphology with a fewer large gel pores and of course larger amount of capillary pores [103]. Similar to a large number of previous studies, Nyame and Illston utilized mercury intrusion porosimetry to evaluate and measure the porosity and surface area of the hardened cement paste samples. The hydraulic radius was computed as the ratio of the intrude pore volume and the surface area of the solid phases accessible to mercury at 200 N/mm<sup>2</sup> [104].

Another common technique utilized in the recent years to investigate the pore structure and pore size distribution of cementitious samples (concrete, mortar and cement paste), is image analysis of backscattered electron (BSE) images [105-107]. Basically, in this technique, the fraction of phases in cement paste (porosity, anhydrous cement content, etc.) is determined [105]. In an image analysis process, the segmentation algorithm should be precise and most importantly reproducible. Then only, such process and analysis may be qualified in order to perform a comparison, and also to formulate relationships. One of the initial and most important challenges in any image analysis is to define the grey level upper threshold.

In their experimental study, Wong and colleagues used image analysis to segment pores from a BSE image of a cementitious material. In the work presented by them, the grey level threshold was identified from the inflection point of the cumulative histogram of all the BSE images analyzed. Based on the results obtained, it was understood that the proposed technique or method was more consistent, and it needed a significantly fewer number of images. In their proposed methodology, a series of images from a single capillary pore with area segmented (white pixels) were obtained with different threshold levels.

As the threshold level increases the segmented area increases as well. Eventually, a sudden increase in the segmented area is observed which indicates the surrounding paste around the capillary pore. At the end, the total area segmented is plotted against the threshold level. Therefore, the selected threshold level will be the intersection of the two linear segments of the plotted curve. After determining the threshold, pores were separated (segmented) from the images using binary segmentation. Finally, the porosity of the material was obtained as the percentage of the segmented pore area to the total paste area [105-107].

### *3.1.3. Surface Area and Gas Sorption Technique*

In order to define the properties of any porous material, the associated surface area has to be analyzed and investigated [108]. The surface area could be obtained by the internal boundary in between the pores and the solid phase of the material under investigation. In materials with a disordered porous microstructure such as cement paste or concrete, understanding and evaluating the surface area will not only provide useful information about the fineness of the pores but also leads to a better understating of properties such as permeability, tortuosity of the pore structure, etc.

However, since cement paste has a complex microstructure (due to the presence of reaction products, unreacted cement particles, etc.), measurement of the corresponding surface area is associated with some difficulties. Nowadays, the surface area of a hardened cement paste sample can be measured by different techniques, which may minimize these difficulties to some extent. One of these difficulties is due to the heterogeneous microstructure of cement paste, containing pores in a wide range. These pores have been previously classified by Mindess and Young (presented below), in terms of their size and the property which can be affected by them [109].

**Table 2.4.** Classification of pores within cement, by Mindess and Young [109]

<b>Designation</b>	<b>Diameter</b>	<b>Description</b>	<b>Properties affected</b>
Capillary pores	> 50 nm	Large capillaries	Strength, permeability
	10 – 50 nm	Medium capillaries	Strength, permeability, Shrinkage (high RH)
Gel pores	2.5 – 10 nm	Small (gel) capillaries	Shrinkage (to 50% RH)
	0.5 – 2.5 nm	Micropores	Shrinkage, creep
	< 0.5 nm	Interlayers	Shrinkage, creep

As stated in Table 2.4, there is an overlap in size range and the affected property.

There are different techniques to measure the surface area of the cement paste and also to investigate the pore structure associated with it [108]. Depending on the feature in mind, one can utilize one of the common methods and study the pore structure of the sample. For instance, the Mercury Intrusion Porosimetry (MIP) method, highlights the larger pores and it cannot be employed to measure the surface in the finest pores. Nevertheless, MIP still

remains as one of the most common techniques for engineers to study cement pore structure. Based on the size classification introduced by Mindess and Young, the larger pores will be very effective in altering the mechanical properties of a cementitious sample, as well as the associated permeability [108].

One of the main challenges in investigating and measuring the surface area of a cement paste sample is determining the boundary between the solid phase and the pores. Basically, the total surface area of a cement sample is determined by the surface area of the C-S-H gel, since it contains the majority of the fine pores (gel pores) [108]. The C-S-H gel which is mostly amorphous is a reaction product forming as a result of the hydration of alite and belite. The C-S-H gel has an extremely high surface area (although it varies a lot) compared to the surface area of unhydrated cement powder or admixtures such as silica fume [110]. As stated by Thomas et al. this challenge becomes even harder since the C-S-H gel contains chemically bound water aside from the water within the gel pores.

Therefore, since defining the correct boundary is not easy, some methods or techniques might under-estimate the surface area whereas some other methods might report a much higher surface area [108].

The most common technique for measuring the surface area is referred to as “gas sorption”, which is also the technique with the most published results. As explored and explained by Gregg and Sing [111] and also by Rarick et al. [112], in the gas sorption technique a monolayer of gas molecules will be adsorbed on to the internal surface area of the material (such as a hardened cement sample). Furthermore, the surface area can be computed according to the equation below [108]:

$$S = \frac{N_m \sigma}{m}$$

Where  $S$  represents the surface area,  $N_m$  is the number of gas molecules in one monolayer,  $\sigma$  stands for the cross-sectional area of a single gas molecule, and  $m$  is the mass of the specimen under investigation. When analyzing a cement specimen, the technique can only be implemented correctly if the sample is pretreated. This pretreatment is associated with the removal of water from the gel pores within the C-S-H gel structure. Furthermore, the gas will be introduced to the specimen and the change in the pressure or the sample weight is recorded and plotted to obtain a sorption isotherm.

In most experiments, desorption isotherm is also recorded in order to observe any possible hysteresis effect. Eventually, based on the obtained isotherm, the amount of gas required to fill in one monolayer of gas onto the specimen is measured, hence the surface area will be evaluated. The most accurate procedure to obtain an isotherm in such experimental analysis is the volumetric method where the gas is introduced into a known volume, then the specimen is transferred to a chamber in order to equilibrate. Finally, the specimen will be isolated and the adsorbed gas will be computed [108].

Another important factor which needs to be taken into consideration is the heat of adsorption of the sportive gas [108]. If the heat of adsorption is high, it means that the gas molecules have formed a monolayer onto the specimen surface, prior to starting the next layer of molecules. Whereas, if the heat of adsorption is low, new molecules have been placed on top of a partially formed layer of molecules (the monolayer is not complete). This is also known as the piling effect. In such a scenario, the specimen being tested has pores with an entrance smaller than the pore radius. These pores will be filled completely

with the gas molecules, but during desorption, it will be very difficult to empty them. Therefore, the hysteresis effect will be observed [108].

The most common method to analyze the sorption isotherm has been derived by Brunauer, Emmet and Teller, referred to as the BET method [113]. In the BET method, it is assumed that the heat of adsorption is constant throughout the formation of the first monolayer, and the heat of adsorption of the next layers will be equal to the heat of condensation of the bulk. Therefore, according to the BET method, one can calculate the surface area based on the relationship between the relative pressure of the gas, and the volume adsorbed per unit specimen mass. The standard BET equation is [108, 113]:

$$\frac{P_{rel}}{V(1-P_{rel})} = \frac{1}{V_m C_{BET}} + \frac{P_{rel}(C_{BET}-1)}{V_m C_{BET}}$$

In this equation,  $P_{rel}$  ( $= P/P_0$ ) is the pressure of the gas in equilibrium with the specimen ( $P$ ), relative to the saturation vapor pressure ( $P_0$ ).  $V$  demonstrated the amount of gas adsorbed at pressure  $P$ , whereas  $V_m$  is the quantity of gas required to form a monolayer. In the BET equation,  $C_{BET}$  is a constant [108, 113].

The BET method has been widely employed in the cement industry in order to measure the surface area of a cementitious sample. As stated earlier there are difficulties in measuring surface area with gas sorption methods. The pores need to be empty of any remaining water. Therefore, the sample has to be dried prior to measuring. This drying process, may alter the C-S-H structure of the cement paste and provide a very different surface area. Different techniques have been proposed for the drying process of cement paste such as oven-drying, vacuum drying [112], D-drying [114] or P-drying [115]. The surface area of

cement paste could be measured by sorption of either water vapor or nitrogen. However, the results will be completely different [108].

According to previous experimental measurements, the surface area of a cementitious sample measured with water vapor is approximately  $200 \text{ m}^2/\text{g}$  of dry cementitious paste [116-118], whereas the surface area measured by nitrogen is much lower [112]. Nowadays, nitrogen is used more than water vapor in BET analysis. Based on the book by Taylor, nitrogen provides surface area measurement as low as  $10 \text{ m}^2/\text{g}$  of dry cementitious paste [14] which is quite different from the measurements obtained with water vapor. Also, surface area measurements using water vapor is not very much dependent to the water-to-cement ratio, whereas if the measurement is executed using nitrogen, the surface area will increase with water-to-cement ratio increasing [119]. It is also understood that the surface area of a cementitious sample will change with age and cement type [108].

In 1998 Thomas et al. [120] measured the effect of water-to-cement ratio on different types of cement powders in order to observe the development of surface area over the initial 3 days of hydration. Different techniques were utilized in their research proposal including neutron scattering and nitrogen adsorption (BET). In the associated report published by them [120], all of the employed techniques demonstrated an increase in the surface area when water-to-cement ratio had increased. In the experimental work conducted, the development of the surface area was monitored at  $30^\circ\text{C}$ . The surface area was seen to develop rapidly in the first 24 hours with heat evolution. However, it gradually leveled off after the first 3 days of investigation, confirming that the further heat evolution was due to the reaction taking place within the cementitious system [120].

Since the solid/pore surface is almost completely formed within the calcium-silicate-hydrate gel, Thomas et al. concluded that two different morphologies of the calcium-silicate-hydrate (C-S-H) gel were present in the cement paste [120]. Their theory stated that there is a high surface area C-S-H gel which occupies the available pores within the first days of hydration, also referred to as the “outer-product”. On the other hand, another C-S-H gel was identified with a lower surface area that predominates at later stages, referred to as “inner-product”. The theory was proved to be accurate after the microscopy studies performed. According to the results published, there was a dramatic increase in the surface area after the first 10 hours, leveling off gradually during the third day [120].

During the past decade, various types of nanomaterials have been employed in cementitious systems, in order to alter the pore structure of the matrix [121, 122]. This would then lead to production or development of high performance and more durable cementitious systems [121, 122]. Among these novel nanoparticles, nanosilica has attracted a significant attention due to its corresponding behavior. Due to the filling effect (to reduce porosity) observed and also the pozzolanic reaction taking place, silica fume has always been considered as an important admixture in the cement industry. Nowadays, nanosilica – which is a siliceous material with a finer particle size and higher purity – is widely utilized to achieve the desired performance in a cementitious system [121].

By introducing nanosilica in Portland cement, Shih et al. [121] investigated the microstructural properties of their cementitious composites. In their experimental study, the surface area of the samples was measured by nitrogen adsorption according to the Brunauer-Emmett-Teller (BET) method. The results indicated that the cementitious samples containing nanosilica had a denser microstructure when compared to the reference

samples (without nanosilica). Consequently, a significant increase in the compressive strength was also observed when nanosilica was incorporated [121].

After investigating the pore structure of the samples using Mercury Intrusion Porosimetry (MIP), Shih et al. also realized that in the regions with pores smaller than 10 nm, pore volume increases by adding nanosilica, whereas the opposite was witnessed for regions with pores larger than 10 nm [121]. However, the accumulated pore volume was reduced when nanosilica was introduced. In this study, cementitious samples containing nanosilica were demonstrating an overall denser microstructure, but in the regions with pores smaller than 10 nm, a looser microstructure was established [121]. Nevertheless, results showed a drop in the total pore volume when nanosilica was added to the mix design. Also, a shift in the pore size distribution was observed, towards finer pore sizes, although not dramatically. These outcomes justified the above findings corresponding to strength gain (due to nanosilica), hence having a more consolidated microstructure was guaranteed when nanosilica was present in the mix [121].

Juenger and Jennings discussed the nitrogen adsorption technique in their published experimental work [123]. In the study performed on cement paste, they investigated the effect of different factors on the surface area measurement using the BET method. They also recognized that variables such as water-to-cement ratio, drying method, age, curing temperature, and presence of admixtures such as calcium chloride will eventually change the measured surface area [123]. In their experimental study, nitrogen was utilized as the adsorption gas. In the technical paper presented by them in 2001, samples that had been oven-dried had the lowest surface area [123]. On the other hand, the obtained results clearly

showed an increase in surface area, with increasing the water-to-cement ratio. These results were in the same trend of the ones presented by Mikhail et al. [117, 119] in the 60s.

According to the concluding remarks of the experimental studies performed by Juenger and Jennings, measuring the surface area of cement paste samples with nitrogen adsorption is extremely dependent to the preparation (mixing, curing, drying, etc.) regime [123]. Therefore, researchers with an intention of measuring porosity using this method need to stay consistent throughout their sample preparation and experimental methods. Also, it was mentioned by them, that the surface area measured using this technique is basically measuring the C-S-H gel's surface area, not the entire surface. Therefore, this method may be used to compare different C-S-H microstructures in different cementitious samples [123].

The data in the literature regarding the effect of curing temperature on the nitrogen surface area are quite different. These results do not follow a single trend. For instance, Blaine and Valis investigate the effect of curing temperature on cement samples and interestingly, find no effect until the age of 84 days [123, 124]. On the other hand, Alunno-Rosetti et al. described an inverse relationship between the curing temperature and the surface area measured [125].

Juenger and Jennings [123] however, identified no influence from the curing temperature on the total pore volume measured by nitrogen but concluded that a change in the pore size distribution was witnessed when the curing temperature was altered. Verbeck and Helmuth [123, 126] also developed a theory insisting that the low temperature curing increases the cement paste surface area. In 2003 Odler describes the factors which may alter the BET surface area results [127]. According to the experimental work conducted and the results

obtained, it was understood that nitrogen adsorption provides different surface area compared to water vapor adsorption. Odler justifies this fact as a consequence of nitrogen's ability to penetrate pores with narrow entrances, known as the ink-bottle pores [127].

### 3.2. Permeability

#### 3.2.1. Theoretical Background

The permeability of a material (porous media) is very dependent on the effective porosity of the material [98]. This means that all the parameters such as grain (particle) size and shape, grain size distribution, cementation and consolidation degree, and interconnectivity of the pores affect the permeability of the material. Similar to porosity, the permeability of a sample can also be mathematically evaluated. Darcy's equation has been employed for decades, in order to compute the permeability value of a core sample [98]. The differential form of this equation is expressed as:

$$v = \frac{q}{A_c} = -\frac{k}{\mu} \frac{dp}{dl}$$

Where

$v$  = Fluid velocity (cm/s)

$q$  = Flow rate (cm<sup>3</sup>/s)

$A_c$  = Cross-sectional area of the core sample (cm<sup>2</sup>)

$k$  = Permeability of the porous media (Darcy, 0.986923 μm<sup>2</sup>)

$\mu$  = Viscosity of the fluid (centipoises)

$l$  = Length of the core sample (cm)

$$\frac{dp}{dl} = \text{Pressure gradient in the direction of the flow (atm/cm)}$$

The expression above can be re-arranged and integrated (with respect to the length of the sample) in order to measure  $k$  such as:

$$k = \frac{q\mu L}{(p_1 - p_2) A_c}$$

Figure 2.2 below demonstrates a schematic diagram of the flow in associate with Darcy's equation [98].

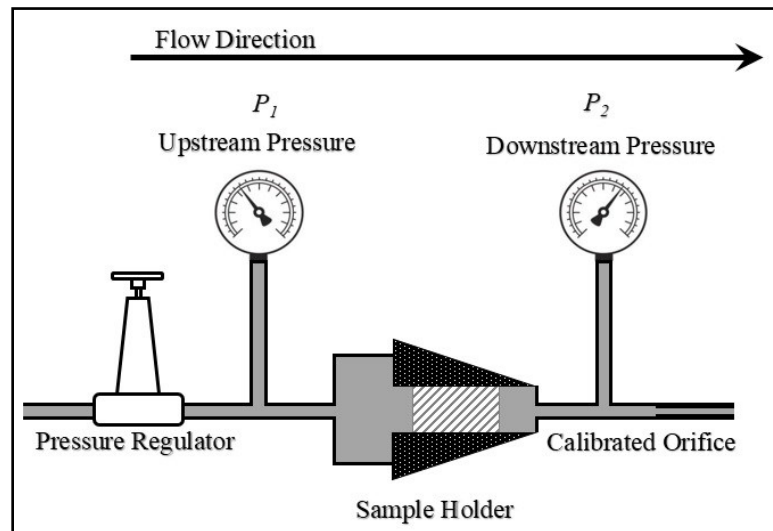


**Figure 2.2.** Schematic diagram of a permeameter [98]

As illustrated in the figure, a pressure gradient between the two ends of the sample allows the liquid to flow through the sample with a specified flow rate. Note that as described in equation 2, the viscosity of the fluid, the length of the core sample and its cross sectional area are also important. The value obtained for permeability ( $k$ ) is basically referring to the effective permeability, unless the porous material is fully saturated with a single liquid or

phase, in that case, it will be describing the absolute permeability. Parameters such as grain (particle) size and shape influence and alter the permeability of a porous media [98].

### *3.2.2. Permeability of Cementitious Systems*

The permeability of a concrete or cementitious sample can be defined as the ease with which liquids, gases and other aggressive ions penetrate the sample. As mentioned by Zhang [100], a higher permeability leads to a greater penetration of aggressive fluids or even water into concrete, which will eventually cause damage and deterioration. Therefore, a concrete with a lower permeability is basically accepted as a more durable concrete. It is also understood that permeability is a function of pore size distribution, thus it is directly influenced by the porosity of the material [128]. Zhang categorizes the main factors which affect the permeability of concrete as: (1) factors influencing the original pore structure of the concrete such as the water-to-cement ratio, (2) factors affecting the development of pore structure of concrete such as age and the curing condition, and (3) factors related to the penetration such as the hydration rate and the chemical composition of the penetration media [100].

While Figg believed [129] that the strength of a concrete sample is indirectly demonstrating the samples durability, he measured the air and water permeability of concrete in an experimental study in order to explain and assess the durability of concrete better. In his proposed methodology and apparatus, Figg drilled a hole inside the concrete specimen and plugged it with a catalyzed liquid silicone rubber to achieve a perfect seal. A hypodermic needle is then pushed through the plugged rubber in a manner which bore of the needle is free and not blocked. A fine plastic cannula is cut to a length such that it passes through the needle described above and touches the bottom of the cavity within the whole. A

syringe filled with water has also been attached to the other end of the apparatus, while there is an adaptor in the middle of the assembly to connect the syringe and the hypodermic needle. There is a third connection to the adapter and that is a glass capillary tube. In order to measure the water permeability of a concrete sample using the apparatus developed by Figg, the water is forced inside the cavity using the syringe attached to the apparatus [129].

A minute after, a water meniscus is brought to a suitable position along the capillary tube and the stopcock attached to the syringe is closed. The time consumed for the meniscus to travel 50 mm is regarded as a measure of the water permeability of the concrete sample. Based on the results obtained by Figg [129], using his developed apparatus, he concluded that the higher the water-to-cement ratio, the higher the permeability of the concrete sample. Also, it was observed that the moisture content of the specimen at the time of the experiment in the permeable samples with higher water-to-cement ratios was less effective compared to the impermeable samples (with a lower permeability). Figg believed that this is mainly due to the fact that the sample with higher water-to-cement ratio has a larger number of capillary channels [129].

In order to measure the water permeability of cement paste samples, Goto and Roy utilized a simple apparatus which was initially developed by White et al. in 1979 [101]. The apparatus had a pressure tank piped to a container. The container itself had a driving piston inside to press down the ionized water on top of the cement sample at the bottom of the container. Thus, when the pressure was released, the piston would press the water towards the sample, and after passing through the sample and a porous plate, the permeated water was collected inside a cylinder. After performing the permeability test, the results presented by Goto and Roy showed that water permeability of cement paste samples increases as the

water-to-cement ratio increases. However, it was observed that the samples cured in a high temperature (60°C) had a higher permeability compared to the ones cured in a lower temperature (27°C). Also, they concluded that pores with a larger radius have a very important effect on the permeability of hard cementitious samples [101].

In 1995, the (water) permeability of cement mortar samples was assessed by Halamickova et al., using a permeability cell [99]. This permeability cell was able to monitor both inflow and outflow in calibrated cylinders, as well as measuring the driving pressure. Each measurement was made in a duration between 200-300 hours, so it was regarded as a time consuming apparatus and system. The outcome of the research indicated that the higher permeability was corresponding to a lower degree of hydration. This was the same trend observed in the porosity assessment of the samples with regards to the degree of hydration (i.e. the higher porosity corresponding to a lower degree of hydration). In their research, the Katz-Thomson relationship was utilized to estimate the porosity, diffusion coefficient and also the permeability of the samples. However, it was concluded that the Katz-Thomson theory [99] overestimates the permeability at  $w/c = 0.5$  and significantly overestimates the permeability at  $w/c = 0.4$  systems.

Some studies related to the permeability of cement paste or concrete, are associated with chloride ingress or diffusion into the concrete or hardened cement paste [130]. As Andrade measures the chloride diffusion coefficient in concrete, insists that the penetration of chloride through concrete is one of the important elements and factors that deteriorates the steel reinforcement inside the concrete. However, in the field of well cementing and in analyzing oil well cement pastes, this factor could result in damaging the casing of the well [130]. According to many studies performed in the past, it is understood that the water

permeability of a cementitious system is lower than its gas permeability. Loosveldt et al. illustrated that this difference may be up to 1 or 2 order of magnitude [131]. They believed that this difference could be explained by phenomena such as rehydration or water adsorption in the thinnest pores [131].

According to the previous experimental studies, researchers have concluded that the permeability of a cementitious system may be influenced by some other factors such as hydraulic radius, the rate of hydration, and also the flow regime [104]. In their experimental study, Nyame and Illston emphasize on the fact that hydraulic radius, porosity and surface area are non-uniquely related to permeability. In fact, for a given age, the measured surface area (by mercury intrusion porosimetry) increases with permeability. The same trend was observed while comparing the hydraulic radius of hardened cement paste samples to the permeability of that [104].

Elsewhere, in a study on water permeability of cement paste, Bantia and Mindess concluded that by increasing the rate of hydration or the curing time, a decrease in the permeability coefficient will be observed [132]. Hosseini and colleagues also investigated the permeability of concrete while stressed and unstressed. They concluded that, evaluating the permeability of concrete is based on achieving an equilibrium in fluid flow. This is mainly due to the fact that Darcy's law (which is used to determine the coefficient of permeability), assumes a slow, unidirectional and steady flow [97].

### **3.3. Mechanical Properties and Strength Development**

#### *3.3.1. Significance*

As stated earlier, when investigating the durability of an oil well cement sheath, the failure associated with stress should be studied and examined efficiently. As elaborated and discussed by Goodwin and Crook in 1992 [8], the expansion of the casing will generally cause radial cracks within the cementitious sheath surrounding the casing. These cracks will eventually influence the oil well performance by decreasing the zonal isolation, especially in the bottom segment of the well (lower one-third or one-quarter of the well) [8]. In their experimental measurements, Goodwin and Crook studied different cementitious systems with different mix designs and compositions.

According to the results published, when pozzolanic materials (such as silica) were added to the mix design, the compressive strength of the cement sheath had enhanced noticeably [8]. Goodwin and Crook described the mechanism by emphasizing on the filler effect of silica [8]. Furthermore, in their investigation, it was concluded that, although the cement sheaths with higher compressive strength (which were more brittle) demonstrated a better support for the casing, their ability to seal the annulus in low internal casing pressure had decreased [8].

#### *3.3.2. Common Strength Enhancing Parameters and Agents*

In 2002, Heinold et al. studied the influence of a number of common additives on the mechanical properties of normal density oil well cement pastes [33]. The cement powder used in their study was the API class G cement, which is known to be one of the most common types of cement utilized in the oil well industry [1]. Heinold et al. tested samples

at two different temperatures ( $38^{\circ}\text{C} \approx 100^{\circ}\text{F}$  and  $93^{\circ}\text{C} \approx 200^{\circ}\text{F}$ ) with the following common additives (solids and polymers): Polyvinyl alcohol (PVA), silica fume (SF), metakaolin (HRM), wollastonite, hydroxyethyl cellulose (HEC), sodium metasilicate (SMS) and latex.

According to Heinold et al. all of the experimented samples were prepared and cured based on the API specifications for oil well cementing. In order to specifically understand the effect of the above mentioned additives on the mechanical properties of oil well cement pastes, the researchers excluded other additives such as retarders and dispersants which are typically used to enhance and optimize the slurry system in parameters and aspects other than mechanical properties [33].

The results published by Heinold et al. [33] demonstrated the effect of each individual additive on the mechanical performance of oil well cement paste. According to the results obtained, not all of the mentioned additives improved the flexural and tensile strength of the cementitious system with high density [33]. It was concluded that the additives utilized were capable of enhancing the mechanical properties, mainly in cementitious systems with low or medium density [33]. In this study, the researchers were also able to optimize the dosage for each individual additive employed.

Some additives demonstrated negative effects (decreasing the strength) after a certain amount of dosage, whereas some other illustrated enhancement with an increase in dosage. Another finding associated with this experimental approach was that some additives proved to be useful at a certain range of temperature. Results verified that when dealing with some of the additives, best results were obtained at lower temperatures, whereas in cases where the same type of additive was utilized at a higher temperature, it showed detrimental effects on the mechanical integrity of cement paste [33].

Heinold et al. explored the influence of the earlier mentioned common additives on compressive strength, tensile strength and flexural strength of cementitious systems at two different temperatures [33]. The first samples evaluated were dosed with polyvinyl alcohol referred to as PVA. In the PVA containing samples examined, there was no significant enhancement witnessed on the flexural strength when tested at 38°C ( $\approx$ 100°F), although when the dosage of PVA reached 1-2% (BWOC), a slight improvement was identified. However, when the same samples were tested at 93°C ( $\approx$ 200°F), improvement in flexural strength was observed only at PVA dosages of 0.5-1% (BWOC). PVA dosages above 1% resulted in a decrease in the flexural strength of the specimens, compared to the reference mix with no PVA additive [33].

Cement samples were also tested to understand the effect of PVA on the tensile strength of specimens. No matter what the testing temperature was, PVA showed no significant influence on the tensile behavior of oil well cement paste samples. Nevertheless, Heinold et al. witnessed a slight improvement when 1% PVA was used, compared to the reference mix [33]. The final PVA-dosed specimens were tested to identify an influence on the compressive strength of oil well cement pastes. Interestingly, the results verified that PVA had no significant impact on the compressive strength when samples were tested at 38°C ( $\approx$ 100°F), whereas the other specimens which were tested at 93°C ( $\approx$ 200°F), demonstrated a slight enhancement in compressive strength (compared to the reference mix with no PVA), at a dosage of 1% (BWOC). Furthermore, a PVA dosage of above 1% decreased the compressive strength noticeably [33].

The second batch of specimens tested by Heinold et al. was dosed with silica fume. This additive was utilized in two different dosages of 2.5% and 5% (BWOC), and samples were

compared to neat specimens with no additive. The flexural strength increased when 2.5% silica fume was employed (at 38°C ≈ 100°F), but it reduced when silica fume reached 5%. On the other hand, when specimens were tested at 93°C (≈200°F), silica fume decreased the flexural strength compared to the mix reference, no matter what the dosage was. Tensile strength also remained unchanged with silica fume, although slight increase and decrease were observed at 38°C (≈100°F) and 93°C (≈200°F), respectively, when silica fume dosage increased. This was again, not significant. Furthermore, the compressive strength of oil well cement specimens tested at 38°C (≈100°F) and 93°C (≈200°F) had all increased with silica fume, demonstrating best results when samples were tested at 93°C [33].

The impact of metakaolin was also examined in this study. Samples tested at 38°C (≈100°F) demonstrated an improvement in flexural strength, when the metakaolin dosage was above 5% (BWOC). However, the influence of metakaolin on the flexural strength of specimens tested at 93°C (≈200°F) was generally undesirable (reduction in strength). The same unwanted effect was witnessed on the tensile behavior of samples tested at both temperatures with all demonstrating a lower tensile strength compared to the reference specimens. Nonetheless, an enhancement in compressive strength was identified when metakaolin was added. Heinold et al. witnessed improvements in compressive strength, especially when metakaolin was employed in the dosage of 10-15% at 38°C (≈100°F) and 5% at 93°C (≈200°F) [33].

Wollastonite was also utilized as an additive in the experimental study performed by Heinold et al. in 2002 [33]. Wollastonite is known to be a white calcium-silicate powder and it is typically referred to as natural fiber [33]. Wollastonite has been used in oil well cement industry for different reasons such as improving permeability, compressive

strength development, sulfate resistance, etc. [33]. Heinold et al. investigated the influence of wollastonite along with other additives described earlier [33]. According to the outcome of the experiment, wollastonite improved flexural strength of oil well cement specimens (at both temperatures), only when used at a dosage above 5% (BWOC).

However, when assessing the tensile strength at 38°C ( $\approx 100^\circ\text{F}$ ) and 93°C ( $\approx 200^\circ\text{F}$ ), an incremental trend was witnessed even at lower dosages (5% and below). Furthermore, a dosage of only 5% (BWOC) of wollastonite, proved to be the optimum amount for achieving best compressive strength at both temperatures tested. Dosages of above 5% proved to reduce the compressive strength of oil well cement paste samples gradually. Nevertheless, wollastonite proved to enhance the compressive strength of neat samples at any dosage [33].

Another interesting additive analyzed in this study was hydroxyethyl cellulose (HEC). Being of the common additives derived from cellulose, HEC has been used in oil well cement industry to address the fluid loss issues [33]. Results achieved by Heinold et al. proved that HEC is most effective in a dosage of 0.5% (BWOC). Even though the influence of HEC on the flexural and tensile strength of oil well cement samples was not significant, but a noticeable increase in compressive strength was observed, especially with the samples tested at 93°C ( $\approx 200^\circ\text{F}$ ) [33].

A similar kind of impact was also observed when sodium metasilicate (SMS) was introduced to the mix design [33]. Although a reduction in the flexural strength (compared to the reference samples) was identified when SMS was employed at both temperatures in this study, an enhancement in the compressive strength was also witnessed, especially at a dosage of 0.75% (BWOC). SMS is generally used to develop low density systems. When

SMS is used alongside Portland cement, it will react with lime to produce calcium silicate gel and consequently improve the compressive strength development of the host mix [33, 4].

Heinold and colleagues also studied the effect of latex on the mechanical properties of oil well cement pastes [33]. In their experimental study, they utilized styrene butadiene latex which is a milky suspension with small spherical particles. This material is generally used in cementitious systems to improve their freeze-thaw resistance. Studies on this material revealed that it will also reduce the permeability of a cementitious system, improve the fluid loss and also enhance the cement-casing bond in oil well cement industry [4].

When Heinold et al. utilized latex in their cementitious samples, slight improvements were observed in the flexural, tensile and compressive strength of the specimens at 38°C ( $\approx 100^\circ\text{F}$ ). However, while investigating specimens which were tested at 93°C ( $\approx 200^\circ\text{F}$ ), it was found that latex improves flexural and tensile strength, but it will reduce the compressive strength of oil well cement specimens [33]. Heinold et al. also concluded (based on the results) that generally, latex would provide a better outcome when used at higher temperatures [33].

Among all additives utilized in cement industry, cellulosic derivatives have been employed widely for a number of features. In recent years, cellulose nanocrystal (CNC) particles have been used as additives in cementitious systems to enhance their mechanical properties such as strength development [133]. In 2015 Cao et al. published their article associated with the influence of cellulose nanocrystal on the performance of cement paste, specifically addressing hydration and strength of pastes dosed with CNC [133]. In their experimental study, the flexural strength of cement pastes dosed with CNC was evaluated at the ages of

3, 7, 21 and 28 days using a ball-on-three-ball flexural test. In their study, CNC was employed in a volume fraction of 0-1.5% (per volume of cement)

As explained earlier in this report, a ball-on-three-ball flexural test is generally selected because the test conditions generate a state of biaxial tensile state in the center of the specimen being tested. Cao et al claim that this test method is more sensitive to defects to all the in-plane directions of the specimen. For instance, the longitudinal cracks which are not likely to be distinguished in the 3-point or 4-point bending tests, are more likely to be identified in the ball-on-three-ball flexural test [133].

Cao and colleagues concluded that the presence of CNC within the mix design will eventually increase the flexural strength of the cement paste [133]. However, the ideal result was obtained when lower dosages of CNC were employed. The researchers involved discussed the fact that an increase in the quantity of CNC, would lead to an agglomeration of CNC particles. This was also in solid agreement with the rheological data. Cao et al. expand the mechanism of action by describing two possible scenarios [133]. The first scenario was believed to be the steric stabilization.

Steric stabilization would lead to a higher degree of hydration in cementitious samples dosed with CNC. However, when these samples were compared to samples dosed with water reducing admixtures (WRA), Cao et al. realized that the steric stabilization could be one of the possible mechanisms of action, but not the only one. Hence, a second scenario was possible to occur simultaneously. Cao and colleagues described the second scenario as a diffusion process in which the trapped CNC particles within the high-density layer of C-S-H around the cement particles would open a path to transport water towards the unhydrated cement grains. They described this process as the short circuit diffusion [133].

Later in 2016, Cao et al. investigated the effect of CNC dispersion on the strength of cementitious systems [134]. For this matter, two different types of samples were prepared and compared with the reference neat specimens (with no CNC): (1) samples with raw CNC and (2) samples with sonicated CNC. According to the findings, the samples containing sonicated CNC particles demonstrated higher strength compared to the samples with raw CNC. On the other hand, another interesting discovery was that, when CNC's were sonicated, even at higher dosages, an increase in strength was observed. Previous experiments [133] revealed that at higher dosages, CNC particles will agglomerate. Therefore, Cao et al. concluded that sonication of the CNC particles could be a possible solution in order to utilize cellulose nanocrystal in a higher dosage, to its complete potential [134].

## **4. CELLULOSE AND CELLULOSIC DERIVATIVES**

### **4.1. Cellulosic Nanomaterials**

#### *4.1.1. Structure of Cellulose*

Moon et al. [135] describe cellulose as a chain of ringed glucose molecules in which the repeat unit consists two anhydroglucose rings [135]. Studies have revealed that the inter-chain hydrogen bonding turns cellulose into a stable polymer and consequently the cellulose fibrils demonstrate a high axial stiffness [135]. Therefore, cellulose fibrils are basically the main reinforcing agents within plants, trees and marine creatures [135]. Furthermore, these cellulose fibrils have segments with chains that are arranged in an order, commonly known as crystalline segments, and also segments with chains which are not arranged in order, referred to as amorphous regions [136]. In recent years, the cellulose

fibrils have been processed and the crystalline regions have been extracted after treatment, leading to the production of cellulose nanocrystals [135].

Basically, cellulose can be extracted from different sources. On the other hand, the hydrolysis treatment to obtain cellulose nanocrystals also influences the final product. Different types of acid hydrolysis processes have been described and explored in this report. Regarding the cellulosic source, different materials have been explored in previous studies [135] such as wood, plant, tunicate, algae and bacteria. If the selected cellulosic source is wood, the extraction procedure begins with purified wood. A purified wood is a wood with the majority of the hemicellulose, lignin and other impurities removed from it [135]. Sometimes, plant fibers are used to produce cellulose nanocrystals. In such cases, the impurities also need to be removed in the same fashion as woods. Plants are known to be a primary source of cellulose nanocrystals mainly because they are abundant. Researchers have studied different types of plants in order to obtain cellulose nanocrystals. Some of the well-known plant materials utilized for this procedure are cottons<sup>1</sup> [137-141]. As stated above, in order to produce cellulose nanocrystals, the cellulose particles should get separated and isolated from the cellulose source material. Moon et al. describe this process in two stages [135]. During the first stage, the cellulosic source material should be purified so that it can react consistently to the treatments. This purification treatment depends on both, the cellulose source and also on the desired morphology for the second stage of treatment [135]. Note that there are different types of purification procedures, however, they have not been explored in this report, since they are beyond the scope of this study.

In the second stage of this process, the purified cellulose material will be separated into microfibrillar and crystalline components. Different approaches are utilized for this purpose. The most common techniques are known to be mechanical treatment [142, 143], acid hydrolysis [142, 143] and enzymatic hydrolysis [142, 143]. The mechanical treatment is usually employed to produce long cellulose fibrils referred as microfibrillated cellulose (MFC), whereas acid hydrolysis is a common technique to produce cellulose nanocrystal (CNC) particles.

#### *4.1.2. Different Types of Cellulose Nanoparticles*

There are different types of cellulose-based particles used globally, and they are generally referred to as cellulose nanoparticle (CN) [135]. This phrase has been assigned to a lot of cellulose-based particles with at least a single nanoscale dimension. The most commonly used cellulose nanoparticles are microcrystalline cellulose (MCC), microfibrillated cellulose (MFC), nanofibrillated cellulose (NFC or CNF), cellulose nanocrystal (CNC) particles and algae cellulose particles (AC) which are obtained from wood fibers (WF) or plant fibers (PF) [135]. These cellulose nanoparticles are mainly different in dimension, surface chemistry and percent crystallinity which could be a result of different factors such as their inherent properties and extraction processes.

MCC is generally employed in the pharmaceutical applications. It has a diameter ranging from 10  $\mu\text{m}$  to 50  $\mu\text{m}$  with a porous structure and they are commonly broken into micron sized rod shaped particles before being added to composites [135]. CNF is also a commonly used nanoparticle. It has a typical length of approximately 500-2000 nm with a width in the range of 4-20 nm, therefore they demonstrate a high aspect ratio [135]. CNC particles (which are the cellulosic nanoparticle utilized in this study) are rod shaped nanoparticles

finer than CNF. The associated aspect ratio of CNC is even higher than CNF with a typical length of 50-500 nm and a width of 3-5 nm. CNC particles are highly crystalline (54% - 88%) [135]. Studies show that if the hydrolysis treatment is not performed rightly, the amorphous region will not be removed completely, therefore, the crystallinity of the CNC produced will decrease and consequently, the morphology will change as well [135].

#### *4.1.3. Properties of Cellulose Nanoparticles*

Assessing and quantifying the mechanical properties of cellulose nanoparticles have always been a challenge for researchers. Due to their small particle size and the limited techniques available, the intrinsic mechanical properties of cellulose nanofibers are not well understood [135]. Also, the reported results of many different studies are quite different (for the same type of cellulose nanofiber). This difference could be due to several reasons such as particle size distribution, crystal structure, percent crystallinity, measuring techniques or methods, etc.

Therefore, it is of great importance to take all these influencing factors into consideration while studying a certain type of CN particle. Majority of the recent studies have concentrated on the elastic behavior of cellulose nanoparticles [135, 144, 145]. Among the studied cellulose nanoparticles, cellulose nanocrystal (CNC) particles have demonstrated the largest value for modulus of elasticity compared to other CN particles [135, 146]. This is basically justified by the percent crystallinity of the CNC particles compared to other CN particles.

Rheological assessments surrounding cellulose nanoparticles have been generally concerned with the gelation properties or liquid crystallinity [135]. Basically, studies and experimental measurements verify the fact that CNC suspensions in dilute regime

demonstrate a shear thinning behavior by increasing the dosage of CNC particles [135]. However, this concentration dependence is greater at lower shear rates. This behavior is a result of the alignment of rod-shaped CNC particles at critical shear rates. Therefore, an ease in flow is eventually obtained [147].

Rheological assessments have also taken place in the presence of CNF particles in suspension. Suspensions containing CNF particles have also shown a shear thinning behavior by increasing the shear rate. In such suspensions, it has been witnessed that the storage modulus will eventually become greater than the loss modulus, with only 0.5% of CNF (assuming wt %) [135]. Another resulting effect after adding cellulose nanoparticles to suspensions is the increase in the associated shear stress and yield stress values. Suspensions with CNC and CNF particles exhibit a rise in shear stress along with an increase in shear viscosity [135, 148].

Klemm et al. claim [149] that the reinforcing influence of nanocellulose particles – when incorporated in composites – depends on parameters such as volume fraction, spatial arrangement and morphology. Studies show that the performance of reinforcing agents rely on the stress transformation from the external source of energy to the reinforcing phase through the matrix [149]. This is basically related to the interface area between the matrix and the reinforcing agent. Therefore, fibers with a higher aspect ratio, sustain the mechanical energy better and distribute it more uniformly over the matrix, compared to shorter fibers [149]. However, these high aspect ratio fibers are more difficult to disperse into the matrix, therefore, the enhancement of the mechanical properties is usually limited [149].

Another key factor which needs to be taken into consideration is the percolation threshold. This percolation threshold is basically a function of distribution and orientation of rods (for instance CNC particles) and also their associated aspect ratio (length/diameter) [149]. Experimental studies show that an increase in the aspect ratio reduces the percolation threshold of the particles/fibers. Experimental measurements have verified the effect and influence of cellulose nanomaterial's length and size on their associated efficiency as a reinforcing agent [150, 151].

Studies show that MFC particles improve the mechanical properties of the host matrix significantly compared to shorter nanocrystal particles [150, 151]. Nevertheless, as stated earlier, the percolation threshold still plays a key role in obtaining optimal enhancement in systems containing cellulose nanoparticles. Studies confirm [152] that the percolation threshold for cellulose whiskers is approximately 1% (v/v) if the aspect ratio of the nanocellulose particle is about 100. Furthermore, if the content of the added nanocellulose particle is high, the matrix modulus will decrease due to the poor particle dispersion within the matrix [149].

## **4.2. Cellulose in Cement**

### *4.2.1. Application*

Cellulose fibers are now produced and utilized in most of the developing and developed countries [153]. As described earlier in this report, they are generally extracted from plants and woods. Due to their associated low density, availability, cost and morphology, they have been employed in different industries, including the cement and concrete industry [153-155]. Perhaps as mentioned in some previous experimental studies, the only drawback

associated with cellulose implementation in cementitious systems could be their durability in the cement matrix, as it is believed that the alkalinity of the matrix weakens the cellulose fibers in long term [156, 157].

Nowadays, scientists modify the surface of the cellulosic fiber in order to obtain better results in cementitious composites [153]. Tonoli et al. utilized two different methods of surface modification on cellulose fibers: (1) Methacryloxypropyltri-methoxysilane (MPTS) and (2) Aminopropyltri-ethoxysilane (APTS). As a result, they obtained a much more durable fiber-cement composite [153]. As described in their published report, the surface modification influenced the microstructure of the composite dramatically. Furthermore, the modulus of rupture (MOR) had also decreased along with the associated toughness of the composite [153].

With the development of cellulosic fibers commercially worldwide, the interest in utilizing such fibers in cementitious composites has increased [158]. This could be expressed as a consequence of being environmentally friendly [158]. Therefore, cellulosic fibers have found their way into the construction industry as reinforcing agents. Cellulose fibers extracted from wood (known as VF or WF) have been added to building materials since ancient times [158], however, the scientific concept of utilizing VF into cement matrix was developed in the 1940s [159]. These fibers were initially considered as replacements for asbestos fibers [159]. Furthermore, cementitious systems containing VF showed an improved toughness, flexural capacity, ductility and also crack resistance, compared to neat cement systems [160-162]. On the other hand, it was identified that these cellulosic fibers would reduce the free plastic shrinkage and also improve the acoustic performance [163, 164].

However, implementing VF has been limited since long term durability has always been an issue when dealing with cellulosic fibers in cement composites. The main reason would be the alkali attack towards the cellulosic fibers which will eventually weaken the fibers and increase the fiber fracture [158]. Nevertheless, cellulosic fibers are still used as reinforcing agents to reduce crack propagation and enhance the post-crack strength of cementitious composites [158]. Researchers have used cellulosic fiber strands as continuous reinforcement in cementitious composites.

Results published by Filho et al. demonstrate an improvement in the mechanical properties after the long cellulosic fibers were introduced to the system [165, 166]. In order to address the durability issues concerning cementitious composites containing cellulosic fibers, different approaches have been investigated by researchers and scientists. Basically, in order to enhance the durability of such systems, two main strategies have been explored. The first strategy is to alter the composition of the matrix in order to reduce the alkaline compounds. The second strategy is to modify the cellulosic fibers using chemical or physical treatments in order to improve their stability in cement's high-alkaline environment [158].

Scientists have reported two main treatments to reduce the portlandite content in the cementitious matrix: (1) adding pozzolanic compounds or (2) carbonation [158]. Many researchers such as Filho [162] and Mohr [167] investigated partial replacement of ordinary Portland cement with pozzolanic materials. A variety of supplementary cementitious materials such as silica fume (SF), ground granulated blast furnace slag (GGBS), different classes of fly ash (FA and CA) and metakaolin (MK) were utilized in

their experimental study. The published results verified the enhancement in the durability of cementitious composites containing both cellulosic fibers and pozzolanic materials.

As mentioned earlier, aside from employing pozzolanic materials in the matrix, accelerated carbonation is also considered as a method to increase the durability of cellulose-based cementitious composites. In their experimental study, Soroushian et al. [168] studied the durability of CO<sub>2</sub>-cured cement composites containing softwood kraft pulp. They realized that the carbonated samples contained less capillary pores and more CaCO<sub>3</sub> content. Also, the bonding of the fibers to the matrix had also been improved. Furthermore, the carbonated samples were examined and tested after diverse accelerated aging effects and exhibited an enhanced weathering resistance and longevity. Thus, Soroushian et al. concluded that the carbonation process had eventually improved the durability of cement composites reinforced with softwood kraft pulp [168].

As stated previously, the second strategy to improve the durability of cellulose-based cementitious composites is to modify the fibers, not the matrix (according to the first strategy described earlier). This is usually addressed with chemical or physical surface treatments in order to enhance the fiber-matrix adhesion and also reduce the sensitivity of the cellulosic fibers regarding the environment and composition associated with the matrix [158]. One of the easiest and cheapest approaches is known to be hornification of cellulose fibers, also referred to as refining the fibers [158]. Researchers have previously applied this method to improve the durability of cellulose-based cementitious composites [169, 170].

Ardanuy describes this hornification process as an irreversible effect on cellulosic fibers subjected to drying and re-wetting cycles [158]. Furthermore, it is understood that hornificated fibers demonstrate a lower water retention ability along with an enhanced

dimensional stability within the host matrix [158, 170]. However, it was later discovered that even though such designed composites were found to be more durable, the hornification process did not prevent partial loss of the mechanical reinforcement caused by cellulose fibers [158]. Nevertheless, modifying the surface of the cellulose nanoparticles still remains as one of the most common techniques utilized by researchers interested in cellulose-based composites, prior to adding them to the host matrix [158].

#### *4.2.2. Hydration of Cement in Presence of Cellulosic Derivatives*

While cellulose and cellulose derivatives are widely used in the cement industry, it is essential to understand the influence of the cellulosic particles on the hydration process of cement. Ridi et al. investigated the effect of cellulosic derivatives on all four phases constituting Portland cement [171]. Tricalcium silicate ( $C_3S$ ), dicalcium silicate ( $C_2S$ ), tricalcium aluminate ( $C_3A$ ) and tetracalcium iron aluminate ( $C_4AF$ ) phases were studied in order to observe the impact of methylhydroxyethyl cellulose (MHEC) during the hydration period. Basically, the calcium silicates ( $C_3S$  and  $C_2S$ ) produce the calcium hydrate silicate (C-S-H) gel, after reacting with water.

The C-S-H gel is an amorphous phase [171], however, the calcium silicate and water reaction also provide a crystalline product known as calcium hydroxide (CH). CH has a hexagonal structure and it is sometimes referred to as portlandite. The hydration reaction of  $C_3S$  takes place in the first month after casting the cement or concrete paste, while the hydration process of  $C_2S$  could take more than 1 year, since the reaction is slower. On the other hand, the hydration products of tricalcium aluminates and tricalcium iron aluminates are known to be cubic structures represented as  $C_3(AF)H_6$  [171].

Ridi et al. claim that when methylhydroxyethyl cellulose (MHEC) is added to the cement paste as an additive, it interacts with the water within the paste and the hydration process becomes more efficient [171]. In this scenario, it is understood that the cellulosic additive releases the water gradually towards the calcium silicates [171]. In their experimental study, Ridi et al. investigated the impact of cellulose on the hydration process by measuring the amount of unreacted water (also known as free water index) vs time, in the matrix, using a differential scanning calorimetry (DSC) method [172, 173].

The free water index (FWI) obtained for the cementitious pastes under study was plotted against the hydration time. These plots illustrated three major segments. During the first segment (period), FWI decreased gradually until reaching the initial time of acceleration period ( $t_i$ ). During the second segment, a dramatic drop was observed in FWI between  $t_i$  and  $t_d$  which indicates the beginning of the diffusion regime. This region would be associated with the nucleation and growth process during hydration of cement paste. Finally, the third segment starts after  $t_d$ , with a slight change in slope of the plot [171].

Interestingly, when the cellulosic additive was utilized, the sharp drop of FWI in between  $t_i$  and  $t_d$  was more dramatic and significant [171]. Ridi et al. realized that the FWI value corresponding to  $t_d$  was much lower in the case where cellulose was consumed. Also, it took longer (time) for the system to reach  $t_i$  and  $t_d$  with the presence of the cellulosic additive. Therefore, according to the FWI evolution, it was concluded that the presence of cellulosic additive would lead towards an increase in the water availability during the acceleration period of cement hydration. This was explained by Ridi et al. as a result of celluloses hydrophilic chemical structure [171]. Ridi et al. emphasize on the fact that in such a scenario there is no need for water to get diffused in order to reach the anhydrous

C<sub>3</sub>S because the hydrophilic cellulosic additive distributes it homogeneously over the paste. Thus, the water is available to hydration in a shorter period of time [171].

#### *4.2.3. Cellulosic Additives: From Fibers to Microcrystals*

In 2012, Hoyos et al. studied the effect of another cellulosic derivative known as cellulose microcrystalline (MCC) particles on the properties of cement composites [77]. MCC particles are utilized in different industries such as food, cosmetics and pharmaceutical. These crystalline cellulose derivatives are known for stabilizing aqueous suspensions, tuning the flow and also reinforcing the host matrix [77, 150, 174]. Hoyos et al. describe the MCC particles as additives with high water retention capability, which will eventually alter the hydration associated with the host cement matrix and its rheology [77].

Based on the obtained results and images, Hoyos et al. identified that the MCC particles link closely with the C-S-H, due to their hydrophilic nature and also their high water retention capacity [77]. The results are further explained by highlighting the interaction between MCC and the hydration products (C-S-H and CH). As elaborated in the literature, MCC particles are made of numerous chains of cellulose with three hydroxyl groups per anhydroglucose unit [175]. Therefore, the free –OH groups allow the MCC particles to interact with compounds having hydrogen atoms in their structure (C-S-H and CH in hydrated cement systems) [77]. According to Hoyos et al. the MCC particles utilized were 4 times larger than the C-S-H crystals [77].

When investigating the influence of MCC particles on the workability and flowability of cementitious composites, Hoyos et al. observed a reduction in the slump value, compared to the neat paste with no MCC [77]. According to the present literature, a fresh cement paste is basically made of many small suspended particles that are interacting with each

other. These interactions are caused and controlled by colloidal forces such as Van der Waals and electrostatic repulsion. In fact, the larger particles may also interact by direct contact (collision or friction). In order to break and interrupt these interactions, a stress is required. This stress is generally referred to as the yield stress ( $\tau_0$ ). The yield stress will eventually separate the particles and thus, the interactions will be terminated [176-179].

In their experimental procedure, Hoyos et al. also studied the effect of MCC particles on the yield stress value [77]. The MCC particles were found to interact with the hydration products, cement particles and also with water (through hydrogen bonds). Consequently, the yield stress value had increased significantly, compared to the neat systems with no MCC added. According to the results published in 2013, Hoyos et al. reported a slight decrease in density after MCC was introduced to the system. However, explained above, the major rheological findings of their study was the decrease in the slump value (mini slump spread diameter) and the increase in the yield stress value [77].

Hoyos et al. also identified that the addition of only 3 wt% of MCC to the cementitious system, delays the hydration reaction [77]. Furthermore, it was concluded that this cellulosic additive reduces the maximum adiabatic temperature. This reduction in maximum adiabatic temperature would be extremely important when large quantities of cement paste or concrete are used. The hydration reaction of cementitious systems generates heat and the temperature will consequently increase.

On one hand, this increase in temperature could cause expansion. On the other hand, if the heat generated is released (especially when released non-uniformly), internal stresses will be produced. Both of these scenarios will eventually cause cracks within the cementitious system. Hoyos et al. emphasize on the fact that if the maximum adiabatic temperature of a

cementitious system is reduced, the heat generated by the hydration reaction will also reduce significantly. Therefore, the reduction in maximum adiabatic temperature, caused by MCC particles will be positive, especially for large scale projects [77].

In cement and concrete industry, polysaccharides have been commonly used as suitable admixtures with a high water retention capability which will eventually delay the hydration reaction. Therefore a great number of researchers have investigated the effect of polysaccharide admixtures on the hydration of cement systems. It is understood that the absorption of polysaccharides on the surface of the unhydrated cement particles and CH crystals, forms a film on the cement particles. This film is known to be water-resistance.

Furthermore, some of the polysaccharides interact with pore water solution (or alkaline solution) and create insoluble derivatives. These derivatives will eventually gather around the unhydrated cement particles and form a protective layer around them, preventing further water ingress [69, 180-183]. Hoyos et al. claim that an approximately similar scenario occurs when MCC is added to the cement mix. Therefore, they conclude that the delay in cement hydration reaction is a consequence of MCC acting like the polysaccharide admixtures [77].

The mechanical properties of cementitious composites hosting MCC were also studied by Hoyos and colleagues [77]. According to the published report and the tabulated results, the addition of MCC particles initially decreased the modulus of elasticity (E) of the cementitious composite. Along with the flexural strength (although slightly). However, when thermal or accelerated curing procedures were utilized, the modulus of elasticity and flexural strength increased.

Hoyos et al. claim the reason behind this development, is the boost in the hydration degree. They have concluded that there will be more water released by the MCC particles and eventually more hydration products are obtained [77]. Furthermore, Hoyos et al. emphasize on the fact that if optimal results are to be witnessed when MCC is added, the curing regime is of great importance. Accelerated or thermal curing will eventually enhance the mechanical properties of MCC-dosed cementitious composites [77].

### **4.3. Cellulose Nanocrystal (CNC)**

#### *4.3.1. From Fibers and Microcrystals to Nanocrystals*

Cellulose is believed to be the most available renewable polymer resource present nowadays [184]. For approximately 150 years, cellulose has been used in different forms such as fibers or other derivatives, and it has been utilized in a wide range of products, materials and applications. However, it has only recently been discovered that when these cellulose fibers are subjected to acid hydrolysis, rod-shaped crystalline residues will be obtained. They are generally referred to as cellulose nanocrystal (CNC) particles. These biopolymeric assemblies have drawn significant attention towards themselves due to their ideal physical and chemical properties, and also because of their inherent renewability and sustainability. In fact, because of their low cost, abundance, light weight, nanoscale dimension and morphology, these nanocrystals have been employed in a wide range of research and studies as a reinforcing agent in nanocomposites [184].

The annual production of cellulose is estimated to be larger than  $7.5 \times 10^{10}$  tons [184]. This amount is basically distributed in plants, marine animals, algae, fungi and bacteria. Basically, this tough fibrous substance (water insoluble), is an important element in

maintaining the structure of a plant cell, initially discovered by Anselme Payen in 1838. No matter what the source is, cellulose is known to demonstrate a high molecular weight. Basically, cellulose is not available as an isolated individual molecule. In fact, cellulose is discovered to be present as assemblies of individual cellulose chain-forming fibers [184].

After being inspired by Nickerson and Habrle [185] who boiled cellulose fibers in acidic solutions in order to observe the degradation, Ranby claimed that colloidal suspension of cellulose is achievable by degrading cellulose fibers using sulfuric acid. In further research, it was identified that these suspensions contain needle shaped particles that have the same crystalline structure of the original cellulose fibers [186]. Later in 1950's, Battista implemented hydrochloric acid degradation on cellulose fibers derived from wood pulps, which led to the development of commercialized microcrystalline cellulose (MCC) [187, 188].

Because of stability, being chemically inactive, and demonstrating binding properties, MCC was soon utilized in pharmaceutical industries, food applications and also composite applications [184]. In 1959, Marchessault et al. optimized the acid hydrolysis settings and were able to develop colloidal suspensions of cellulose nanocrystals that demonstrated nematic liquid crystalline alignment. Furthermore, improvements in the mechanical properties of nanocomposites were observed after introducing cellulose nanocrystals, thus the amount of interest also increased [189, 190].

#### *4.3.2. Preparation of Cellulose Nanocrystals*

Acid hydrolysis is the main procedure utilized to separate cellulose nanocrystals from the cellulose fibers [184]. In this procedure, the disordered segments of cellulose are favorably hydrolyzed, but the crystalline regions demonstrate a higher resistance to this acid attack

and remain undamaged [191, 192]. Therefore, this acid treatment results in the removal of the microfibrils and rod shaped nanocrystals are produced.

Studies and experimental measurements reveal that the morphology and crystallinity of cellulose nanocrystals are the same as the original cellulose fibers [184]. Basically, the technique for production of cellulose nanocrystals requires subjecting the cellulosic material to strong acid hydrolysis under defined controlled conditions. The temperature, time, nature of the acid involved and acid-to-cellulosic fiber ratio are known to be the influencing factors or parameters affecting the preparation and final product. The obtained suspension is diluted with water, washed with centrifuges and then dialyzed with distilled water to remove the free acid molecules [184].

For the purpose of producing cellulose nanocrystals, different types of acids such as sulfuric acid, hydrochloric acid, phosphoric acid and hydrobromic acid have been tested by researchers around the world, however, the first two types remain the most common ones used [184]. Depending on the type of acid being used, the final cellulose nanocrystal product exhibits different properties. For instance, if the hydrolyzing agent used is hydrochloric acid, the cellulose nanocrystal prepared shows a limited ability to disperse. On the other hand, if the cellulosic source is subjected to sulfuric acid, the cellulose nanocrystal produced will demonstrate a higher dispersion ability.

This is mainly due to the fact that the sulfuric acid used reacts with the surface hydroxyl groups of cellulose and eventually lead to the production of charged surface sulfate esters that promote dispersion of CNC [184]. Another example could be the effect of the type of acid (hydrolyzing agent) used on the rheological properties of suspensions having CNC particles. Studies show that suspensions containing CNC's produced by sulfuric acid

hydrolysis demonstrate a viscosity which is not time-dependent, whereas suspensions having CNC's prepared by hydrochloric acid treatment show a thixotropic behavior at CNC concentrations above 0.5% (w/v) and anti-thixotropic behavior at CNC concentrations below 0.3% [193]. Another interesting scenario is when both sulfuric acid and hydrochloric acid have been used in the treatment process. In such a case, the morphology of the cellulose nanocrystal produced is different and the final product generated is not a rod shaped nanoparticle, but a spherical cellulose nanocrystal particle. These spherical CNC's contain less amount of sulfate groups on their surface and therefore show an improved thermal stability [194].

In the past decade, researchers decided to optimize the hydrolysis treatment process using a factorial design matrix. The parameters varied were the concentration of the cellulosic material which was microcrystalline cellulose in their experiment (MCC), the concentration of sulfuric acid, the hydrolysis time and temperature, and the ultrasonic treatment time [195-198]. The measured parameters were the median size of the cellulose particle and the associated reaction yield. Eventually, Bondenson et al. [195] revealed that if the concentration of the sulfuric acid is 63.5% (w/w) with a hydrolysis duration of 2 hours, the final product will be cellulose nanocrystals with a length of 200-400 nm and a width of less than 10 nm. It was also reported in this study that if the hydrolysis duration is increased, the length of the CNC particles produced will decrease.

#### *4.3.3. Morphology and Dimension of Cellulose Nanocrystal*

As stated earlier and mentioned in the literature, the geometrical dimension (length and width) of the cellulose nanocrystal produced depends on the preparation and treatment (hydrolysis) condition and also the nature of the cellulosic material utilized [184].

However, for a given source of cellulosic material, this variation in size could be minimized by performing filtration, differential centrifuges or ultracentrifugation [184]. Furthermore, the morphology of the final product could be investigated and studied using microscopy techniques such as TEM [199], light scattering techniques such as SANS [200], or polarized and depolarized dynamic light scattering techniques such as DLS and DDLS [201].

Nowadays, TEM is a common technique employed worldwide to assess the aggregation of CNC particles [184]. On the other hand, another well-known technique used widely to investigate the surface topography of cellulose nanocrystal particles is atomic force microscopy (AFM) [199, 202]. However, even though AFM provides the surface topography at length scales as low as angstrom level, it will demonstrate rounded cross section profiles where other shapes are expected [184].

#### *4.3.4. Properties of Cellulose Nanocrystal Based Composites*

Due to the nanoscale dimension of cellulose nanocrystal particles and their mechanical properties, they are widely used to enhance mechanical properties of other materials (composites) [184]. Research shows that the axial Young's modulus of cellulose nanocrystal is even greater than that of steel and quite in the same range of Kevlar [184].

The Young's modulus values mentioned in the literature for cellulose nanocrystal varies from 105 GPa to approximately 167.5 GPa, depending on the cellulosic source of CNC production [146, 184, 203, 204]. Favier et al. were the first group to implement cellulose nanocrystal as a reinforcing agent [189, 190]. According to the experimental study performed by them, a significant enhancement was observed in the mechanical properties

of the host material. Storage modulus was among the aspects that had been dramatically improved by introducing cellulose nanocrystal particles.

Habibi [184] claims that when cellulose nanocrystal is utilized to improve the mechanical properties of a host material, the mechanical properties are improved basically because of the dimensions of cellulose nanocrystals and the interaction between the host matrix and cellulose nanocrystal particles at the interface. Habibi insists that the aspect ratio or the dimensions of the cellulose nanocrystal particle used determines the percolation threshold value which will eventually alter the mechanical properties of the host material or composite [184]. Experimental results reveal that cellulose nanocrystals with a higher aspect ratio demonstrate the best reinforcing effect since a lower amount is required to witness percolation.

However, this is still reliant on the initial cellulosic source of CNC production [184]. This mechanical enhancement is basically originated because of the rigid network formed between cellulose nanocrystals attached by hydrogen bonds [184]. Furthermore, factors such as the nature of the host matrix and also the surface energy of CNC particles will affect the formation of this network and eventually alter the mechanical properties of the obtained composite.

Another interesting phenomenon witnessed is the tendency of CNC to reduce the elastic modulus of the final product (composite), if there is a significantly good compatibility between CNC particles and the host matrix. Studies show that this behavior is mainly due to the restricted movements of CNC particles. Hence, in such a scenario, CNC particles will interact with the host matrix rather than extending to themselves in order to form a

network [184]. For instance, this behavior is observed when CNC (extracted from cottonseed linters) is used to reinforce glycerol-plasticized starch [184, 205].

In other studies, while investigating the influence of cellulose nanocrystals on the thermal behavior of composites, researchers have identified that no matter what the host material or the cellulosic source of CNC is, the glass-rubber transition temperature,  $T_g$ , is not affected [150, 206]. However, there are a number of studies showing that the addition of cellulose nanocrystal particles as a filler could change  $T_g$ , especially in moisture sensitive host materials [207]. Habibi claims that this could be related to the powerful interaction between CNC particles and the host matrix [184].

#### **4.4. Cellulose Nanocrystal (CNC) Particles in Cementitious Systems**

##### *4.4.1. Application*

In recent years, cellulose nanocrystal particles have been introduced to cementitious systems [133, 134, 208]. However, in these experimental studies, CNC particles have been basically utilized as reinforcing agents to enhance the strength of a cementitious material. For instance, in their experimental approach, Cao et al. described cellulose nanocrystal (CNC) particles as an ideal reinforcing material for cementitious systems [133]. Based on the available knowledge in the literature, CNC was believed to demonstrate unique characteristics such as high aspect ratio, high elastic modulus, high strength, reactive surface and also a low density [133, 135].

Due to its small size and dimension, Cao et al. expected a great amount of interaction between cement particles and CNC particles, prior to performing the analysis. On the other hand, the inter-fiber spacing was also believed to be low, hence leading towards more

interaction between CNC and cement grains [133]. Since CNC particles were much smaller than previously used fibers in the cement industry, Cao et al. could not claim that the CNC particles would delay the crack propagation like other (larger) fibers, hence the mechanism of work and the CNC-cement particle interaction needed to be studied and investigated with a series of experimental measures. The first step was to understand the influence of CNC particles on the cement hydration reaction.

#### *4.4.2. Effect of CNC on the Degree of Hydration*

Cao et al. discovered an increase in the cumulative heat evolution (caused by cement hydration) when cellulose nanocrystal (CNC) is added to the cement paste, using isotherm calorimetry (IC) [133]. This cumulative heat evolution is directly related to the degree of hydration and also to the rate of hydration [133]. This means that the degree of hydration also increased when CNC was introduced to the cementitious system. However, this trend was not observed until 25 hours after mixing. Additionally, the total mass of the chemically bound water (CBW) was also measured using thermogravimetric analysis (TGA), in order to compare the degree of hydration between neat cement pastes and cement pastes dosed with CNC.

The results obtained by Cao et al. clearly demonstrated that the samples with CNC had a lower final weight compared to the reference mixes with no CNC. Therefore, Cao et al. concluded that more water had reacted with cement grains, in the presence of CNC particles within the mix [133]. The TGA results along with the IC results, verified the initial hypothesis made by Cao et al. regarding an improvement in the degree of hydration when CNC is present. It was further reported that by increasing the dosage of CNC, the degree of hydration would also increase [133].

#### 4.4.3. *Interaction between CNC and Cement Particles*

As stated earlier, it was essential to understand the CNC-cement particle interaction, in order to employ CNC as an additive in cementitious systems. Hence, Cao et al. performed a series of experiments to clarify and understand this interaction [133]. First, the water adsorption of CNC was assessed using an adsorption/desorption equipment. This assessment was executed in order to understand or anticipate the influence of CNC, on the designated water-to-cement ratio of the cementitious system in mind. The results obtained by Cao et al. showed that only 0.7% of the total water used in the experimental study was adsorbed by CNC. This was considered a negligible amount in cement or concrete mixing procedure, therefore Cao et al. concluded that any change in the rheological or fresh properties of cement paste dosed with CNC should not be associated with CNC's water adsorption ability [133].

Furthermore, Cao et al investigated the rheological properties of cement pastes with and without CNC in order to observe the effect of cellulose nanocrystal particles on parameters such as the yield stress and viscosity. The rheological results demonstrated that if the dosage of CNC used (as additive) is less than 0.3% (volume fraction of cement), the yield stress of the cement paste would be lower than that of a neat paste with no CNC added. However, as soon as the dosage increases (greater than 0.3%), the yield stress of the cement paste increases dramatically, compared to the neat mix [133]. This increase and decrease in the yield stress value with respect to the dosage of the CNC employed could be explained by at least two mechanisms which have been previously observed in cementitious systems. The decrease in the yield stress witnessed could be a result of the steric stabilization, which is also known as the controlling mechanism for water reducing admixtures [133, 209].

However, Cao et al. describe the increase in the yield stress value observed, as a possible result of the CNC agglomeration in the paste pore solution. In such a scenario, it is believed that CNC particles form a strong network that requires a greater amount of force to break them, or at least align them. Thus, an increase in the yield stress of the cement paste dosed with CNC is inevitable. Subsequently, according to the results presented by Cao et al. in 2015, when the dosage of the CNC added (to cement paste) is below 0.3%, steric stabilization is the controlling mechanism, whereas if the dosage is greater than 0.3%, particle agglomeration is the observed mechanism of action [133].

Cao et al. also investigated cement hydration of samples dosed with CNC, by monitoring the heat flow rate using isothermal calorimetry (IC) [133]. It is generally understood that if a non-reactive material is added to the mix design, it might get attached to the surface of the cement particles and perhaps prevent them from reacting with water. Water reducing admixtures are a clear example of this mechanism [109, 133]. Results obtained by Cao et al. verified the fact that by increasing the dosage of CNC, the heat flow rate decreased noticeably [133]. Cao et al. claim that the reference samples (with no CNC), reached the heat flow peak after approximately 12 hours, whereas for samples with only 1.5% CNC (volume fraction of cement), this was achieved after approximately 17 hours. Evidently, CNC's addition to the cementitious mix had retarded the hydration reaction [133].

Interestingly, the BSE-SEM and optical images taken from neat samples and samples with CNC, illustrated a significant difference between the two types of mixes, at the age of 7 days. In the samples with CNC, Cao et al. observed a ring (or shell) around the unhydrated cement grains. This was in fact, in complete agreement with the steric stabilization

mechanism discussed earlier. The concentration of CNC was seen to be higher around unhydrated cement particles, compared to the hydration products [133].

The cement-CNC particle interaction was further explored by Cao et al. to see whether steric stabilization is the only mechanism of action or not. Initially, the zeta potential of CNC and cement particles were compared in two different environments: (1) A neutral environment ( $\text{pH} = 7$ ) and (2) An alkaline environment with a  $\text{pH}$  similar to fresh cement paste ( $\text{pH} = 12.71$ ). The second environment was simulated and prepared using the composition defined by Rajabipour et al. [133, 210]. According to the results, Cao et al. realized that zeta potential of both CNC and cement particles were not noticeably altered by the change in environment ( $\text{pH}$ ) [133]. Knowing that the zeta potential of CNC was much greater than that of cement, Cao et al. concluded that the cement particles have a tendency to agglomerate, compared to CNC particles.

This was further clarified by Cao et al. by emphasizing on the fact that the CNC particles tend to adhere to the cement particle surfaces, instead of agglomerating [133]. This was again in solid agreement with the steric stabilization effect discussed earlier. However, this mechanism (steric stabilization) requires the CNC particles to disperse perfectly into the matrix and separate the cement particles from each other, but the zeta potentials had revealed that the attraction between cement particles is stronger than the one between cement and CNC, therefore, Cao et al. argued that the steric stabilization effect might not be the only mechanism of action within the cement matrix dosed with CNC particles [133]. To follow up, Cao et al. compared the samples which were dosed with CNC, to samples containing polycarboxylate- based WRA.

The effect of WRA on the degree of hydration is well known and it is believed that steric stabilization is the mechanism of action for such additives. After comparing the degree of hydration between samples having CNC and samples containing WRA, Cao et al. recognized a 4% increase in the degree of hydration, when 1% (volume fraction of cement) WRA was employed, whereas 1% (volume fraction of cement) CNC increased the degree of hydration by approximately 8% (twice the amount increased by WRA). They concluded that perhaps, steric stabilization is not the only mechanism of action in cement-CNC particle interaction scenario [133].

As described earlier, when investigating microscopic images, Cao et al. identified rings (shells) around the unhydrated cement grains, which were in fact, C-S-H layers with high a density [133]. It is claimed by them that the high density C-S-H shell slows the water diffusion rate in this case. However, the CNC present in this high density C-S-H layer would eventually open a path to transport water towards the unhydrated cement grains. Thus, cement samples dosed with CNC would ultimately establish a larger portion of hydrated cement particles, compared to the reference neat samples with no CNC [133].

Cao et al. name this mechanism as short-circuit-diffusion (SCD) [133]. Therefore, the higher degree of hydration (DOH) obtained and observed experimentally, in cementitious samples dosed with CNC, may be a consequence of two mechanisms: (1) steric stabilization and (2) short-circuit-diffusion (SCD). However, Cao et al. claim that SCD may only be possible when a critical concentration of CNC is present in the mix design, since for this mechanism of action to occur, it is essential to have CNC present in the high density C-S-H ring around the unhydrated cement particles [133].

#### 4.4.4. *Influence of CNC on the Microstructure and Strength*

CNC's effect on the flexural strength of cement paste samples was also investigated [133]. A ball-on-three-ball flexural test was performed. This experimental method was selected over the conventional flexural tests because it is found to be more sensitive to defects all over the in-plane directions (of the disk sample tests) [133, 211, 212]. Cao et al. clarify that this is basically possible due to the geometry and loading condition where a biaxial tensile state would occur in the center of the specimen [133].

Therefore, defects such as longitudinal cracks – which are less likely to be detected in traditional three point or four point bending tests – would be identified in this experimental method [133, 213]. In this section of the study, two different types of samples were prepared: (1) samples with WRA and (2) samples with CNC. The obtained results verified that the samples with CNC had shown a greater flexural strength at different ages compared to the samples with WRA. This was consistent with the degree of hydration plots reported in the earlier stages of their study (from isothermal calorimetry analysis), where CNC-dosed samples reflected a higher degree of hydration compared to samples containing WRA [133].

Later in 2016, Cao et al. decided to investigate the influence of dispersion factor of CNC in cementitious samples. Therefore, two different sets of samples were prepared. The first set was made using raw CNC particles (similar to their previous study [133]), whereas the second set of samples benefited from sonicated CNC particles [134, 208]. Sonication was performed for 30 minutes, in order to achieve a better CNC dispersion in the aqueous suspension [134, 208]. Cao et al. defined two types of CNC particles within the fresh cement paste: (1) aCNC which were adsorbed on the surface of the cement particles and

(2) fCNC which were the free CNC particles (not adsorbed on the cement grain surface) [208].

In their experimental study, Cao et al. realized that the sonication process did not change the quantity of aCNC particles. Furthermore, isothermal calorimetry analysis also verified that sonication did not change the hydration process, even though the CNC particles were dispersed better. Additionally, porosity reduction was observed in the presence of CNC, however, this reduction was larger when sonicated CNC was utilized in the cementitious mix. The pore size distribution study revealed that the sonicated CNC reduced porosity mainly at larger pore sizes (such as capillary pores) [208]. Different types of cellulose nanocrystal (CNC) particles are currently utilized in cementitious systems. Table 2.5 introduces a variety of these cellulosic nanomaterials along with their associated physical properties. The cellulose nanocrystal (CNC) particles used in this study are also described in the last row with an aspect ratio between 10-60.

**Table 2.5.** Different types of cellulose nanocrystal (CNC) particles

Source	Form	Average Length (nm)	Aspect Ratio
Wood pulp [214]	Aqueous suspension	93	13
Cotton fiber [214]	Aqueous suspension	127	14
Algae [214]	Aqueous suspension	966	46
Wood pulp [214]	Dry powder	90	12
Wood pulp [214]	Dry powder	85	11
Wood pulp (this study)	Dry powder	100-300	10-60

## REFERENCES

- [1] Shahriar, A. (2011). *Investigation on rheology of oil well cement slurries* (Doctoral dissertation, The University of Western Ontario).

- [2] Specification, A. P. I. (2010). 10A. *Cements and Materials for Well Cementing*.
- [3] Smith, D. K. (1989). *Cementing*. SPE Monograph Series. Society of Petroleum Engineers, Richardson, Texas.
- [4] Nelson, E. B. (Ed.). (1990). *Well cementing* (Vol. 28). Newnes.
- [5] Kumar, S., Singh, C. J., Singh, R. P., & Kachari, J. (2002, April). Microfine cement: special superfine Portland cement. In Proc., Seventh NCB International Seminar, New Delhi, India.
- [6] Orchard, D. F. (1962). *Concrete Technology, Vol. 1, Properties of Materials*. 358p.
- [7] Joshi, R. C., & Lohita, R. P. (1997). *Fly ash in concrete: production, properties and uses* (Vol. 2). CRC Press.
- [8] Goodwin, K. J., & Crook, R. J. (1992). Cement sheath stress failure. *SPE Drilling Engineering*, 7(04), 291-296.
- [9] Cooke Jr, C. E., Kluck, M. P., & Medrano, R. (1983). Field measurements of annular pressure and temperature during primary cementing. *Journal of Petroleum Technology*, 35(08), 1-429.
- [10] Carter, L. G. (1968). *Effect of bore-hole stresses on set cement* (Doctoral dissertation, University of Oklahoma).
- [11] Burkowsky, M., Ott, H. P., & Schillinger, H. (1981). Cemented pipe-in-pipe casing strings solve field problems. *World Oil*; (United States), 193(5).

- [12] Ravi, K., Bosma, M., & Gastebled, O. (2002, January). Improve the economics of oil and gas wells by reducing the risk of cement failure. In *IADC/SPE Drilling Conference*. Society of Petroleum Engineers.
- [13] Zhang, J., Weissinger, E. A., Peethamparan, S., & Scherer, G. W. (2010). Early hydration and setting of oil well cement. *Cement and Concrete research*, *40*(7), 1023-1033.
- [14] Taylor, H. F. (1997). *Cement chemistry*. Thomas Telford.
- [15] Parrott, L. J., Geiker, M., Gutteridge, W. A., & Killoh, D. (1990). Monitoring Portland cement hydration: comparison of methods. *Cement and Concrete Research*, *20*(6), 919-926.
- [16] Sant, G., Dehadrai, M., Bentz, D., Lura, P., Ferraris, C. F., Bullard, J. W., & Weiss, J. (2009). Detecting the fluid-to-solid transition in cement pastes. *Concrete international*, *31*(06), 53-58.
- [17] Jupe, A. C., Wilkinson, A. P., Luke, K., & Funkhouser, G. P. (2005). Class H oil well cement hydration at elevated temperatures in the presence of retarding agents: an in situ high-energy X-ray diffraction study. *Industrial & engineering chemistry research*, *44*(15), 5579-5584.
- [18] Vidick, B., Fletcher, P., & Michaux, M. (1989). Evolution at early hydration times of the chemical composition of liquid phase of oil-well cement pastes with and without additives Part II. Cement pastes containing additives. *Cement and Concrete Research*, *19*(4), 567-578.

- [19] Jupe, A. C., Wilkinson, A. P., Luke, K., & Funkhouser, G. P. (2007). Slurry Consistency and In Situ Synchrotron X-Ray Diffraction during the Early Hydration of Portland Cements with Calcium Chloride. *Journal of the American Ceramic Society*, 90(8), 2595-2602.
- [20] Justnes, H., Van Loo, D., Reyniers, B., Skalle, P., Sveen, J., & Sellevold, E. J. (1995). Chemical shrinkage of oil well cement slurries. *Advances in cement research*, 7(26), 85-90.
- [21] Justnes, H., Skalle, P., Sveen, J., & Øye, B. A. (1995). Porosity of oil well cement slurries during setting. *Advances in Cement Research*, 7(25), 5-12.
- [22] Vlachou, P. V., & Piau, J. M. (1997). The influence of the shear field on the microstructural and chemical evolution of an oil well cement slurry and its rheometric impact. *Cement and Concrete Research*, 27(6), 869-881.
- [23] Zhang, J., Xu, M., Yan, Z., & Gao, L. (2008). Hydration and hardening of Class G oilwell cement with and without silica sands under high temperatures. *J Chin Ceram Soc*, 36(7), 935-941.
- [24] Backe, K. R., Skalle, P., Lile, O. B., Lyomov, S. K., Justnes, H., & Sveen, J. (1998). Shrinkage of oil well cement slurries. *Journal of Canadian Petroleum Technology*, 37(09).
- [25] Ramachandran, V. S. (1996). *Concrete admixtures handbook: properties, science and technology*. William Andrew.

- [26] Bentz, D. P., Coveney, P. V., Garboczi, E. J., Kleyn, M. F., & Stutzman, P. E. (1994). Cellular automaton simulations of cement hydration and microstructure development. *Modelling and Simulation in Materials Science and Engineering*, 2(4), 783.
- [27] Bermudez, M. (2007, January). Effect of sugar on the thickening time of cement slurries. In *SPE Annual Technical Conference and Exhibition*. Society of Petroleum Engineers.
- [28] Broni-Bediako, E., Joel, O. F., & Ofori-Sarpong, G. (2016). Oil Well Cement Additives: A Review of the Common Types. *Oil & Gas Research*, 2, 112.
- [29] Magarini, P., Lanzetta, C., Galletta, A. (1999) Drilling Design Manual Eni-Agip Division 97-107.
- [30] API, R. (2005). 10B-2. *recommended practice for testing well cements*.
- [31] Bett, E. K. (2011). Geothermal well cementing, materials and placement techniques.
- [32] Cowan, K. M., & Eoff, L. (1993, January). Surfactants: additives to improve the performance properties of cements. In *SPE International Symposium on Oilfield Chemistry*. Society of Petroleum Engineers.
- [33] Heinold, T., Dillenbeck, R. L., & Rogers, M. J. (2002, January). The effect of key cement additives on the mechanical properties of normal density oil and gas well cement systems. In *SPE Asia Pacific Oil and Gas Conference and Exhibition*. Society of Petroleum Engineers.
- [34] Salim, P., & Amani, M. (2013). Special considerations in cementing high pressure high temperature wells. *International Journal of Engineering*, 1(4), 2305-8269.

- [35] Mueller, D. T., & Bray, W. S. (1993, January). Characterization of surfactant-enhanced cement fluid-loss additives. In *SPE Production Operations Symposium*. Society of Petroleum Engineers.
- [36] Adams, N., & Charrier, T. (1985) *Drilling Engineering: A Complete Well Planning Approach* Penn Well Publishing Company. Tulsa Oklahoma USA 297-303.
- [37] Wilson, M. A., & Sabins, F. L. (1988). A laboratory investigation of cementing horizontal wells. *SPE drilling engineering*, 3(03), 275-280.
- [38] Bach, D., & Vijn, P. (2002, January). Environmentally Acceptable Cement Fluid Loss Additive. In *SPE International Conference on Health, Safety and Environment in Oil and Gas Exploration and Production*. Society of Petroleum Engineers.
- [39] Shuker, M. T., Memon, K. R., Tunio, S. Q., & Memon, M. K. (2014). Laboratory investigation on performance of cement using different additives schemes to improve early age compressive strength. *Research Journal of Applied Sciences, Engineering and Technology*, 7(11), 2298-2305.
- [40] Slagle, K. A., & Carter, L. G. (1959, January). Gilsonite-A Unique Additive for Oil-well Cements. In *Drilling and Production Practice*. American Petroleum Institute.
- [41] Davis, N. I., & Tooman, C. E. (1989). New laboratory tests evaluate the effectiveness of gilsonite resin as a borehole stabilizer. *SPE drilling engineering*, 4(01), 47-56.
- [42] Tattersall, G. H. (2003). *Workability and quality control of concrete*. CRC Press.
- [43] Tattersall, G. H., & Banfill, P. F. (1983). *The rheology of fresh concrete* (Vol. 759). London: Pitman.

- [44] Beaupre, D. (1994). *Rheology of high performance shotcrete* (Doctoral dissertation, University of British Columbia).
- [45] Laskar, A. I., & Talukdar, S. (2008). Rheological behavior of high performance concrete with mineral admixtures and their blending. *Construction and Building materials*, 22(12), 2345-2354.
- [46] De Larrard, F., Hu, C., Sedran, T., Sztikar, J. C., Joly, M., Claux, F., & Derkx, F. (1997). A new rheometer for soft-to-fluid fresh concrete. *Materials Journal*, 94(3), 234-243.
- [47] Ferraris, C., De Larrard, F., & Martys, N. (2001). Fresh concrete rheology: recent developments. *Materials Science of Concrete VI, Amer. Cer. Soc. Ed. S. Mindess, J. Skalny*, 215-241.
- [48] Ferraris, C. F. (1999). Measurement of the rheological properties of high performance concrete: state of the art report. *Journal of research of the national institute of standards and technology*, 104(5), 461.
- [49] Hanehara, S., & Yamada, K. (1999). Interaction between cement and chemical admixture from the point of cement hydration, absorption behaviour of admixture, and paste rheology. *Cement and Concrete Research*, 29(8), 1159-1165.
- [50] Uchikawa, H., Uchida, S., Ogawa, K., & Hanehara, S. (1984). Influence of  $\text{CaSO}_4 \cdot 2\text{H}_2\text{O}$ ,  $\text{CaSO}_4 \cdot 12\text{H}_2\text{O}$  and  $\text{CaSO}_4$  on the initial hydration of clinker having different burning degree. *Cement and Concrete Research*, 14(5), 645-656.
- [51] Uchikawa, H., Ogawa, K., & Uchida, S. (1983). Effect of admixtures on the rheology of fly ash cement. In *JCA Proceedings of Cement & Concrete* (Vol. 37, pp. 53-56).

- [52] Uchikawa, H., Sawaki, D., & Hanehara, S. (1995). Influence of kind and added timing of organic admixture on the composition, structure and property of fresh cement paste. *Cement and Concrete Research*, 25(2), 353-364.
- [53] Kinoshita, M., Yamaguchi, S., Yamamoto, T., & Tomosawa, F. (1990). Chemical structure and performance of new type high-range water-reducing AE agent. In *JCA Proceedings of Cement & Concrete* (Vol. 44, pp. 222-227).
- [54] Matsuhisa, M., Yamada, K., Ishimori, M., & Kaneda, Y. (1998). Effects of cement character on the fluidity of cement paste added with beta-naphthalene sulfonate type or polycarboxylate type superplasticizers. *Proceedings of the Japan Concrete Institute*, 20(2), 67-72.
- [55] Ohno, A., & Yamamoto, T. (1997). Fluidity of various cement pastes added polycarboxylic acid type admixture. In *JCA Proceedings of Cement & Concrete* (Vol. 51, pp. 258-263).
- [56] Ghio, V. A., Monteiro, P. J., & Demsetz, L. A. (1994). The rheology of fresh cement paste containing polysaccharide gums. *Cement and concrete research*, 24(2), 243-249.
- [57] Poinot, T., Bartholin, M. C., Govin, A., & Grosseau, P. (2015). Influence of the polysaccharide addition method on the properties of fresh mortars. *Cement and Concrete Research*, 70, 50-59.
- [58] Khayat, K. H. (1998). Viscosity-enhancing admixtures for cement-based materials—an overview. *Cement and Concrete Composites*, 20(2-3), 171-188.
- [59] Khayat, K. H., & Yahia, A. (1997). Effect of welan gum-high-range water reducer combinations on rheology of cement grout. *Materials Journal*, 94(5), 365-372.

- [60] Rols, S., Ambroise, J., & Pera, J. (1999). Effects of different viscosity agents on the properties of self-leveling concrete. *Cement and Concrete Research*, 29(2), 261-266.
- [61] Lachemi, M., Hossain, K. M. A., Lambros, V., Nkinamubanzi, P. C., & Bouzoubaâ, N. (2004). Self-consolidating concrete incorporating new viscosity modifying admixtures. *Cement and Concrete Research*, 34(6), 917-926.
- [62] Paiva, H., Silva, L. M., Labrincha, J. A., & Ferreira, V. M. (2006). Effects of a water-retaining agent on the rheological behaviour of a single-coat render mortar. *Cement and Concrete Research*, 36(7), 1257-1262.
- [63] Sonebi, M. (2006). Rheological properties of grouts with viscosity modifying agents as diutan gum and welan gum incorporating pulverised fly ash. *Cement and Concrete Research*, 36(9), 1609-1618.
- [64] Leemann, A., & Winnefeld, F. (2007). The effect of viscosity modifying agents on mortar and concrete. *Cement and Concrete Composites*, 29(5), 341-349.
- [65] Cappellari, M., Daubresse, A., & Chaouche, M. (2013). Influence of organic thickening admixtures on the rheological properties of mortars: Relationship with water-retention. *Construction and Building Materials*, 38, 950-961.
- [66] Brumaud, C., Baumann, R., Schmitz, M., Radler, M., & Roussel, N. (2014). Cellulose ethers and yield stress of cement pastes. *Cement and concrete research*, 55, 14-21.
- [67] Patural, L., Marchal, P., Govin, A., Grosseau, P., Ruot, B., & Deves, O. (2011). Cellulose ethers influence on water retention and consistency in cement-based mortars. *Cement and Concrete Research*, 41(1), 46-55.

- [68] Bertrand, L., Maximilien, S., & Guyonnet, R. (2004, June). Wedge Splitting Test: a test to measure the polysaccharide influence on adhesion of mortar on its substrate. In *Proceedings of the 11th International Congress on Polymers in Concrete, Berlin, Germany* (pp. 569-576).
- [69] Peschard, A., Govin, A., Grosseau, P., Guilhot, B., & Guyonnet, R. (2004). Effect of polysaccharides on the hydration of cement paste at early ages. *Cement and Concrete Research*, 34(11), 2153-2158.
- [70] Ruot, B., Goto, T., & Pourchez, J. (2007). Some aspects of cellulose ethers and latexes influence on the properties of cement-based materials—examples of results obtained within the CEReM. *Proceedings of the VII SBTA (7 Simposio Brasileiro De Tecnologia Das Argamassas)*.
- [71] Pourchez, J., Peschard, A., Grosseau, P., Guyonnet, R., Guilhot, B., & Vallée, F. (2006). HPMC and HEMC influence on cement hydration. *Cement and Concrete Research*, 36(2), 288-294.
- [72] Pourchez, J., Grosseau, P., Guyonnet, R., & Ruot, B. (2006). HEC influence on cement hydration measured by conductometry. *Cement and Concrete Research*, 36(9), 1777-1780.
- [73] Ferraris, C. F., & Martys, N. S. (2003). Relating fresh concrete viscosity measurements from different rheometers. *Journal of research of the National Institute of Standards and Technology*, 108(3), 229.
- [74] Barnes, H. A., & Nguyen, Q. D. (2001). Rotating vane rheometry—a review. *Journal of Non-Newtonian Fluid Mechanics*, 98(1), 1-14.

- [75]Nehdi, M., & Rahman, M. A. (2004). Estimating rheological properties of cement pastes using various rheological models for different test geometry, gap and surface friction. *Cement and concrete research*, 34(11), 1993-2007.
- [76]Yahia, A., & Khayat, K. H. (2001). Analytical models for estimating yield stress of high-performance pseudoplastic grout. *Cement and Concrete Research*, 31(5), 731-738.
- [77]Hoyos, C. G., Cristia, E., & Vázquez, A. (2013). Effect of cellulose microcrystalline particles on properties of cement based composites. *Materials & Design*, 51, 810-818.
- [78]Nilsson, J., & Sargenius, P. (2011). Effect of microfibrillar cellulose on concrete equivalent mortar fresh and hardened properties.
- [79]Sun, X., Wu, Q., Zhang, J., Qing, Y., Wu, Y., & Lee, S. (2017). Rheology, curing temperature and mechanical performance of oil well cement: Combined effect of cellulose nanofibers and graphene nano-platelets. *Materials & Design*, 114, 92-101.
- [80]Sun, X., Wu, Q., Ren, S., & Lei, T. (2015). Comparison of highly transparent all-cellulose nanopaper prepared using sulfuric acid and TEMPO-mediated oxidation methods. *Cellulose*, 22(2), 1123-1133.
- [81]Deshpande, A. P., Krishnan, J. M., & Kumar, S. Rheology of complex fluids. 2010.
- [82]Mezger, T. G. (2006). *The rheology handbook: for users of rotational and oscillatory rheometers*. Vincentz Network GmbH & Co KG.
- [83]Barnes, H. A., Hutton, J. F., & Walters, K. (1989). *An introduction to rheology* (Vol. 3). Elsevier.

- [84] Larson, R. G. (1999). *The structure and rheology of complex fluids* (Vol. 150). New York: Oxford university press.
- [85] Malkin, A. Y., & Isayev, A. I. (2017). *Rheology: concepts, methods, and applications*. Elsevier.
- [86] Malkin, A. Y., Askadsky, A. A., Kovriga, V. V., & Chalykh, A. E. (1983). Experimental methods of polymer physics. *Measurement of mechanical properties, viscosity and diffusion* (Mir, Moscow, 1983).
- [87] Whorlow, R. (1980). Rheological techniques.
- [88] Nachbaur, L., Mutin, J. C., Nonat, A., & Choplin, L. (2001). Dynamic mode rheology of cement and tricalcium silicate pastes from mixing to setting. *Cement and Concrete Research*, 31(2), 183-192.
- [89] Shaughnessy, R., & Clark, P. E. (1988). The rheological behavior of fresh cement pastes. *Cement and Concrete Research*, 18(3), 327-341.
- [90] Schultz, M. A., & Struble, L. J. (1993). Use of oscillatory shear to study flow behavior of fresh cement paste. *Cement and Concrete Research*, 23(2), 273-282.
- [91] Betioli, A. M., Gleize, P. J. P., Silva, D. A., John, V. M., & Pileggi, R. G. (2009). Effect of HMEC on the consolidation of cement pastes: isothermal calorimetry versus oscillatory rheometry. *Cement and concrete Research*, 39(5), 440-445.
- [92] Nachbaur, L., Nonat, A., Mutin, J. C., & Choplin, L. (2000). Dynamic mode rheology of cement pastes. In *Proceedings of the 2 nd International RILEM Workshop on Hydration and Setting, RILEM publications* (pp. 281-293).

- [93] Schultz, M. A. (1991). *Rheological studies of fresh cement pastes* (Doctoral dissertation, University of Illinois at Urbana-Champaign).
- [94] Papo, A., & Caufin, B. (1991). A study of the hydration process of cement pastes by means of oscillatory rheological techniques. *Cement and concrete research*, 21(6), 1111-1117.
- [95] Yongliang, L., Xiangming, K., Yanrong, Z., & Peiyu, Y. (2012). Static and dynamic mechanical properties of cement-asphalt composites. *Journal of Materials in Civil Engineering*, 25(10), 1489-1497.
- [96] Zhang, Z., Wang, P., & Wu, J. (2012). Dynamic mechanical properties of EVA polymer-modified cement paste at early age. *Physics Procedia*, 25, 305-310.
- [97] Hoseini, M., Bindiganavile, V., & Banthia, N. (2009). The effect of mechanical stress on permeability of concrete: a review. *Cement and Concrete Composites*, 31(4), 213-220.
- [98] Tiab, D., & Donaldson, E. C. (2015). *Petrophysics: theory and practice of measuring reservoir rock and fluid transport properties*. Gulf professional publishing.
- [99] Halamickova, P., Detwiler, R. J., Bentz, D. P., & Garboczi, E. J. (1995). Water permeability and chloride ion diffusion in Portland cement mortars: relationship to sand content and critical pore diameter. *Cement and concrete research*, 25(4), 790-802.
- [100] Zhang, M. H., & Li, H. (2011). Pore structure and chloride permeability of concrete containing nano-particles for pavement. *Construction and Building Materials*, 25(2), 608-616.

- [101] Goto, S., & Roy, D. M. (1981). The effect of w/c ratio and curing temperature on the permeability of hardened cement paste. *Cement and Concrete Research*, 11(4), 575-579.
- [102] Page, C., Short, N. R., & El Tarras, A. (1981). Diffusion of chloride ions in hardened cement pastes. *Cement and concrete research*, 11(3), 395-406.
- [103] Jennings, H. M., Thomas, J. J., Gevrenov, J. S., Constantinides, G., & Ulm, F. J. (2007). A multi-technique investigation of the nanoporosity of cement paste. *Cement and Concrete Research*, 37(3), 329-336.
- [104] Nyame, B. K., & Illston, J. M. (1981). Relationships between permeability and pore structure of hardened cement paste. *Magazine of Concrete Research*, 33(116), 139-146.
- [105] Yang, R., & Buenfeld, N. R. (2001). Binary segmentation of aggregate in SEM image analysis of concrete. *Cement and Concrete Research*, 31(3), 437-441.
- [106] Wong, H. S., Head, M. K., & Buenfeld, N. R. (2006). Pore segmentation of cement-based materials from backscattered electron images. *Cement and Concrete Research*, 36(6), 1083-1090.
- [107] Wong, H. S., Buenfeld, N. R., & Head, M. K. (2006). Estimating transport properties of mortars using image analysis on backscattered electron images. *Cement and Concrete Research*, 36(8), 1556-1566.
- [108] Thomas, J. J., Jennings, H. M., & Allen, A. J. (1999). The surface area of hardened cement paste as measured by various techniques. *Concrete Science and Engineering*, 1(1), 45-64.

- [109] Mindess, S., Young, J. F., & Darwin, D. (2003). *Concrete*. Prentice Hall.
- [110] Mehta, P. K. (1986). *Concrete. Structure, properties and materials*.
- [111] Gregg, S. J., Sing, K. S. W., & Salzberg, H. W. (1967). Adsorption surface area and porosity. *Journal of the Electrochemical Society*, 114(11), 279C-279C.
- [112] Rarick, R. L., Bhatti, J. I., & Jennings, H. M. (1995). Surface area measurement using gas sorption: application to cement paste. *Material Science of Concrete IV, American Ceramic Society*, 1-41.
- [113] Brunauer, S., Emmett, P. H., & Teller, E. (1938). Adsorption of gases in multimolecular layers. *Journal of the American chemical society*, 60(2), 309-319.
- [114] Copeland, L. E., & Hayes, J. C. (1953). *The determination of non-evaporable water in hardened portland cement paste* (No. 47).
- [115] Copeland, L. E., & Bragg, R. H. (1954). The hydrates of magnesium perchlorate. *The Journal of Physical Chemistry*, 58(12), 1075-1077.
- [116] Powers, T. C., & Brownyard, T. L. (1946, September). Studies of the physical properties of hardened Portland cement paste. In *Journal Proceedings* (Vol. 43, No. 9, pp. 101-132).
- [117] Mikhail, R. S., Copeland, L. E., & Brunauer, S. (1964). Pore structures and surface areas of hardened Portland cement pastes by nitrogen adsorption. *Canadian Journal of Chemistry*, 42(2), 426-438.
- [118] Kalousek, G. L., Richard, J. O., Ziems, K. L., & Saxer, E. L. (1953, November). Relation of shrinkage to moisture content in concrete block. In *Journal Proceedings* (Vol. 50, No. 11, pp. 225-240).

- [119] Mikhail, R. S., & Selim, S. A. (1966). Adsorption of organic vapors in relation to the pore structure of hardened Portland cement pastes. *Highway Research Board Special Report*, (90).
- [120] Thomas, J. J., Jennings, H. M., & Allen, A. J. (1998). The surface area of cement paste as measured by neutron scattering: evidence for two CSH morphologies. *Cement and Concrete Research*, 28(6), 897-905.
- [121] Shih, J. Y., Chang, T. P., & Hsiao, T. C. (2006). Effect of nanosilica on characterization of Portland cement composite. *Materials Science and Engineering: A*, 424(1), 266-274.
- [122] Pitkethly, M. J. (2004). Nanomaterials—the driving force. *Materials today*, 7(12), 20-29.
- [123] Juenger, M. C. G., & Jennings, H. M. (2001). The use of nitrogen adsorption to assess the microstructure of cement paste. *Cement and Concrete Research*, 31(6), 883-892.
- [124] Blaine, R. L. (1949). Surface available to nitrogen in hardened Portland cements. *Journal of Research of the National Bureau of Standards Monograph*, 42(3), 257-267.
- [125] Alunno-Rossetti, V., Chiochio, G., & Collepardi, M. (1974). Low pressure steam hydration of tricalcium silicate. *Cement and Concrete Research*, 4(2), 279-288.
- [126] Verbeck, G. J. (1968). Structures and physical properties of cement paste, Invited Paper. In *5th International Symposium on the Chemistry of Cement, Tokyo* (pp. 1-32).
- [127] Odler, I. (2003). The BET-specific surface area of hydrated Portland cement and related materials. *Cement and Concrete Research*, 33(12), 2049-2056.

- [128] Živica, V. (1997). Relationship between pore structure and permeability of hardened cement mortars: on the choice of effective pore structure parameter. *Cement and Concrete Research*, 27(8), 1225-1235.
- [129] Figg, J. W. (1973). Methods of measuring the air and water permeability of concrete. *Magazine of Concrete Research*, 25(85), 213-219.
- [130] Andrade, C. (1993). Calculation of chloride diffusion coefficients in concrete from ionic migration measurements. *Cement and concrete research*, 23(3), 724-742.
- [131] Loosveldt, H., Lafhaj, Z., & Skoczylas, F. (2002). Experimental study of gas and liquid permeability of a mortar. *Cement and Concrete Research*, 32(9), 1357-1363.
- [132] Banthia, N., & Mindess, S. (1989). Water permeability of cement paste. *Cement and Concrete Research*, 19(5), 727-736.
- [133] Cao, Y., Zavatterri, P., Youngblood, J., Moon, R., & Weiss, J. (2015). The influence of cellulose nanocrystal additions on the performance of cement paste. *Cement and Concrete Composites*, 56, 73-83.
- [134] Cao, Y., Zavattieri, P., Youngblood, J., Moon, R., & Weiss, J. (2016). The relationship between cellulose nanocrystal dispersion and strength. *Construction and Building Materials*, 119, 71-79.
- [135] Moon, R. J., Martini, A., Nairn, J., Simonsen, J., & Youngblood, J. (2011). Cellulose nanomaterials review: structure, properties and nanocomposites. *Chemical Society Reviews*, 40(7), 3941-3994.
- [136] Nishiyama, Y. (2009). Structure and properties of the cellulose microfibril. *Journal of Wood Science*, 55(4), 241-249.

- [137] Elazzouzi-Hafraoui, S., Nishiyama, Y., Putaux, J. L., Heux, L., Dubreuil, F., & Rochas, C. (2007). The shape and size distribution of crystalline nanoparticles prepared by acid hydrolysis of native cellulose. *Biomacromolecules*, 9(1), 57-65.
- [138] Saito, T., Nishiyama, Y., Putaux, J. L., Vignon, M., & Isogai, A. (2006). Homogeneous suspensions of individualized microfibrils from TEMPO-catalyzed oxidation of native cellulose. *Biomacromolecules*, 7(6), 1687-1691.
- [139] Helbert, W., Cavaille, J. Y., & Dufresne, A. (1996). Thermoplastic nanocomposites filled with wheat straw cellulose whiskers. Part I: processing and mechanical behavior. *Polymer composites*, 17(4), 604-611.
- [140] Alemdar, A., & Sain, M. (2008). Isolation and characterization of nanofibers from agricultural residues—Wheat straw and soy hulls. *Bioresource technology*, 99(6), 1664-1671.
- [141] Zimmermann, T., Bordeanu, N., & Strub, E. (2010). Properties of nanofibrillated cellulose from different raw materials and its reinforcement potential. *Carbohydrate Polymers*, 79(4), 1086-1093.
- [142] Hubbe, M. A., Rojas, O. J., Lucia, L. A., & Sain, M. (2008). Cellulosic nanocomposites: a review. *BioResources*, 3(3), 929-980.
- [143] Siró, I., & Plackett, D. (2010). Microfibrillated cellulose and new nanocomposite materials: a review. *Cellulose*, 17(3), 459-494.
- [144] Lahiji, R. R., Xu, X., Reifenberger, R., Raman, A., Rudie, A., & Moon, R. J. (2010). Atomic force microscopy characterization of cellulose nanocrystals. *Langmuir*, 26(6), 4480-4488.

- [145] Wagner, R., Moon, R. J., & Raman, A. (2016). Mechanical properties of cellulose nanomaterials studied by contact resonance atomic force microscopy. *Cellulose*, *23*(2), 1031-1041.
- [146] Rusli, R., & Eichhorn, S. J. (2008). Determination of the stiffness of cellulose nanowhiskers and the fiber-matrix interface in a nanocomposite using Raman spectroscopy. *Applied Physics Letters*, *93*(3), 033111.
- [147] Orts, W. J., Godbout, L., Marchessault, R. H., & Revol, J. F. (1998). Enhanced ordering of liquid crystalline suspensions of cellulose microfibrils: A small angle neutron scattering study. *Macromolecules*, *31*(17), 5717-5725.
- [148] Lasseguette, E., Roux, D., & Nishiyama, Y. (2008). Rheological properties of microfibrillar suspension of TEMPO-oxidized pulp. *Cellulose*, *15*(3), 425-433.
- [149] Klemm, D., Kramer, F., Moritz, S., Lindström, T., Ankerfors, M., Gray, D., & Dorris, A. (2011). Nanocelluloses: A new family of nature-based materials. *Angewandte Chemie International Edition*, *50*(24), 5438-5466.
- [150] Azizi Samir, M. A. S., Alloin, F., & Dufresne, A. (2005). Review of recent research into cellulosic whiskers, their properties and their application in nanocomposite field. *Biomacromolecules*, *6*(2), 612-626.
- [151] Siqueira, G., Bras, J., & Dufresne, A. (2010). Cellulosic bionanocomposites: a review of preparation, properties and applications. *Polymers*, *2*(4), 728-765.
- [152] Favier, V., Dendievel, R., Canova, G., Cavaille, J. Y., & Gilormini, P. (1997). Simulation and modeling of three-dimensional percolating structures: case of a latex matrix reinforced by a network of cellulose fibers. *Acta Materialia*, *45*(4), 1557-1565.

- [153] Tonoli, G. H. D., Rodrigues Filho, U. P., Savastano, H., Bras, J., Belgacem, M. N., & Lahr, F. R. (2009). Cellulose modified fibres in cement based composites. *Composites Part A: Applied Science and Manufacturing*, 40(12), 2046-2053.
- [154] Dufresne, A. (2005). A special issue devoted to cellulose-based composites. *Compos Interf*, 12, 1-2.
- [155] Savastano, H., & Warden, P. G. (2005). Special theme issue: Natural fibre reinforced cement composites.
- [156] Agopyan, V., Savastano, H., John, V. M., & Cincotto, M. A. (2005). Developments on vegetable fibre–cement based materials in São Paulo, Brazil: an overview. *Cement and Concrete Composites*, 27(5), 527-536.
- [157] Bentur, A., & Akers, S. A. S. (1989). The microstructure and ageing of cellulose fibre reinforced cement composites cured in a normal environment. *International Journal of Cement Composites and Lightweight Concrete*, 11(2), 99-109.
- [158] Ardanuy, M., Claramunt, J., & Toledo Filho, R. D. (2015). Cellulosic fiber reinforced cement-based composites: a review of recent research. *Construction and building materials*, 79, 115-128.
- [159] Tonoli, G. H. D., Santos, S. F., Savastano, H., Delvasto, S., de Gutiérrez, R. M., & de Murphy, M. D. M. L. (2011). Effects of natural weathering on microstructure and mineral composition of cementitious roofing tiles reinforced with fique fibre. *Cement and Concrete Composites*, 33(2), 225-232.

- [160] Savastano, H., Warden, P. G., & Coutts, R. S. P. (2003). Mechanically pulped sisal as reinforcement in cementitious matrices. *Cement and Concrete Composites*, 25(3), 311-319.
- [161] Morton, J. H., Cooke, T., & Akers, S. A. S. (2010). Performance of slash pine fibers in fiber cement products. *Construction and building materials*, 24(2), 165-170.
- [162] Toledo Filho, R. D., Ghavami, K., England, G. L., & Scrivener, K. (2003). Development of vegetable fibre–mortar composites of improved durability. *Cement and concrete composites*, 25(2), 185-196.
- [163] Toledo Filho, R. D., Ghavami, K., Sanjuán, M. A., & England, G. L. (2005). Free, restrained and drying shrinkage of cement mortar composites reinforced with vegetable fibres. *Cement and Concrete Composites*, 27(5), 537-546.
- [164] Neithalath, N., Weiss, J., & Olek, J. (2004). Acoustic performance and damping behavior of cellulose–cement composites. *Cement and Concrete Composites*, 26(4), 359-370.
- [165] De Andrade Silva, F., Mobasher, B., & Toledo Filho, R. D. (2010). Fatigue behavior of sisal fiber reinforced cement composites. *Materials Science and Engineering: A*, 527(21), 5507-5513.
- [166] De Andrade Silva, F., Mobasher, B., Soranakom, C., & Toledo Filho, R. D. (2011). Effect of fiber shape and morphology on interfacial bond and cracking behaviors of sisal fiber cement based composites. *Cement and Concrete Composites*, 33(8), 814-823.

- [167] Mohr, B. J., Biernacki, J. J., & Kurtis, K. E. (2007). Supplementary cementitious materials for mitigating degradation of kraft pulp fiber-cement composites. *Cement and Concrete Research*, 37(11), 1531-1543.
- [168] Soroushian, P., Won, J. P., & Hassan, M. (2012). Durability characteristics of CO<sub>2</sub>-cured cellulose fiber reinforced cement composites. *Construction and Building Materials*, 34, 44-53.
- [169] Ardanuy, M., Claramunt, J., García-Hortal, J. A., & Barra, M. (2011). Fiber-matrix interactions in cement mortar composites reinforced with cellulosic fibers. *Cellulose*, 18(2), 281-289.
- [170] Claramunt, J., Ardanuy, M., García-Hortal, J. A., & Tolêdo Filho, R. D. (2011). The hornification of vegetable fibers to improve the durability of cement mortar composites. *Cement and Concrete Composites*, 33(5), 586-595.
- [171] Ridi, F., Fratini, E., Mannelli, F., & Baglioni, P. (2005). Hydration process of cement in the presence of a cellulosic additive. A calorimetric investigation. *The Journal of Physical Chemistry B*, 109(30), 14727-14734.
- [172] Damasceni, A., Dei, L., Fratini, E., Ridi, F., Chen, S. H., & Baglioni, P. (2002). A novel approach based on differential scanning calorimetry applied to the study of tricalcium silicate hydration kinetics. *The Journal of Physical Chemistry B*, 106(44), 11572-11578.
- [173] Ridi, F., Dei, L., Fratini, E., Chen, S. H., & Baglioni, P. (2003). Hydration kinetics of tri-calcium silicate in the presence of superplasticizers. *The Journal of Physical Chemistry B*, 107(4), 1056-1061.

- [174] Reier, G. E., & Shangraw, R. F. (1966). Microcrystalline cellulose in tableting. *Journal of Pharmaceutical Sciences*, 55(5), 510-514.
- [175] Fengel, D., & Wegener, G. (Eds.). (1983). *Wood: chemistry, ultrastructure, reactions*. Walter de Gruyter.
- [176] Roussel, N. (2005). Steady and transient flow behaviour of fresh cement pastes. *Cement and concrete research*, 35(9), 1656-1664.
- [177] Roussel, N., Stefani, C., & Leroy, R. (2005). From mini-cone test to Abrams cone test: measurement of cement-based materials yield stress using slump tests. *Cement and Concrete Research*, 35(5), 817-822.
- [178] Coussot, P., Proust, S., & Ancy, C. (1996). Rheological interpretation of deposits of yield stress fluids. *Journal of Non-Newtonian Fluid Mechanics*, 66(1), 55-70.
- [179] Banfill, P. F. G. (2006). Rheology of fresh cement and concrete. *Rheology reviews*, 2006, 61.
- [180] Grosseau, P., Pourchez, J., Guilhot, B., Guyonnet, R., & Ruot, B. (2007). Impact of cellulose ethers on the C3S hydration. In *International Congress on the Chemistry of Cement*.
- [181] Pourchez, J., Govin, A., Grosseau, P., Guyonnet, R., Guilhot, B., & Ruot, B. (2006). Alkaline stability of cellulose ethers and impact of their degradation products on cement hydration. *Cement and Concrete Research*, 36(7), 1252-1256.
- [182] Peschard, A., Govin, A., Pourchez, J. A. E., Fredon, E., Bertrand, L., Maximilien, S., & Guilhot, B. (2006). Effect of polysaccharides on the hydration of cement suspension. *Journal of the European Ceramic Society*, 26(8), 1439-1445.

- [183] Khan, B., & Baradan, B. (2002). The effect of sugar on setting-time of various types of cements. *Quarterly science vision*, 8(1), 71-78.
- [184] Habibi, Y., Lucia, L. A., & Rojas, O. J. (2010). Cellulose nanocrystals: chemistry, self-assembly, and applications. *Chemical reviews*, 110(6), 3479-3500.
- [185] Nickerson, R. F., & Habrle, J. A. (1947). Cellulose intercrystalline structure. *Industrial & Engineering Chemistry*, 39(11), 1507-1512.
- [186] Mukherjee, S. M., & Woods, H. J. (1953). X-ray and electron microscope studies of the degradation of cellulose by sulphuric acid. *Biochimica et biophysica acta*, 10, 499-511.
- [187] Battista, O. A. (1950). Hydrolysis and crystallization of cellulose. *Industrial & Engineering Chemistry*, 42(3), 502-507.
- [188] Battista, O. A., Coppick, S., Howsmon, J. A., Morehead, F. F., & Sisson, W. A. (1956). Level-off degree of polymerization. *Industrial & Engineering Chemistry*, 48(2), 333-335.
- [189] Favier, V., Canova, G. R., Cavaillé, J. Y., Chanzy, H., Dufresne, A., & Gauthier, C. (1995). Nanocomposite materials from latex and cellulose whiskers. *Polymers for Advanced Technologies*, 6(5), 351-355.
- [190] Favier, V., Chanzy, H., & Cavaille, J. Y. (1995). Polymer nanocomposites reinforced by cellulose whiskers. *Macromolecules*, 28(18), 6365-6367.
- [191] Angles, M. N., & Dufresne, A. (2001). Plasticized starch/tunicin whiskers nanocomposite materials. 2. Mechanical behavior. *Macromolecules*, 34(9), 2921-2931.

- [192] Ruiz, M. M., Cavaille, J. Y., Dufresne, A., Gerard, J. F., & Graillat, C. (2000). Processing and characterization of new thermoset nanocomposites based on cellulose whiskers. *Matériaux & Techniques*, 88(7-8), 63-68.
- [193] Araki, J., Wada, M., Kuga, S., & Okano, T. (1998). Flow properties of microcrystalline cellulose suspension prepared by acid treatment of native cellulose. *Colloids and Surfaces A: Physicochemical and Engineering Aspects*, 142(1), 75-82.
- [194] Wang, N., Ding, E., & Cheng, R. (2007). Thermal degradation behaviors of spherical cellulose nanocrystals with sulfate groups. *Polymer*, 48(12), 3486-3493.
- [195] Bondeson, D., Mathew, A., & Oksman, K. (2006). Optimization of the isolation of nanocrystals from microcrystalline cellulose by acid hydrolysis. *Cellulose*, 13(2), 171-180.
- [196] Pranger, L., & Tannenbaum, R. (2008). Biobased nanocomposites prepared by in situ polymerization of furfuryl alcohol with cellulose whiskers or montmorillonite clay. *Macromolecules*, 41(22), 8682-8687.
- [197] Capadona, J. R., Shanmuganathan, K., Trittschuh, S., Seidel, S., Rowan, S. J., & Weder, C. (2009). Polymer nanocomposites with nanowhiskers isolated from microcrystalline cellulose. *Biomacromolecules*, 10(4), 712-716.
- [198] Oksman, K., & Sain, M. (Eds.). (2006). *Cellulose nanocomposites: processing, characterization, and properties*. American Chemical Society.
- [199] Miller, A. F., & Donald, A. M. (2003). Imaging of anisotropic cellulose suspensions using environmental scanning electron microscopy. *Biomacromolecules*, 4(3), 510-517.

- [200] Terech, P., Chazeau, L., & Cavaille, J. Y. (1999). A small-angle scattering study of cellulose whiskers in aqueous suspensions. *Macromolecules*, 32(6), 1872-1875.
- [201] De Souza Lima, M. M., Wong, J. T., Paillet, M., Borsali, R., & Pecora, R. (2003). Translational and rotational dynamics of rodlike cellulose whiskers. *Langmuir*, 19(1), 24-29.
- [202] Hanley, S. J., Giasson, J., Revol, J. F., & Gray, D. G. (1992). Atomic force microscopy of cellulose microfibrils: comparison with transmission electron microscopy. *Polymer*, 33(21), 4639-4642.
- [203] Šturcová, A., Davies, G. R., & Eichhorn, S. J. (2005). Elastic modulus and stress-transfer properties of tunicate cellulose whiskers. *Biomacromolecules*, 6(2), 1055-1061.
- [204] Cao, X., Dong, H., & Li, C. M. (2007). New nanocomposite materials reinforced with flax cellulose nanocrystals in waterborne polyurethane. *Biomacromolecules*, 8(3), 899-904.
- [205] Lu, Y., Weng, L., & Cao, X. (2005). Biocomposites of plasticized starch reinforced with cellulose crystallites from cottonseed linter. *Macromolecular Bioscience*, 5(11), 1101-1107.
- [206] Dufresne, A. (2008). Polysaccharide nano crystal reinforced nanocomposites. *Canadian Journal of Chemistry*, 86(6), 484-494.
- [207] Roohani, M., Habibi, Y., Belgacem, N. M., Ebrahim, G., Karimi, A. N., & Dufresne, A. (2008). Cellulose whiskers reinforced polyvinyl alcohol copolymers nanocomposites. *European polymer journal*, 44(8), 2489-2498.

- [208] Cao, Y., Tian, N., Bahr, D., Zavattieri, P. D., Youngblood, J., Moon, R. J., & Weiss, J. (2016). The influence of cellulose nanocrystals on the microstructure of cement paste. *Cement and Concrete Composites*, 74, 164-173.
- [209] Nawa, T. (2006). Effect of chemical structure on steric stabilization of polycarboxylate-based superplasticizer. *Journal of Advanced Concrete Technology*, 4(2), 225-232.
- [210] Rajabipour, F., Sant, G., & Weiss, J. (2008). Interactions between shrinkage reducing admixtures (SRA) and cement paste's pore solution. *Cement and Concrete Research*, 38(5), 606-615.
- [211] With, G., & Wagemans, H. H. (1989). Ball-on-Ring Test Revisited. *Journal of the American Ceramic Society*, 72(8), 1538-1541.
- [212] Börger, A., Supancic, P., & Danzer, R. (2002). The ball on three balls test for strength testing of brittle discs: stress distribution in the disc. *Journal of the European Ceramic Society*, 22(9), 1425-1436.
- [213] Lee, J. H., Park, S. E., Lee, H. J., & Lee, H. L. (2002). Thermal shock behaviour of alumina ceramics by ball-on-3-ball test. *Materials Letters*, 56(6), 1022-1029.
- [214] Fu, T., Montes, F., Suraneni, P., Youngblood, J., & Weiss, J. (2017). The Influence of Cellulose Nanocrystals on the Hydration and Flexural Strength of Portland Cement Pastes. *Polymers*, 9(9), 424.

## Chapter III

# *The Influence of Cellulose Nanocrystal (CNC) Particles on Steady Shear Rheology, Workability and Fluid Loss Properties of Oil Well Cement Paste*

### **ABSTRACT**

In this study, cellulose nanocrystal (CNC) is utilized as a replenishable, non-toxic additive to oil well cement paste, in order to tailor the rheology of the system. The rheological behavior of various colloidal suspensions containing bentonite and CNC was investigated first. Subsequently, the rheological parameters were assessed upon fresh oil well cement paste followed by static filtration tests to evaluate fluid loss. It was found that adding CNC to colloids and oil well cement paste leads to shear thinning which manifests as lower slump for the cement based slurry. As well, there was a favorable synergy between CNC and the bentonite resulting in an increase in the time required to collect a given amount of filtrate.

*Keywords: Oil Well Cement, Cellulose Nanocrystal, Workability, Rheology, Fluid Loss*

This chapter has been partially presented at the ConMAT '15 conference. (Dousti, M. R., Boluk, Y., & Bindiganavile, V. *The influence of cellulose nanocrystals on the fresh properties of oil well cement paste. Proc. CONMAT, 15.*)

## 1. INTRODUCTION

Oil consumption has increased significantly over the past 50 years [1]. This continuously puts pressure on exploration and extraction that consume the least time, energy and money. The effort is on towards using advanced technologies and materials to the address this issue [2]. At the same time, a poorly designed oil well may trigger oil spills or release of other toxic substances [2]. Hence, well cementing becomes a crucial step in the commissioning of an oil well. This involves an oil well cement paste that is poured to fill the annular space between the casing string and the ground formation within the drilled hole (see Figure 3.1). The cement paste used in an oil well has exclusive functions to perform namely, (i) restrict the movement of hydrocarbons and/or water in between the permeable zones, (ii) provide a suitable mechanical support for the casing string and in turn, the geological formation, and (iii) protect the casing from possible physical damage through corrosion. Along with these functional demands, the material is almost always a neat paste, devoid of aggregates. Also, a relatively large volume of water is used in producing oil well cement slurry, in order to make it pumpable. Thus, the properties of fresh oil well cement, especially its rheology and subsequent deposition, are of primary concern.

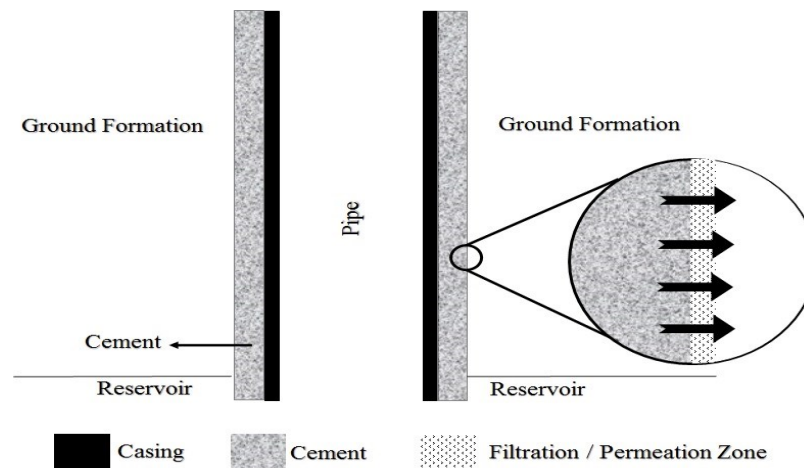


**Figure 3.1.** A schematic view of a section of an oil well

The American Petroleum Institute (API) recognizes different classes of oil well cement, based on the usage and purpose of the well and certain influencing factors viz., the depth of the well, resistance to sulfate attack, early age strength gain, rheological properties and, susceptibility to high pressure and temperature [3]. The cement slurry, which is pumped into the oil or gas wells, is a combination of Portland cement, certain additives (depending on the desired characteristic) and water [4]. These additives are employed to control such characteristics of the slurry as thickening time, compressive strength, or density. Among them, bentonite occurs as an inevitable pollutant through the drilling fluids.

Fluid loss is an inevitable part of the cementing process during well completion. One will ideally not want a large amount of fluid loss, since the slurry becomes significantly viscous and difficult to pump. Neat oil well cement paste (i.e. with no special additives) usually demonstrates a fluid loss rate of approximately 2000 cc/hour or higher [5]. It has been demonstrated that almost 50% of this water loss is due to filtration, even though the presence of mud cake decreases the filtration [6]. Bentonite is known to reduce fluid loss, while organic colloids like carboxymethyl hydroxyethyl cellulose (CMHEC) is effective [6]. In permeable sections or formations, the loss of cement filtrate will result in the dehydration of parts of the cement slurry. Eventually, this prevents the flow and influences it negatively. As a result, a decrease in the slurry flow rate is observed and hence, the performance of the cement slurry will be inferior [5, 7, 8].

There could also be some circulating pressure restricting the annular space that could possibly break down the formation. The resulting residue, known as the filter cake, occurs through the deposit on the near side of the permeable cement paste even as the fluid filters through. This filter cake is to an extent desirable, as it isolates the surrounding formation

from the drilling fluids. However, an external filter cake is preferable to one that forms partly inside the formation as the latter may cause damage to the formation [9].

In many studies, static filtration has been utilized as an experimental approach and methodology, to investigate and measure the fluid loss of cementitious slurries. In their proposed methodology, Plank et al. employed a copolymer of N,N-dimethylacrylamide and calcium 2-acrylamido-2-methylpropanesulfonate as a fluid loss additive and investigated the effect of such polymer on the fluid loss behavior using static filtration. In a static filtration process, a filter cake is usually formed from the paste under examination [10]. Note that the filter cake (if formed) permeability of a cement slurry is of great importance.

To clarify, Plank and colleagues [10] describe the process (static filtration) in three mechanisms. Firstly, the effective pore diameter of cement may decrease by adsorption of large macromolecules. In the second mechanism, some of the pores may be plugged by the hydrated and swollen polymers in the slurry. Finally, the third mechanism is described as the modification and change in the filter cake structure (such as increase in its compaction). At the end of their experimental work, it was concluded that the fluid loss additive used, reduced the fluid loss and also the filter cake permeability of the oil well cement slurry by adsorption (of the polymer) on the hydrating cement particles.

In another study performed by Plank et al. in 2010 [11], the effect of water-soluble copolymers in the presence of welan gum, on the fluid loss of oil well cement slurry was examined. Similar to the previous study, static filtration was performed to measure the fluid loss and obtain a filter cake. It was observed that the polymer controlled the fluid loss mainly by adsorption onto the cement particles. However, as demonstrated in the results,

if this adsorption is prevented, fluid loss control will not be observed [10, 11]. Picandet et al. also performed a static filtration test, in order to understand the hydro-mechanical behavior (fluid loss and permeability characteristics) of cement paste [12]. For this purpose, a common soil permeameter was used with a hydraulic head applied.

In a recent study on cement paste, Pierre et al. used cellulose ether admixtures in order to enhance the permeability and water retaining properties of cementitious systems [13]. In their experimental work, the effect of cellulose ether on the filtration of cement paste through oedometric filters was examined. The results obtained from the test illustrated that the addition of cellulose ether modified the rheological behavior of the cementitious pastes prepared. The apparent viscosity had increased which lead to a decrease in the materials apparent permeability. Furthermore, it was witnessed that the water retaining ability of the cement pastes increased after introducing the cellulose ether admixtures. This clearly limited the amount of bleed water associated with the cement pastes [13].

Cellulose nanocrystal (CNC) particles are rod shaped nanoparticles derived from cellulose after separating the amorphous phases present in the nanofiber (Figure 3.2) [14]. Bondeson et al. [15] prepared CNC by acid hydrolysis after dissolving wood pulp or cotton with 65% concentrated sulfuric acid. Commercially available CNC has a rod-like morphology with a diameter between 5 to 10 nm and under 300 nm in length. As described by Boluk et al. [16], the appearance of sulfate groups on their surface renders CNC with a pronouncedly negative charge when in an aqueous solution. However, the disintegration of the sulfate group occurs only beyond 200°C, which eliminates any concern related to possible sulfate attack to the cementitious system [14, 17]. In recent years, much has been documented with regard to its mechanical, optical and surface properties [17-19].

It possesses high strength and elastic modulus but at the same time, is lightweight, non-toxic, chemically tunable and, as opposed to most other nanomaterials, is sustainably bio-sourced and considerably inexpensive. The cellulose molecule has an extremely complex hydrogen-bonding network with multiple isotropic and anisotropic phases, as elaborated by Dufresne in 2012 [20]. The fibrils (substructure of cellulose) are orientated in the same direction in an isotropic phase whereas in an anisotropic phase, there are several layers of isotropic phases stacked upon each other to form a fibril layer in different orientations [17]. This is mainly important because these isotropic and anisotropic phases impact and influence their final dimensions and aspect ratio. This suite of attributes makes it attractive not merely as an additive but in fact to nano-engineer cement based systems.

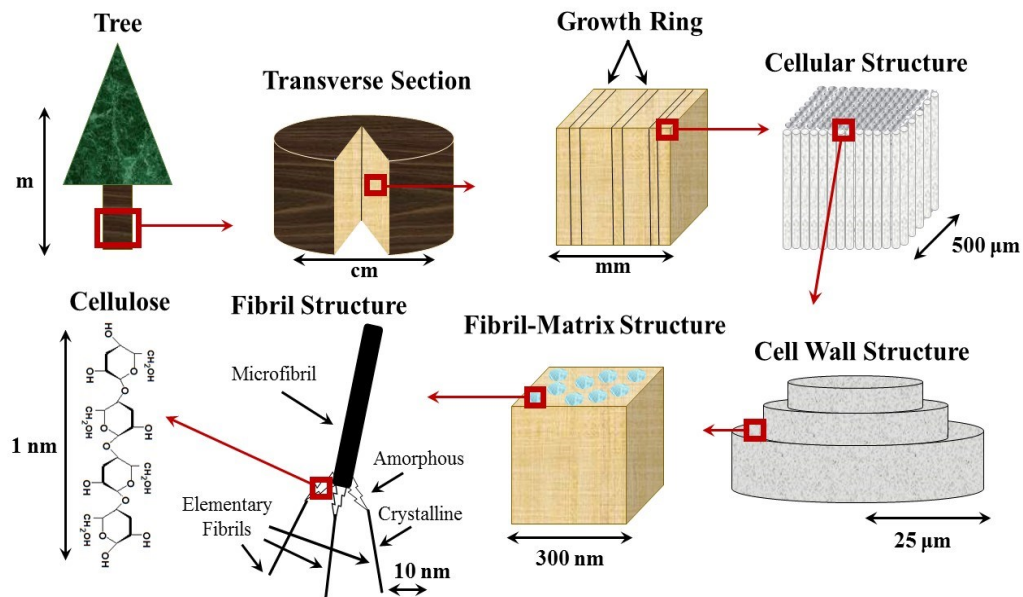


**Figure 3.2.** A schematic demonstration of CNC hierarchy [14]

Synthetic polymers and latex are added to arrest leak-off of water into rock, while maintaining key characteristics such as thickening time, rheology, and strength development and, avoid build-up of the filter cake. Although there are limited studies that

focus on modifying the rheology of suspensions containing CNC [16, 19, 21-26] and in their strategic promotion of the hydration process [27, 28], the impact of CNC on the rheology, fluid flow and filtration in oil well cementing has not been examined. In the study reported here, CNC is employed as a rheology modifying admixture to obtain a favorable flow behavior as well as filtration performance.

## 2. EXPERIMENTAL DETAILS

### 2.1. Materials

As stated earlier, the cementitious slurry examined here was composed of water, Type G oil well cement [3], bentonite and CNC. Information regarding each of these specific materials used in this system is presented below.

#### 2.1.1. *Oil Well Cement Type G*

The cement used here was a Type G cement, based on the American Petroleum Institute (API) classification, Specification 10A, for oil well cements [3]. A water/cement ratio of 0.44 is recommended and the cement itself was comparable to CSA Type MS (ASTM Type II) or CSA Type HS (Type V Portland cement) per [29, 30] in their respective jurisdiction. Tables 3.1 and 3.2, describe the physical properties and chemical composition of this type of cement, respectively.

**Table 3.1.** Physical properties of Type G cement (prepared by Lafarge Canada, December 8<sup>th</sup>, 2015)

<b>Physical Analysis</b>	
Thickening Time (Schedule 5)	99 min.

Max. Consis. 15-30 min.	23 Bc
Fineness 45 $\mu\text{m}$ sieve	93.9%
Blaine	311 $\text{m}^2/\text{kg}$
Free Fluid	4.4 %

**Table 3.2.** Chemical composition of Type G cement (prepared by Lafarge Canada, December 8<sup>th</sup>, 2015)

<b>Chemical Analysis</b>	
Silica ( $\text{SiO}_2$ )	20.9%
Alumina ( $\text{Al}_2\text{O}_3$ )	3.8%
Iron Oxide ( $\text{Fe}_2\text{O}_3$ )	4.7%
Calcium Oxide, Total (TCaO)	62.9%
Magnesium Oxide (MgO)	4.5%
Sulphur Trioxide ( $\text{SO}_3$ )	2.6%
Loss on Ignition	0.66%
Insoluble Residue	0.13%
Equivalent Alkali (as $\text{Na}_2\text{O}$ )	0.48%
$\text{C}_3\text{S}$	57.9%
$\text{C}_2\text{S}$	16.1%
$\text{C}_3\text{A}$	2.0%
$\text{C}_4\text{AF}$	14.3%
$\text{C}_4\text{AF} + 2\text{X } \text{C}_3\text{A}$	18.3%

### 2.1.2. Cellulose Nanocrystal (CNC)

Figure 3.3 illustrates a micrograph of the CNC employed in this study. The diameter was between 5-10 nm, while the aspect ratio lay between 10-60. It was locally sourced from Canada's second largest production facility in Edmonton, Alberta. The material is produced from kraft pulp produced by the provincial pulp and paper industry.

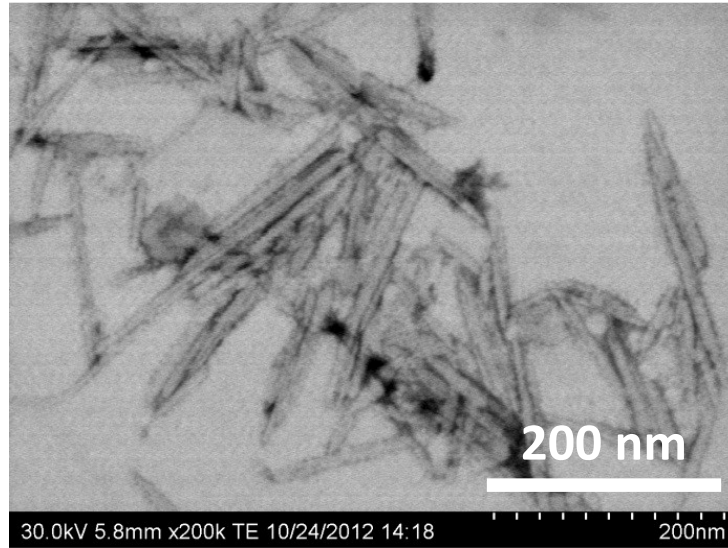


**Figure 3.3.** Scanning electron micrograph of the cellulose nanocrystal (CNC) particles used in this study

#### 2.1.3. Bentonite

Generally, clay minerals are used in industries such as ceramic production, drilling fluids, molding sands, and cementing. An important reason is their ability to provide adequate particle dispersion in order to have a uniform and stable system [31]. In some cases, clay particles may become aggregated. This aggregation which may occur under a certain specific combination of pressure and temperature will eventually vary the flow behavior [32]. There are different viscosity modifying agents added to bentonite in order to stabilize it and prevent any sort of aggregation. The de-coagulant, in this case, was Carboxymethyl Cellulose (CMC). The bentonite employed in this study is commercially referred to as Wyoming Gel.

#### 2.1.4. Carboxymethyl Cellulose (CMC)

Carboxymethyl cellulose (CMC) is added to improve the rheological properties of clay suspensions [33]. Given that bentonite was used in suspensions examined here,

carboxymethyl cellulose (CMC), with a molecular weight of 700 kDa, was deemed suitable not only to modify the viscosity of the suspension but also control the mud flow loss under conditions of high temperature and pressure [34]. Often used in producing cosmetics and toothpaste, it binds, thickens and stabilizes the product. It is frequently employed in drilling fluids as a dispersion agent. Here, it was commercially sourced as a powder.

## **2.2. Preparation**

There were two stages of preparing the desired materials for this research. In the first stage, the colloidal suspensions were made on which the rheology tests were carried out. In the second stage, the cementitious slurry was prepared, directed in part by the prior composition of the colloid. The slurry was subsequently examined for rheological parameters and static filtration performance.

### *2.2.1. Colloidal Suspensions*

In the first stage of this study, three suspensions were prepared as follows: The first had only bentonite and CMC, while the second carried bentonite and CNC. The third suspension included bentonite, CMC and CNC. Recall that bentonite reaches the drilling fluid and in turn almost always contaminates the oil well cement slurry. Carboxymethyl cellulose (CMC) was required to aid in stabilizing bentonite in the suspension. Based on field observations, the bentonite occurs at between 0.5-3% mass fraction (of cement) in the drilling fluid [35]. Accordingly, in this study, its dosage was set to 3% mass fraction in water. Preliminary trials by the authors demonstrated that a dosage of CMC at 0.25% by mass of water was suitable to de-coagulate the bentonite. The cellulose nanocrystals were added in the third suspension at 1% mass fraction of water. Each of these constituent

materials was mixed with a third of the total water using a high shear mixer. They were mixed together to render the total water amount as the second stage of mixing, in order to get a better dispersion and a more uniform system.

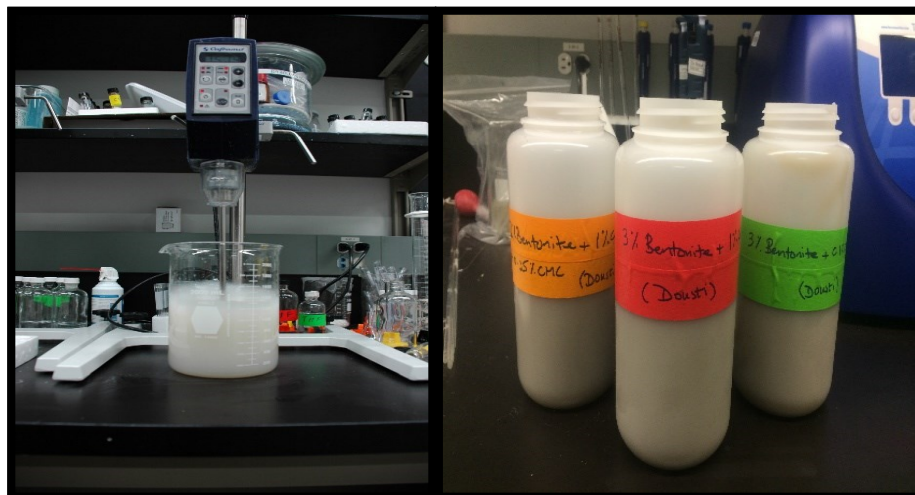


**Figure 3.4.** Homogenizing the CNC into a colloidal suspension (left) and prepared suspensions containing variously, CNC, CMC and Bentonite (right)

These suspensions were stored in a refrigerator until further testing. For each suspension examined in this study, rheological tests were performed with at least three replicates. Table 3.3 demonstrates a sample mix design identical to the mix design used in this research study.

**Table 3.3.** Mix design (sample) for preparation of colloidal suspensions

<b>Colloidal Suspension (Mix Design)</b>	
Water	100 g
Bentonite	3 g
Cellulose nanocrystal (CNC) particles	1 g
Carboxymethyl cellulose (CMC) particles	0.25 g

### 2.2.2. Cementitious System (Slurry)

In the second stage of this study, a series of cementitious slurry was prepared based on the suspensions examined previously. A control mixture was prepared first containing a mixture of water and oil well cement. Two further mixtures were prepared to contain in addition to water and oil well cement, bentonite and cellulose nanocrystal (CNC) particles, respectively. The fourth mixture contained both bentonite and CNC in the same slurry. In all cases, the water-to-cement ratio was 0.44, which is per the API specification 10A [3].



**Figure 3.5.** High shear mixer (left) and the prepared cementitious slurry samples (right)

Note that CMC was excluded in the cementitious slurry, as the bentonite gel was deemed stable enough and well dispersed. In keeping with the suspensions in the first stage of this study, the bentonite was brought in once again at 3% mass fraction of the total amount of water in the mix design. Similarly, the CNC was introduced at 1% of the design amount of water. Table 3.4 demonstrates a sample mix design identical to the mix design used in this research study.

**Table 3.4.** Mix design (sample) for preparation of cement paste

<b>Oil Well Cement Paste (Mix Design)</b>	
Cement	1000 kg
Water	440 kg
Bentonite	13.2 kg
Cellulose nanocrystal (CNC) particles	4.4 kg

As was done earlier, again, the bentonite and CNC were individually homogenized in a suitable fraction of the mix water. The oil well cement was mixed first with the remaining water to prepare a slurry. The bentonite and CNC, now in their own suspensions, were then added to the slurry and the mixture was agitated further for 5 minutes. The resulting fresh paste was then tested for rheological characterization and performance under static filtration.

Note that due to the inherent properties of cellulose nanocrystal (CNC) particles, the dosage being added to the mix design (in this case 1% of the total amount of water or approximately 0.5% mass fraction of the total amount of cement powder used), and their associated mechanism of adsorption with the water molecules, any change to the water-to-cement ratio of the prepared cementitious system will be negligible. Recent studies have also confirmed that despite their hydrophilic nature, even with higher dosages of CNC used, at a high relative humidity (approximately 97% where CNC particles are immersed in water), the water adsorption of dry CNC particles is in the region of 34% which is only about 0.7% of the total mixing water in mass [27]. In this study, considering the fact that CNC particles are added to the mix design in the form of an aqueous solution (similar high relative humidity as the mentioned study), the adsorbed water on CNC will be approximately 0.3% of the total mixing water in mass. Therefore, based on Table 3.4, the

water-to-cement ratio will change from a value of “440 kg / 1000 kg = 0.44” to a revised value of “441.5 kg / 1000 kg = 0.4415”, which is negligible.

## 2.3. Test Methods

### 2.3.1. Steady Shear Rheological Parameters

The rheometer employed in this study is shown in Figure 3.6. The authors realized that it was required first to select the appropriate geometry for the contacting surfaces in the rheometer.

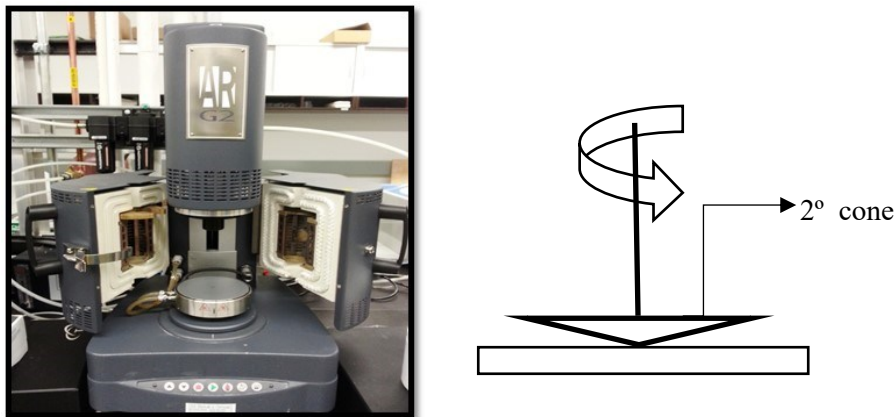


**Figure 3.6.** Dynamic shear rheometer utilized for steady shear rheology assessment (left) and the schematic showing cone and plate geometry (right)

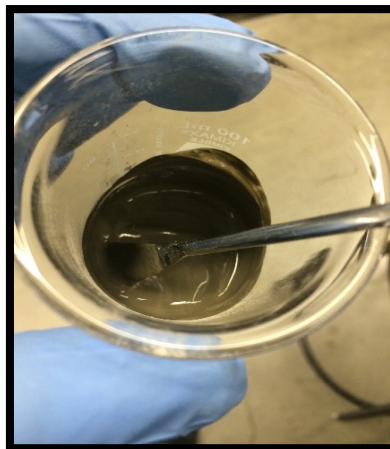


**Figure 3.7.** Prepared sample for rheological measurements

After trial and error, a calibrated cone (SST) geometry was selected with a cone angle of 2 degrees and a diameter of 60 mm (Figure 3.6). For the cementitious slurry, the same rheometer required a different cone-plate setup, this time with a diameter of 20 mm and grated surface.

In order to perform the test, the rheometer was turned on together with the water pump and air pipes attached to it. After assembling the cone and plate assembly, the selected geometry was assembled and set into the rheometer. A tablespoonful sample of each suspension or cementitious mixture was placed on the flat plate within this assembly in the rheometer (Figure 3.7). Note that the tests were performed at 25°C and normal atmospheric pressure. The tests were carried out to achieve 20 different shear rates between 1 s<sup>-1</sup> to 200 s<sup>-1</sup> with a continuous rotation of 10 seconds at each shear rate. Based on prior experience with this instrument, the shear rate was examined in a descending order from 200 s<sup>-1</sup>.

### 2.3.2. *Workability of Fresh Cement Paste*

The cementitious slurry was examined for slump and flow. In the first instance, a mini slump test was performed as shown. A total of six measurements were made for the slump (height) and the spread (diameter) upon releasing the paste under gravity. In the second instance, a flow table was utilized to measure the height and spread of the cementitious paste. As is well known, this test requires that the sample frustum of paste be subjected to agitation associated with the rise and fall of the base. In each case, the number of blows required to spread the sample to a predetermined diameter was recorded. As well, the diameter of spread was recorded once after 2 blows and then after 25 blows. Again, a total of three measurements were made for the diameter to capture the variability. In like

manner, the height of the paste (ie. elevation from the top of the spread sample to the surface of the flow table) was also recorded.



**Figure 3.8.** Flow table (left) and mini slump cone (right) employed to investigate the workability of prepared cement paste.

### 2.3.3. *Static Filtration*

The cementitious slurry was examined further under static filtration using the apparatus recommended by API Standard [36] and shown in Figure 3.9. The sample was placed in a cell and allowed to rest on a filter medium. The filter medium employed for this study was a Whatman #50 grade filter paper with a thickness of 115  $\mu\text{m}$ . The particle retention (in liquid) associated with the filter medium was 2.7  $\mu\text{m}$ .

Furthermore, pressure ( $\Delta P = 100$  psi) was applied to the sample and a hydraulic head was introduced. This led to water percolation, which was measured. The following parameters were measured: (i) Time required to collect 100 ml of filtrate from the cementitious system; (ii) Time required to collect 150 ml of filtrate from the same system; (iii) Total amount of fluid loss from the cementitious system after 30 minutes.



**Figure 3.9.** The static filtration test setup

### 3. RESULTS AND DISCUSSION

#### 3.1. Colloidal Suspensions

Figures 3.10 and 3.11 illustrate the variation in yield shear stress and the viscosity, respectively, across the different suspensions examined. Notwithstanding other available rheological models, it was deemed more practical to settle for a Bingham model for these suspensions, as shown.

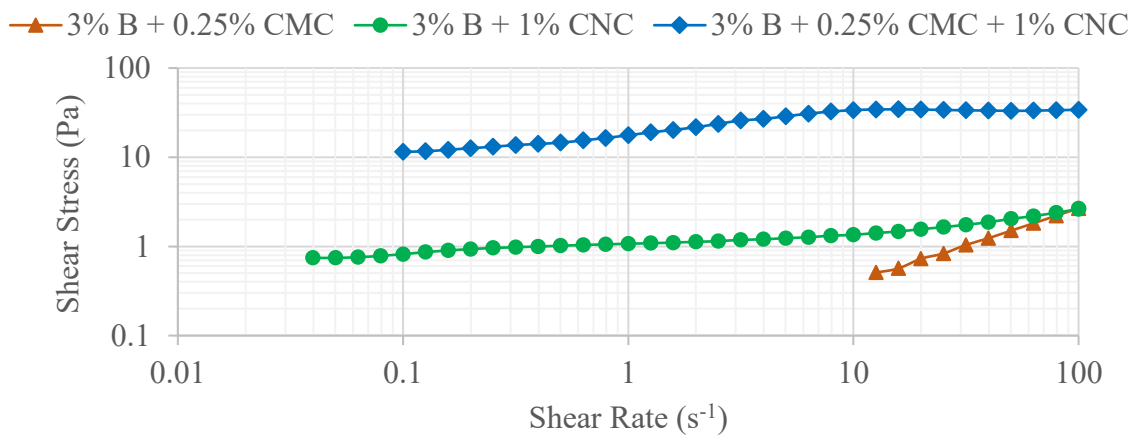


**Figure 3.10.** Variation in yield shear stress across different suspensions (in the presence of cellulose nanocrystal particles)

It is seen that the suspension containing no cellulose nanocrystal (CNC) was not stable at low shear rates (shear rates below  $1 \text{ s}^{-1}$ ). On the other hand, those suspensions that contained CNC were stable, especially at lower shear rates. Although adding CMC does not improve the stability of the suspension, however, the viscosity and the yield shear stress were significantly higher upon adding CMC. This should be perceived as a disadvantage in the oil well cementing process. In this study, therefore, it was CNC and not CMC that appeared to be apt as a rheology modifying agent for oil well application.

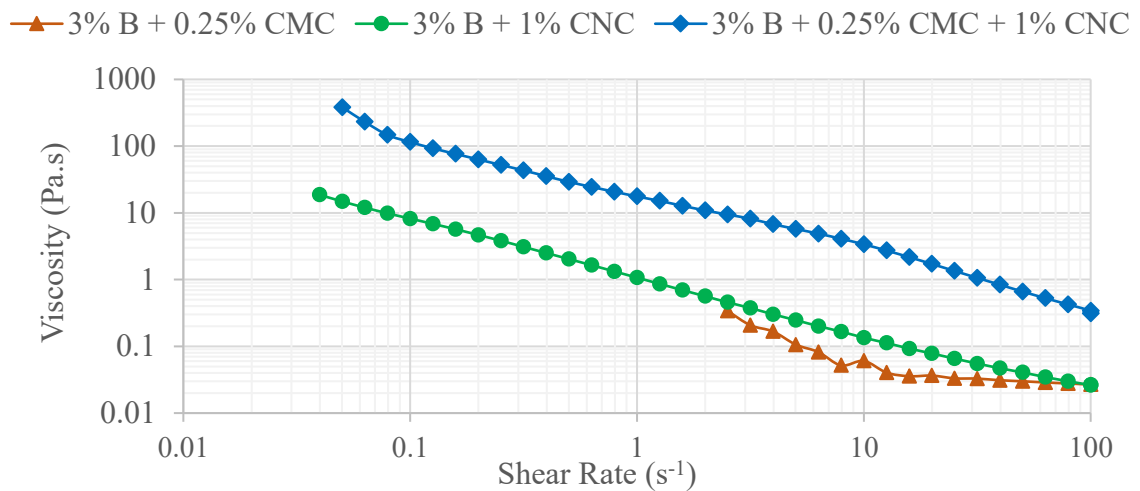


**Figure 3.11.** Variation in viscosity across different suspensions (in the presence of cellulose nanocrystal particles)

### 3.2. Fresh Cementitious Paste

As described earlier in Section 2.2, and 2.3., the colloidal suspensions were introduced into cement paste and the resulting slurry was examined firstly for its rheological parameters and secondly for its workability.

### 3.2.1. Steady Shear Rheology of Fresh Cement Paste

After the colloidal suspensions were evaluated for yield stress and viscosity, the mixtures of cementitious slurry were examined similarly. Again, the Bingham model was utilized here. The variation in yield shear stress and the viscosity of each sample with the applied strain rate is listed in Figures 3.12 and 3.13, respectively. The yield shear stress and viscosity corresponding to each mixture as derived from the Bingham model are listed in Table 3.5.

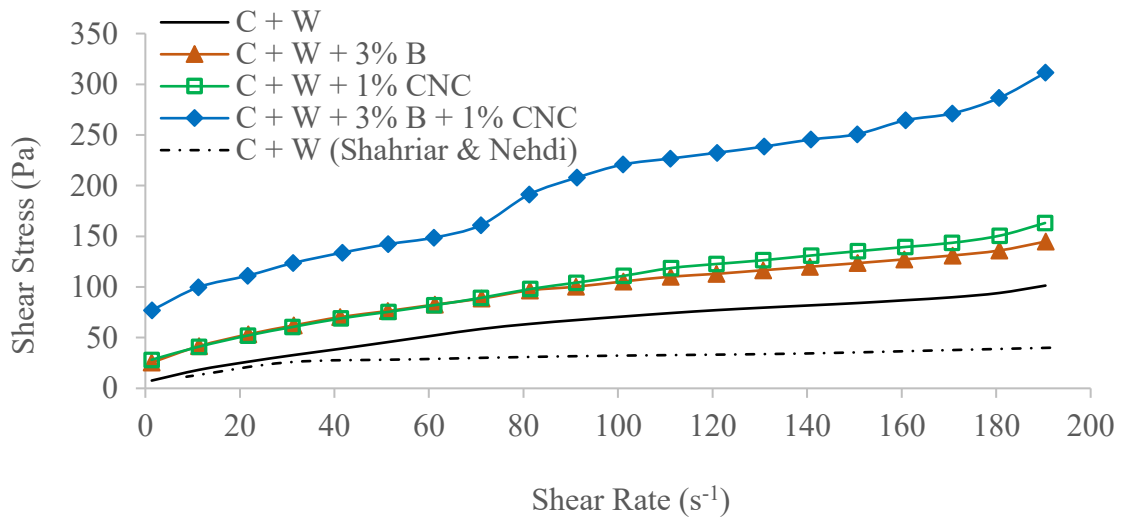


**Figure 3.12.** Effect of mixture composition on rheological behavior of fresh oil well cement paste (1): shear stress profile

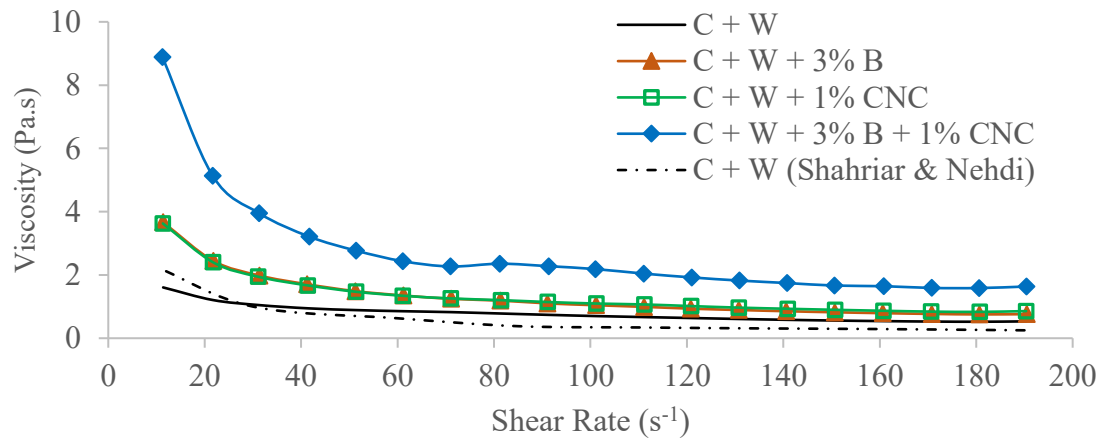


**Figure 3.13.** Effect of mixture composition on rheological behavior of fresh oil well cement paste (2): viscosity profile

**Table 3.5.** Cement paste rheology results

Mix Type	Yield Shear Stress (Pa)	Viscosity (Pa.s)
1) Cement + Water	19.95	0.44
2) Cement + Water + Bentonite	43.47	0.55
3) Cement + Water + CNC	39.68	0.65
4) Cement + Water + Bentonite + CNC	87.05	1.15

A prior study on oil well cement paste by Shahriar and Nehdi had identical water-to-cement ratio [37]. In Figures 3.12 and 3.13, the result from that study is plotted along with those from the present work and was found comparable. Note that there is an increase in the yield shear stress as well as the viscosity of the paste, upon adding CNC. Whereas adding bentonite also results in an increase in these two parameters, the effect was less so compared to adding CNC. Further, the mixture containing both bentonite and CNC displayed the highest viscosity and yield shear stress. Recall that adding CNC and bentonite whether separately or together, had the same effect upon the rheology of the colloidal suspension. In the range of shear stress that was examined here, a shear thinning response was witnessed across all of the mixtures in this study.

### 3.2.2. *Workability of Fresh Cement Paste*

The average diameter and height respectively, of the various mixtures subjected to the mini slump test, are shown in Figure 3.14. Note that in this instance, there was no external load on the paste. As expected from the preceding results using the rheometer, the diameter was smaller upon adding CNC, while there was a drop in the slump for those corresponding mixtures. The yield stress was also calculated (Table 3.6) using the spread diameter

obtained from the mini slump test and the following equation employed by Hoyos et al. [38]:

$$\tau_0 = \frac{225 \cdot \rho \cdot g \cdot V^2}{128 \cdot \pi^2 \cdot R^5}$$

Where V is the tested sample volume and R is the spread diameter measured.

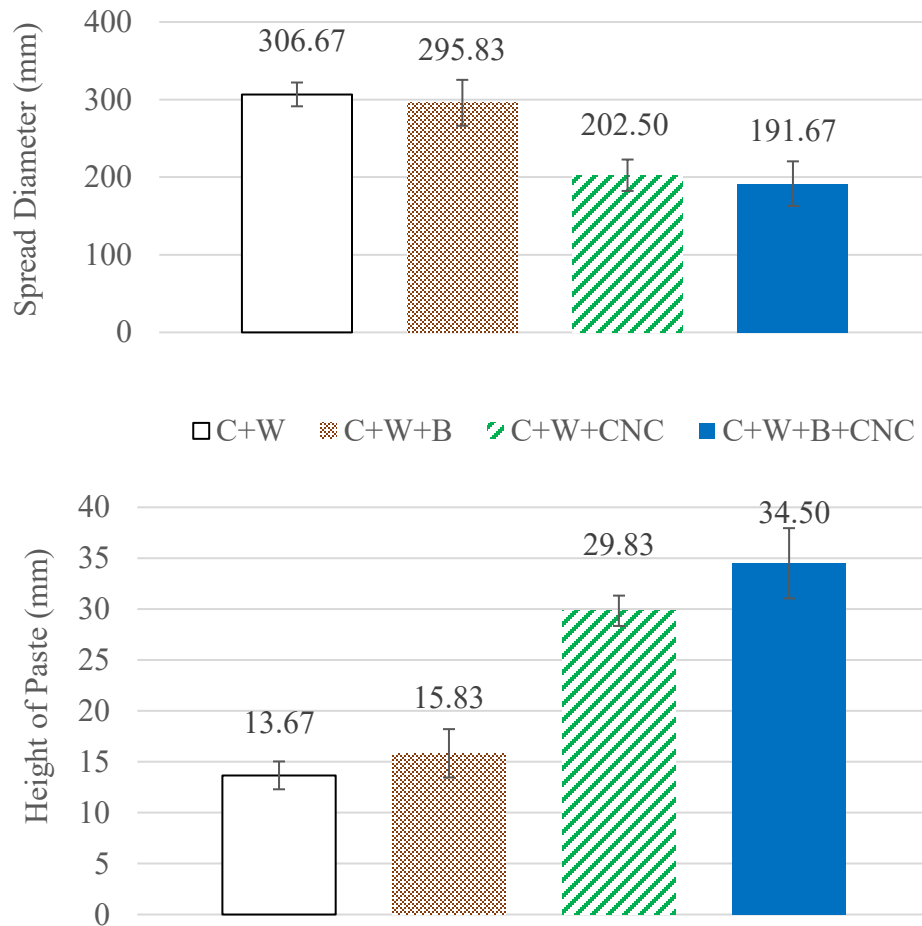


**Figure 3.14.** Results from mini slump test: spread diameter (top) and residual height measured from the base (bottom)

**Table 3.6.** Yield shear stress computed using the equation employed by Hoyos et al. [38]

Mix Type	Yield Shear Stress (Pa)
1) Cement + Water	0.145

2) Cement + Water + Bentonite	0.174
3) Cement + Water + CNC	1.155
4) Cement + Water + Bentonite + CNC	1.520

When the yield shear stress values calculated using the equation are compared to the yield stress values obtained from the rheometer, one can realize that the equation underestimates the yield stress and is not efficient. This may be due to the fact that the provided equation does not consider the surface tension (during the slump test). Therefore, even though it demonstrates the correct pattern (increase in yield stress after CNC and bentonite are added), it is not accurate.

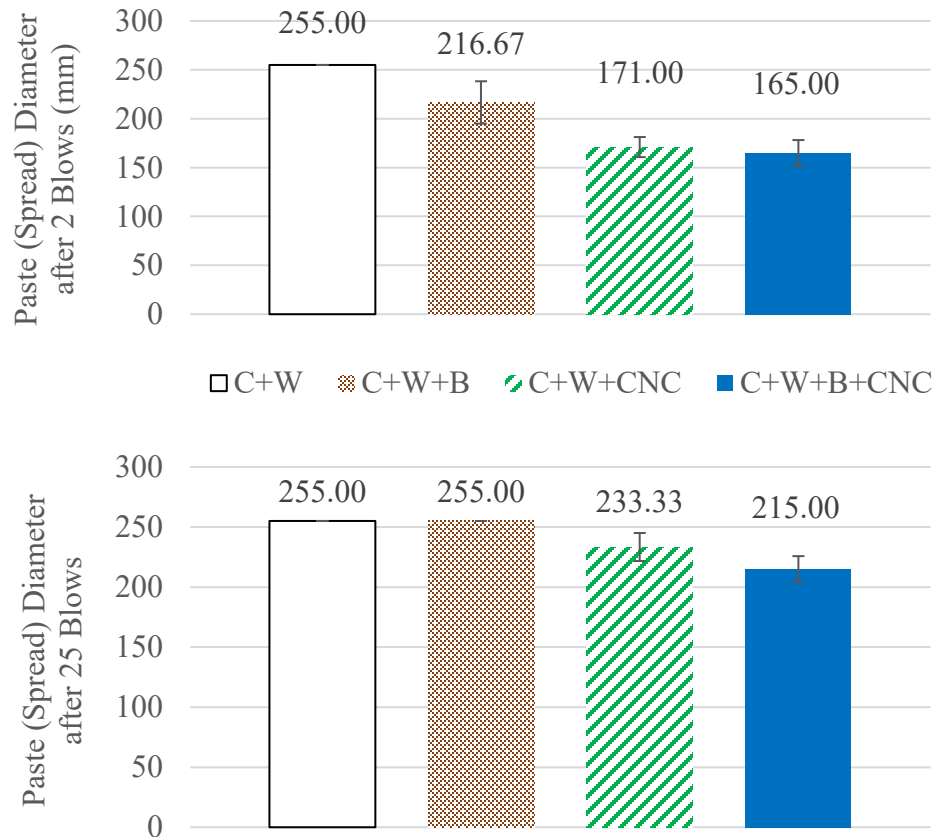


**Figure 3.15.** Flow table test results: spread diameter after 2 blows (top) and spread diameter after 25 blows (bottom)

Moreover, as stated earlier, the flow table test captures the workability of the oil well cement paste, under pressure. It is seen from Figure 3.15 that mixes without CNC could not resist the twenty-five blows on the flow table. On the other hand, after the CNC was introduced to the cementitious system, not only was the diameter significantly lower after only 2 blows but compared to the other mixes, mixes with CNC were able also to withstand the complete twenty-five blow regime on the flow table. This was expected since the yield stress of the cementitious system with CNC is higher than the pastes with no CNC. Note also that the combination of CNC and bentonite was the most desirable in that a higher yield stress is required to cause flow. These results are recorded in Tables 3.7, 3.8 and 3.9 of this chapter.

**Table 3.7.** Flow table spread diameters after 2 blows

<b>Mix Type</b>	<b>C+W</b>	<b>C+W+B</b>	<b>C+W+CNC</b>	<b>C+W+B+CNC</b>
Attempt 1	255	220	167	165
Attempt 2	255	225	174	170
Attempt 3	255	205	172	160
<i>Average</i>	$255.00 \pm 0$	$216.67 \pm 10.41$	$171.00 \pm 3.61$	$165.00 \pm 5$

**Table 3.8.** Flow table spread diameters after 25 blows

<b>Mix Type</b>	<b>C+W</b>	<b>C+W+B</b>	<b>C+W+CNC</b>	<b>C+W+B+CNC</b>
Attempt 1	255	255	230	210
Attempt 2	255	255	235	220
Attempt 3	255	255	235	215
<i>Average</i>	$255.00 \pm 0$	$255.00 \pm 0$	$233.33 \pm 2.89$	$215.00 \pm 5$

**Table 3.9.** Flow table height of residual paste (spread) after 2 blows

Mix Type	C+W	C+W+B	C+W+CNC	C+W+B+CNC
Height of Paste	9	12	19	21

### 3.2.3. Filtration of Fresh Cement Paste

As illustrated in Figure 3.16a, the average time required to collect 100 ml of filtrate from a neat oil well cement paste (with no additive) in the static filtration test, was 73 seconds. However, when CNC was added to the oil well cement paste samples as a fluid loss control additive, this required time was increased to 82 seconds. According to the results obtained, the best performance (slower rate of fluid loss) was observed when both CNC and bentonite were present in the mix design. In this case, it took an average period of 107 seconds to collect 100 ml of filtrate. This was a significant reduction in fluid loss and filtration rate.

Furthermore, Figure 3.16b demonstrates the 2<sup>nd</sup> stage of the experimental measurement. This figure illustrates the required amount of time to collect 150 ml filtrate from the oil well cement paste samples. Based on the obtained results, it took an average period of 582 seconds to collect a filtrate volume of 150 ml from the neat oil well cement paste samples, whereas in the case where oil well cement paste was dosed with CNC particles, this time period increased to 956 seconds, which was almost twice the period required to collect 150ml for neat oil well cement paste. These results show the effect of CNC on the fluid loss behavior of oil well cement pastes. Once again, the effect of cellulose nanocrystal was enhanced when bentonite was also involved in the mix, which confirms the previous stage result.

Eventually, the experiment was carried out for a total duration of 30 minutes, in order to compare the total amount of filtrate volume at the end of the test procedure.

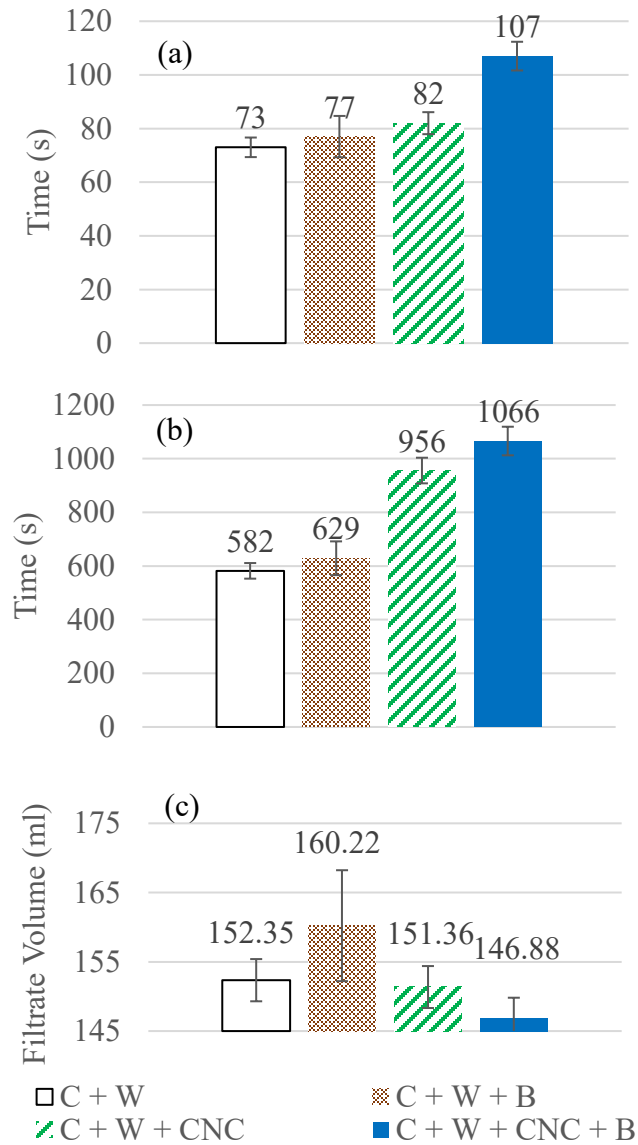


**Figure 3.16.** Static filtration test results; a) Time required to collect 100ml of filtrate volume; b) Time required to collect 150ml of filtrate volume; c) Total amount of filtrate volume after 30 minutes of static filtration

Figure 3.16c illustrates the total amount of fluid loss from each cementitious system and compares all 4 different type of samples. Based on the obtained results, the total amount of fluid loss after 30 minutes was not noticeably different, however, based on Figures 3.16a and 3.16b, the rate of fluid loss was significantly slower when CNC was introduced. The fact that the total amount of fluid loss was almost equal in all cases, could be due to the reason that the duration of the test (30 minutes) for the prepared amount of sample was longer than required.

Interestingly, the oil well cement paste sample including bentonite only (no CNC), showed the worst result in terms of total amount of fluid loss from the system. However, when cellulose nanocrystal particles are introduced to the same system (C+W+CNC+B), the system demonstrates the best performance in terms of fluid loss. Therefore, the presence of both CNC and bentonite at the same time in the mix, not only decreases the filtration rate of the cementitious system but also decreases the total amount of fluid loss and enhances the overall fluid loss behavior of the oil well cement paste sample.

In the studies reported by Plank et al. [10, 11], the additive employed had reduced the filtration (fluid loss) by adsorbing onto the surface of hydrating cement particles. When added to the cementitious system, some of the cellulose nanocrystal particles are also believed to be adsorbed onto the cement particles [27, 28]. Furthermore, the synergic effect between cellulose nanocrystal and bentonite within the cement mix has proved to be significantly beneficial and useful, even though bentonite was initially considered to be a cross contamination agent. The analysis of this synergic effect is not in the scope of this research study, nevertheless, this synergy led to an unexpected improvement in oil well cement paste filtration properties.

#### 4. CONCLUDING REMARKS

The rheological behavior of different types of colloidal suspensions were assessed by to examine the effect of bentonite along with cellulose nanocrystals. Significant changes in viscosity and shear strain were observed due to the addition of the CNC. The trend seen with the rheology testing on colloidal suspensions were utilized to anticipate and predict the behavior of cementitious systems with CNC. The following specific findings were observed:

- The rheological parameters indicate that cellulosic nanocrystals increase the viscosity of bentonite suspensions. As well, CNC makes the suspension stable at low shear rates.
- All the suspensions examined here demonstrated a shear-thinning behaviour. This was more manifest in mixes containing CNC.
- Flow tests on cementitious slurry made with the colloidal suspensions and oil well cement illustrate that adding CNC makes for stable slurries that can survive the 25-blow regime. Whereas adding bentonite alone had very minor effect on the flow diameter and height, the addition of CNC significantly stiffened the mix as expected from the associated low shear rate.
- The rheological results obtained from the cement paste samples match the rheological results obtained from the colloidal suspensions and also the flow test results (on cement paste samples).
- According to the rheological results obtained from the colloidal suspensions, both bentonite and CNC are increasing the yield shear stress and the viscosity of neat

cement paste. However, combining both of the mentioned material together illustrates a significant increase in the parameters discussed.

- The influence of bentonite and CNC on yield shear stress and viscosity (flow behavior) of the cementitious pastes, was almost similar to their influence on the flow behavior of the colloidal suspensions.
- Cellulose nanocrystal (CNC) particles reduced the rate of filtration and fluid loss in oil well cement pastes, therefore, when compared to neat oil well cement slurry, a longer duration was required to collect a specific amount of filtrate when CNC was added.
- Aside from slowing down the filtration process, the total amount of filtrate also decreased (however not significantly) by adding CNC to the system.
- When bentonite was present in the oil well cement paste system, the total amount of fluid loss increased, no matter what the filtration rate was. However, when bentonite was paired with cellulose nanocrystal particles, in an oil well cement paste system, the rate of fluid loss decreased noticeably.
- When cellulose nanocrystal particles and bentonite were both present in the oil well cement paste system at the same time (as additive or cross contamination agent), the oil well cementitious system demonstrated a significantly lower fluid loss.
- A synergic effect between cellulose nanocrystal particles and bentonite was observed within the oil well cementitious system, however, the study and analysis of this effect is not within the scope of this research.

## ACKNOWLEDGMENT

The authors are grateful to Alberta Innovates – Bio Solution for funding the project. Thanks are also due to Alberta Innovates Technology Futures (AITF) and Alpac for supplying CNC samples and to Lafarge Canada for providing the oil well cement employed in this study.

## REFERENCES

- [1] Yahaba, N. (2010). *How Does A Decrease In Oil Production Affect The World Economy?*. Australia-Japan Research Centre.
- [2] Shahriar, A. (2011). *Investigation on rheology of oil well cement slurries* (Doctoral dissertation, The University of Western Ontario).
- [3] Specification, A. P. I. (2010). 10A. *Cements and Materials for Well Cementing*.
- [4] George, C., & Gerke, R. R. (1985). U.S. Patent No. 4,557,763. Washington, DC: U.S. Patent and Trademark Office.
- [5] Smith, D. K. (1989). *Cementing*. SPE Monograph Series. *Society of Petroleum Engineers, Richardson, Texas*.
- [6] Bülichen, D., & Plank, J. (2012). Mechanistic study on carboxymethyl hydroxyethyl cellulose as fluid loss control additive in oil well cement. *Journal of Applied Polymer Science*, 124(3), 2340-2347.

- [7] Bannister, C. E. (1978, January). Evaluation of Cement Fluid-Loss Behavior Under Dynamic Conditions. In *SPE Annual Fall Technical Conference and Exhibition*. Society of Petroleum Engineers.
- [8] Brice Jr, J. W., & Holmes, B. C. (1964). Engineered Casing Cementing Programs Using Turbulent Flow Techniques. *Journal of Petroleum Technology*, 16(05), 503-508.
- [9] Nelson, E. B. (Ed.). (1990). *Well cementing* (Vol. 28). Newnes.
- [10] Plank, J., Brandl, A., Zhai, Y., & Franke, A. (2006). Adsorption behavior and effectiveness of poly (N, N-dimethylacrylamide-co-Ca 2-acrylamido-2-methylpropanesulfonate) as cement fluid loss additive in the presence of acetone-formaldehyde-sulfite dispersant. *Journal of applied polymer science*, 102 (5), 4341-4347.
- [11] Plank, J., Lummer, N. R., & Dugonjić-Bilić, F. (2010). Competitive adsorption between an AMPS®-based fluid loss polymer and Welan gum biopolymer in oil well cement. *Journal of applied polymer science*, 116(5), 2913-2919.
- [12] Picandet, V., Rangeard, D., Perrot, A., & Lecompte, T. (2011). Permeability measurement of fresh cement paste. *Cement and Concrete Research*, 41(3), 330-338.
- [13] Pierre, A., Perrot, A., Picandet, V., & Guevel, Y. (2015). Cellulose ethers and cement paste permeability. *Cement and Concrete Research*, 72, 117-127.
- [14] Dufresne, A. (2013). Nanocellulose: a new ageless bionanomaterial. *Materials Today*, 16(6), 220-227.

- [15] Bondeson, D., Mathew, A., & Oksman, K. (2006). Optimization of the isolation of nanocrystals from microcrystalline cellulose by acid hydrolysis. *Cellulose*, 13(2), 171-180.
- [16] Boluk, Y., Lahiji, R., Zhao, L., & McDermott, M. T. (2011). Suspension viscosities and shape parameter of cellulose nanocrystals (CNC). *Colloids and Surfaces A: Physicochemical and Engineering Aspects*, 377(1), 297-303.
- [17] Habibi, Y., Lucia, L. A., & Rojas, O. J. (2010). Cellulose nanocrystals: chemistry, self-assembly, and applications. *Chemical reviews*, 110(6), 3479-3500.
- [18] Venere, E. (2013). Cellulose nanocrystals possible green wonder material. *Science Daily*.
- [19] Kamal, M. R., & Khoshkava, V. (2015). Effect of cellulose nanocrystals (CNC) on rheological and mechanical properties and crystallization behavior of PLA/CNC nanocomposites. *Carbohydrate polymers*, 123, 105-114.
- [20] Dufresne, A. (2012). *Nanocellulose: from nature to high performance tailored materials*. Walter de Gruyter.
- [21] Shafeiei Sabet, S., Hamad, W. Y., & Hatzikiriakos, S. G. (2013). Influence of degree of sulfation on the rheology of cellulose nanocrystal suspensions. *Rheologica Acta*, 52(8-9), 741-751.
- [22] Shafeiei Sabet, S. (2013). *Shear rheology of cellulose nanocrystal (CNC) aqueous suspensions* (Doctoral dissertation, University of British Columbia).

- [23] Wu, Q., Meng, Y., Wang, S., Li, Y., Fu, S., Ma, L., & Harper, D. (2014). Rheological behavior of cellulose nanocrystal suspension: influence of concentration and aspect ratio. *Journal of Applied Polymer Science*, 131(15).
- [24] Ureña-Benavides, E. E., Ao, G., Davis, V. A., & Kitchens, C. L. (2011). Rheology and phase behavior of lyotropic cellulose nanocrystal suspensions. *Macromolecules*, 44(22), 8990-8998.
- [25] Qiao, C., Chen, G., Zhang, J., & Yao, J. (2016). Structure and rheological properties of cellulose nanocrystals suspension. *Food Hydrocolloids*, 55, 19-25.
- [26] Li, M. C., Wu, Q., Song, K., Qing, Y., & Wu, Y. (2015). Cellulose nanoparticles as modifiers for rheology and fluid loss in bentonite water-based fluids. *ACS applied materials & interfaces*, 7(8), 5006-5016.
- [27] Cao, Y., Zaverri, P., Youngblood, J., Moon, R., & Weiss, J. (2015). The influence of cellulose nanocrystal additions on the performance of cement paste. *Cement and Concrete Composites*, 56, 73-83.
- [28] Cao, Y., Tian, N., Bahr, D., Zavattieri, P. D., Youngblood, J., Moon, R. J., & Weiss, J. (2016). The influence of cellulose nanocrystals on the microstructure of cement paste. *Cement and Concrete Composites*, 74, 164-173.
- [29] Canadian Standards Association. (2013). CSA A3000–13 Cementitious materials compendium. *CSA Group*.
- [30] Standard, A. S. T. M. "C150/C150M-17 (2017)." *Standard specification for Portland cement* (2017).

- [31] Grim, R. E. (1955). Clay mineralogy, 1968. *Karl Jasmund, Die silicatischen Tonminerale, 2nd enlarged ed.*
- [32] Luckham, P. F., & Rossi, S. (1999). The colloidal and rheological properties of bentonite suspensions. *Advances in Colloid and Interface Science*, 82(1), 43-92.
- [33] Coussot, P., Bertrand, F., & Herzhaft, B. (2004). Rheological behavior of drilling muds, characterization using MRI visualization. *Oil & gas science and technology*, 59(1), 23-29.
- [34] Benchabane, A., & Bekkour, K. (2008). Rheological properties of carboxymethyl cellulose (CMC) solutions. *Colloid and Polymer Science*, 286(10), 1173-1180.
- [35] Zomorrodian, M. A. (2014). *Wellbore integrity: Modifying and characterizing oil well cement to enhance wellbore logging and prevent perforating damages in hydraulic fractured wells.* (Master's Thesis, University of Houston).
- [36] API, R. (2005). 13B-2. *Recommended Practice for Field Testing of Oil-based Drilling Fluids.*
- [37] Shahriar, A., & Nehdi, M. L. (2012). Rheological properties of oil well cement slurries. *Proceedings of the ICE-Construction Materials*, 165(1), 25-44.
- [38] Hoyos, C. G., Cristia, E., & Vázquez, A. (2013). Effect of cellulose microcrystalline particles on properties of cement based composites. *Materials & Design*, 51, 810-818.

## Chapter IV

# *Dynamic Mechanical Properties of Oil Well Cement Paste Dosed with Cellulose Nanocrystal (CNC) Particles*

### **ABSTRACT**

This study examines the effect of cellulose nanocrystal (CNC) particles on the dynamic mechanical properties of oil well cement paste. Using oscillatory rheology, the linear viscoelastic range of CNC-dosed oil well cement paste was determined and the frequency sweep test was performed at the critical strain. According to the results obtained, the presence of CNC enhances the complex viscosity, rigidity, hydration rate and solidification of oil well cement paste.

*Keywords: Oil Well Cement, Cellulose Nanocrystal, Dynamic Mechanical Properties, Oscillatory Rheology, Viscoelastic Behavior, Hydration, Solidification*

## **1. INTRODUCTION**

### **1.1. Oil Well Cement**

Oil well cement paste is placed inside the annular space between the casing and the ground formation [1]. It is believed that the main functions of an oil well cement paste present in a wellbore, is to restrict the movement of the fluids between formations and to protect and support the casing from any kind of damage [1, 2]. The oil well cement paste designed and prepared is pumped inside the wellbore, therefore the flow behavior and rheology of it is of great importance [3]. Furthermore, Shahriar claims that the productivity of an oil or gas well is reliant on the quality of cement sheath in between the casing and the ground formation [3].

Oil well cement needs to be perfectly pumpable and flowable while fresh (before setting), however, loss circulation should also be taken into account, while tuning the rheological behavior of the paste [3]. Rheological characterization of materials is performed by utilizing different controlled methods such as steady shear method, stress relaxation method, oscillatory method, etc. Furthermore, the obtained results and findings are quantified and assessed using material functions such as viscosity, storage and loss modulus, creep, etc. [4].

### **1.2. Oscillatory (Dynamic Mode) Rheology**

The most common technique used to study the rheological behavior of nonlinear viscous materials is known to be the steady shear measurement technique. In this technique, a steady stress response of the material is measured at different strain rates applied. Therefore, one is able to differentiate different types of behavior (such as shear thinning or

shear thickening behavior). On the other hand, the most common technique employed to study the rheological behavior of a viscoelastic material under linear deformation is the oscillatory shear measurement [4-6]. Dynamic mechanical analysis of any (viscoelastic) material is examined by conducting a set of oscillatory tests. These tests or experiments are usually referred to as dynamic mechanical analysis [7]. Majority of the rheological studies on cementitious systems are steady shear rheological assessments [8, 9], which only provide information about the workability and flowability of the cementitious system [10]. Furthermore, steady shear rheology analysis does not deliver fundamental information regarding the evolution of the structure of the paste and the forces responsible for its associated mechanical properties [10]. Therefore, for such information, dynamic mode rheology (oscillatory rheology) is utilized as an ideal technique [10]. However, according to Schultz and Struble [11], dynamic mechanical analysis or oscillatory rheology would only be acceptable if it is performed in the linear viscoelastic domain of the material. Hence, the shear strain value selected for such measurements needs to be below the critical strain and in the linear region [10, 11].

### **1.3. Objectives of Study**

The aim of this study is to investigate and study the influence of cellulose nanocrystal (CNC) particles on the dynamic mechanical properties of oil well cement paste. In order to understand the impact caused by CNC particles, different types of samples are prepared and a number of parameters such as storage modulus and loss modulus are assessed. Furthermore, by obtaining and plotting the damping (loss) factor associated with each individual mix design, the influence of CNC particles on the hydration process is also

explored. Finally, the results obtained from the oscillatory rheology are compared to the shear rheology results achieved previously.

## 2. EXPERIMENTAL DETAILS

### 2.1. Materials

The cementitious systems prepared and tested in this study were composed of water, oil well cement Type G, cellulose nanocrystal (CNC) and bentonite.

#### 2.1.1. Oil Well Cement Type G

The cement used for this experimental study was Type G cement, based on the American Petroleum Institute (API) classification, specification 10A for oil well cements [12]. Type G cement is comparable to CSA Type MS (ASTM Type II) or CSA Type HS (Type V Portland cement) [13, 14]. It is recommended by the API classification 10A to use a water-to-cement ratio of 0.44 for this type of cement. Hence, all the pastes prepared and tested in this study have a water-to-cement ratio of 0.44. Tables 4.1 and 4.2, describe the physical properties and chemical composition of this type of cement, respectively.

**Table 4.1.** Physical properties of Type G cement (prepared by Lafarge Canada, December 8<sup>th</sup>, 2015)

<b>Physical Analysis</b>	
Thickening Time (Schedule 5)	99 min.
Max. Consis. 15-30 min.	23 Bc
Fineness 45 $\mu\text{m}$ sieve	93.9%
Blaine	311 $\text{m}^2/\text{kg}$
Free Fluid	4.4 %

**Table 4.2.** Chemical composition of Type G cement (prepared by Lafarge Canada, December 8<sup>th</sup>, 2015)

<b>Chemical Analysis</b>	
Silica (SiO <sub>2</sub> )	20.9%
Alumina (Al <sub>2</sub> O <sub>3</sub> )	3.8%
Iron Oxide (Fe <sub>2</sub> O <sub>3</sub> )	4.7%
Calcium Oxide, Total (TCaO)	62.9%
Magnesium Oxide (MgO)	4.5%
Sulphur Trioxide (SO <sub>3</sub> )	2.6%
Loss on Ignition	0.66%
Insoluble Residue	0.13%
Equivalent Alkali (as Na <sub>2</sub> O)	0.48%
C <sub>3</sub> S	57.9%
C <sub>2</sub> S	16.1%
C <sub>3</sub> A	2.0%
C <sub>4</sub> AF	14.3%
C <sub>4</sub> AF + 2X C <sub>3</sub> A	18.3%

### 2.1.2. Cellulose Nanocrystal (CNC)

The additive proposed and utilized in this study was cellulose nanocrystal (CNC). Cellulose is believed to be the most available renewable polymer resource present nowadays [15]. For approximately 150 years, cellulose has been used in different forms such as fibers or other derivatives, and it has been utilized in a wide range of products, materials and applications. However, it has only recently been discovered that when these cellulose fibers are subjected to acid hydrolysis, rod-shaped crystalline residues will be obtained. They are generally referred to as cellulose nanocrystal (CNC) particles [15].

These biopolymeric assemblies have drawn significant attention towards themselves due to their ideal physical and chemical properties, and also because of their inherent renewability and sustainability. In fact, because of their low cost, abundance, light weight, nanoscale dimension and morphology, these nanocrystals have been employed in a wide range of research and studies as a reinforcing agent in nanocomposites [15]. In this study, the aspect ratio (length/diameter) of the cellulose nanocrystal (CNC) particles used, are in between 10-60 with a dosage of 1% (w/v of water).

### *2.1.3. Bentonite*

Bentonite is employed in different industries, because of their unique ability to provide adequate particle dispersion [16]. Also, it is believed that when bentonite particles are added as additives to a certain host material (or matrix), they tend to stabilize the system [16]. However, it is well understood that due to the possible aggregation of bentonite particles (in different pressure and temperature conditions), the flow behavior of the system containing bentonite will eventually change and parameters such as viscosity and yield will be affected [17].

Bentonite particles are widely used in drilling procedures and are one of the most common constituent materials in drilling fluids [16]. Since the cementing operation in a wellbore takes place after the drilling process, bentonite contamination is a possibility. Therefore, in this study bentonite is employed as a cross contamination agent with a dosage of 3% (w/v of water). Note that the bentonite utilized in this study is commercially referred to as Wyoming Gel.

## 2.2. Slurry Preparation

In this experimental study, 4 different types of slurries were designed and prepared. The composition (formulation) of these cementitious systems is described and presented in Table 4.3:

**Table 4.3.** Formulation and designation of the samples prepared

	Composition (w/c = 0.44)	Designation
<i>Sample 1</i>	Cement and water (Neat, no additive)	C+W
<i>Sample 2</i>	Cement, water and 3% bentonite	C+W+B
<i>Sample 3</i>	Cement, water and 1% CNC	C+W+CNC
<i>Sample 4</i>	Cement, water, 3% bentonite and 1% CNC	C+W+B+CNC

Note that bentonite and cellulose nanocrystal particles were mixed with water using a high shear mixer, then added to the cement mixer in the form of a suspension. The mixing water used in this part of the preparation was later deducted from the total water calculated (in the mix design), in order to prevent or minimize any change in the water-to-cement ratio.



**Figure 4.1.** Mixers used to prepare bentonite/CNC suspensions (left) and oil well cement slurry (right)

Table 4.4 demonstrates a sample mix design identical to the mix design used in this research study.

**Table 4.4.** Mix design (sample) for preparation of cement paste

<b>Oil Well Cement Paste (Mix Design)</b>	
Cement	1000 kg
Water	440 kg
Bentonite	13.2 kg
Cellulose nanocrystal (CNC) particles	4.4 kg

As was done earlier, again, the bentonite and CNC were individually homogenized in a suitable fraction of the mix water. The oil well cement was mixed first with the remaining water to prepare a slurry. The bentonite and CNC, now in their own suspensions, were then added to the slurry and the mixture was agitated further for 5 minutes. The resulting fresh paste was then tested for dynamic mechanical properties and oscillatory rheological assessment. Note that due to the inherent properties of cellulose nanocrystal (CNC) particles, the dosage being added to the mix design (in this case 1% of the total amount of water or approximately 0.5% mass fraction of the total amount of cement powder used), and their associated mechanism of adsorption with the water molecules, any change to the water-to-cement ratio of the prepared cementitious system will be negligible. Recent studies have also confirmed that despite their hydrophilic nature, even with higher dosages of CNC used, at a high relative humidity (approximately 97% where CNC particles are immersed in water), the water adsorption of dry CNC particles is in the region of 34% which is only about 0.7% of the total mixing water in mass [18]. In this study, considering the fact that CNC particles are added to the mix design in the form of an aqueous solution (similar high relative humidity as the mentioned study), the adsorbed water on CNC will

be approximately 0.3% of the total mixing water in mass. Therefore, based on Table 4.4, the water-to-cement ratio will change from a value of “440 kg / 1000 kg = 0.44” to a revised value of “441.5 kg / 1000 kg = 0.4415” which is negligible.

### **2.3. Test Methods**

The dynamic mode (oscillatory) rheology measurement procedure employed in this study had two major parts.

#### *2.3.1. Part (I): Strain Amplitude Sweep Test*

Nowadays, modern and well-designed rheometers are utilized to carry out such investigations. As mentioned by Mezger in the “Rheology Handbook”, these modern rheometers measure the torque and also the deflection angle is determined by an optoelectronic incremental position sensor [7]. This test was performed to identify the linear viscoelastic range where both storage modulus and loss modulus display constant plateau values. This part of the experiment was executed at a temperature of 25°C and normal atmospheric pressure with an angular frequency of 1 rad/sec. After the cement paste samples were prepared as described in the previous section, a small portion of it was placed on the surface of a TA rheometer used for shear and oscillatory rheology tests. For the cementitious pastes prepared, the rheometer required a cone-plate setup, with a diameter of 20 mm and grated surface. In order to perform the test, the rheometer was turned on together with the water pump and air pipes attached to it. After assembling the cone and plate assembly, the selected geometry was assembled and set into the rheometer. The plate used in this experiment would also be identical to the one used in shear rheology test explained earlier in this thesis. Furthermore, the results from this part of the experiment

also verify whether the storage modulus of the material is greater than the loss modulus or not. This clarifies the fact that whether the material demonstrates a gel-like character in the linear viscoelastic range or a viscoelastic liquid character.

### 2.3.2. Part (II): Frequency Sweep Test

After observing the linear viscoelastic range of the material and the character it represents, it was necessary to investigate the time-dependent deformation behavior of the cement paste in mind. This test was performed at various frequencies, with a controlled shear strain usually referred to as the critical strain value [19]. Note that this measurement must be carried out in the linear viscoelastic range, therefore the shear strain selected for this stage of the experiment, should lie within the linear viscoelastic range of the strain amplitude sweep measurements performed earlier. Finally, the storage and the loss modulus of the material were plotted against the varying angular frequency to identify which one is frequency dependent. Furthermore, as claimed by Zhang et al [20], by obtaining the damping factor ( $\tan\delta$ ) from the phase angle ( $\delta$ ), and plotting it against angular velocity, the influence of cellulose nanocrystal (CNC) particles on the hydration of oil well cement paste was also explored and studied. The relationship between phase angle, loss modulus and storage modulus can be written as below [7]:

$$\tan\delta = G'' / G'$$

## 3. RESULTS AND DISCUSSION

As described earlier in this chapter, in order to understand the viscoelastic behavior of the oil well cement paste developed in this experimental study, and specifically the effect of cellulose nanocrystal (CNC) particles on that, the dynamic mechanical properties of fresh

oil well cement paste were assessed and studied using a set of oscillatory tests. The results are reported below.

### 3.1. Strain Amplitude Sweep Test Results

#### 3.1.1. Linear Viscoelastic Domain (Range) and Critical Strain $\gamma_c$

The first step was to perform a strain amplitude sweep test on the fresh cementitious pastes developed, to identify the linear viscoelastic domain associated with each sample. The critical strain value ( $\gamma_c$ ) needs to be identified prior to any dynamic mode rheological experiments. After evaluating the critical strain value, dynamic mode rheology is then possible, provided that the strain is kept below the critical value.

Based on the results obtained from testing the prepared samples using the strain amplitude sweep test, the critical strain value was found to be approximately 0.01% strain for all of the samples. This value (0.01%) was in agreement and very close to the values reported in the literature, whereas Nachbaur [10] has reported a critical strain value of 0.03% and Betioli et al. [19] have recorded their critical strain value as 0.01%. These values are in the same order of magnitude as the critical strain value obtained in this study.

Hence, this value was selected to perform the frequency sweep tests. The strain amplitude sweep test results associated with the fresh cementitious samples prepared in this study are illustrated further in this chapter (Figures 4.2-4.5 demonstrate the linear viscoelastic domain (range) for each of the tested samples). In all of the samples tested storage modulus was found to be greater than loss modulus ( $G' > G''$ ). This justifies the fact that the tested material demonstrates a solid-like behavior [7, 10].

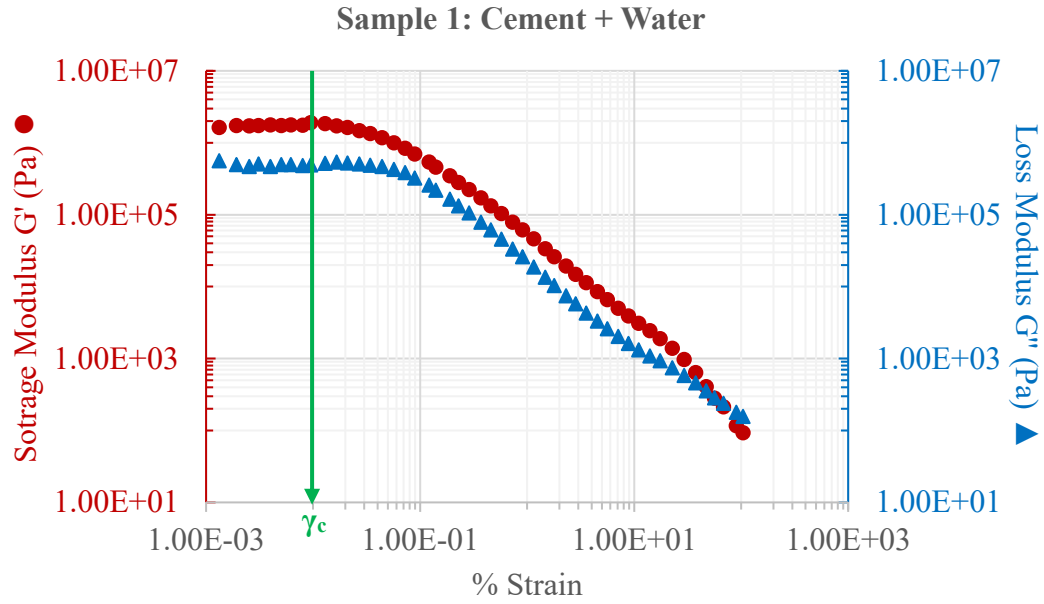


**Figure 4.2.** Strain amplitude sweep test result demonstrating the linear viscoelastic range associated with sample 1 (C+W)

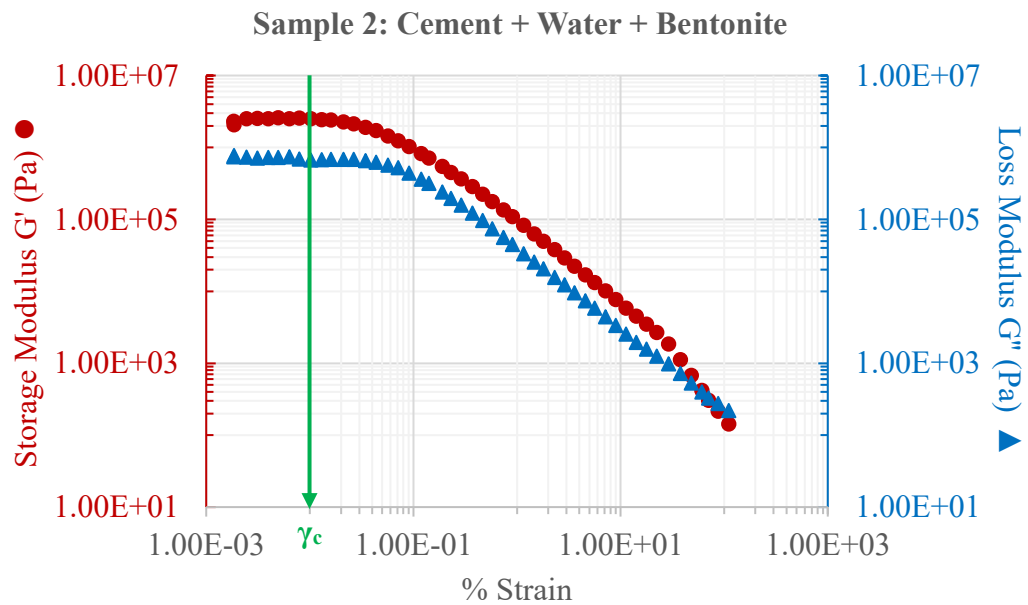


**Figure 4.3.** Strain amplitude sweep test result demonstrating the linear viscoelastic range associated with sample 2 (C+W+B)

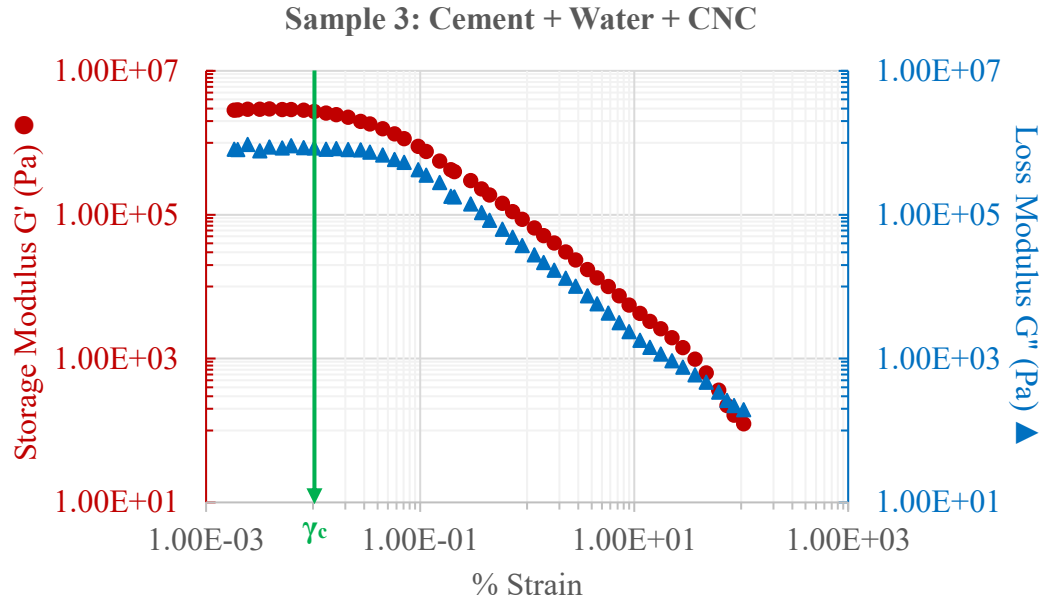


**Figure 4.4.** Strain amplitude sweep test result demonstrating the linear viscoelastic range associated with sample 3 (C+W+CNC)

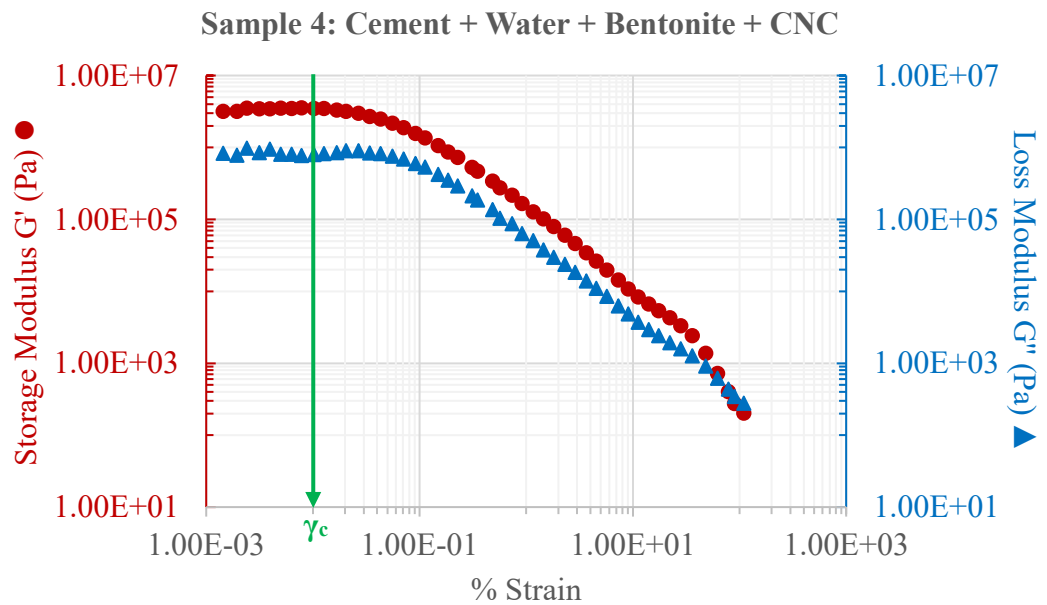


**Figure 4.5.** Strain amplitude sweep test result demonstrating the linear viscoelastic range associated with sample 4 (C+W+B+CNC)

### 3.1.2. Effect of CNC on Storage Modulus ( $G'$ ) and Loss Modulus ( $G''$ )

Based on the present literature, storage modulus ( $G'$ ) illustrates the elastic behavior of the material under examination and loss modulus ( $G''$ ) represents the viscous behavior associated with it [7]. According to the results obtained in this study, both Storage Modulus ( $G'$ ) and Loss Modulus ( $G''$ ) increased after cellulose nanocrystal particles were introduced to the cementitious system, within the viscoelastic range. The cementitious system containing both bentonite and cellulose nanocrystal (CNC) particles demonstrated the highest storage and loss modulus. However, this increase and enhancement were more noticeable in the storage modulus, whereas the loss modulus did not follow a linear trend. Figures 4.6 and 4.7 illustrate the change in storage modulus ( $G'$ ) and loss modulus ( $G''$ ) with strain, in the viscoelastic domain, for all of the samples prepared.

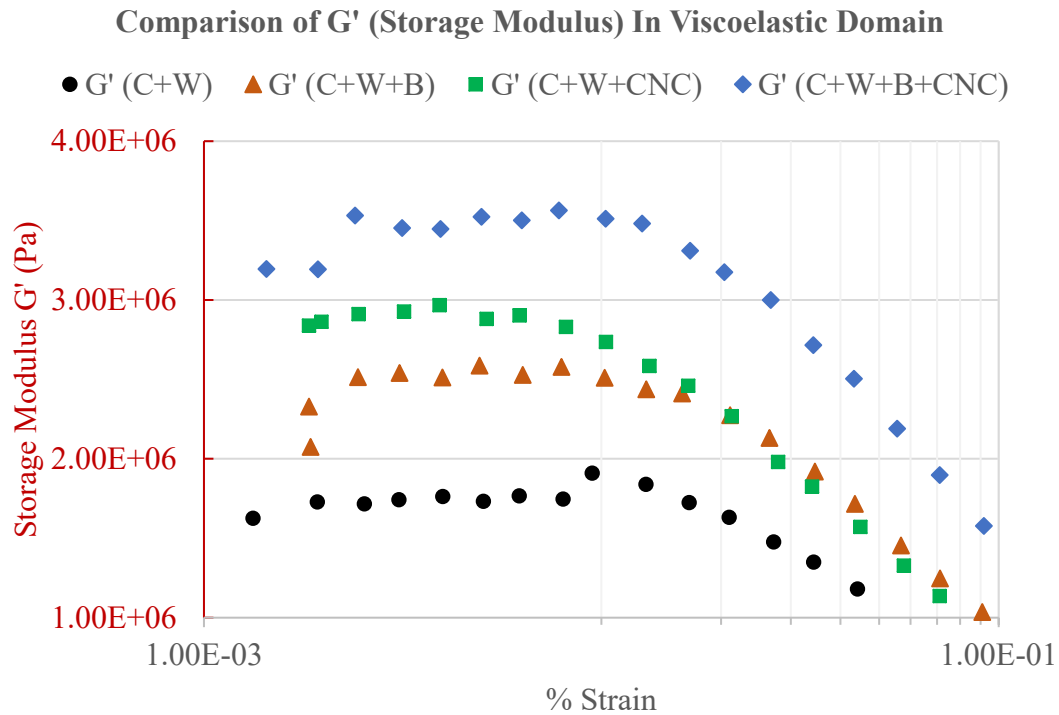


**Figure 4.6.** Strain amplitude sweep test result demonstrating the change in storage modulus ( $G'$ ), in the viscoelastic domain for all samples

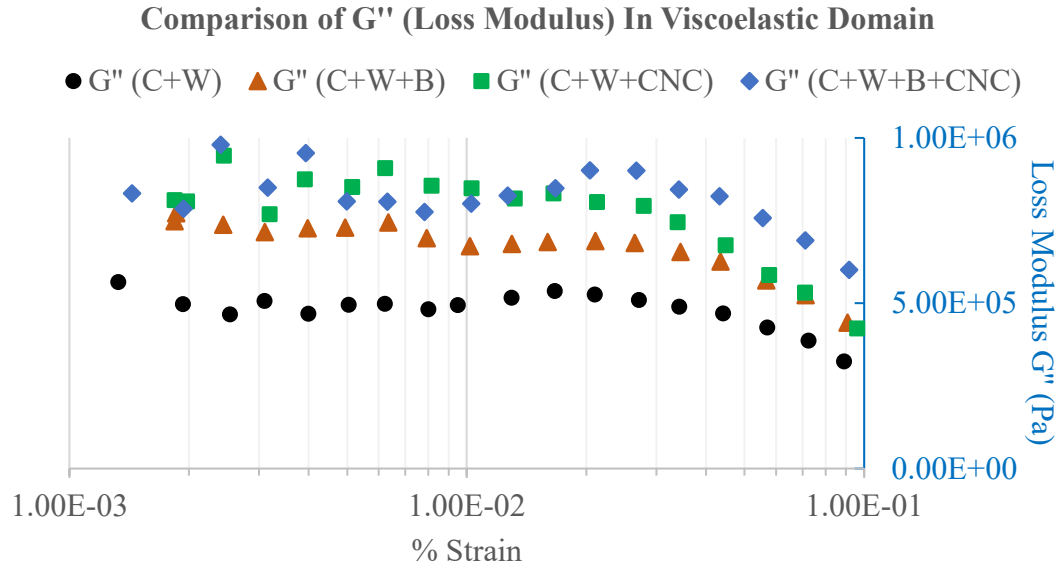


**Figure 4.7.** Strain amplitude sweep test result demonstrating the change in loss modulus ( $G''$ ), in the viscoelastic domain for all samples

### 3.2. Frequency Sweep Test Results

After identifying the linear viscoelastic domain associated with each sample, the critical strain value ( $\gamma_c$ ) was selected to perform the frequency sweep test. As mentioned earlier the critical strain value ( $\gamma_c$ ) chosen at this stage of the experimental study presented here was 0.01% for all 4 types of samples under examination.

#### 3.2.1. Evolution of Storage Modulus ( $G'$ ) and Loss Modulus ( $G''$ )

When a material undergoes a shear process and deforms, a deformation energy is stored in it. The storage modulus ( $G'$ ) of a material is basically a measure of this stored energy [7]. This energy is available after unloading the sample or the specimen and will unveil itself as a driving force in order to partially or completely compensate the deformation developed in the structure of the material. Hence, it may be concluded that the storage modulus ( $G'$ )

illustrates the elastic behavior of the material under examination and it is usually represented in Pa (as its unit) [7]. This parameter is associated with the stiffness of the material [7]. According to Figures 4.8-4.11 (provided in this chapter), the storage modulus ( $G'$ ) of oil well cement paste increases with an increase in angular velocity. This increase was even greater when cellulose nanocrystal was present in the mix. Furthermore, the storage modulus ( $G'$ ) can be compared to the proportional limit range on the stress-strain diagram. On the other hand, the loss modulus ( $G''$ ) of oil well cement paste was found to be independent of the angular velocity. In other words, the storage modulus can be labeled as frequency dependent (in oil well cement) while the loss modulus cannot. Also, an increase in storage modulus justifies the fact that the energy stored in the material while shearing it has also increased. Additionally, this could be further interpreted by declaring an increase in solidification process of the CNC dosed cement paste, compared to the neat sample. This increase in stored energy and solidification could be a sign of an increase in the rate of hydration, in a cementitious system.

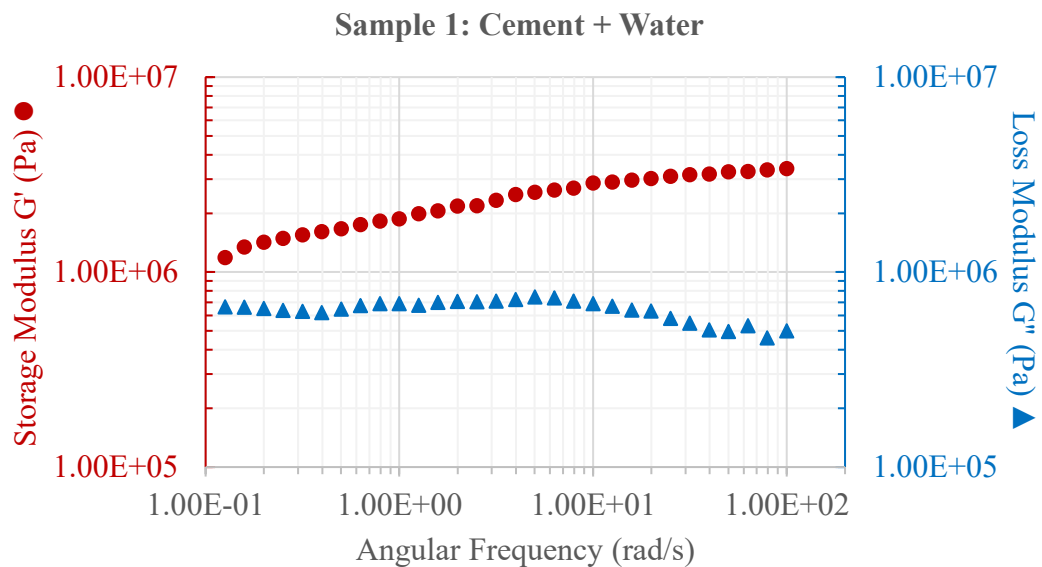


**Figure 4.8.** Variation in storage modulus ( $G'$ ) and loss modulus ( $G''$ ) of sample 1 (C+W) with respect to angular frequency

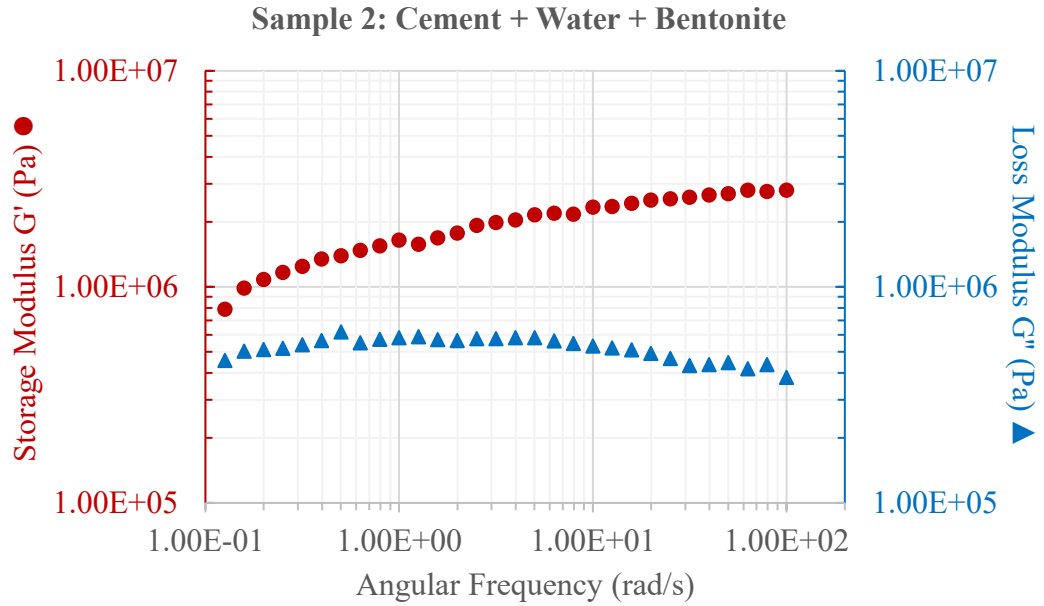


**Figure 4.9.** Variation in storage modulus ( $G'$ ) and loss modulus ( $G''$ ) of sample 2 (C+W+B) with respect to angular frequency

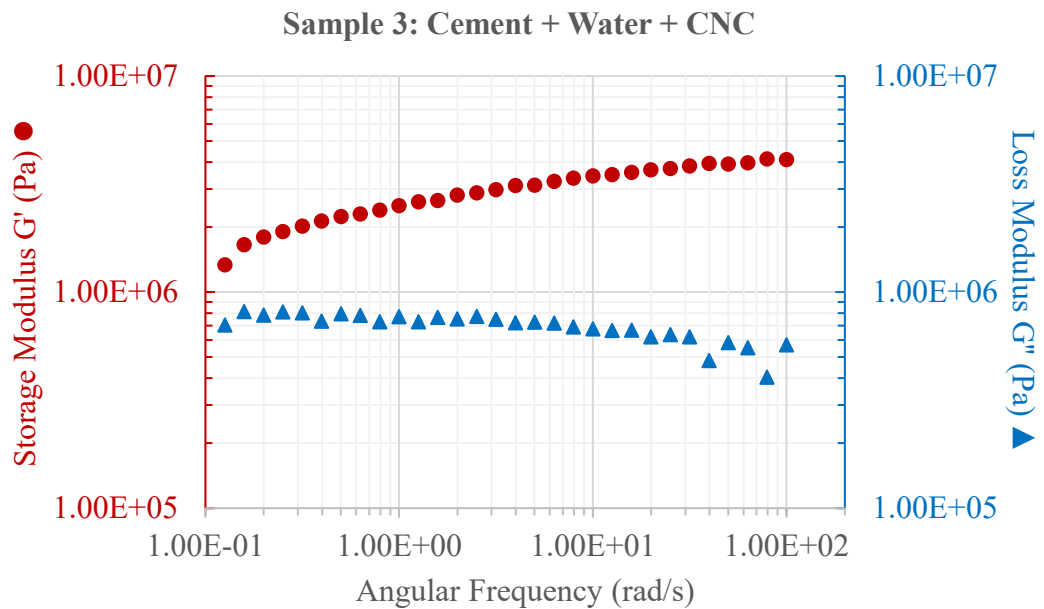


**Figure 4.10.** Variation in storage modulus ( $G'$ ) and loss modulus ( $G''$ ) of sample 3 (C+W+CNC) with respect to angular frequency

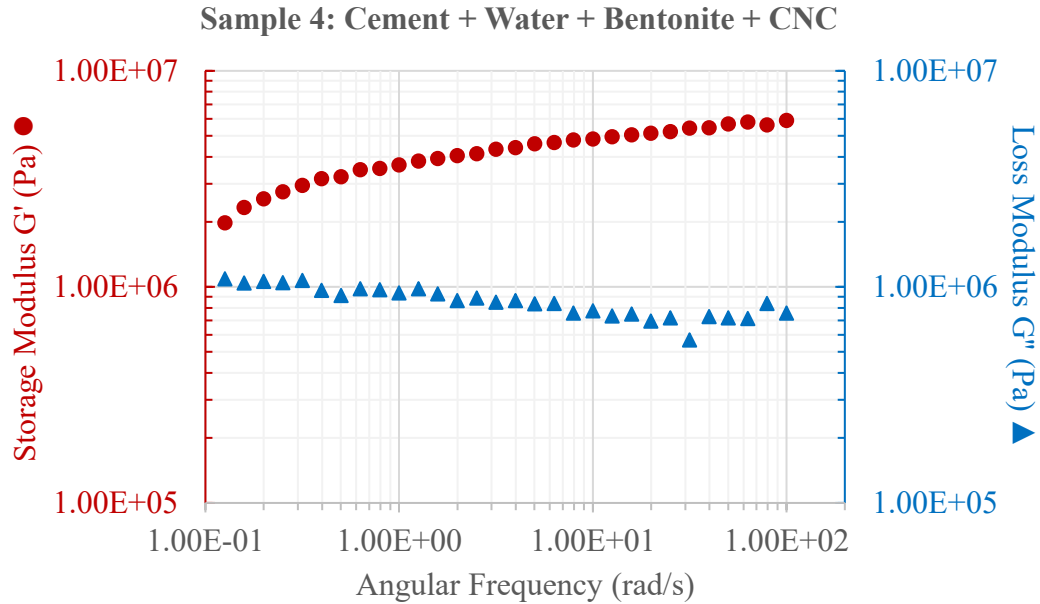


**Figure 4.11.** Variation in storage modulus ( $G'$ ) and loss modulus ( $G''$ ) of sample 4 (C+W+B+CNC) with respect to angular frequency

Moreover, Figures 4.12 and 4.13 provide a better comparison in between the samples prepared. As clearly illustrated, all 4 cementitious samples prepared and tested in this experimental study, show an enhancement in their storage modulus ( $G'$ ) with an increase in angular velocity. This justifies the fact that the storage modulus ( $G'$ ) in cement paste is frequency dependent. Furthermore, Figure 4.12 proves that the cementitious sample containing both bentonite and cellulose nanocrystal (CNC) particle demonstrates the greatest storage modulus values within the angular velocity range investigated. In sample 3 where CNC is employed without bentonite, an increase in storage modulus ( $G'$ ) is still witnessed, although not as much as sample 4. Zhang et al [20] claim that an increase in the storage modulus justifies an increase in cement hydration. Therefore, with such a justification, CNC particles could prove to enhance the cement hydration, with or without bentonite. On the other hand, no significant change in loss modulus ( $G''$ ) was observed

when angular velocity increased, verifying the fact that loss modulus was not frequency dependent. Note that, the presence of CNC also increased the loss modulus compared to the neat cementitious sample (C+W).

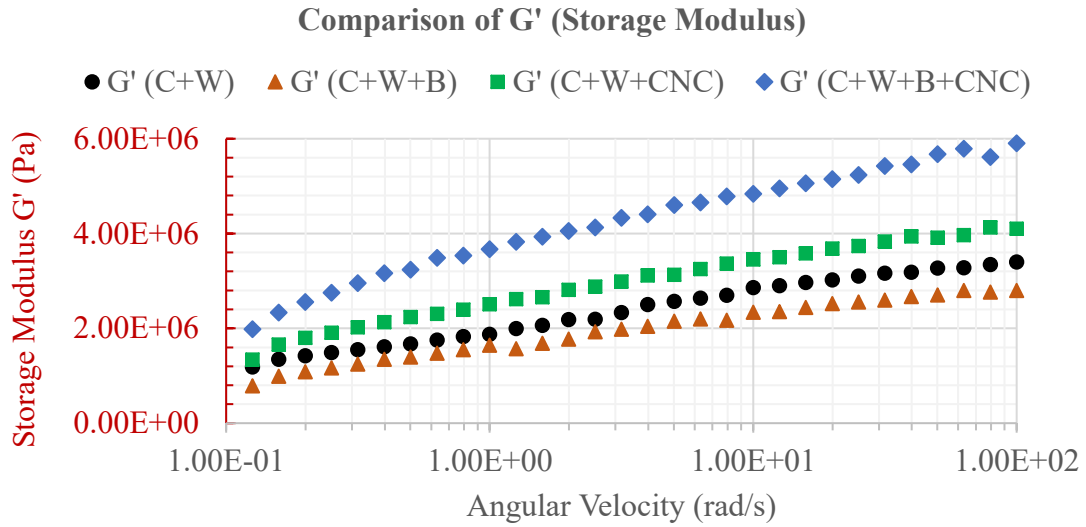


**Figure 4.12.** Change in storage modulus ( $G'$ ) with respect to angular frequency for all cementitious samples

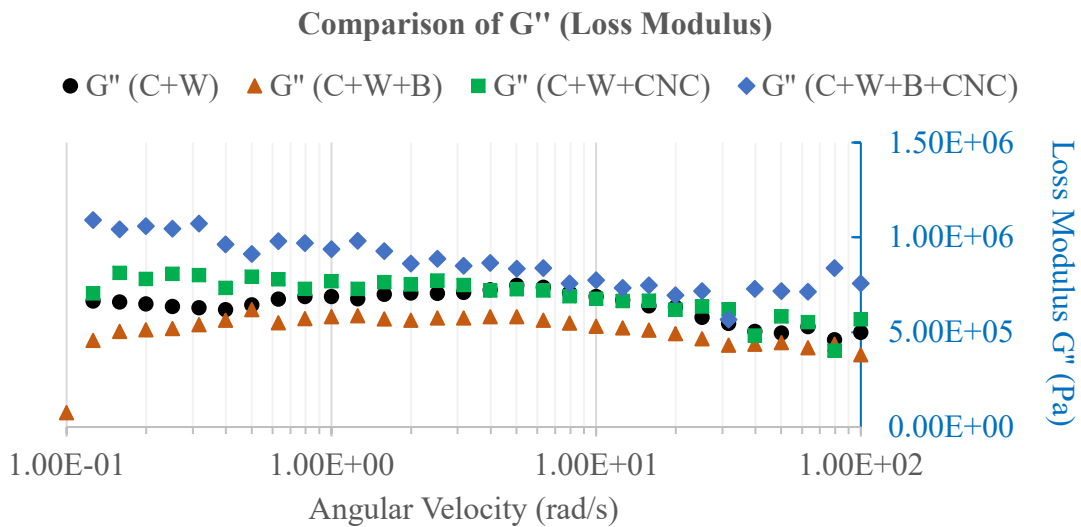


**Figure 4.13.** Change in loss modulus ( $G''$ ) with respect to angular frequency for all cementitious samples

### 3.2.2. Complex Shear Modulus ( $G^*$ ) and Complex Viscosity ( $\eta^*$ )

In contrary to normal shear modulus ( $G$ ) measurement, where a constant shear strain or shear stress is applied for each measuring point (steady shear), the complex shear modulus ( $G^*$ ) is obtained from a harmonic-periodic (for instance sinusoidal) shear process, usually known as a set of oscillatory tests. Practically, the complex shear modulus ( $G^*$ ) is a parameter to express the rigidity of the material being tested [7]. Figure 4.14a describes the relationship between the storage modulus ( $G'$ ), loss modulus ( $G''$ ) and complex shear modulus ( $G^*$ ) in vector form.

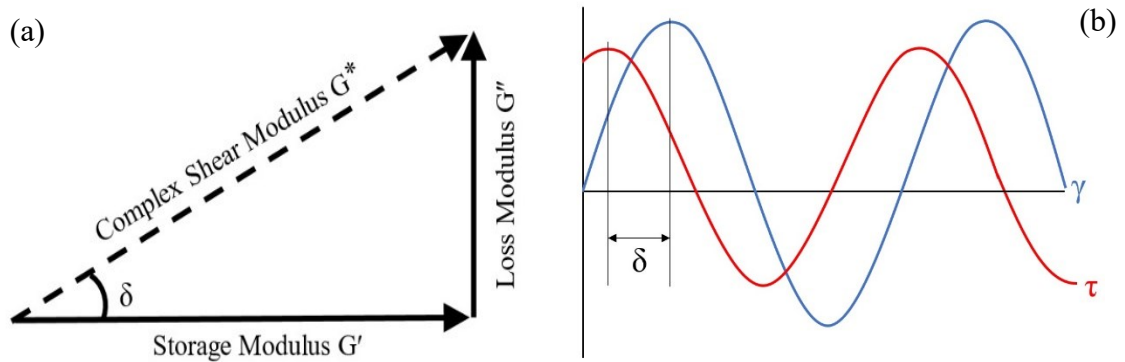


**Figure 4.14.** a) Relationship between storage modulus ( $G'$ ), loss modulus ( $G''$ ) and the resulting complex shear modulus ( $G^*$ ); b) Schematic demonstration of a preset shear strain function ( $\gamma$ ) and the resulting shear stress function ( $\tau$ ) with a phase shift angle ( $\delta$ )

Furthermore, the complex viscosity ( $\eta^*$ ) of a material is also obtained from a set of oscillatory tests where the material does not undergo a steady shear during the measurement procedure. The frequency sweep test not only describes the change in loss and storage modulus of a substance or a cementitious sample prepared but also allows one to observe the change in complex (dynamic) viscosity  $\eta^*$  of the sample. The complex viscosity consists of two main vector components: (1) viscous behavior component ( $\eta'$ )

also known as real component and (2) elastic behavior component ( $\eta''$ ) also known as the imaginary component. Note that the complex viscosity should not be confused with the common shear viscosity measured during the steady shear rheology.

In this experimental study, the complex shear modulus ( $G^*$ ) of all 4 types of samples was obtained and plotted against angular velocity ( $\omega$ ). The results verified an increase in complex shear modulus ( $G^*$ ) when cellulose nanocrystal particles were added to the mix design, hence an increase in the host materials rigidity. Evidently, when both bentonite and cellulose nanocrystal (CNC) particles were present in the mix design, the cementitious system exhibited a higher rigidity. Figure 4.15 clearly illustrates an increase in rigidity (complex shear modulus) when cellulose nanocrystal (CNC) is employed in the cement mix.

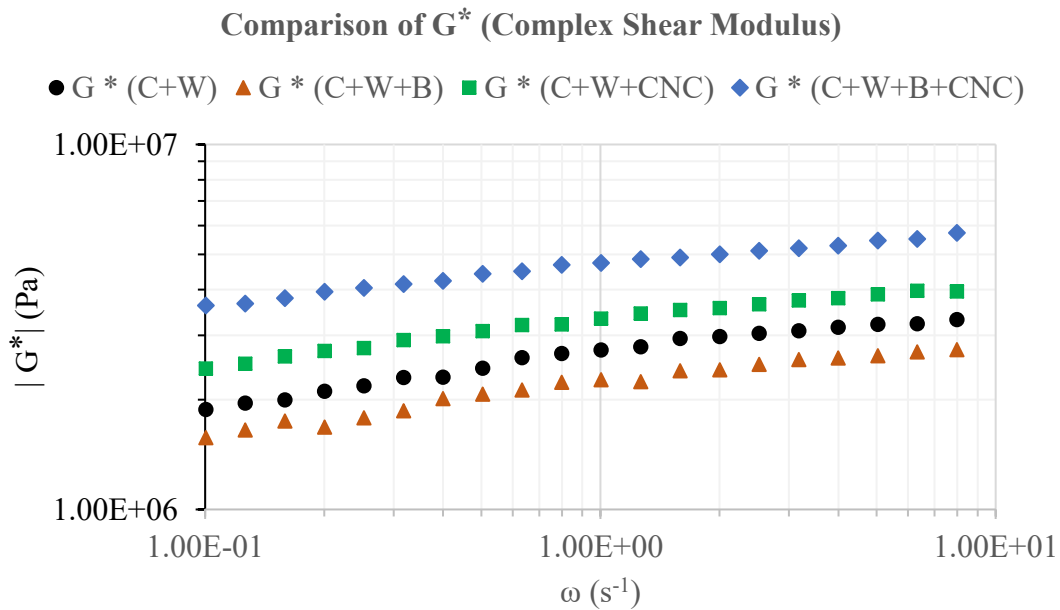


**Figure 4.15.** Change in complex shear modulus ( $G^*$ ) with respect to angular frequency for all cementitious samples

Moreover, the complex viscosity ( $\eta^*$ ) parameter was also plotted against the angular velocity in order to report the flow behavior and viscosity profile of the tested cementitious samples.

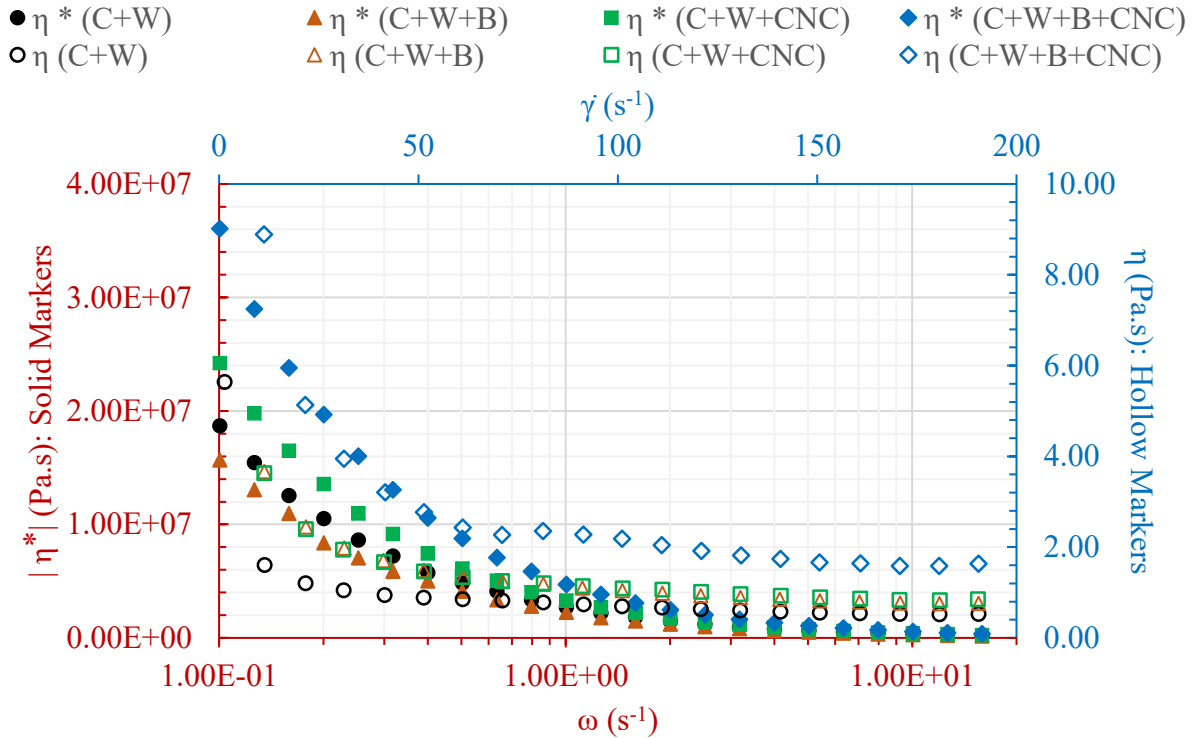


**Figure 4.16.** Change in complex viscosity ( $\eta^*$ ) with respect to angular frequency for all cementitious samples compared to the change in shear viscosity ( $\eta$ ) with respect to shear strain (obtained from Chapter 3)

As expected, samples 3 (C+W+CNC) and 4 (C+W+B+CNC) displayed a higher viscosity throughout the angular velocity range tested, compared to the neat sample and the sample containing only bentonite. Interestingly, when bentonite was utilized alone, the complex viscosity dropped, compared to the neat cement paste. However, when CNC was added to the bentonite and cement matrix (sample 4), the most viscous behavior was observed among all 4 types of samples. Such a synergy between CNC and bentonite was also

observed in the steady shear rheology tests conducted in this comprehensive study (chapter 3). Note that the interaction between CNC and bentonite is beyond the scope of this research. Similar to the steady shear rheology results, all of the samples demonstrated a shear thinning behavior. The complex viscosity ( $\eta^*$ ) profile of the samples tested in this experimental study is illustrated in Figure 4.16.

### 3.2.3. Damping Factor ( $\tan\delta$ )

Another dynamic mode rheology parameter assessed and compared in this experimental study was the damping factor ( $\tan\delta$ ) which is sometimes referred to as the loss factor. Generally, when a viscoelastic material is subjected to a preset shear strain, the resulting shear stress will appear with the same frequency, however with a phase shift angle ( $\delta$ ) expressed in degrees. Figure 4.14b describes this phenomenon. The phase shift angle  $\delta$  for an ideal elastic behavior is  $0^\circ$  and for an ideal viscous material, the corresponding  $\delta$  is  $90^\circ$ . Therefore, for a viscoelastic material  $0^\circ < \delta < 90^\circ$ . This practically means that the shear stress generated under preset shear strain will appear with a delay. Furthermore, as described earlier in section 2.3.2 the damping (loss) factor is computed as the ratio of the viscous and the elastic portion of a viscoelastic deformation behavior ( $\tan\delta = G''/G'$ ) [7]. Accordingly, for a liquid state material  $\tan\delta > 1$  since  $G'' > G'$  and for a gel (solid) state material  $\tan\delta < 1$  since  $G' > G''$ .

Figure 4.17 demonstrates the change in damping factor ( $\tan\delta$ ) with respect to the angular velocity. According to the plot presented here, the addition of cellulose nanocrystal (CNC) particles as an additive reduced the damping factor ( $\tan\delta$ ) associated with the cementitious system prepared. Furthermore, this reduction was more significant when cellulose nanocrystal was coupled with bentonite which was added to the mix design in this part of

the study. Previous studies [20] claim that when the hydration increases in a cementitious system, the damping factor ( $\tan\delta$ ) associated with that system drops.

This occurrence was well witnessed within this study. Previous plots and results reported in this chapter declared an enhancement in the solidification of the cement past (increase in storage modulus) when cellulose nanocrystal was added. The results were further justified by observing a drop in the damping factor ( $\tan\delta$ ) when CNC was present in the mix design. Since a drop in the damping factor is a sign of improvement in cement hydration, one can claim that the presence of CNC particles (with or without bentonite) had enhanced the hydration process.

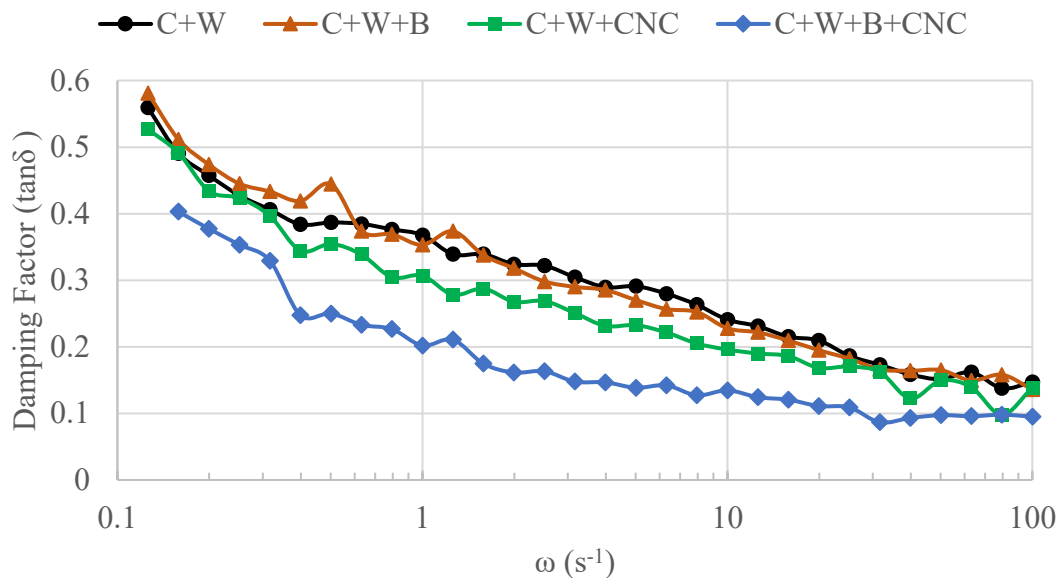


**Figure 4.17.** Change in damping factor ( $\tan\delta$ ) with respect to angular velocity

#### 4. CONCLUDING REMARKS

The dynamic mechanical properties of different oil well cement pastes were investigated and studied by performing a set of oscillatory rheology tests, in order to understand the

structural development and solidification associated with them. 4 different samples were prepared in order to witness the influence of cellulose nanocrystal (CNC) particles as an additive (alone or coupled with bentonite), on the dynamic mechanical properties of Type G oil well cement paste. Consequently, the following findings were observed:

- The strain amplitude sweep test results verified the solid/gel behavior of the cementitious systems examined by proving that the storage modulus was greater than the loss modulus in all cases.
- The linear viscoelastic domain (range) was identified and the critical strain value selected for the frequency sweep test was 0.01% for all samples.
- The frequency sweep test results proved that the storage modulus ( $G'$ ) of the samples increased with angular velocity, unlike the loss modulus ( $G''$ ), which is expected due to the solid structure.
- Introducing cellulose nanocrystal (CNC) particles to oil well cement paste led to an increase in the storage modulus ( $G'$ ) and also the loss modulus ( $G''$ ).
- The storage modulus ( $G'$ ) represents the stiffness of the material under oscillatory shear deformation, hence an increase in  $G'$  could be interpreted as an increase in solidification of the material.
- The dynamic mechanical analysis reported in this chapter indicated an increase in the rigidity ( $G^*$ ) of oil well cement paste with the addition of cellulose nanocrystal (CNC) particles.
- The complex viscosity ( $\eta^*$ ) profiles associated with the samples confirmed an increase in complex viscosity ( $\eta^*$ ) when CNC is present in the mix design.

- The complex viscosity ( $\eta^*$ ) profiles achieved from the dynamic mechanical analysis, followed the same trend as the viscosity profiles obtained from the steady shear rheology.
- When cellulose nanocrystal (CNC) particles were added to oil well cement paste, a drop in damping factor ( $\tan\delta$ ) was observed. According to the present literature, this phenomenon represents an increase in cement hydration. Hence, this could be further interpreted by stating the fact that the CNC particles enhanced the cement hydration.
- When cellulose nanocrystal is coupled with bentonite, the increase in storage modulus and drop in damping factor is more significant. The same synergy was observed during the steady shear rheology measurements.

## **ACKNOWLEDGEMENTS**

The authors would like to express their gratitude to Alberta Innovates – Bio Solution for funding this project. Furthermore, the authors would like to thank Alberta Innovates Technology Futures (AITF) and Alpac for providing the cellulose nanocrystal (CNC) samples, and Lafarge Canada for supplying the oil well cement utilized throughout this study.

## **REFERENCES**

- [1] Nelson, E. B. (Ed.). (1990). Well cementing (Vol. 28). Newnes.
- [2] Smith, D. K. (1989). Cementing. SPE Monograph Series. Society of Petroleum Engineers, Richardson, Texas.

- [3] Shahriar, A. (2011). *Investigation on rheology of oil well cement slurries* (Doctoral dissertation, The University of Western Ontario).
- [4] Deshpande, A. P., Krishnan, J. M., & Kumar, S. Rheology of complex fluids. 2010.
- [5] Bird, R. B., Armstrong, R. C., & Hassager, O. (1987). Dynamics of polymeric liquids. Volume 1: fluid mechanics. A Wiley-Interscience Publication, John Wiley & Sons.
- [6] Larson, R. G. (1999). *The structure and rheology of complex fluids* (Vol. 150). New York: Oxford university press.
- [7] Mezger, T. G. (2006). *The rheology handbook: for users of rotational and oscillatory rheometers*. Vincentz Network GmbH & Co KG.
- [8] Tattersall, G. H., & Banfill, P. F. (1983). *The rheology of fresh concrete* (Vol. 759). London: Pitman.
- [9] Shaughnessy, R., & Clark, P. E. (1988). The rheological behavior of fresh cement pastes. *Cement and Concrete Research*, 18(3), 327-341.
- [10] Nachbaur, L., Mutin, J. C., Nonat, A., & Choplin, L. (2001). Dynamic mode rheology of cement and tricalcium silicate pastes from mixing to setting. *Cement and Concrete Research*, 31(2), 183-192.
- [11] Schultz, M. A., & Struble, L. J. (1993). Use of oscillatory shear to study flow behavior of fresh cement paste. *Cement and Concrete Research*, 23(2), 273-282.
- [12] Specification, A. P. I. (2010). 10A. *Cements and Materials for Well Cementing*.
- [13] Canadian Standards Association. (2013). CSA A3000–13 Cementitious materials compendium. CSA Group.

- [14] Standard, A. S. T. M. "C150/C150M-17 (2017)." Standard specification for Portland cement (2017).
- [15] Habibi, Y., Lucia, L. A., & Rojas, O. J. (2010). Cellulose nanocrystals: chemistry, self-assembly, and applications. *Chemical reviews*, 110(6), 3479-3500.
- [16] Grim, R. E. (1955). Clay mineralogy, 1968. Karl Jasmund, Die silicatischen Tonminerale, 2nd enlarged ed.
- [17] Luckham, P. F., & Rossi, S. (1999). The colloidal and rheological properties of bentonite suspensions. *Advances in Colloid and Interface Science*, 82(1), 43-92.
- [18] Cao, Y., Zavaterra, P., Youngblood, J., Moon, R., & Weiss, J. (2015). The influence of cellulose nanocrystal additions on the performance of cement paste. *Cement and Concrete Composites*, 56, 73-83
- [19] Betioli, A. M., Gleize, P. J. P., Silva, D. A., John, V. M., & Pileggi, R. G. (2009). Effect of HMEC on the consolidation of cement pastes: isothermal calorimetry versus oscillatory rheometry. *Cement and concrete Research*, 39(5), 440-445.
- [20] Zhang, Z., Wang, P., & Wu, J. (2012). Dynamic mechanical properties of EVA polymer-modified cement paste at early age. *Physics Procedia*, 25, 305-310.

## Chapter V

# *The Effect of Cellulose Nanocrystal (CNC) Particles on the Porosity and Strength Development of Hardened Oil Well Cement Paste*

### **ABSTRACT**

In this chapter, the effect of cellulose nanocrystal (CNC) particles on the pore structure and porosity of hardened oil well cement paste are investigated using the gas sorption technique. Furthermore, the strength development (compressive and tensile) of CNC-dosed oil well cement paste was measured at different ages in order to recognize the impact of this nanomaterial on the mechanical properties of hardened oil well cement paste. According to the results presented in this chapter, CNC particles reduced the porosity and surface area of hardened oil well cement paste and enhanced the mechanical properties.

*Keywords: Oil Well Cement, Cellulose Nanocrystal, Porosity, Surface Area, Mechanical Properties, Strength Development*

## **1. INTRODUCTION**

### **1.1. Oil Well Cement**

Nowadays, the human culture is extremely dependant on oil and chemical feedstock. Therefore, the oil industry's influence on the current modern technological society is significant [1]. Even though alternative renewable energy sources have been introduced to the modern life, research and investigations show that consumption of oil and oil-related products have dramatically increased in the past few decades [2]. Nevertheless, due to the limited source present on earth, a decrease in oil production is desired. The remaining oil needs to be extracted, placed and used adequately, thus oil wells need to be designed properly in order to prevent severe economic losses. Aside from the economic point of view, a poorly designed well might lead to oil spills. This will eventually cause environmental disasters due to the toxic substances being released. The oil industry has been investigating and spending billions of dollars to minimize such risks and optimize oil production around the globe [1].

In the design process of an oil well, the cementing job is a crucial step towards completion. It takes place at the end of the drilling process. An improper cementing job could possibly lead to remedial cementing which means a large amount of time, energy and money will be spent to overcome the poorly performed initial cementing operation. The well cementing operation is basically placing the cement paste in the annular space between the casing and the geological formation surrounding the wellbore. The cement paste utilized in oil wells should demonstrate an adequate flow behavior since it needs to be pumped into the wellbore. Furthermore, the oil well cement paste placed in the annulus needs to provide an

acceptable zonal isolation to protect the well casing from any kind of damage [1, 3]. Therefore, the integrity and strength of the oil well cement sheath are also of great importance.

A cementitious system is known to be a heterogeneous and porous material [4]. The pores within the material are in different shapes and sizes [4]. It is understood and acknowledged that the pore structure and air void network of a cementitious system influence many of the properties associated with that system [5, 6]. For instance, properties such as permeability and strength are heavily influenced by any change in the porosity and pore structure of the material [7]. It is generally agreed that the pore structure of a cementitious system plays a significant role in determining its durability. Hence, studying the pore structure of any type of cementitious system is essential.

## **1.2. Porosity**

### *1.2.1. Theoretical Background*

A fluid is able to undergo different transport mechanisms such as permeability, migration and diffusion, within cementitious systems. All of the named mechanisms are significantly influenced by the effective porosity of that cementitious system. The effective porosity may be defined as the degree of continuity of the pore system. In other words, transport of any fluid within cement paste or concrete is highly related to the inherent micro-cracks and the interconnected pore network within the cementitious system's core [8]. In mathematical terms, porosity can be written as:

$$\varphi = \frac{V_p}{V_b}$$

Where

$\varphi$  = Porosity

$V_p$  = Pore volume

$V_b$  = Bulk volume

Based on the definition and the mathematical expression above, the porosity of a porous media (material) could be any number. However, there are some factors affecting the porosity value. One of the most influencing ones is the particle or grain size of the material. A material with smaller particles will demonstrate a lower porosity compared to the one with larger grains. Another well-known parameter affecting the porosity magnitude of a substance is the degree of cementation (also referred to as consolidation). As this increases, the porosity tends to decrease and a lower value is obtained. In any porous material, some pores are interconnected whereas some other are completely isolated. Therefore, this affects the measuring value of the porosity of a material. As a result, two different porosity values may be obtained from one material, depending on which pore spaces have been analyzed.

This phenomenon leads to two categories of porosity: (1) Absolute or total porosity and (2) effective porosity. Absolute porosity is basically the ratio of the total void space to the bulk volume of the sample, as described above mathematically. Effective porosity, on the other hand, is influenced by many factors such as heterogeneity of grain sizes, packing of the grains, pore channels, etc. These factors should be taken into account while measuring effective porosity [9]. It should be understood and highlighted that the porosity and the pore structure of a hydrated concrete specimen are different from that of a hydrated cement

paste specimen. Since there is no aggregates included in an oil well cement paste, the porosity of the material is basically a function of the paste pore structure, whereas in concrete the aggregate-paste interface has a significant effect on the porosity. This is mainly due to the fact that the aggregates have higher porosity and larger pores.

### *1.2.2. Different Measuring Techniques*

There are different techniques to measure the surface area of the cement paste and also to investigate the pore structure associated with it [10]. Depending on the feature in mind, one can utilize one of the common methods and study the pore structure of the sample. For instance, the Mercury Intrusion Porosimetry (MIP) method, highlights the larger pores and it cannot be employed to measure the surface in the finest pores. Nevertheless, MIP still remains as one of the most common techniques for engineers to study cement pore structure [10].

Another common technique utilized to investigate the pore structure and pore size distribution of cementitious samples (concrete, mortar and cement paste), in the recent years, is image analysis of backscattered electron (BSE) images. Basically, in this technique, the fraction of phases in cement paste (porosity, anhydrous cement content, etc.) is determined [11]. In an image analysis process, the segmentation algorithm should be precise and most importantly reproducible. Then only, such process and analysis may be qualified in order to perform a comparison, and also to formulate relationships. One of the initial and most important challenges in any image analysis is to define the grey level upper threshold. In their experimental study, Wong and colleagues used image analysis to segment pores from a BSE image of a cementitious material. In the work presented by

them, the grey level threshold was identified from the inflection point of the cumulative histogram of all the BSE images analyzed. Based on the results obtained, it was understood that the proposed technique or method was more consistent, and it needed a significantly fewer number of images [11].

In their proposed methodology, a series of images from a single capillary pore with area segmented (white pixels) were obtained with different threshold levels. As the threshold level increases the segmented area increases as well. Eventually, a sudden increase in the segmented area is observed which indicates the surrounding paste around the capillary pore. At the end, the total area segmented is plotted against the threshold level. Therefore, the selected threshold level will be the intersection of the two linear segments of the plotted curve. After determining the threshold, pores were separated (segmented) from the images using binary segmentation. Finally, the porosity of the material was obtained as the percentage of the segmented pore area to the total paste area [11-13].

The most common technique for measuring the surface area is referred to as “gas sorption”, which is also the technique with the most published results. As explored and explained by Gregg and Sing [14] and also by Rarick et al. [15], in the gas sorption technique a monolayer of gas molecules will be adsorbed on to the internal surface area of the material (such as a hardened cement sample). The most common method to analyze the sorption isotherm has been derived by Brunauer, Emmet and Teller, referred to as the BET method [16]. In the BET method, it is assumed that the heat of adsorption is constant throughout the formation of the first monolayer, and the heat of adsorption of the next layers will be equal to the heat of condensation of the bulk. Therefore, according to the BET method, one

can calculate the surface area based on the relationship between the relative pressure of the gas, and the volume adsorbed per unit specimen mass.

The BET method has been widely employed in the cement industry in order to measure the surface area of a cementitious sample. As stated earlier there are difficulties in measuring surface area with gas sorption methods. The pores need to be empty of any remaining water. Therefore, the sample has to be dried prior to measuring. This drying process, may alter the C-S-H structure of the cement paste and provide a very different surface area. Different techniques have been proposed for the drying process of cement paste such as oven-drying, vacuum drying [15], D-drying [17] or P-drying [18]. The surface area of cement paste could be measured by sorption of either water vapor or Nitrogen. However, the results will be completely different.

In 2003 Odler describes the factors which may alter the BET surface area results [19]. According to the experimental work conducted and the results obtained, it was understood that Nitrogen adsorption provides different surface area compared to water vapor adsorption. Odler justifies this fact as a consequence of Nitrogen's ability to penetrate pores with narrow entrances, known as the ink-bottle pores [19].

### *1.2.3. Previous Studies on the Pore Structure of Cementitious Systems*

As stated earlier, researchers have employed different techniques to study and evaluate the porosity and pore structure of a cementitious material. In an experimental study performed by Goto and Roy in 1981, the effect of water-to-cement ratio and curing temperature on permeability and pore size distribution of different cement pastes were investigated [20]. They developed an equation to measure the porosity of their samples based on the weight

of the dried samples. The pore size distribution of the samples was also evaluated using a mercury intrusion porosimetry. Their work demonstrated the fact that as the water-to-cement ratio of the cement paste sample increases, the porosity of it also increases, however, a decrease in the porosity was observed when the samples were cured in a higher temperature [20]. Page and colleagues investigated the chloride penetration in cement. Based on the work published and presented by them, as the water-to-cement ratio (w/c) increased, the porosity increased as well, and also an increase in the penetration volume was observed [21].

In a research conducted by Halamickova et al., the effect of pore structure on the transport properties (such as water permeability) of cement mortars were investigated. In their study, the pore structure of different mortars with different water-to-cement ratios was measured using mercury intrusion porosimetry (MIP). After determining the critical radius using the Katz-Thompson method (inflection point on the volume intrusion measured versus the radius curve), it was concluded that higher pore sizes lead to higher degree of hydration. Based on the Katz-Thompson theory, the critical radius is the radius of the smallest pore (that are subsets of a larger pore) that can create a connected path through the sample [22].

In 2006, the nanoporosity of different samples were investigated by Jennings et al. and based on the results, it was understood that the samples hydrated at 20°C produce a low density calcium-silicate-hydrate (C-S-H) gel structure whereas drying the samples in a higher temperature (60°C) will result in to a denser morphology with a fewer large gel pores and of course larger amount of capillary pores [23]. Nyame and Illston also utilized mercury intrusion porosimetry to evaluate and measure the porosity and surface area of the hardened cement paste samples. The hydraulic radius was computed as the ratio of the

intrude pore volume and the surface area of the solid phases accessible to mercury at 200 N/mm<sup>2</sup> [24].

#### *1.2.4. The Effect of Additives on Porosity*

During the past couple of decades, various types of nanomaterials have been employed in cementitious systems, in order to alter the pore structure of the matrix. This would then lead to production or development of high performance and more durable cementitious systems [25]. Among these novel nanoparticles, nanosilica has attracted a significant attention due to its corresponding behavior. Because of the filling effect (to reduce porosity) observed and also the pozzolanic reaction taking place, silica fume has always been considered as an important admixture in the cement industry. Nowadays, nanosilica – which is a siliceous material with a finer particle size and higher purity – is widely utilized to achieve the desired performance in a cementitious system [25].

In another experimental approach, Zhang and Li investigated the influence of nano-TiO<sub>2</sub> and nano-SiO<sub>2</sub> on the pore structure of concrete [4]. Based on the results obtained, the authors concluded that the presence of such nanoparticles alters the pore structure of concrete [4]. The cumulative pore volume of concrete had decreased when Zhang and Li introduced nano-TiO<sub>2</sub> and nano-SiO<sub>2</sub> into the mix design [4]. Interestingly, the addition of nano-SiO<sub>2</sub> did not refine the cementitious system to the same extent as nano-TiO<sub>2</sub>. Samples containing nano-TiO<sub>2</sub> had a finer pore structure compared to samples containing nano-SiO<sub>2</sub>. Although both types of nanoparticles studied by Zhang and Li, reduced the cumulative pore volume of concrete, only nano-TiO<sub>2</sub> particles reduced the average pore diameter noticeably. Hence, nano-SiO<sub>2</sub> particles had reduced the total pore volume without

making any significant change to the pore size distribution. The authors claim that this is mainly attributed to the fact that nano-SiO<sub>2</sub> particles are smaller than nano-TiO<sub>2</sub> particles and exhibit a larger surface area and water demand. Furthermore, Zhang and Li identified an enhancement in strength and resistance to chloride penetration in samples containing the nanoparticles mentioned above. According to the reported results, it was concluded that the finer the pore structure of the cementitious sample, the lower the chloride penetration would be [4].

### **1.3. Mechanical Properties of Oil Well Cement Paste**

#### *1.3.1. Importance of Strength in Oil Wells*

When investigating the durability of an oil well cement sheath, the failure associated with stress should be studied and examined efficiently. As elaborated and discussed by Goodwin and Crook in 1992 [26], the expansion of the casing will generally cause radial cracks within the cementitious sheath surrounding the casing. These cracks will eventually influence the oil well performance by decreasing the zonal isolation, especially in the bottom segment of the well (lower one-third or one-quarter of the well) [26].

#### *1.3.2. Common Additives to Enhance Mechanical Properties*

In the study mentioned earlier, Goodwin and Crook also assessed the mechanical properties of different cementitious systems with different compositions [26]. The main objective was to investigate the effect of pozzolanic materials on the mechanical properties of oil well cement systems. According to the results published, when pozzolanic materials (such as silica) were added to the mix design, the compressive strength of the cement sheath had enhanced noticeably [26]. Goodwin and Crook described the mechanism by emphasizing

on the filler effect of silica [26]. Furthermore, in their investigation, it was concluded that, although the cement sheaths with higher compressive strength (which were more brittle) demonstrated a better support for the casing, their ability to seal the annulus in low internal casing pressure had decreased [26].

Furthermore, in 2002, Heinold et al. studied the influence of a number of common additives on the mechanical properties of normal density oil well cement pastes [27]. The cement powder used in their study was the API Type G cement, which is known to be one of the most common types of cement utilized in the oil well industry [1]. Heinold et al. tested samples at two different temperatures (100°F and 200°F) with the following common additives: Polyvinyl alcohol (PVA), silica fume (SF), metakaolin (HRM), wollastonite, hydroxyethyl cellulose (HEC), sodium metasilicate (SMS) and latex.

According to Heinold et al. all of the experimented samples were prepared and cured based on the API specifications for oil well cementing. In order to specifically understand the effect of the above mentioned additives on the mechanical properties of oil well cement pastes, the researchers excluded other additives such as retarders and dispersants which are typically used to enhance and optimize the slurry system in parameters and aspects other than mechanical properties [27].

As described in depth in Chapter 2 of this dissertation, the effect of each individual additive was measured and reported by Heinold et al. however, according to the results obtained, not all of the mentioned additives improved the flexural and tensile strength of the cementitious system with high density [27]. It was concluded that the additives utilized were capable of enhancing the mechanical properties, mainly in cementitious systems exhibiting low or medium density [27].

## 1.4. Objectives of Study

In the study presented here, cellulose nanocrystal (CNC) particles have been proposed and utilized, as a novel bio-based and non-toxic additive, to improve the durability of oil well cement by modifying and enhancing the pore structure and mechanical properties associated with it.

## 2. EXPERIMENTAL DETAILS

### 2.1. Materials

#### 2.1.1. Oil Well Cement Type G

Oil well cements are made from Portland cement clinker. The prepared paste will be pumped inside the oil well through the interior section of the casing and forced back to the surface from the base of the borehole, in order to fill the annulus [1, 3, 28]. Currently, the API Specifications for Materials and Testing for Well Cements [29] provides different classes of oil well cement. This classification is based on their Tricalcium Aluminate content [1]. The API classifies oil well cement into ordinary, moderate sulfate resistance, and high sulfate resistance [29]. Therefore, the chemical composition of the cement is practically what separates one API class from another.

Note that oil well cements are different from regular Portland cements. The difference is mainly attributed to the  $C_3A$  content. Generally, oil well cements have lower  $C_3A$  compared to the regular Portland cements used for other applications. The cement used for this experimental study was Type G cement, based on the American Petroleum Institute (API) classification, specification 10A for oil well cements [29].

Type G and Type H oil well cements are currently the most commonly used in the oil well cementing operations [30]. Type G oil well cement is comparable to ASTM Type II or Type V Portland cement. The water-to-cement ratio used in this experimental study is 0.44, as recommended by the API Specification 10A. Tables 5.1 and 5.2, describe the physical properties and chemical composition of this type of cement, respectively.

**Table 5.1.** Physical properties of Type G cement (prepared by Lafarge Canada, December 8<sup>th</sup>, 2015)

<b>Physical Analysis</b>	
Thickening Time (Schedule 5)	99 min.
Max. Consis. 15-30 min.	23 Bc
Fineness 45 $\mu\text{m}$ sieve	93.9%
Blaine	311 $\text{m}^2/\text{kg}$
Free Fluid	4.4 %

**Table 5.2.** Chemical composition of Type G cement (prepared by Lafarge Canada, December 8<sup>th</sup>, 2015)

<b>Chemical Analysis</b>	
Silica ( $\text{SiO}_2$ )	20.9%
Alumina ( $\text{Al}_2\text{O}_3$ )	3.8%
Iron Oxide ( $\text{Fe}_2\text{O}_3$ )	4.7%
Calcium Oxide, Total (TCaO)	62.9%
Magnesium Oxide (MgO)	4.5%
Sulphur Trioxide ( $\text{SO}_3$ )	2.6%
Loss on Ignition	0.66%
Insoluble Residue	0.13%
Equivalent Alkali (as $\text{Na}_2\text{O}$ )	0.48%
$\text{C}_3\text{S}$	57.9%

C <sub>2</sub> S	16.1%
C <sub>3</sub> A	2.0%
C <sub>4</sub> AF	14.3%
C <sub>4</sub> AF + 2X C <sub>3</sub> A	18.3%

---

### 2.1.2. Cellulose Nanocrystal (CNC)

Cellulose nanocrystals are rod shaped, non-toxic nanoparticles derived from cellulose [31]. Cellulose fibers have been employed in different applications for over 150 years, however, only in the past decade scientific and industrial interest has led to the development of cellulose nanocrystals [32]. Cellulose nanocrystals are novel bio based materials with a wide range of applications which can also be incorporated in construction materials [33]. In order to have a better understanding of cellulose nanocrystals, one should know that a cellulose molecule has an extremely complex hydrogen-bonding network with multiple isotropic and anisotropic phases, as elaborated by Dufresne in 2012 [34]. The fibrils (substructure of cellulose) are orientated in the same direction in an isotropic phase whereas, in an anisotropic phase, there are several layers of isotropic phases stacked upon each other to form a fibril layer in different orientations [31]. Note that in both isotropic and anisotropic phases, the disordered regions of cellulose are hydrolyzed by acid, in order to manufacture and produce cellulose nanocrystals from raw cellulose. In this scenario different acids are used to produce CNC, such as sulfuric acid, hydrochloric acid, phosphoric acid, hydrobromic acid, etc. but the most effective one is the sulfuric acid in order to break apart the cellulose in hand [31, 35].

In 2013, Zavattieri et al. used quantum physics as a tool in order to prove that cellulose nanocrystals have a stiffness comparable and close to steel, based on Young's moduli values obtained in experimental works. This fact was mainly due to the extreme anisotropies in the density of cellulose nanocrystals. Note that Young's moduli values obtained for steel lie within a range of 120-190 GPa whereas the stiffness of cellulose nanocrystals was evaluated as 206 GPa [36]. Venere [33] described cellulose nanocrystal as one of the most novel biomaterials that are employed and utilized in a wide range of industrial applications.

Cellulose is intrinsically hydrophilic [31]. Hence, they tend to dissolve easily into water. On the other hand, they have the tendency to hold water inside their structure because of their hydrogen network [31]. Cellulose nanocrystals are also widely employed as reinforcing agents in nanocomposites, electro-optical materials, bio carrier, etc. due to their low cost, availability, inherent renewability, nanoscale dimension, unique morphology, light weight, sustainability and abundance. Furthermore, the ability of CNC holding and releasing excess water (gradually) is of great importance in order to improve the hydration of cement particles [31, 37, 38]. In this research, the aspect ratio or the shape parameter (length/diameter) of the CNC particles are in between 10-60 with a dosage of 1% (w/v of water).

## **2.2. Specimen Preparation**

The oil well cement paste studied in this experimental research was prepared based on the API Specifications 10A [29]. As described earlier in this article, Type G cement was selected among the available API cement categories. The water-to-cement ratio utilized in

this experimental approach was 0.44 and a high shear mixer was employed for the mixing process. For the purpose of the study, 2 different type of samples were designed: (1) neat oil well cement paste with no additive (C+W) and (2) oil well cement dosed with cellulose nanocrystal particles (C+W+CNC). In this study, after measuring the required amount of water for each mix, CNC particles were mixed separately with an adequate amount of water (deducted from the initial measured amount). Furthermore, these suspensions were introduced to the high shear mixer where the cement powder and remaining water were present. Table 5.3 demonstrates a sample mix design identical to the mix design used in this research study.

**Table 5.3.** Mix design (sample) for preparation of cement paste

<b>Oil Well Cement Paste (Mix Design)</b>	
Cement	1000 kg
Water	440 kg
Cellulose nanocrystal (CNC) particles	4.4 kg

As was done earlier, again, the CNC particles were individually homogenized in a suitable fraction of the mix water. The oil well cement was mixed first with the remaining water to prepare a slurry. The CNC particles, now in their own suspension, were then added to the slurry and the mixture was agitated further for 5 minutes. Note that due to the inherent properties of cellulose nanocrystal (CNC) particles, the dosage being added to the mix design (in this case 1% of the total amount of water or approximately 0.5% mass fraction of the total amount of cement powder used), and their associated mechanism of adsorption with the water molecules, any change to the water-to-cement ratio of the prepared cementitious system will be negligible. Recent studies have also confirmed that despite

their hydrophilic nature, even with higher dosages of CNC used, at a high relative humidity (approximately 97% where CNC particles are immersed in water), the water adsorption of dry CNC particles is in the region of 34% which is only about 0.7% of the total mixing water in mass [37]. In this study, considering the fact that CNC particles are added to the mix design in the form of an aqueous solution (similar high relative humidity as the mentioned study), the adsorbed water on CNC will be approximately 0.3% of the total mixing water in mass. Therefore, based on Table 5.3, the water-to-cement ratio will change from a value of “440 kg / 1000 kg = 0.44” to a revised value of “441.5 kg / 1000 kg = 0.4415”, which is negligible.

## **2.3. Test Methods**

### *2.3.1. Porosity Assessment*

The influence of cellulose nanocrystal (CNC) on the porosity and pore structure of hardened oil well cement paste was characterized using gas sorption (adsorption/desorption) method. For this purpose, a Quantachrome Autosorb iQ apparatus was used. After 28 days of curing, hardened oil well cement samples were fragmented into small pieces (with a diameter less than 10 mm), outgassed at room temperature and placed inside the tubes attached to the Quantachrome Autosorb iQ apparatus. The samples were outgassed at room temperature to prevent any possible damage to the microstructure of the cement paste. In this study, Nitrogen was employed for the analysis and sorption was performed at a temperature of 77 K. Furthermore, the Nitrogen isotherm associated with each type of sample was obtained.

After obtaining the isotherms, in order to express the porosity and pore structure of the cementitious samples and report the effect of cellulose nanocrystals, the surface area of neat and CNC-dosed specimens was computed using the Brunauer-Emmet-Teller (BET) equation. Additionally, the total (cumulative) pore volume and pore size distribution of the cementitious samples were obtained using the density functional theory (DFT) and the Barrett-Joyner-Halenda (BJH) method. Ultimately, using the three methods named above (BET, DFT and BJH), the porosity data associated with neat cement pastes are compared to the data achieved by testing the CNC-dosed specimens.

### *2.3.2. Investigation of the Mechanical Properties*

In order to understand the effect of cellulose nanocrystal (CNC) particles on the mechanical properties and strength development of oil well cement paste, samples were tested at different ages. As described earlier, in this study, two different type of specimens were designed and prepared: (1) Neat samples (with no additive) containing only Type G oil well cement and water; (2) samples dosed with cellulose nanocrystal (CNC) particles. Furthermore, the mixed slurry was placed inside cylindrical molds with a height of 150 mm and width of 75 mm. The prepared samples were allowed to set and cure inside the humidity room (humidity 100%) at room temperature ( $25^{\circ}\text{C} \pm 2$ ). The objective of this study was to monitor and measure the compressive and tensile strength development of neat and CNC-dosed oil well cement pastes at different ages. Hence, the samples were tested after 1, 7, 28 and 56 days of curing. Therefore, a hydraulic load frame was utilized to apply load on the cylinders at a rate of 0.25 mm/min and measurements were recorded using linear variable differential transformers (LVDT's) and compressometer. A data acquisition system was also employed to record the data. As mentioned above, in this study,

the compressive strength of the specimens was obtained at different ages, however, the stress-strain response of the specimens cured for 28 days was also obtained to understand the behavior of the samples in compression. Moreover, another set of cylindrical specimens was selected to undergo the split (tensile) test in order to evaluate their corresponding tensile strength after 1, 7, 28 and 56 days of curing. Eventually, the effect of cellulose nanocrystal (CNC) particles on the tensile strength development of oil well cement paste was observed and reported.

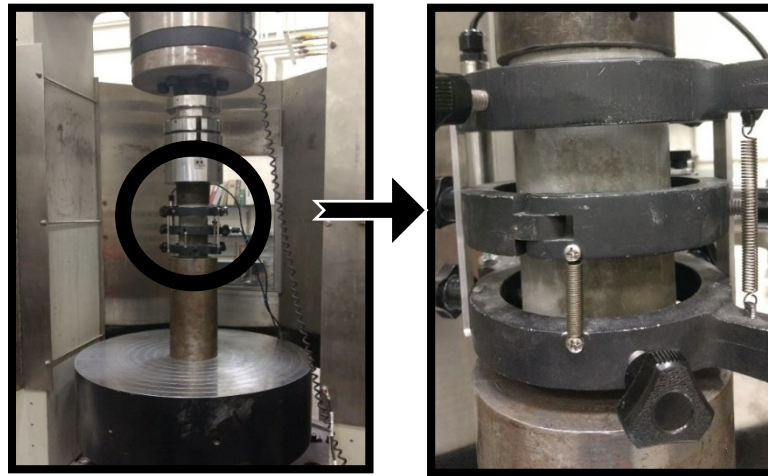


**Figure 5.1.** Compression test setup

### **3. RESULTS AND DISCUSSION**

As described in section 2 of this chapter, 2 different set of measurements and assessments took place in this study, which are reported here. First, the influence of cellulose nanocrystal (CNC) particles on the porosity and pore structure of oil well cement paste are demonstrated. Furthermore, the impact of such cellulosic additive on the mechanical properties and strength development of Type G oil well cement paste is assessed and elaborated.

### 3.1. Porosity

In this experimental study, the porosity of neat and CNC-dosed oil well cement paste has been investigated, by using the gas sorption technique. As described in section 2.3.1 of this chapter, Nitrogen has been selected in order to obtain the isotherm graphs associated with the cementitious samples. The isotherm is illustrated in Figure 5.2. Furthermore, different models have been selected to describe the pore structure and porosity of the samples. Note that the samples tested in this study were all cured for approximately 28 days in a similar condition (humidity of 100% and temperature of  $25^{\circ}\text{C} \pm 2$ ). All of the samples had a water-to-cement ratio of 0.44 which was selected based on the API standard [29]. The only difference in the composition and mix design is the presence of cellulose nanocrystal particles.

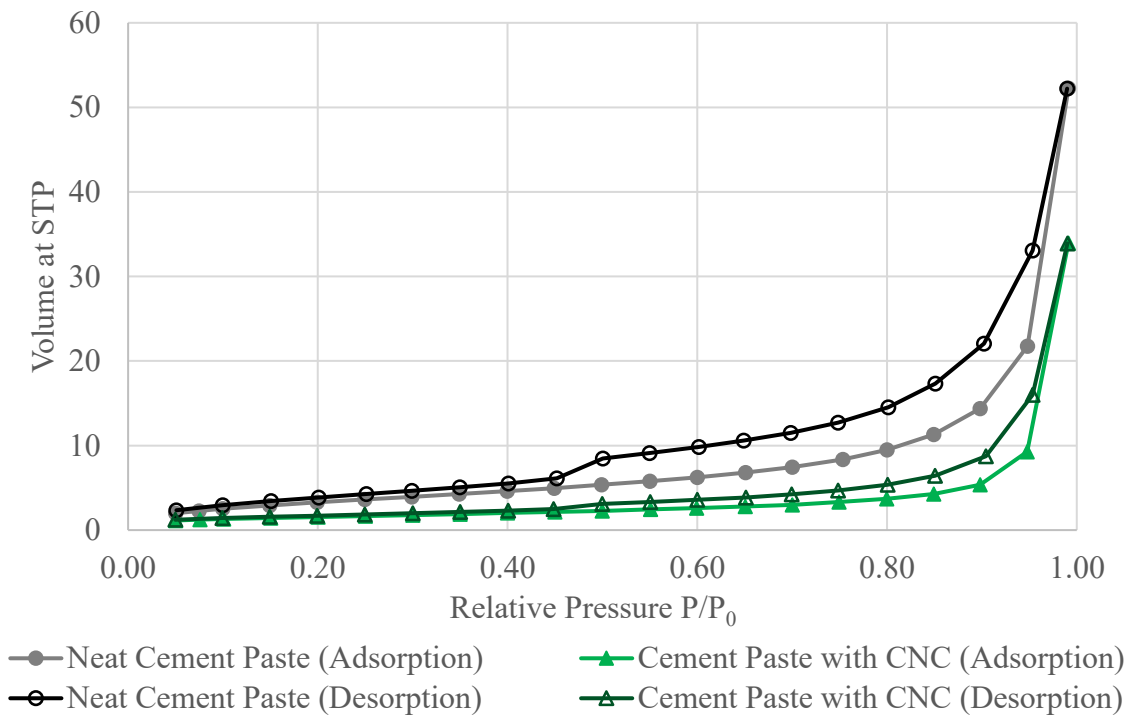


**Figure 5.2.** Nitrogen isotherm associated with neat and CNC-dosed cementitious samples

### 3.1.1. Influence of CNC on the Surface Area of Oil Well Cement Paste

Although the Brunauer-Emmet-Teller (BET) model is generally employed to compute the surface area of different materials, the surface area has been also obtained using the density functional theory (DFT) and the Barrett-Joyner-Halenda (BJH) method. The surface area value obtained from each individual model was then compared in order to verify the results and influence of cellulose nanocrystal particles on this parameter. Note that the surface area calculated using the BET method is the most reliable value. According to the data presented in Table 5.4 and Figure 5.3, all three models (BET, DFT and BJH) demonstrated a dramatic and significant decrease in surface area of the cementitious samples, when cellulose nanocrystal (CNC) was introduced as an additive. The difference in surface area could only be attributed to the presence of cellulose nanocrystal (CNC) since every other aspect of the samples were identical (composition, water-to-cement ratio, age, curing, etc.). All three models showed a reduction of more than 50% in surface area.

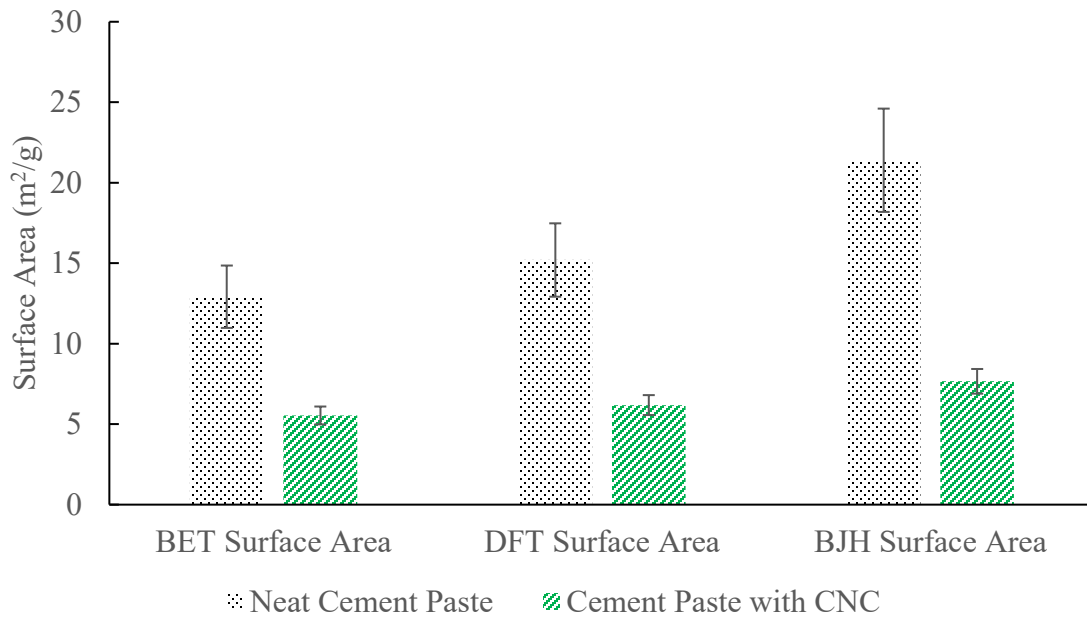


**Figure 5.3.** Visual comparison of surface area obtained from different models

**Table 5.4.** The surface area of neat and CNC-dosed oil well cement paste samples obtained using different models

	Surface Area (m <sup>2</sup> /g)		
	<i>Neat Cement Paste</i>	<i>Cement Paste with CNC</i>	<i>% Difference</i>
<i>BET</i>	12.917	5.542	57.1
<i>DFT</i>	15.198	6.186	59.3
<i>BJH</i>	21.396	7.662	64.2

According to the data provided in Figure 5.3 and Table 5.4, the presence of CNC (which is the only difference in the specimen composition) modified the porosity of oil well cement paste noticeably. The Brunauer-Emmet-Teller (BET) model which is known to be the most accurate and reliable method of evaluating the surface area of materials, reported a significant reduction of 57.1% when CNC was added to the mix design. This decrease in surface area verified the change in porosity, as expected. However, the cumulative pore volume and also the pore size distribution should also be investigated in order to understand and clarify the mechanism of action of such cellulosic additive. As mentioned earlier in this report, Cao et al. [37, 38] have already reported that the addition of cellulose nanocrystal particles to concrete increases strength and modifies the porosity. Furthermore, in this thesis, the impact of cellulose nanocrystal (CNC) particles on the strength, pore volume and also pore size distribution of hardened cement paste is explored.

### 3.1.2. Influence of CNC on Pore Volume and Pore Size Distribution

As stated above, the next step in unfolding the influence of cellulose nanocrystal (CNC) particles on the pore structure of hardened oil well cement paste was to assess the overall impact on the total pore volume and also the size distribution of pores. One of the most common techniques utilized in defining the pore size distribution of concrete specimens is

Mercury Intrusion Porosimetry (MIP). However, the MIP test method is more sensitive to larger pores (<100 nm). As specified in detail previously, the cellulose nanocrystal (CNC) particles used in this study have an aspect ratio of 10-60, with a diameter in the range of 5-10 nm. Therefore, aside from the short-circuit-diffusion (SCD) mechanism defined by Cao et al. [37, 38] where CNC enhances the hydration of cement grains and tunes the available pores (by changing the pore diameter), the possibility of other mechanisms such as pore-clogging should be investigated. Hence, the gas sorption technique (with Nitrogen) was once again employed to obtain and observe the effect of cellulose nanocrystal (CNC) particles on the pore size distribution and cumulative pore volume of hardened oil well cement pastes dosed with such cellulosic additive. As illustrated below, in this part of the experimental study, two different models have been used: (1) Density function theory (DFT) and the Barrett-Joyner-Halenda (BJH) method. Using both models, neat oil well cementitious samples have been compared to CNC-dosed samples.

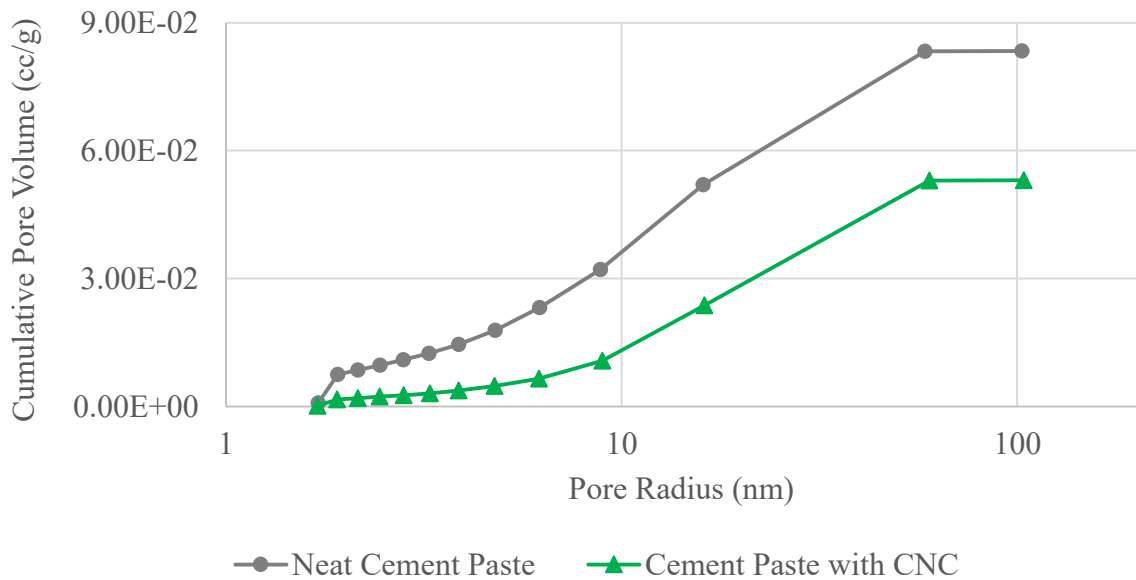


**Figure 5.4.** The effect of cellulose nanocrystal (CNC) particles on the cumulative pore volume of hardened oil well cement paste, obtained using the BJH method

As presented in Figure 5.4, by implementing the BJH model on the Nitrogen isotherm (obtained initially), the cumulative pore volumes associated with both types of specimens were obtained. Although the BJH model and the gas sorption test method used have only proved to be sensitive to pores with a radius of approximately 100 nm or less, the influence of CNC particles is clearly noticeable. Note that the plateau observed at the end of the representative curves above could be indicative of no further significant change in pore volumes measured.

However, this is actually due to the nature of the employed technique since this test method is generally utilized to identify and study the narrow pores. Furthermore, the DFT model was also employed to generate the cumulative pore volume graphs associated with neat and CNC-dosed samples. Basically, the DFT model is known to be more accurate and precise in defining the pore size distribution and pore volume of various materials, compared to the BJH model. However, the model is sensitive to smaller pore sizes. Moreover, in order to justify the BJH plots obtained in this experimental study, the pore size distributions of the tested samples were also generated and compared using the DFT model.

Note that Figure 5.5 demonstrates a trend very similar to the one witnessed in Figure 5.4 regarding the volume of the total pores identified. The presence of cellulose nanocrystal (CNC) particles had reduced the cumulative pore volume of the cementitious specimen dramatically, even though the identified and considered pores were limited to the narrow pores (pores with a radius of less than 40 nm). The cumulative pore volume values obtained from both BJH and DFT models (utilized in this study) are tabulated below.

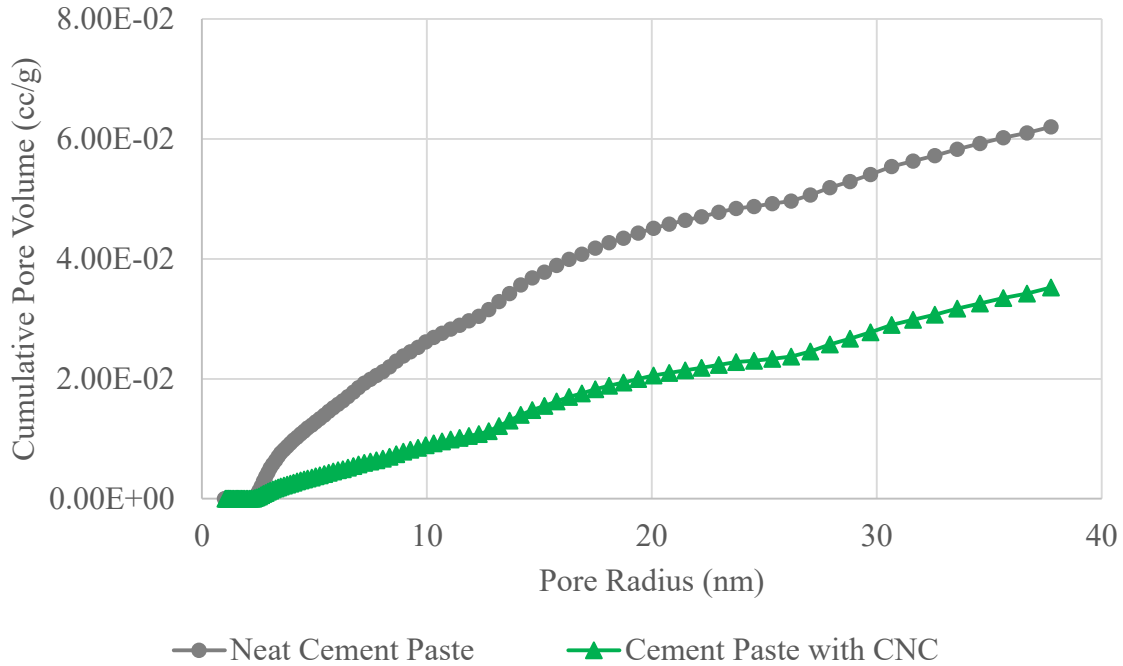


**Figure 5.5.** The effect of cellulose nanocrystal (CNC) particles on the cumulative pore volume of hardened oil well cement paste, obtained using the DFT method

**Table 5.5.** Cumulative pore volume of hardened oil well cement pastes

	Cumulative Pore Volume (cc/g)		
	Neat Cement Paste	Cement Paste with CNC	% Difference
<b>DFT</b>	0.062	0.035	43.5
<b>BJH</b>	0.083	0.053	36.1

Both models verify the fact that cellulose nanocrystal (CNC) particles had reduced the total amount of pores within the cementitious system. However, further investigations proved that the cellulosic additive used, did not refine or alter the pore size distribution within the range tested (narrow pores).

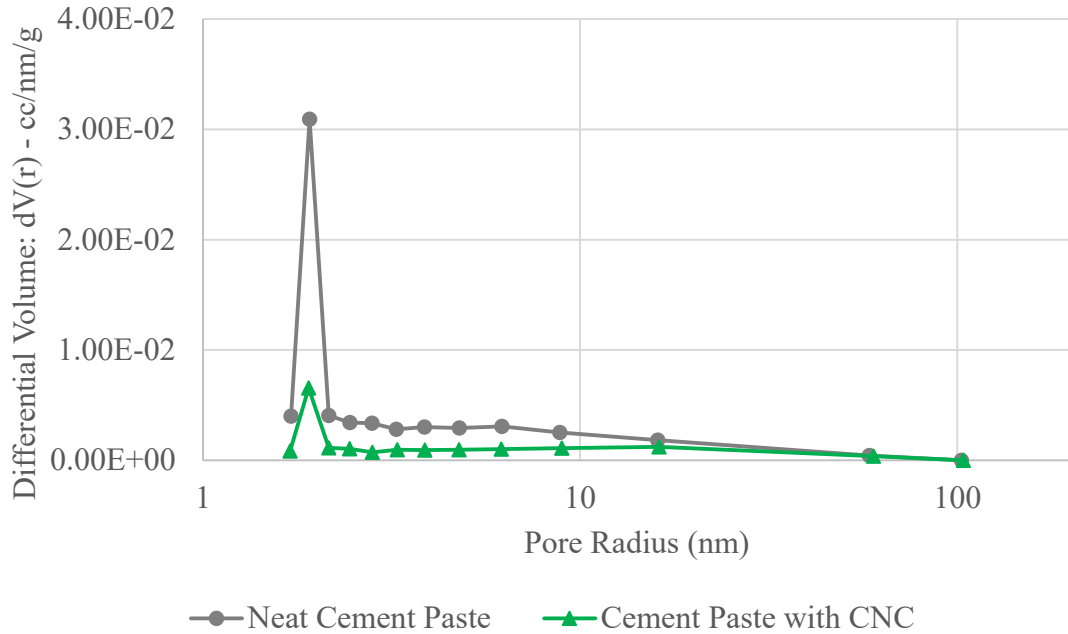


**Figure 5.6.** The effect of cellulose nanocrystal (CNC) particles on the pore size distribution of hardened oil well cement paste, obtained using the BJH method

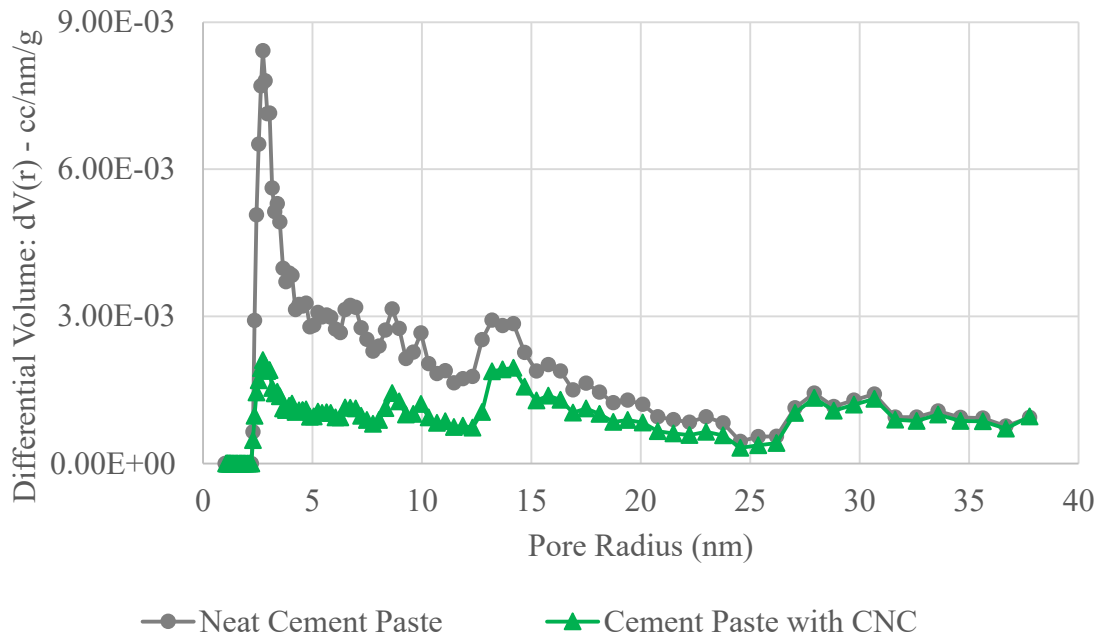


**Figure 5.7.** The effect of cellulose nanocrystal (CNC) particles on the pore size distribution of hardened oil well cement paste, obtained using the DFT method

According to Figure 5.6 and Figure 5.7, when CNC was added to the mix design, the pore size distribution pattern remained the same within the region investigated in this study. However, this does not mean that the overall pore size distribution (beyond the narrow pores and the region studied here) of the samples dosed with CNC will be similar to the neat samples. In fact, the increase in hydration due to the presence of CNC is likely to tune the larger pores and refine the pore size distribution. The investigation presented in this experimental study suggests a second mechanism of action associated with the influence of CNC particles on the porosity of cementitious systems. The results plotted and reported, verified a change in cumulative pore volume whereas the pore size distribution was not altered. This phenomenon suggests that the narrow pores with a radius of less than 100 nm were practically clogged by the rod shaped nanoparticles added to the mix design.

This has previously been witnessed when additives such as nanosilica have been added to the mix design. For instance, Zhang and Li observed the same mechanism of action when they added nano-SiO<sub>2</sub> particles to the mix design. According to their experimental study, the nano-SiO<sub>2</sub> particles had reduced the total pore volume without making any significant change to the pore size distribution [4]. Furthermore, such a mechanism has also been observed in material other than concrete. In a recent study, Niknaddaf et al. investigated the pore structure and porosity of three different carbon fiber cloths. They realized that some of the carbon fibers utilized reduced the total pore volume of the host material without altering the pore size distribution associated with that [39]. This was further clarified as a pore-clogging incident caused by the carbon fiber used in their experimental study. Therefore, the cellulose nanocrystal (CNC) particles may not only alter the porosity by enhancing the cement hydration using the short-circuit-diffusion method [37, 38] where

they act as seeding agents for the hydration process, but also change and reduce the porosity of the cementitious system by clogging the narrow pores. Figures 5.8-5.11 provide a better understanding regarding the volume of narrow pores present and their associated size distribution.

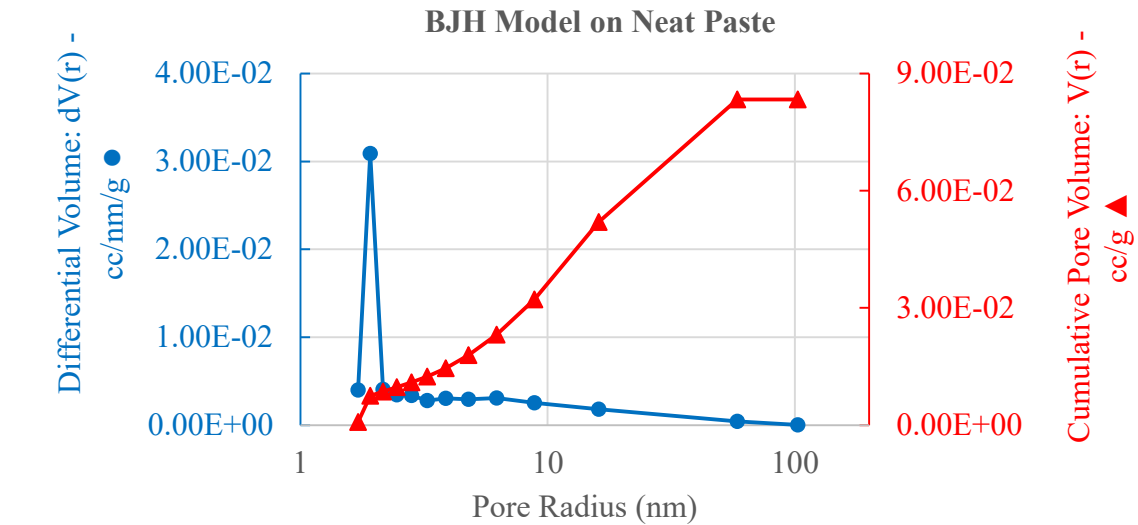


**Figure 5.8.** Porosity profile of neat hardened oil well cement paste obtained using the BJH method

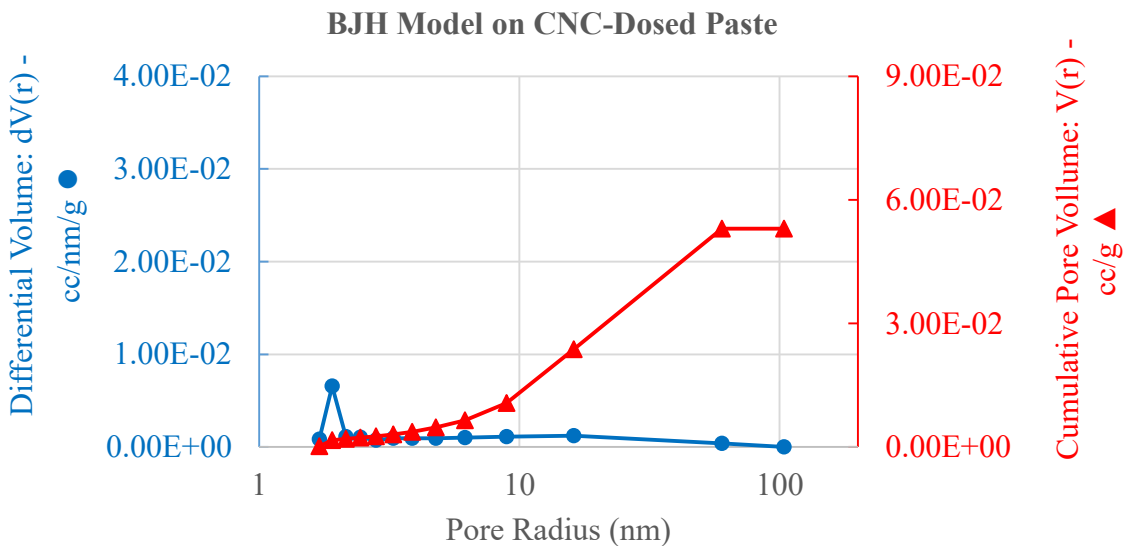


**Figure 5.9.** Porosity profile of CNC-dosed hardened oil well cement paste obtained using the BJH method

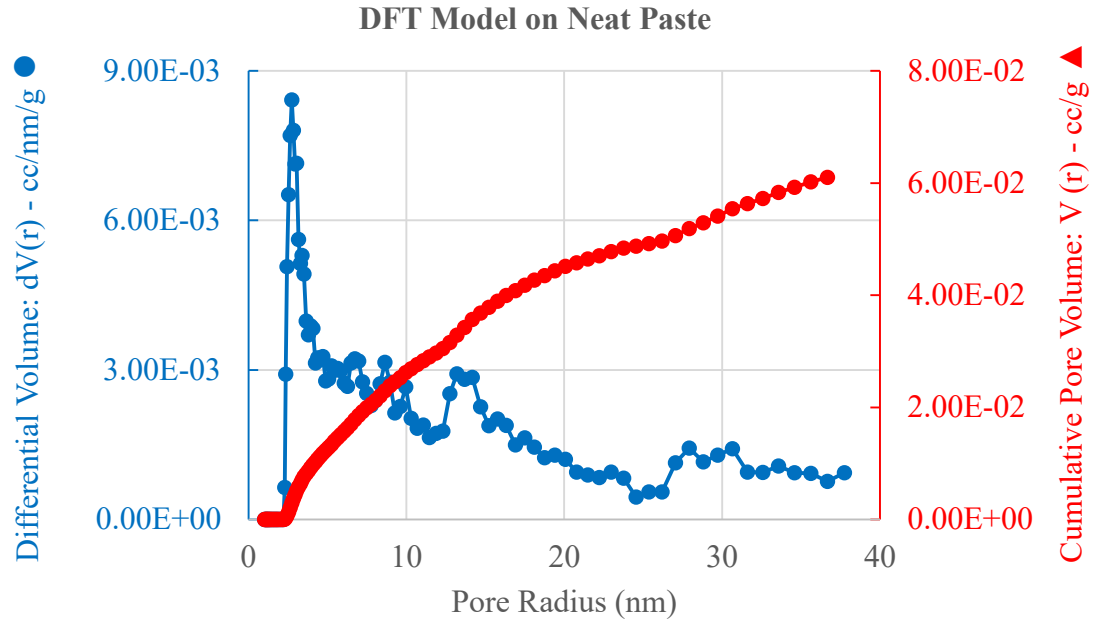


**Figure 5.10.** Porosity profile of neat hardened oil well cement paste obtained using the DFT method

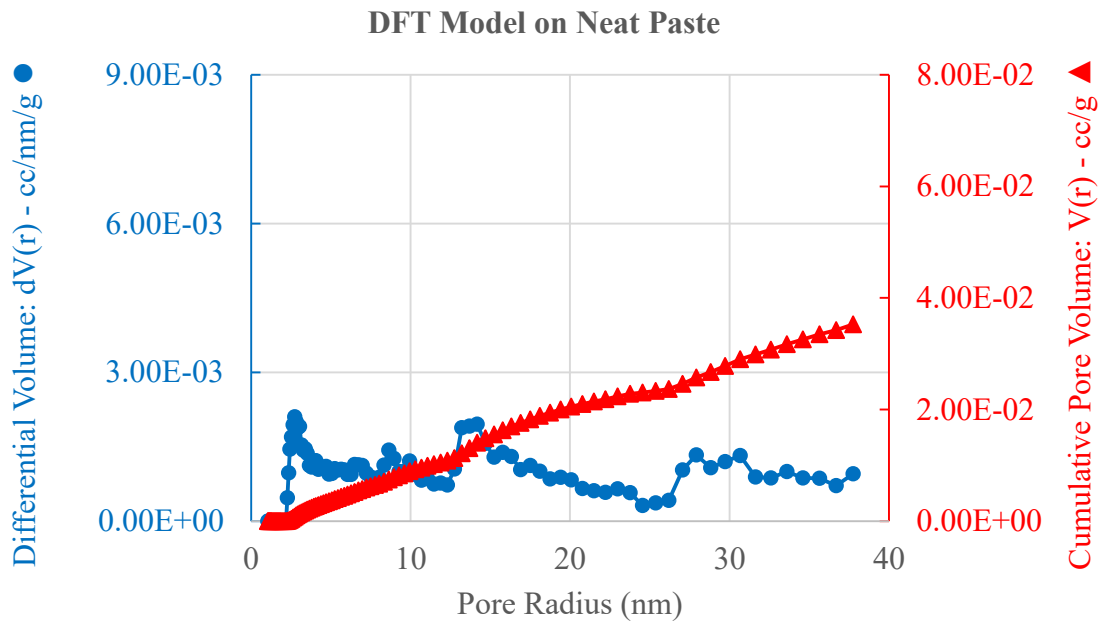


**Figure 5.11.** Porosity profile of CNC-dosed hardened oil well cement paste obtained using the DFT method

### 3.2. Mechanical Properties

#### 3.2.1. Impact of CNC on Strength Development of Oil Well Cement Paste

As described in section 2.3.2 of this chapter, the compressive strength and tensile strength of the prepared specimens were measured and compared at different ages. Therefore, the influence of cellulose nanocrystal on the mechanical properties and strength development of hardened oil well cement paste was identified. Figure 5.12, demonstrates the compressive strength development of neat and CNC-dosed oil well cement paste. To obtain the mentioned plot, the compressive strength of the prepared specimens was tested after 1, 7, 28 and 56 days of curing. The mix design and composition of the samples were kept identical and the only difference between the two sets of specimens was the presence of cellulose nanocrystal (CNC) particles. Note that all of the tested specimens have been cured in the same manner (as explained earlier). The water-to-cement selected for this stage of this experimental study was 0.44 according to the specifications provided in the API standards.

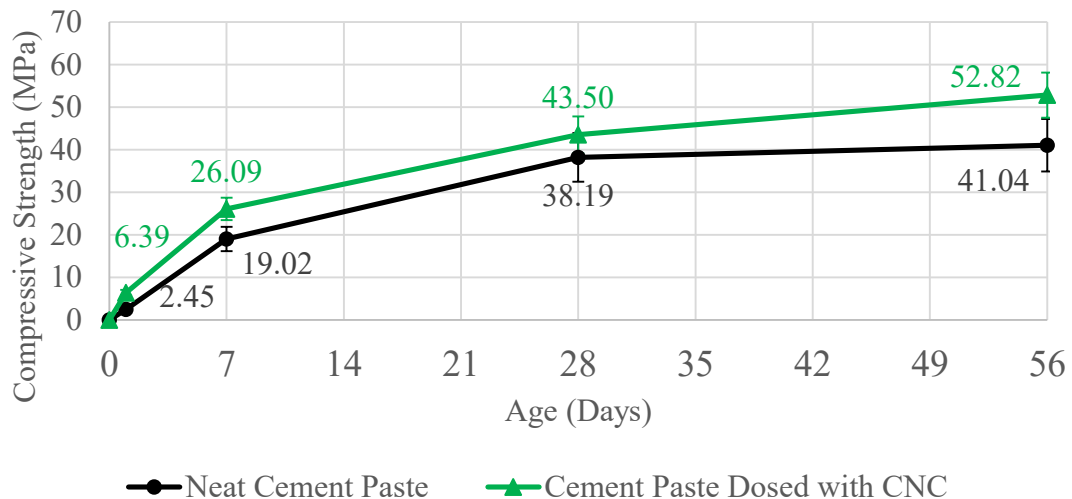


**Figure 5.12.** Influence of CNC on the compressive strength development of class G oil well cement paste

Based on Figure 5.12, the cementitious samples dosed with CNC particles demonstrated a higher compressive strength throughout the experiment timeline, compared to the neat samples with no additives. The compressive strength of the samples containing cellulose nanocrystal particles was measured to be higher, even at the early stages and on the first day of the testing schedule. Since the water-to-cement ratio of the samples, curing regime and the composition of the specimens were identical, the increase in compressive strength and early compressive strength development of the CNC-dosed samples was believed to be attributed to the presence of such cellulosic additives.

Current literature verifies that the CNC particles enhance cement hydration significantly. Furthermore, previous results of the study presented here also revealed a decrease in porosity when CNC was added to the mix design. Interestingly, according to the results obtained, the hydration process in the CNC-dosed cementitious samples seemed to be ongoing with a higher rate compared to the neat samples.

Figure 5.12 shows that in the final region of the plot (after 28 days), the slope of the curve associated with the CNC-dosed samples is noticeably greater than the slope of the curve associated with the neat samples. In fact, this figure shows that after 28 days of curing, the strength development curve of the neat cementitious samples almost converts to a plateau, whereas the green curve corresponding to the CNC-dosed samples is still rising. This may be documented as an enhancement in the hydration reaction of oil well cement pastes since no other external parameter (curing condition, additive, etc.) was found to affect the experiment at this stage.

The same trend was also observed on the tensile strength development curves generated in this study. With a similar test routine and curing condition, samples were prepared and tested (split tensile test) in order to observe the impact of CNC particles on the tensile strength of oil well cement paste. Figure 5.13 illustrates the tensile strength profile of oil well cement samples tested after 1, 7, 28 and 56 days of curing.

Similar to the compressive strength development observed earlier, the tensile strength of CNC-dosed samples was measured to be higher even on the first day. Ultimately, results obtained verified a noticeable increase in the tensile strength of oil well cement paste (at any age) when cellulose nanocrystal particles were added to the mix design. This may also be attributed to the enhancement of the cement hydration reaction.

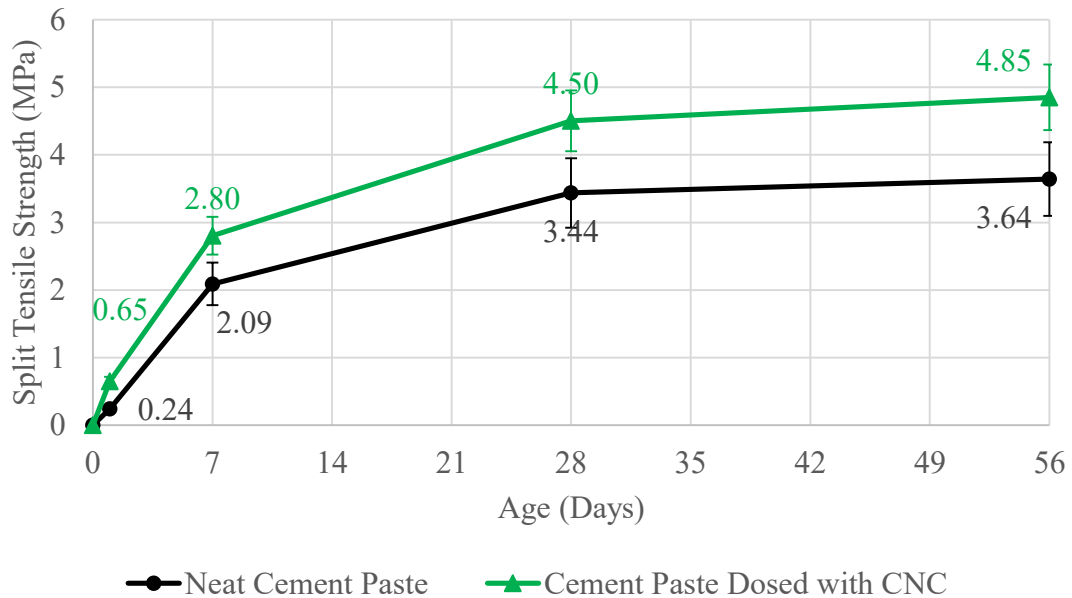


**Figure 5.13.** Influence of CNC on the tensile strength development of class G oil well cement paste

### 3.2.2. Effect of CNC on the Stress-Strain Profile of Oil Well Cement

Furthermore, the stress-strain profile associated with each type of sample was obtained using a load frame and a compressometer (as described in section 2.3.2 of this chapter). Figure 5.14 displays the mentioned profiles after 28 days of curing. According to the demonstration provided in this chapter, the addition of cellulose nanocrystal (CNC) particles to oil well cement paste, not only increased the ultimate compressive strength but also enhanced the modulus of elasticity (E).

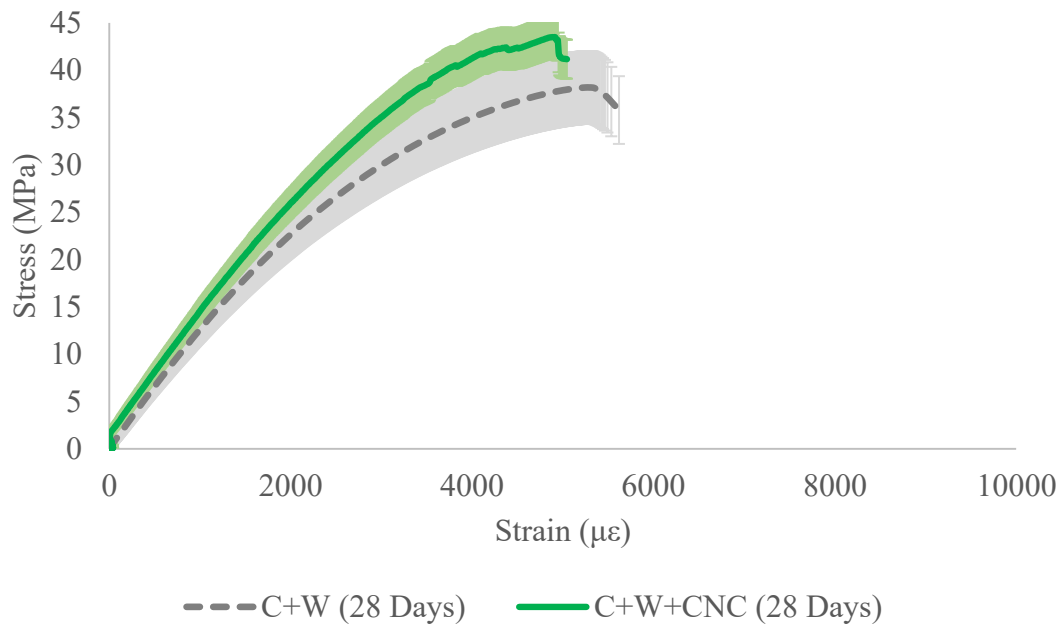


**Figure 5.14.** Stress-strain diagram of neat and CNC-dosed class G oil well cement paste after 28 days

It is well understood that cellulose nanocrystal (CNC) particles enhance the cement hydration when utilized in the cementitious systems [37, 38]. Based on the results reported in the literature [37, 38] and the findings in the previous sections of this comprehensive

study, the influence of CNC particles on the porosity and dynamic mechanical properties of cementitious systems (Chapter 4), verify the fact that the CNC particles improved the cement hydration. Evidently, the cellulose nanocrystal (CNC) particles acted as seeding agents to diffuse water towards the unhydrated cement grains (Figure 5.15). Furthermore, the porosity results obtained here verified that the CNC particles also alter the porosity using a second mechanism described as a pore-clogging mechanism. Therefore, the increase in strength and enhancement in the mechanical properties caused by cellulose nanocrystal particles have not been beyond expectation.

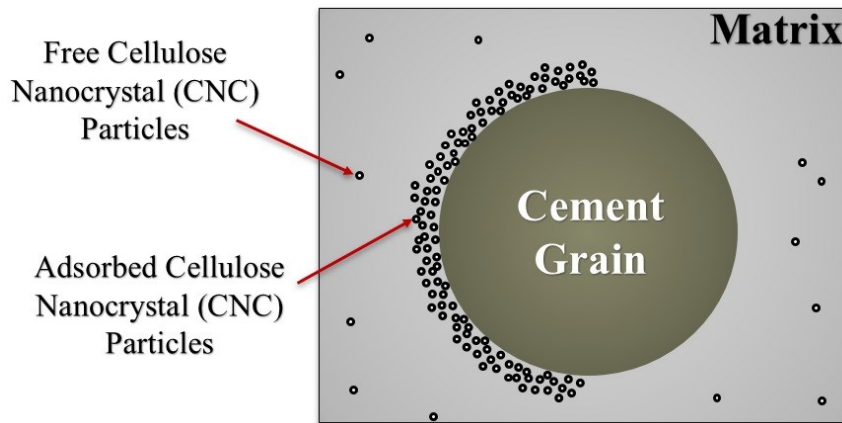


**Figure 5.15.** Schematic demonstration of adsorbed CNC particles on a cement grain (seeding agents) and free CNC particles in the matrix

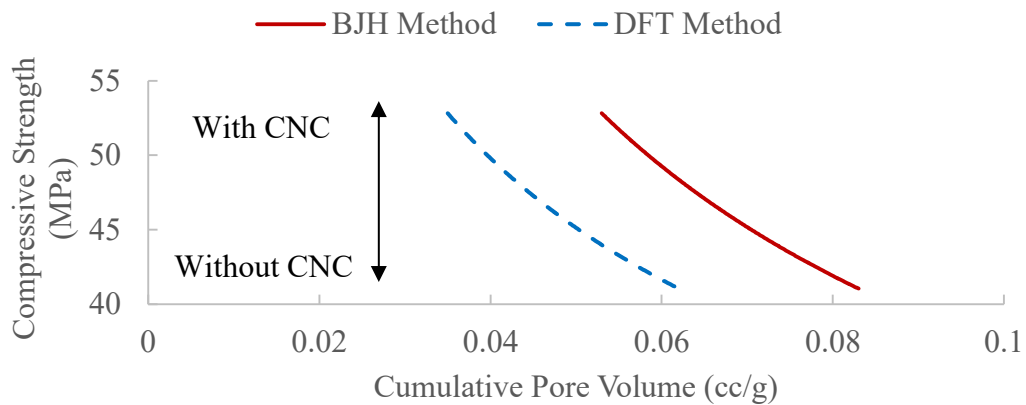


**Figure 5.16.** Compressive strength vs cumulative pore volume (the impact of CNC)

As illustrated in Figure 5.16, samples containing CNC particles eventually demonstrated a higher compressive strength and a lower cumulative pore volume. Moreover, the dynamic mechanical analysis performed earlier in this study (Chapter 4) also led to an understanding that the CNC particles enhance the complex shear modulus ( $G^*$ ) of the paste while it is still fresh. An increase in  $G^*$  is believed to be an enhancement in the rigidity of the cementitious system while the development of the structure of the system is occurring. Results obtained in this section also proved that the addition of CNC particles as an additive increased both compressive and tensile strength associated with oil well cement paste. Also, an enhancement in Young's modulus ( $E$ ) verified the stiffness enhancement reported earlier. However, note that previous studies [31, 40] claim that if the cellulose nanocrystal particles are not dispersed well enough, Young's modulus of the host material might decrease.

#### 4. CONCLUDING REMARKS

In the study presented here, the effect of cellulose nanocrystal (CNC) particles on the porosity and mechanical properties of hardened oil well cement paste was evaluated. In order to recognize and appreciate the impact caused by cellulose nanocrystal particles, the results obtained were compared to the ones achieved by examining neat oil well cement paste (containing no additive). Eventually, the following findings were reported:

- The addition of cellulose nanocrystal (CNC) particles reduced the surface area of the host material (oil well cement paste) significantly.
- The gas sorption measuring technique was utilized to investigate the effect of CNC on porosity. Different models were employed and all reported a decrease in cumulative pore volume with the addition of CNC.

- Since the gas sorption measuring technique is limited to narrow pores, no significant change in pore size distribution was observed.
- The cellulose nanocrystal particles had eliminated a significant amount of narrow pores (radius < 100nm).
- Previous studies had proved that CNC particles modify the pore structure of a cementitious system by enhancing the hydration and tuning large pores. However, the findings of this study declared that tuning the large pores may not be the only mechanism of action when CNC is present. In fact, the narrow pores were clogged by the CNC particles and the overall pore volume was reduced significantly.
- The cellulose nanocrystal (CNC) particles improved the compressive and the tensile strength of oil well cement paste by more than 60% during the first 24 hours. This is extremely beneficial since the early strength development of cement paste is crucial during well cementing operations.
- The stress-strain profile of oil well cementitious samples examined in this study verified an increase in Young's modulus of a hardened oil well cement paste by addition of CNC particles.
- Results obtained here were in complete agreement with the dynamic mechanical properties assessed in Chapter 4 of this comprehensive study. The dynamic mechanical analysis performed on fresh cement paste suggested an increase in rigidity and cement hydration should be expected when CNC particles are added to oil well cement paste.

## ACKNOWLEDGMENT

The authors would like to express their gratitude to Alberta Innovates Technology Futures (AITF), Alberta Innovates Bio Solutions, Alberta Pacific Forest Industries (Alpac) and Lafarge Canada for providing the material and funding required for this experimental study.

## REFERENCES

- [1] Shahriar, A. (2011). *Investigation on rheology of oil well cement slurries* (Doctoral dissertation, The University of Western Ontario).
- [2] Yahaba, N. (2010). *How Does A Decrease In Oil Production Affect The World Economy?*. Australia-Japan Research Centre.
- [3] Calvert, D.G. (2006). Preface. In: Nelson, E.B. and Guillot, D. (Ed.), *Well Cementing*, Schlumberger, Texas, pp. 1-11.
- [4] Zhang, M. H., & Li, H. (2011). Pore structure and chloride permeability of concrete containing nano-particles for pavement. *Construction and Building Materials*, 25(2), 608-616.
- [5] Živica, V. (1997). Relationship between pore structure and permeability of hardened cement mortars: on the choice of effective pore structure parameter. *Cement and Concrete Research*, 27(8), 1225-1235.
- [6] Tanaka, K., & Kurumisawa, K. (2002). Development of technique for observing pores in hardened cement paste. *Cement and Concrete Research*, 32(9), 1435-1441.

- [7] Poon, C. S., Wong, Y. L., & Lam, L. (1997). The influence of different curing conditions on the pore structure and related properties of fly-ash cement pastes and mortars. *Construction and Building Materials*, 11(7-8), 383-393.
- [8] Hoseini, M., Bindiganavile, V., & Banthia, N. (2009). The effect of mechanical stress on permeability of concrete: a review. *Cement and Concrete Composites*, 31(4), 213-220.
- [9] Tiab, D., & Donaldson, E. C. (2015). *Petrophysics: theory and practice of measuring reservoir rock and fluid transport properties*. Gulf professional publishing.
- [10] Thomas, J. J., Jennings, H. M., & Allen, A. J. (1999). The surface area of hardened cement paste as measured by various techniques. *Concrete Science and Engineering*, 1(1), 45-64.
- [11] Yang, R., & Buenfeld, N. R. (2001). Binary segmentation of aggregate in SEM image analysis of concrete. *Cement and Concrete Research*, 31(3), 437-441.
- [12] Wong, H. S., Head, M. K., & Buenfeld, N. R. (2006). Pore segmentation of cement-based materials from backscattered electron images. *Cement and Concrete Research*, 36(6), 1083-1090.
- [13] Wong, H. S., Buenfeld, N. R., & Head, M. K. (2006). Estimating transport properties of mortars using image analysis on backscattered electron images. *Cement and Concrete Research*, 36(8), 1556-1566.
- [14] Gregg, S. J., Sing, K. S. W., & Salzberg, H. W. (1967). Adsorption surface area and porosity. *Journal of the Electrochemical Society*, 114(11), 279C-279C.

- [15] Rarick, R. L., Bhatta, J. I., & Jennings, H. M. (1995). Surface area measurement using gas sorption: application to cement paste. *Material Science of Concrete IV, American Ceramic Society*, 1-41.
- [16] Brunauer, S., Emmett, P. H., & Teller, E. (1938). Adsorption of gases in multimolecular layers. *Journal of the American chemical society*, 60(2), 309-319.
- [17] Copeland, L. E., & Hayes, J. C. (1953). *The determination of non-evaporable water in hardened portland cement paste* (No. 47).
- [18] Copeland, L. E., & Bragg, R. H. (1954). The hydrates of magnesium perchlorate. *The Journal of Physical Chemistry*, 58(12), 1075-1077.
- [19] Odler, I. (2003). The BET-specific surface area of hydrated Portland cement and related materials. *Cement and Concrete Research*, 33(12), 2049-2056.
- [20] Goto, S., & Roy, D. M. (1981). The effect of w/c ratio and curing temperature on the permeability of hardened cement paste. *Cement and Concrete Research*, 11(4), 575-579.
- [21] Page, C., Short, N. R., & El Tarras, A. (1981). Diffusion of chloride ions in hardened cement pastes. *Cement and concrete research*, 11(3), 395-406.
- [22] Halamickova, P., Detwiler, R. J., Bentz, D. P., & Garboczi, E. J. (1995). Water permeability and chloride ion diffusion in Portland cement mortars: relationship to sand content and critical pore diameter. *Cement and concrete research*, 25(4), 790-802.

- [23] Jennings, H. M., Thomas, J. J., Gevrenov, J. S., Constantinides, G., & Ulm, F. J. (2007). A multi-technique investigation of the nanoporosity of cement paste. *Cement and Concrete Research*, 37(3), 329-336.
- [24] Nyame, B. K., & Illston, J. M. (1981). Relationships between permeability and pore structure of hardened cement paste. *Magazine of Concrete Research*, 33(116), 139-146.
- [25] Shih, J. Y., Chang, T. P., & Hsiao, T. C. (2006). Effect of nanosilica on characterization of Portland cement composite. *Materials Science and Engineering: A*, 424(1), 266-274.
- [26] Goodwin, K. J., & Crook, R. J. (1992). Cement sheath stress failure. *SPE Drilling Engineering*, 7(04), 291-296.
- [27] Heinold, T., Dillenbeck, R. L., & Rogers, M. J. (2002, January). The effect of key cement additives on the mechanical properties of normal density oil and gas well cement systems. In *SPE Asia Pacific Oil and Gas Conference and Exhibition*. Society of Petroleum Engineers.
- [28] Powers, C. A., Holman, G. B., & Smith, R. C. (1977). U.S. Patent No. 4,036,301. Washington, DC: U.S. Patent and Trademark Office.
- [29] Specification, A. P. I. (2010). 10A. *Cements and Materials for Well Cementing*.
- [30] Nelson, E. B., Baret, J. F., & Michaux, M. (1990). 3 Cement Additives and Mechanisms of Action. *Developments in Petroleum Science*, 28, 3-1.

- [31] Habibi, Y., Lucia, L. A., & Rojas, O. J. (2010). Cellulose nanocrystals: chemistry, self-assembly, and applications. *Chemical reviews*, 110(6), 3479-3500.
- [32] Pietz, L. M., & Thomas, E. A. (2014). Strengthening Construction Materials Via Incorporation of Cellulose Nanocrystals: A Sustainable Biomaterial.
- [33] Venere, E. (2013). Cellulose nanocrystals possible green wonder material. *Science Daily*.
- [34] Dufresne, A. (2012). *Nanocellulose: from nature to high performance tailored materials*. Walter de Gruyter.
- [35] Eichhorn, S. J., Dufresne, A., Aranguren, M., Marcovich, N. E., Capadona, J. R., Rowan, S. J., & Gindl, W. (2010). Review: current international research into cellulose nanofibres and nanocomposites. *Journal of materials science*, 45(1), 1.
- [36] Dri, F. L., Hector, L. G., Moon, R. J., & Zavattieri, P. D. (2013). Anisotropy of the elastic properties of crystalline cellulose I $\beta$  from first principles density functional theory with Van der Waals interactions. *Cellulose*, 20(6), 2703-2718.
- [37] Cao, Y., Zavaterra, P., Youngblood, J., Moon, R., & Weiss, J. (2015). The influence of cellulose nanocrystal additions on the performance of cement paste. *Cement and Concrete Composites*, 56, 73-83.
- [38] Cao, Y., Tian, N., Bahr, D., Zavattieri, P. D., Youngblood, J., Moon, R. J., & Weiss, J. (2016). The influence of cellulose nanocrystals on the microstructure of cement paste. *Cement and Concrete Composites*, 74, 164-173.

- [39] Niknaddaf, S., Atkinson, J. D., Shariaty, P., Lashaki, M. J., Hashisho, Z., Phillips, J. H., Anderson, J. E. & Nichols, M. (2016). Heel formation during volatile organic compound desorption from activated carbon fiber cloth. *Carbon*, 96, 131-138.
- [40] Klemm, D., Kramer, F., Moritz, S., Lindström, T., Ankerfors, M., Gray, D., & Dorris, A. (2011). Nanocelluloses: A new family of nature-based materials. *Angewandte Chemie International Edition*, 50(24), 5438-5466.

## Chapter VI

# *Permeability of Early Aged Oil Well Cement Paste Dosed with Cellulose Nanocrystal (CNC) Particles*

### **ABSTRACT**

In this chapter, cellulose nanocrystal (CNC) is utilized as a bio-based and non-toxic additive to oil well cement paste, in order to reduce the permeability of the system. The mass flow rate of early aged hollow cylindrical specimens dosed with CNC was measured by using a pressurized permeability cell. Furthermore, the water permeability of the specimens was evaluated using Darcy's law for laminar flow. The results were then compared to the mass flow rate and water permeability of neat oil well cement paste samples with no additive. Based on the results presented in this chapter, the water permeability of oil well cement paste was reduced with the addition of cellulose nanocrystal (CNC) particles.

*Keywords: Oil Well Cement, Cellulose Nanocrystal, Permeability, Early Age Cement Paste, Additive, Durability*

This chapter has been partially presented at the ICBBM EcoGRAFI conference. (Dousti, M. R., Boluk, Y., & Bindiganavile, V. *The effect of cellulose nanocrystal (CNC) on the water permeability of early aged oil well cement. Proc. ICBBM 2017, 2nd International Conference On Bio-Based Building Materials. RILEM*)

## **1. INTRODUCTION**

### **1.1. Oil Well Cement**

During the past few decades, oil consumption has increased significantly, especially from 1964 to 2008 [1]. This is mainly due to the fact that today, modern technology and culture is very much dependent on oil and oil-related products, although alternative renewable energy sources have propagated their way into human lives. The limited amount of oil present on earth has gradually forced everyone to extract, place and consume it properly, with the least time, energy and money wasted on this path. Thus, a large amount of money has been used in the oil industry to introduce and invent appropriate, suitable and advanced technologies to the address this issue [2]. In order to adequately design an oil well, different aspects, dimensions and parameters should be considered and addressed within the design. A poorly designed oil well might lead to incidents such as oil spill or other environmental disasters (due to toxic substances) [2]. Well cementing is one of the most crucial and important steps in any well completion. However, since it takes place at the end of the drilling process, a satisfying and acceptable job is rarely done. Hence, a large and significant amount of time and energy is then spent in order to do the required remedial cementing.

In the oil well cementing process, cement is used to fill the annular space between the casing string and the ground formation within the drilled hole. The cement used in an oil well has exclusive functions to perform. These include restricting the movement of hydrocarbons and/or water in between the permeable zones, providing a suitable mechanical support for the casing string, protecting the casing from any sort of physical damage including corrosion, and supporting the wellbore walls in order to prevent the

collapse of formation. Note that the difference between construction cement and oil well cement is that there is no aggregate added to oil well cement and also a large volume of water is used in oil well cement, in order to make the slurry pump-able. A vast number of additives are nowadays available to meet and achieve any kind of desired characteristics.

Durability is one of the main concerns when dealing with any kind of cementitious material or cementitious specimen. In structural applications of cementitious materials, maximum load and strength limits are rarely witnessed, therefore durability of the concrete and the reinforcement within the concrete plays a significant role in the failure of structures. Stressed or unstressed, cracks will be observed on any cementitious member. Transport and penetration of different types of harmful fluids into the cementitious member will eventually lead to the failure of the member. Therefore, the permeability of any cementitious material is one of the key factors affecting its durability. The permeability of a concrete or cementitious sample can be defined as the ease with which liquids, gases and other aggressive ions penetrate the sample. As mentioned by Zhang and Li [3], a higher permeability leads to a greater penetration of aggressive fluids or even water into concrete, which will eventually cause damage and deterioration. Therefore, a concrete with a lower permeability is basically accepted as a more durable concrete.

## **1.2. Permeability of Oil Well Cement**

While pumped into the annular space between the casing and the ground formation, oil well cement has to isolate and protect the casing from any kind of damage. Therefore, the durability of the cement paste utilized in oil well cementing is extremely important to any individual involved in the oil industry. In the absence of aggregates, concerns arise both in the short term performance including fluid loss (filtration) and flowability, and in the long

term as in shrinkage cracking and permeability of the cementitious slurry. The amount of water penetrated into the cementitious system should be minimized since the ions dissolved in water may also cause serious damage to the microstructure of the system [4].

The permeability of a material (porous media) is very dependent on the effective porosity of the material. This means that all the parameters such as grain (particle) size and shape, grain size distribution, cementation and consolidation degree, and interconnectivity of the pores affect the permeability of the material. Similar to porosity, the permeability of a sample can also be mathematically evaluated. Darcy's equation has been employed for decades, in order to compute the permeability value of a core sample [5]. The permeability of a concrete or cementitious sample can be defined as the ease with which liquids, gases and other aggressive ions penetrate the sample. As mentioned in the literature [3], a higher permeability leads to a greater penetration of aggressive fluids or even water into concrete, which will eventually cause damage and deterioration. Therefore, a concrete with a lower permeability is basically accepted as a more durable concrete. It is also understood that permeability is a function of pore size distribution, thus it is directly influenced by the porosity of the material [6]. Zhang and Li categorize the main factors which affect the permeability of concrete as: (1) factors influencing the original pore structure of the concrete such as the water-to-cement ratio, (2) factors affecting the development of pore structure of concrete such as age and the curing condition, and (3) factors related to the penetration such as the hydration rate and the chemical composition of the penetration media [3].

The permeability of cement paste has always been a concern and it has been investigated through several methods and experimental designs. In one of the early studies to measure

the water permeability of cement paste samples, Goto and Roy utilized a simple apparatus which was initially developed by White et al. in 1979 [7]. The apparatus had a pressure tank piped to a container. The container itself had a driving piston inside to press down the ionized water on top of the cement sample at the bottom of the container. Thus, when the pressure was released, the piston would press the water towards the sample, and after passing through the sample and a porous plate, the permeated water was collected inside a cylinder.

After performing the permeability test, the results presented by Goto and Roy showed that water permeability of cement paste samples increases as the water-to-cement ratio increases. However, it was observed that the samples cured in a high temperature (60 °C) had a higher permeability compared to the ones cured in a lower temperature (27 °C). Also, they concluded that pores with a larger radius have a very important effect on the permeability of hard cementitious samples [7]. In 1995, the (water) permeability of cement mortar samples was assessed by Halamickova et al., using a permeability cell [8]. This permeability cell was able to monitor both inflow and outflow in calibrated cylinders, as well as measuring the driving pressure.

Each measurement was made in a duration between 200-300 hours, so it was regarded as a time consuming apparatus and system. The outcome of the research indicated that the higher permeability was corresponding to a lower degree of hydration. This was the same trend observed in the porosity assessment of the samples with regards to the degree of hydration (i.e. the higher porosity corresponding to a lower degree of hydration). In their research, the Katz-Thompson relationship was utilized to estimate the porosity [8], diffusion coefficient and also the permeability of the samples. However, it was concluded

that the Katz-Thomson theory overestimated the permeability at  $w/c = 0.5$  and significantly overestimated the permeability at  $w/c = 0.4$  systems [8].

Some studies related to the permeability of cement paste or concrete, are associated with chloride ingress or diffusion into the concrete or hardened cement paste. Andrade measured the chloride diffusion coefficient in concrete, insisting that the penetration of chloride through concrete is one of the important elements and factors that deteriorates the steel reinforcement inside the concrete. However, in oil well cement pastes, this factor could result in damaging the casing of the well [9]. Furthermore, studies performed in the past, justify the fact that the water permeability of a cementitious system is lower than its gas permeability. Loosveldt et al. clarified that this difference may be up to 1 or 2 order of magnitude. They believed that this difference could be explained by phenomena such as rehydration or water adsorption in the thinnest pores [10].

Based on previous experimental studies, researchers have concluded that the permeability of a cementitious system may be influenced by some other factors such as hydraulic radius, the rate of hydration, and also the flow regime. In their experimental study, Nyame and Illston emphasized on the fact that hydraulic radius, porosity and surface area are non-uniquely related to permeability. In fact, they observed, for a given age, the measured surface area (by mercury intrusion porosimetry) increased with permeability. The same trend was observed while comparing the hydraulic radius of hardened cement paste samples to the permeability of that [11].

Elsewhere, in a study on water permeability of cement paste, Bantia and Mindess concluded that by increasing the degree of hydration or the curing time, a decrease in the permeability coefficient will be observed [12]. Hoseini and colleagues also investigated

the permeability of concrete while stressed and unstressed. In their experimental approach, the permeability of concrete was evaluated after achieving an equilibrium in fluid flow. This is mainly due to the fact that Darcy's law (which is used to determine the coefficient of permeability), assumes a slow, unidirectional and steady flow [13].

### **1.3. Objective of Study**

Nowadays, various commercial additives are produced and employed to address the durability issues in cementitious systems. The objective of this study is to propose cellulose nanocrystal (CNC) as a novel and non-toxic additive to improve the durability of a cementitious system by decreasing the water permeability associated with that system. Although cellulose nanocrystal has been widely used in different industrial applications, it has not been utilized in oil well cement industry up to now. In recent studies, the effect of CNC on the mechanical performance of ordinary cement paste has been studied [14], whereas in the experimental study presented in this section, emphasize is mainly on the improvement of the transport properties of oil well cement paste, under the influence of this innovative nanomaterial.

## **2. EXPERIMENTAL DETAILS**

### **2.1. Materials**

#### *2.1.1. Oil Well Cement Type G*

The cement used for this experimental study was Type G cement, based on the American Petroleum Institute (API) classification, specification 10A for oil well cements [15]. Type G cement is comparable to ASTM Type II or Type V Portland cement. It is recommended

to use a water-to-cement ratio of 0.44 for this type of cement. Tables 6.1 and 6.2, describe the physical properties and chemical composition of this type of cement, respectively.

**Table 6.1.** Physical properties of Type G cement (prepared by Lafarge Canada, December 8<sup>th</sup>, 2015)

<b>Physical Analysis</b>	
Thickening Time (Schedule 5)	99 min.
Max. Consis. 15-30 min.	23 Bc
Fineness 45 $\mu\text{m}$ sieve	93.9%
Blaine	311 $\text{m}^2/\text{kg}$
Free Fluid	4.4 %

**Table 6.2.** Chemical composition of Type G cement (prepared by Lafarge Canada, December 8<sup>th</sup>, 2015)

<b>Chemical Analysis</b>	
Silica ( $\text{SiO}_2$ )	20.9%
Alumina ( $\text{Al}_2\text{O}_3$ )	3.8%
Iron Oxide ( $\text{Fe}_2\text{O}_3$ )	4.7%
Calcium Oxide, Total (TCaO)	62.9%
Magnesium Oxide (MgO)	4.5%
Sulphur Trioxide ( $\text{SO}_3$ )	2.6%
Loss on Ignition	0.66%
Insoluble Residue	0.13%
Equivalent Alkali (as $\text{Na}_2\text{O}$ )	0.48%
$\text{C}_3\text{S}$	57.9%
$\text{C}_2\text{S}$	16.1%
$\text{C}_3\text{A}$	2.0%
$\text{C}_4\text{AF}$	14.3%
$\text{C}_4\text{AF} + 2\text{X } \text{C}_3\text{A}$	18.3%

### 2.1.2. Cellulose Nanocrystal (CNC)

Cellulose whiskers or cellulose nanocrystals are non-toxic rod shaped nanoparticles derived from cellulose [16, 17]. There has been a significant trend in employing and utilizing CNC in many research areas due to its unique strength, optical and surface properties. In order to have a better understanding of cellulose nanocrystals, one should know that a cellulose molecule has an extremely complex hydrogen-bonding network with multiple isotropic and anisotropic phases, as elaborated by Dufresne [16].

The fibrils (substructure of cellulose) are orientated in the same direction in an isotropic phase where as in an anisotropic phase, there are several layers of isotropic phases stacked upon each other to form a fibril layer in different orientations [17]. This is mainly important because these isotropic and anisotropic phases impact and influence the physical properties of cellulose. Furthermore, it is understood that the rod shaped cellulose nanocrystal particles in aqueous solutions have negative electrical charges. This could be explained as a result of the formation of sulfate groups on their surface, as described by Boluk et al. [18].

The applications of CNC varies from case to case. In some cases, it has been used in drug industry whereas the construction industry has also had its share. Cellulose nanocrystals are also widely employed as reinforcing agents in nanocomposites, electro-optical materials, bio carrier, etc. due to their low cost, availability, inherent renewability, nanoscale dimension, unique morphology, light weight, sustainability and abundance. Nowadays, mechanical high shear disintegration and high pressure homogenization are utilized to isolate nanofibrillated cellulose from raw commercial pulp and straw. Venere described cellulose nanocrystal as one of the most novel biomaterials that are employed

and employed in a wide range such as structural components of electronic sensors, water purification filters, and also the strengthening of construction materials [19].

There are different methods of producing and preparing cellulose nanocrystals nowadays. In their experimental work, Bondeson and colleagues prepared some rod shaped cellulose nanocrystals by acid hydrolysis of dissolving pulp or cotton with 65% concentrated sulfuric acid [20]. The outcome of their experimental work was preparation and production of certain cellulose nanocrystals with a width of generally 5-10 nm and a length of 100-300 nm. In this study, the aspect ratio or the shape parameter (length/diameter) of the CNC particles are in between 10-60.

## **2.2. Specimen Preparation**

The paste was initially formulated based on a mixture of water and oil well cement (Type G). Furthermore, cellulose nanocrystal (CNC) particles were added in form of an aqueous solution. As described earlier, the water-to-cement ratio selected for this purpose was 0.44 based on the API specification 10A [15]. For the mixing process, a high shear cement (concrete) mixer was utilized and the mixing took place at a noticeably high speed. In this process, firstly the amount of water was calculated based on the water-to-cement ratio. This amount was then used to evaluate the desired amount of CNC. Note that only a dosage of 1% (w/v of water) CNC has been used in this experimental study. Furthermore, as described earlier, the CNC particles were mixed with an adequate amount of water (deducted from the total amount of water so that the water-to-cement ratio would not change). After mixing the cement powder with the remaining water (while the mixer is turned on), the CNC solution was added to the high shear mixer.



**Figure 6.1.** EIRICH high shear mixer (left) and the prepared cementitious paste (right)



**Figure 6.2.** Hollow cylindrical samples prepared for the permeability test

Note that in this experimental study, two different types of samples were designed and prepared in the form of hollow cylinders: (1) samples cast from cement and water only (referred to as C+W in this chapter) and (2) samples cast from the combination of cement, water and CNC (referred to as C+W+CNC in this chapter). The inside and outside diameters of these cylinders were 50 mm and 100 mm respectively, with a specimen height of 200

mm. In order to take the effect of curing time into consideration in this study, a group of prepared specimens were cured in a humidity room (humidity = 100% and temperature =  $25^{\circ}\text{C} \pm 2$ ) for a period of 1 day, whereas another set of specimens were cured for 1 week prior to testing. Figure 6.2 demonstrates a prepared hollow cylindrical sample which has been demolded using a hydraulic jack and cured for a week and it is ready to be tested.

**Table 6.3.** The prepared and tested specimens (for permeability measurement)

<b>Specimen Code</b>	<b>w/c</b>	<b>CNC Content</b>	<b>Curing Period (day)</b>
(1) C+W	0.44	0% (w/v of water)	1
(2) C+W+CNC	0.44	1% (w/v of water)	1
(3) C+W	0.44	0% (w/v of water)	7
(4) C+W+CNC	0.44	1% (w/v of water)	7

Table 6.4 demonstrates a sample mix design identical to the mix design used in this research study.

**Table 6.4.** Mix design (sample) for preparation of cement paste

<b>Oil Well Cement Paste (Mix Design)</b>	
Cement	1000 kg
Water	440 kg
Cellulose nanocrystal (CNC) particles	4.4 kg

As was done earlier, again, the CNC particles were individually homogenized in a suitable fraction of the mix water. The oil well cement was mixed first with the remaining water to prepare a slurry. The CNC particles, now in their own suspension, were then added to the slurry and the mixture was agitated further for 5 minutes. Note that due to the inherent properties of cellulose nanocrystal (CNC) particles, the dosage being added to the mix

design (in this case 1% of the total amount of water or approximately 0.5% mass fraction of the total amount of cement powder used), and their associated mechanism of adsorption with the water molecules, any change to the water-to-cement ratio of the prepared cementitious system will be negligible. Recent studies have also confirmed that despite their hydrophilic nature, even with higher dosages of CNC used, at a high relative humidity (approximately 97% where CNC particles are immersed in water), the water adsorption of dry CNC particles is in the region of 34% which is only about 0.7% of the total mixing water in mass [14]. In this study, considering the fact that CNC particles are added to the mix design in the form of an aqueous solution (similar high relative humidity as the mentioned study), the adsorbed water on CNC will be approximately 0.3% of the total mixing water in mass. Therefore, based on Table 6.4, the water-to-cement ratio will change from a value of “440 kg / 1000 kg = 0.44” to a revised value of “441.5 kg / 1000 kg = 0.4415” which is negligible.

### **2.3. Test Method**

The specimens were tested by using a pressurized permeability cell developed by Hoseini et al. at the University of Alberta, which has been adapted from Biparva's apparatus [21]. However, in this research, the permeability test was not executed under load and the specimens remained unstressed. The test setup is demonstrated in Figure 6.3. By utilizing this permeability test setup, in this proposed method, pressurized water (approximately 100 psi  $\approx$  0.69 MPa) was introduced to the outer wall of the cylindrical specimens (inside the permeability cell). Note that the specimens were sealed (by using silicon) within the permeability cell, to prevent any leakage. Consequently, the water permeated through the specimen and eventually the mass of the outflow was collected in a beaker which had been

rested on top of a sensitive weighing scale. The scale was connected to a computer device and real-time measurement and recording of the outflow mass were performed. Note that in this method, the flow was monitored until a steady-state condition was reached.

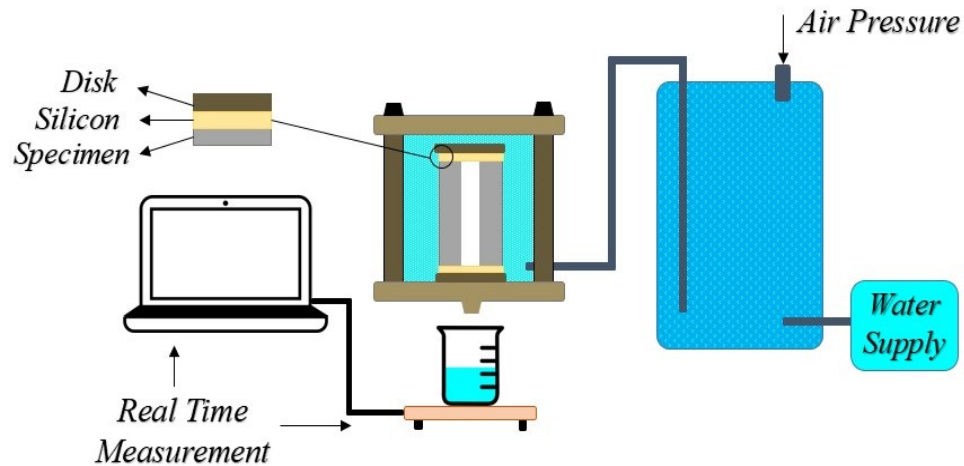


**Figure 6.3.** A schematic diagram of the permeability test setup employed [13, 21]

After reaching the steady state condition on each sample (which depending on the mix design and composition, could be a matter of few minutes or a few hours after starting the test), the mass flow rate was evaluated and by utilizing Darcy's law for laminar flow, the water permeability of each cementitious sample was evaluated.

### 3. RESULTS AND DISCUSSION

#### 3.1. Mass Flow Rate

After performing the experiment on the specimens with and without cellulose nanocrystals, the mass flow rate profile of the cementitious specimens was obtained. Figure 6.4 demonstrates the flow rate profile of specimens after just 1 day of curing, whereas in Figure 6.5, the flow rate profile of the cementitious specimens after 7 days of curing is presented.

Based on the curves and the results obtained, it was concluded that the oil well cement paste samples containing cellulose nanocrystals reached the steady state condition at a much lower flow rate compared to the neat oil well cement paste samples. According to Figure 6.4 and Figure 6.5, after adding the cellulose nanocrystal additive to the cementitious system, a significant drop in the mass flow rate was witnessed during the experiment.

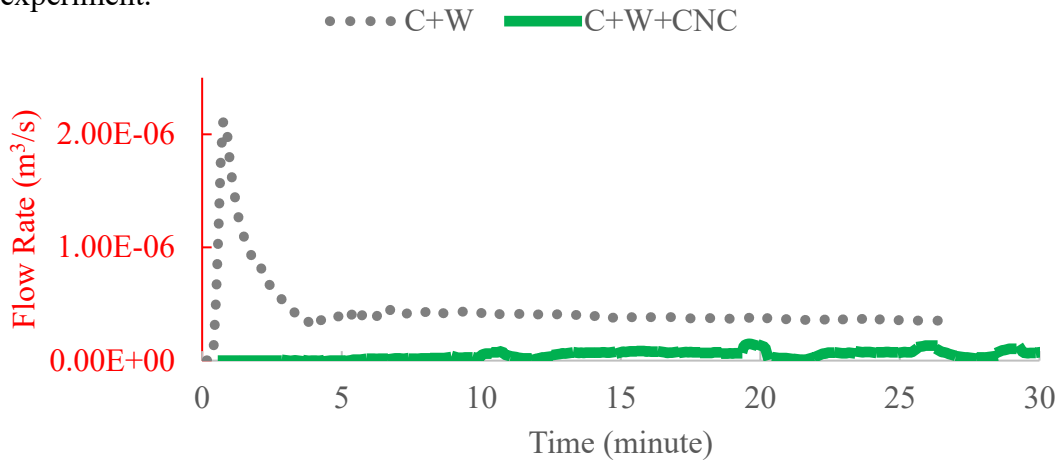


**Figure 6.4.** The mass flow rate profile of hardened oil well cement paste samples after 1 day of curing time

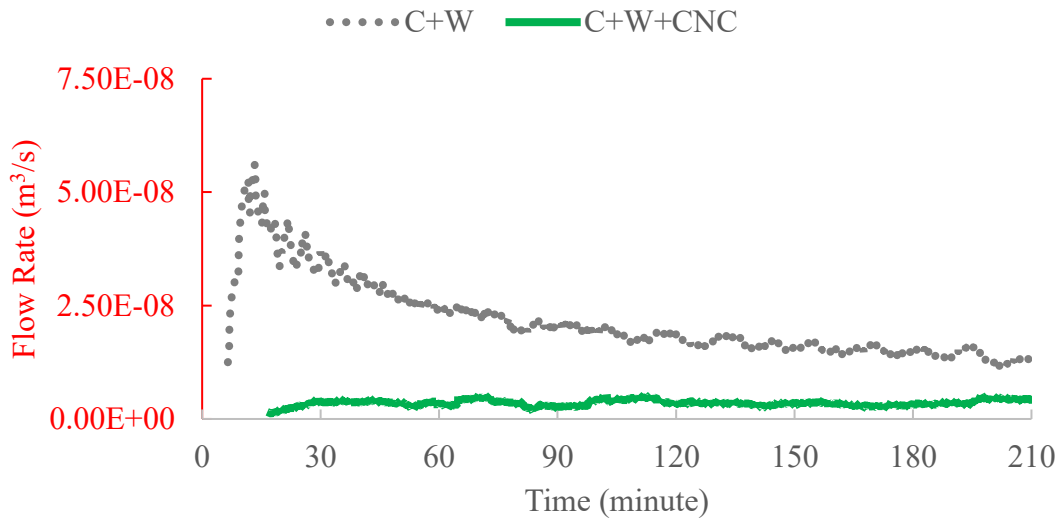


**Figure 6.5.** The mass flow rate profile of hardened oil well cement paste samples after 7 days of curing time

Furthermore, in oil well systems containing cellulose nanocrystals, steady state was reached much faster compared to the neat oil well cement paste. This phenomenon is related to the water diffusion within the cementitious systems experimented.

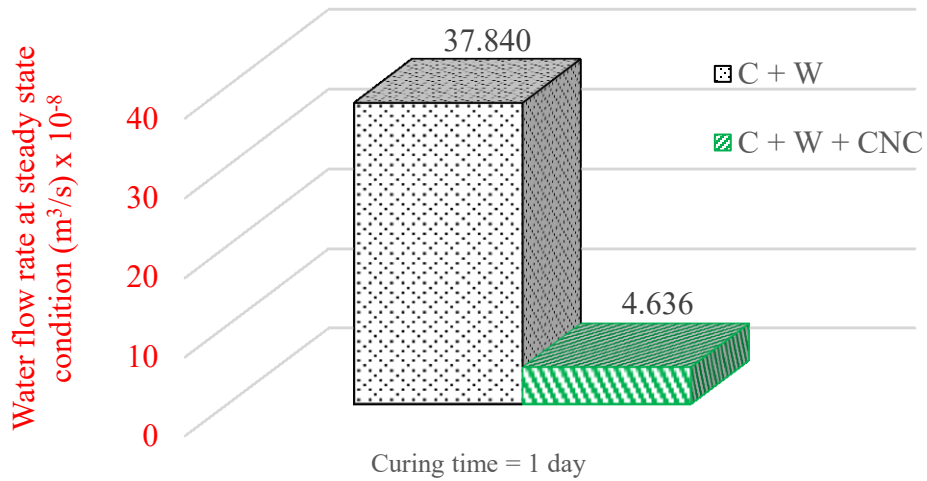


**Figure 6.6.** Flow rate comparison of cementitious systems at steady state condition with and without cellulose nanocrystal (CNC) particles after 1 day of curing time

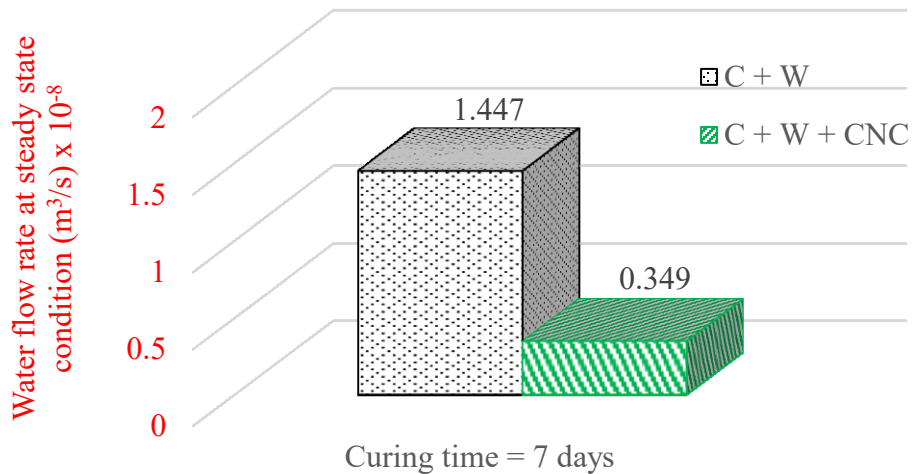


**Figure 6.7.** Flow rate comparison of cementitious systems at steady state condition with and without cellulose nanocrystal (CNC) particles after 7 days of curing time

In oil well cement pastes with cellulose nanocrystals as an additive, the pores were saturated within a shorter period of time, whereas in the neat oil well cement paste, the pores were fully saturated in a much slower pace. Figure 6.6 compares the value of flow rate ( $Q$ ) at the steady state, for systems with and without cellulose nanocrystals, after just 1 day of curing time, whereas Figure 6.7 demonstrates the same comparison after 7 days of curing. Table 6.5 summarizes the effect of cellulose nanocrystal (CNC) particles as an additive on the flow rate of oil well cementitious systems.

**Table 6.5.** The effect of CNC particles on the flow rate of cementitious samples

<b><math>Q_{1 \text{ day}} \text{ (cm}^3\text{/min)}</math></b>		<b><math>Q_{7 \text{ days}} \text{ (cm}^3\text{/min)}</math></b>	
<i>C+W</i>	<i>C+W+CNC</i>	<i>C+W</i>	<i>C+W+CNC</i>
22.704	2.782	0.868	0.209
<i>Reduction (%)</i>		75.92%	
87.75%			

Based on data tabulated above, the effect of cellulose nanocrystal particles on the flow rate was still significant after 7 days of curing (75.92% reduction). However, this reduction was even larger in early aged samples which had only been cured for a single day (87.75% reduction). Note that the flow rate ( $Q$ ) values presented above are associated with the steady state condition of the cementitious system and not prior to that. These values were later utilized to compute and evaluate the water permeability of the samples. This is further explained and expanded in the next section.

### 3.2. Water Permeability

After performing the experiment and collecting the desired data (flow rate profile of the samples) using the digital scale and the data acquisition system connected to the permeability apparatus, the water permeability coefficient of the specimens was calculated according to Darcy's law for laminar flow. Note that at this stage of the study, the water permeability coefficient of the samples was computed based on the flow rate ( $Q$ ) measured at steady state condition (when pores are fully saturated). The equations employed can be summarized as below:

$$k_w = k_i \left( \frac{\rho \cdot g}{\mu} \right)$$

$$k_i = \left( \frac{Q \cdot \mu \cdot L}{A \cdot \Delta P} \right)$$

Where:

$k_w$ : water permeability coefficient (m/s);

$k_i$ : intrinsic permeability (m<sup>2</sup>);

$\rho$ : density of water (kg/m<sup>3</sup>);

$g$ : gravitational acceleration (m/s<sup>2</sup>);

$\mu$ : viscosity of water (kg/ms);

$Q$ : rate of water flow (m<sup>3</sup>/s);

$L$ : specimen's thickness (m);

$A$ : permeation area (m<sup>2</sup>);

$\Delta P$ : pressure difference introduced (Pa – N/m<sup>2</sup>)

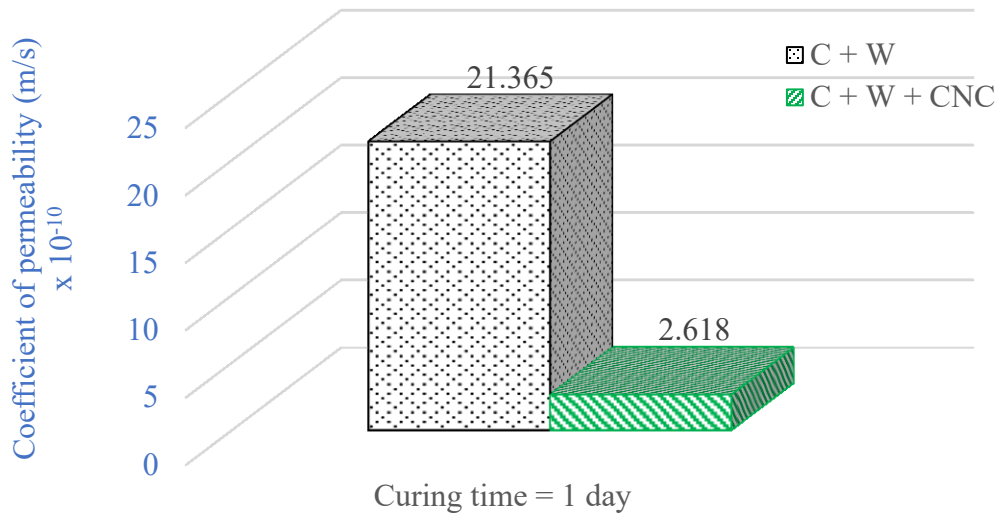


**Figure 6.8.** Coefficient of water permeability ( $k_w$ ) in early aged oil well cement pastes with and without cellulose nanocrystal (CNC) particles, after 1 day of curing

Figures 6.8 and 6.9, demonstrate the effect of cellulose nanocrystal particles (as additive) on the water permeability coefficient of oil well cement paste samples. Therefore, 2 different type of samples were investigated: (1) neat oil well cement paste samples (with no CNC) and (2) oil well cement paste samples dosed with 1% (w/v of water) CNC. Similar to the previous section of this study, the water permeability of samples were assessed at the early age. Results presented below are associated with samples cured for 1 day and samples cured for 7 days.

**Table 6.6.** The effect of CNC particles on the coefficient of water permeability of oil well cementitious samples

$k_w, 1 \text{ day } (\text{m/s}) \times 10^{-10}$		$k_w, 7 \text{ days } (\text{m/s}) \times 10^{-10}$	
<i>C+W</i>	<i>C+W+CNC</i>	<i>C+W</i>	<i>C+W+CNC</i>
21.365	2.618	0.817	0.197
<i>Reduction (%)</i>		75.89%	

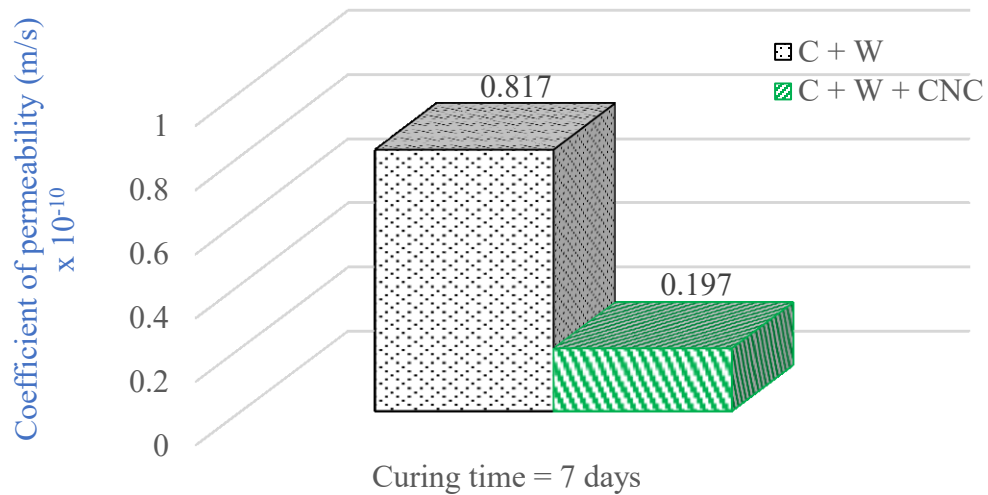


**Figure 6.9.** Coefficient of water permeability ( $k_w$ ) in early aged oil well cement pastes with and without cellulose nanocrystal (CNC) particles, after 7 days of curing

Furthermore, Table 6.6 summarizes the effect of cellulose nanocrystal (CNC) particles as an additive on the coefficient of water permeability ( $k_w$ ) of oil well cementitious systems. According to the results obtained and computed, a decrease in the coefficient of water permeability ( $k_w$ ) was observed by introducing cellulose nanocrystal (CNC) particles as an additive to the cementitious mix design. This could be due to the fact that CNC particles may have changed the pore structure and pore size distribution of the specimen. Note that previous studies and investigations show that the addition of cellulose nanocrystal particles will increase the strength of the cementitious system [14].

In this study, the compressive strength of the tested samples was also considered. Moreover, an increase in strength was also observed in the samples prepared and tested in this experimental study. Hardened oil well cement samples which did not include any dosage of cellulose nanocrystal particles, demonstrated an average compressive strength of 2.45 MPa after a single day of curing.

However, when the CNC particles were introduced to the mix design, the average compressive strength of the samples (after 1 day of curing) was found to be 6.39 MPa. The same procedure was utilized for the samples which were tested after 7 days of curing. At this stage, the average compressive strength of neat oil well cement (without CNC) samples was 19.02 MPa whereas the average compressive strength of the samples with CNC particles was recorded as 26.09 MPa. Hence, the decrease in permeability could be related to this change of strength. Cellulose nanocrystal particles tend to host the hydration and act as a seeding agent. This phenomenon is believed to lead towards an increase in hydration and also in strength development, resulting in a less permeable oil well cement paste.

On the other hand, the permeability results obtained in this study could be justified using the information gained from the porosity assessment performed earlier. The pore structure of neat and CNC-dosed oil well cement paste was analyzed using the gas sorption technique and different models such as BET, BJH and DFT were implemented to recognize the influence of cellulose nanocrystal (CNC) particles on the pore volume of the specimens prepared.

Using the Nitrogen isotherm, the surface area of different oil well cement samples was computed and compared. Table 6.7 and Figure 6.10 demonstrate a comparison between the measured surface area associated with neat samples and the surface area corresponding to the samples containing CNC particles. All three models utilized for this investigation declared that the presence of CNC particles reduced the surface area of the cementitious system. Note that the Brunauer-Emmet-Teller (BET) model is believed to be the most accurate method for expressing the surface area of a material.

**Table 6.7.** The surface area of neat and CNC-dosed oil well cement paste samples obtained using different techniques

	Surface Area ( $\text{m}^2/\text{g}$ )		
	Neat Cement Paste	Cement Paste with CNC	% Difference
<i>BET</i>	12.917	5.542	57.1
<i>DFT</i>	15.198	6.186	59.3
<i>BJH</i>	21.396	7.662	64.2

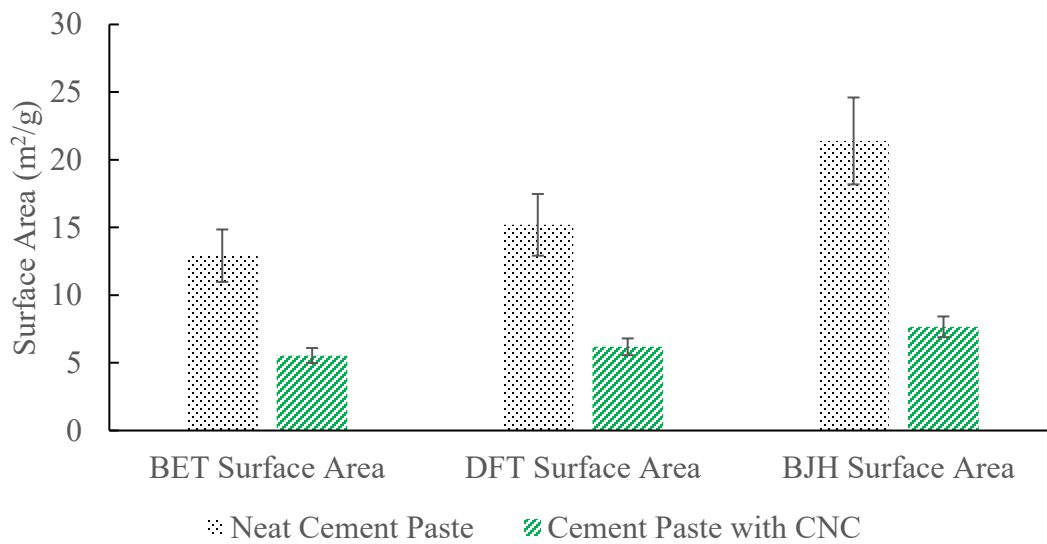


**Figure 6.10.** A visual comparison of surface area obtained from different models

Previous studies [22] indicate that the presence of CNC particles in the cement matrix reduces porosity in larger pores by enhancing hydration. Thus, the larger pores are tuned and the pore size distribution changes [22]. However, the gas sorption technique displays its own limits in terms of pore size recognition. Porosity assessment completed in this study was limited to narrow pores with radius  $< 100$  nm. According to the results, the presence of cellulose nanocrystal (CNC) particles reduced the cumulative pore volume dramatically, whereas no significant change in pore size distribution was witnessed within the examined

range. Even though the pores considered in this method are basically small gel pores and medium capillary pores, enhancement of cement hydration is still a probable scenario. However, this might not be the only mechanism of action in altering the porosity.

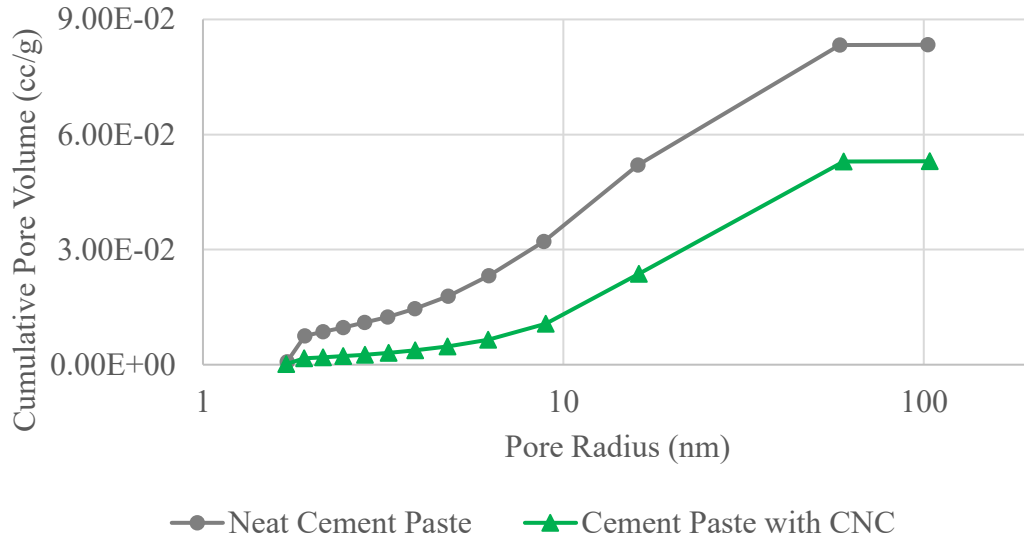


**Figure 6.11.** The effect of cellulose nanocrystal (CNC) particles on the cumulative pore volume of hardened oil well cement paste, obtained using the BJH method

Figure 6.11 and Figure 6.12 verify that a large number of narrow pores were eliminated when CNC was introduced to the cementitious system. The rod like cellulose nanocrystal (CNC) particles are believed to have altered the pore structure of the hardened oil well cement paste by another well-known mechanism called pore-clogging. A similar kind of behavior has also been witnessed in other studies where nano-SiO<sub>2</sub> particles had reduced the total pore volume of a cementitious system without making any significant change to the pore size distribution associated with it [3].

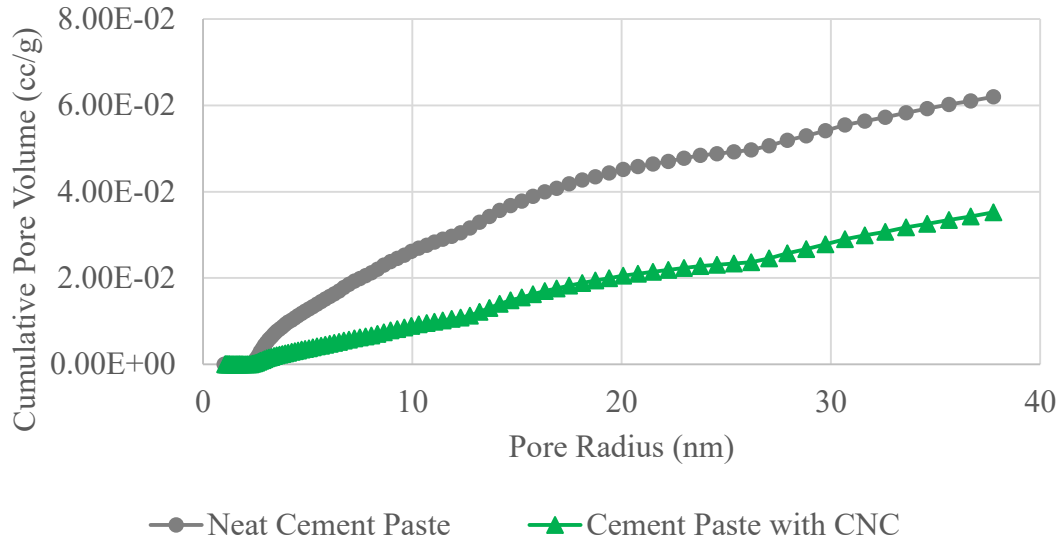


**Figure 6.12.** The effect of cellulose nanocrystal (CNC) particles on the cumulative pore volume of hardened oil well cement paste, obtained using the DFT method

Therefore, the reduction in mass flow rate and consequently the drop in water permeability in CNC-dosed hardened oil well cement samples is not only attributed to the increase in strength, but also to the change in porosity caused by the novel cellulosic additive (CNC) implemented in this experimental study.

#### 4. CONCLUDING REMARKS

In this experimental study, the water permeability of hardened early aged oil well cement paste samples was investigated in order to study and understand the effect of cellulose nanocrystal (CNC) particles as an additive on the permeability. Hollow cylindrical specimens were prepared with 2 different formulations, one excluding cellulose nanocrystal particles and the other including 1% (w/v of water) of this bio-based nanomaterial. One group of the samples were cured for only 1 day whereas another group were cured for a duration of 7 days after demolding, prior to the permeability test. The

experiment was conducted under a differential pressure of 0.69 MPa ( $\approx 100$  psi) and the cylindrical specimens were fully sealed to avoid leakage. The apparatus was connected to a digital scale and a data acquisition system and real-time data logging was performed. The following specific findings were observed:

- Whether cured for a single day or 7 days, the addition of cellulose nanocrystal particles led to a significant decrease in the flow rate of hardened oil well cement samples.
- Oil well cement paste samples dosed with cellulose nanocrystals reached a steady state flow condition sooner than the neat oil well cement paste samples.
- Introducing cellulose nanocrystal particles as an additive, reduced the water permeability of hardened early aged oil well cement samples dramatically.
- The permeability reduction percentage corresponding to samples containing cellulose nanocrystal particles was found to be 87.75% for samples tested after 1 day, and 75.89% for samples tested after 7 days of curing.
- The compressive strength of oil well cement paste samples also improved by introducing cellulose nanocrystal particles, confirming previous studies performed in this area.
- As previously reported (Chapter 5), the cellulose nanocrystal (CNC) particles had also reduced the surface area and total pore volume of the hardened oil well cement paste samples. Hence, the drop in water permeability could also be attributed to the change in porosity.

The above mentioned concluding remarks were clearly observed in all the samples tested, verifying the consistency of the results.

## ACKNOWLEDGMENTS

The authors would like to express their gratitude to Alberta Innovates Technology Futures (AITF), Alberta Innovates Bio Solutions, Alberta Pacific Forest Industries (Alpac) and Lafarge Canada.

## REFERENCES

- [1] Yahaba, N. (2010). *How Does A Decrease In Oil Production Affect The World Economy?*. Australia-Japan Research Centre.
- [2] Shahriar, A. (2011). *Investigation on rheology of oil well cement slurries* (Doctoral dissertation, The University of Western Ontario).
- [3] Zhang, M. H., & Li, H. (2011). Pore structure and chloride permeability of concrete containing nano-particles for pavement. *Construction and Building Materials*, 25(2), 608-616.
- [4] Russo, V., Ferrari, G., Salvioni, D., Valentini, L., Artioli, G., & Stefancic, M. (2017, April). Study of the effect a novel metal-silicate nanodispersion on the water permeability of concrete. Proceedings of the 39th International Cement Microscopy Association Conference, Toronto (pp. 198-206).
- [5] Tiab, D., & Donaldson, E. C. (2015). *Petrophysics: theory and practice of measuring reservoir rock and fluid transport properties*. Gulf professional publishing.
- [6] Živica, V. (1997). Relationship between pore structure and permeability of hardened cement mortars: on the choice of effective pore structure parameter. *Cement and Concrete Research*, 27(8), 1225-1235.

- [7] Goto, S., & Roy, D. M. (1981). The effect of w/c ratio and curing temperature on the permeability of hardened cement paste. *Cement and Concrete Research*, 11(4), 575-579.
- [8] Halamickova, P., Detwiler, R. J., Bentz, D. P., & Garboczi, E. J. (1995). Water permeability and chloride ion diffusion in Portland cement mortars: relationship to sand content and critical pore diameter. *Cement and concrete research*, 25(4), 790-802.
- [9] Andrade, C. (1993). Calculation of chloride diffusion coefficients in concrete from ionic migration measurements. *Cement and concrete research*, 23(3), 724-742.
- [10] Loosveldt, H., Lafhaj, Z., & Skoczylas, F. (2002). Experimental study of gas and liquid permeability of a mortar. *Cement and Concrete Research*, 32(9), 1357-1363.
- [11] Nyame, B. K., & Illston, J. M. (1981). Relationships between permeability and pore structure of hardened cement paste. *Magazine of Concrete Research*, 33(116), 139-146.
- [12] Banthia, N., & Mindess, S. (1989). Water permeability of cement paste. *Cement and Concrete Research*, 19(5), 727-736.
- [13] Hoseini, M., Bindiganavile, V., & Banthia, N. (2009). The effect of mechanical stress on permeability of concrete: a review. *Cement and Concrete Composites*, 31(4), 213-220.
- [14] Cao, Y., Zavaterra, P., Youngblood, J., Moon, R., & Weiss, J. (2015). The influence of cellulose nanocrystal additions on the performance of cement paste. *Cement and Concrete Composites*, 56, 73-83.

- [15] Specification, A. P. I. (2010). 10A. *Cements and Materials for Well Cementing*.
- [16] Dufresne, A. (2012). *Nanocellulose: from nature to high performance tailored materials*. Walter de Gruyter.
- [17] Habibi, Y., Lucia, L. A., & Rojas, O. J. (2010). Cellulose nanocrystals: chemistry, self-assembly, and applications. *Chemical reviews*, 110(6), 3479-3500.
- [18] Boluk, Y., Lahiji, R., Zhao, L., & McDermott, M. T. (2011). Suspension viscosities and shape parameter of cellulose nanocrystals (CNC). *Colloids and Surfaces A: Physicochemical and Engineering Aspects*, 377(1), 297-303.
- [19] Venere, E. (2013). Cellulose nanocrystals possible green wonder material. *Science Daily*.
- [20] Bondeson, D., Mathew, A., & Oksman, K. (2006). Optimization of the isolation of nanocrystals from microcrystalline cellulose by acid hydrolysis. *Cellulose*, 13(2), 171-180.
- [21] Hoseini, M. (2013). *Effect of compressive loading on transport properties of cement-based materials* (Doctoral dissertation, University of Alberta).
- [22] Cao, Y., Tian, N., Bahr, D., Zavattieri, P. D., Youngblood, J., Moon, R. J., & Weiss, J. (2016). The influence of cellulose nanocrystals on the microstructure of cement paste. *Cement and Concrete Composites*, 74, 164-173.

## Chapter VII

# *Summary and Conclusions*

### **ABSTRACT**

In this chapter, an overview and summary of the dissertation are presented. Furthermore, the overall concluding remarks associated with the study is provided along with recommendations for future research in this area.

*Keywords: Oil Well Cement, Cellulose Nanocrystal, Additive, Rheology, Filtration, Porosity, Strength, Permeability, Durability*

## 1. OVERVIEW OF THE DISSERTATION

Oil well cementing is known to be one of the most crucial steps during well completion [1]. Failure of the cementitious system (sheath) provided in the annular space between ground formation and casing could lead to economic disasters or remedial cementing. Therefore, the properties associated with the cement paste designed is of great importance [1]. The cement paste utilized in oil well industry is basically placed by pumping inside the wellbore. Thus, the flowability, pumpability and rheological characteristics of the paste are critical [2]. Also, a well-designed cement paste with adequate viscosity and yield stress will eventually reduce the amount of lost circulation during the cementing operation [1].

Moreover, the fluid loss or filtration rate associated with the fresh cementitious system designed is considered to be a major concern [3]. The fluid loss will alter the water-to-cement ratio of the cement paste and consequently, a large number of properties will be affected. Furthermore, the hardened cement sheath placed in an oil well should demonstrate adequate compressive and tensile strength in order to prevent failure under stress [1]. Failure of cement sheath around the casing could possibly influence the zonal isolation and formation stability [1, 2]. Nevertheless, the steel casing could also corrode if aggressive agents propagate their way through the cracked cement sheath. Moreover, the permeability of hardened oil well cement paste should also be minimized to reduce the penetration of external agents [1].

In order to address the above discussed characteristics, a vast number of additives are produced and utilized in the composition of oil well cement systems [1]. According to the desired properties and environmental conditions, specific additives are employed to alter the behavior of cementitious systems. The main goal of this study was to develop a durable

cementitious system by addressing all of the major failure contributing factors mentioned above. For this purpose, a novel, non-toxic innovative nanomaterial derived from cellulose known as cellulose nanocrystal (CNC) was proposed as an additive. Cellulosic additives have previously been used in cement applications, however, cellulose nanocrystal (CNC) particles had never been implemented in designing an oil well cement sheath.

A set of objectives were defined to investigate the influence of this nanomaterial on the behavior of fresh and hardened cement paste. During the course of this study, the workability, rheological characteristics, fluid loss and filtration rate, dynamic mechanical properties, porosity, mechanical properties and permeability of CNC-dosed oil well cement paste were assessed and the performance of the newly developed oil well cement system was compared to the performance of neat cementitious system with no additive.

## **2. OVERALL CONCLUDING REMARKS**

The following are the significant findings of this comprehensive study on the influence of cellulose nanocrystal (CNC) particles on the overall behavior of oil well cement paste:

- In order to gain primary knowledge on the effect of CNC on rheological parameters, shear rheology measurement was initially performed on colloidal suspensions. Presence of cellulose nanocrystal (CNC) particles led to an increase in viscosity and yield stress of colloidal suspensions and when utilized in oil well cement system, the same trend was observed. The shear-thinning behavior of oil well cement system was more manifest when CNC particles were introduced to the mix design.

- Conventional workability tests were carried out to verify the rheological measurements. Results obtained from mini slump and flow table tests confirmed an increase in viscosity and yield stress as a result of CNC addition to the matrix. Samples containing CNC particles showed a smaller spread diameter in both tests.
- When investigating the fresh properties of oil well cement pastes dosed with CNC, bentonite was also introduced to the mix design. Since cementing operation takes place after the drilling process, bentonite contamination is believed to be inevitable. Both rheological measurements and workability test results proved that the presence of CNC and bentonite at the same time increases the viscosity and yield stress significantly.
- The impact of cellulose nanocrystal (CNC) particles on the fluid loss and filtration rate of oil well cement paste was studied using static filtration test regime. CNC particles reduced the rate of filtration along with the total amount of filtrate volume. Bentonite was also employed in this procedure. Test results proved that the presence of bentonite alone led to an increase in fluid loss, however, when paired with CNC the rate of fluid loss and filtrate volume was significantly lower than neat samples.
- Oscillatory rheology (DMA) was also performed to investigate the effect of CNC particles on the dynamic mechanical properties and hydration of oil well cement paste. DMA results demonstrated that introducing CNC particles increased both storage modulus ( $G'$ ) and loss modulus ( $G''$ ).
- DMA results also proved that CNC particles increased both complex shear modulus ( $G^*$ ) and complex viscosity ( $\eta^*$ ). It was also recognized that the addition of CNC

particles led towards a drop in damping factor ( $\tan\delta$ ). This phenomenon is mainly attributed to an increase and enhancement in cement hydration.

- DMA results showed that when CNC was paired with bentonite, the increase in storage modulus ( $G'$ ), loss modulus ( $G''$ ), complex shear modulus ( $G^*$ ) and complex viscosity ( $\eta^*$ ) was more significant whereas the drop in damping factor ( $\tan\delta$ ) was also more noticeable.
- The oscillatory rheology results followed the same trend as the steady shear rheology results.
- Gas sorption technique was selected to understand the influence of cellulose nanocrystal (CNC) particles on the porosity and pore structure of hardened oil well cement paste. Different theoretical models (BET, BJH and DFT) were implemented on the nitrogen isotherms obtained. The reported results showed that presence of CNC particles led to a significant reduction in the surface area and total pore volume of hardened oil well cement specimens tested.
- According to the literature, CNC particles enhance cement hydration and therefore tune the large capillary pores [4-6]. The DMA results also confirmed an enhancement in solidification after CNC was added to the mix design. However, the results presented in this report declared that pore tuning may not be the only mechanism of action in this scenario. Since a large number of narrow capillary pores (radius < 100 nm) were eliminated after introducing CNC to the system, pore-clogging may have been another mechanism of action.
- The compressive and tensile strength of hardened oil well cement samples were measured at different ages to monitor and observe the impact of CNC particles on

the mechanical properties. The obtained results proved that the addition of CNC particles led to an increase in compressive strength, tensile strength and also modulus of elasticity. This was another sign of improvement in cement hydration. The dynamic mechanical analysis performed earlier had suggested an increase in rigidity (increase in  $G^*$ ) and hydration rate (drop in  $\tan\delta$ ). Therefore, the strength development enhancement justified the DMA results.

- Whether cured for a single day or a week, the mass flow rate and water permeability coefficient of hardened oil well cement paste had decreased significantly, when cellulose nanocrystal (CNC) was utilized as an additive in the mix design. However, by observing a reduction in porosity and enhancement in strength, a decrease in permeability was expected in the presence of such cellulosic additives (CNC particles).

Table 7.1 summarizes the concluding remarks mentioned above.

**Table 7.1.** The effect of cellulose nanocrystal (CNC) particles as an additive, on the critical parameters associated with oil well cement paste

Parameter	Influence of CNC
Viscosity	↑
Shear yield stress	↑
Fluid loss	↓
Filtration rate	↓
Storage modulus	↑
Loss modulus	↑
Complex shear modulus	↑
Complex viscosity	↑
Damping factor	↓

Mass flow rate	↓
Water permeability	↓
Total pore volume	↓
Surface area	↓
Compressive strength	↑
Tensile strength	↑
Modulus of elasticity	↑

---

Evidently, all of the major failure contributing parameters (affecting oil well cement systems) described earlier in this dissertation have been addressed and the obtained results verified the development of a more durable cementitious system by utilizing a single type of additive, cellulose nanocrystal.

The test methods and experimental procedures provided in this research study have been engineered in order to ease the cementing operation. With the rheological profiles (associated with the cement paste) available, parameters such as the pumping and the thickening time can be managed easier during the placement. Furthermore, understanding the filtration and mechanical properties of the CNC-dosed oil well cement paste can help predict the behavior of the prepared cement sheath. In a cementitious system, the performance (impact) of cellulose nanocrystal (CNC) particles depends on the type of the cement powder used. CNC particles have a large amount of sulfate, hence they will perform better in systems with less aluminate content such as cement type HS (Canada) and Type V (USA).

### 3. RECOMMENDATIONS FOR FUTURE RESEARCH

The research presented in this dissertation is a comprehensive study on the influence of cellulose nanocrystal (CNC) particles on the overall behavior of conventional oil well cement paste. The results, discussions and concluding remarks provided in this study clarify the impact of CNC, however, the area could be explored and expanded further in order to gain a broader knowledge. Based on the findings of this research, following recommendations are made for future investigation:

- The cellulose nanocrystal (CNC) particles were added to the cementitious system in a dosage of 1% (w/v of water). Future studies could examine the influence of this additive in other dosages in order to identify an optimized dosage.
- The rheological analysis and fluid loss assessments were performed at room temperature and atmospheric pressure. Further investigation should be carried out under elevated temperature and in high pressure condition.
- While investigating the fresh properties of CNC-dosed oil well cement paste, a clear synergy between CNC and bentonite was observed. In future studies, the interaction between CNC and bentonite particles should be studied to understand the synergy reported here.
- The dynamic mechanical properties of CNC-dosed oil well cement paste were measured at a constant temperature during the course of this study. Future investigations should consider the effect of temperature elevation on the dynamic mechanical analysis.

- The effect of cellulose nanocrystal (CNC) particles on the water permeability of oil well cement paste was evaluated in this experimental study. Further, the gas permeability of CNC-dosed oil well cement paste should also be examined.
- CNC with sulfated surface groups was studied in this research. Future studies could examine the effect of carboxylate cellulose nanocrystals and cellulose nanofibers in oil well cement systems.
- In future studies, the CNC-dosed cement samples could be cured in different temperatures, in order to witness the influence of curing temperature on the impact of cellulose nanocrystal particles.
- The overall performance of CNC-dosed oil well cement systems should be validated in actual field conditions (thermal and stress cycles).

## REFERENCES

- [1] Nelson, E. B. (Ed.). (1990). Well cementing (Vol. 28). Newnes.
- [2] Shahriar, A. (2011). *Investigation on rheology of oil well cement slurries* (Doctoral dissertation, The University of Western Ontario).
- [3] Bonett, A., & Pafitis, D. (1996). Getting to the root of gas migration. *Oilfield Review*, 8(1), 36-49.
- [4] Cao, Y., Zavaterra, P., Youngblood, J., Moon, R., & Weiss, J. (2015). The influence of cellulose nanocrystal additions on the performance of cement paste. *Cement and Concrete Composites*, 56, 73-83.

- [5] Cao, Y., Zavattieri, P., Youngblood, J., Moon, R., & Weiss, J. (2016). The relationship between cellulose nanocrystal dispersion and strength. *Construction and Building Materials*, 119, 71-79.
- [6] Cao, Y., Tian, N., Bahr, D., Zavattieri, P. D., Youngblood, J., Moon, R. J., & Weiss, J. (2016). The influence of cellulose nanocrystals on the microstructure of cement paste. *Cement and Concrete Composites*, 74, 164-173.

# *Bibliography*

- Adams, N., & Charrier, T. (1985) *Drilling Engineering: A Complete Well Planning Approach* Penn Well Publishing Company. Tulsa Oklahoma USA 297-303.
- Agopyan, V., Savastano, H., John, V. M., & Cincotto, M. A. (2005). Developments on vegetable fibre–cement based materials in São Paulo, Brazil: an overview. *Cement and Concrete Composites*, 27(5), 527-536.
- Alemdar, A., & Sain, M. (2008). Isolation and characterization of nanofibers from agricultural residues–Wheat straw and soy hulls. *Bioresource technology*, 99(6), 1664-1671.
- Alunno-Rossetti, V., Chiochio, G., & Collepardi, M. (1974). Low pressure steam hydration of tricalcium silicate. *Cement and Concrete Research*, 4(2), 279-288.
- Andrade, C. (1993). Calculation of chloride diffusion coefficients in concrete from ionic migration measurements. *Cement and concrete research*, 23(3), 724-742.
- Angles, M. N., & Dufresne, A. (2001). Plasticized starch/tunicin whiskers nanocomposite materials. 2. Mechanical behavior. *Macromolecules*, 34(9), 2921-2931.
- API, R. (2005). 10B-2. *recommended practice for testing well cements*.
- API, R. (2005). 13B-2. *Recommended Practice for Field Testing of Oil-based Drilling Fluids*.

- Araki, J., Wada, M., Kuga, S., & Okano, T. (1998). Flow properties of microcrystalline cellulose suspension prepared by acid treatment of native cellulose. *Colloids and Surfaces A: Physicochemical and Engineering Aspects*, 142(1), 75-82.
- Ardanuy, M., Claramunt, J., García-Hortal, J. A., & Barra, M. (2011). Fiber-matrix interactions in cement mortar composites reinforced with cellulosic fibers. *Cellulose*, 18(2), 281-289.
- Ardanuy, M., Claramunt, J., & Toledo Filho, R. D. (2015). Cellulosic fiber reinforced cement-based composites: a review of recent research. *Construction and building materials*, 79, 115-128.
- Azizi Samir, M. A. S., Alloin, F., & Dufresne, A. (2005). Review of recent research into cellulosic whiskers, their properties and their application in nanocomposite field. *Biomacromolecules*, 6(2), 612-626.
- Bach, D., & Vijn, P. (2002, January). Environmentally Acceptable Cement Fluid Loss Additive. In *SPE International Conference on Health, Safety and Environment in Oil and Gas Exploration and Production*. Society of Petroleum Engineers.
- Backe, K. R., Skalle, P., Lile, O. B., Lyomov, S. K., Justnes, H., & Sveen, J. (1998). Shrinkage of oil well cement slurries. *Journal of Canadian Petroleum Technology*, 37(09).
- Banfill, P. F. G. (2006). Rheology of fresh cement and concrete. *Rheology reviews*, 2006, 61.

- Bannister, C. E. (1978, January). Evaluation of Cement Fluid-Loss Behavior Under Dynamic Conditions. In *SPE Annual Fall Technical Conference and Exhibition*. Society of Petroleum Engineers.
- Banthia, N., & Mindess, S. (1989). Water permeability of cement paste. *Cement and Concrete Research*, 19(5), 727-736.
- Barnes, H. A., Hutton, J. F., & Walters, K. (1989). *An introduction to rheology* (Vol. 3). Elsevier.
- Barnes, H. A., & Nguyen, Q. D. (2001). Rotating vane rheometry—a review. *Journal of Non-Newtonian Fluid Mechanics*, 98(1), 1-14.
- Battista, O. A. (1950). Hydrolysis and crystallization of cellulose. *Industrial & Engineering Chemistry*, 42(3), 502-507.
- Battista, O. A., Coppick, S., Howsmon, J. A., Morehead, F. F., & Sisson, W. A. (1956). Level-off degree of polymerization. *Industrial & Engineering Chemistry*, 48(2), 333-335.
- Benchabane, A., & Bekkour, K. (2008). Rheological properties of carboxymethyl cellulose (CMC) solutions. *Colloid and Polymer Science*, 286(10), 1173-1180.
- Bentur, A., & Akers, S. A. S. (1989). The microstructure and ageing of cellulose fibre reinforced cement composites cured in a normal environment. *International Journal of Cement Composites and Lightweight Concrete*, 11(2), 99-109.
- Bentz, D. P., Coveney, P. V., Garboczi, E. J., Kleyn, M. F., & Stutzman, P. E. (1994). Cellular automaton simulations of cement hydration and microstructure

- development. *Modelling and Simulation in Materials Science and Engineering*, 2(4), 783.
- Bermudez, M. (2007, January). Effect of sugar on the thickening time of cement slurries. In *SPE Annual Technical Conference and Exhibition*. Society of Petroleum Engineers.
- Bertrand, L., Maximilien, S., & Guyonnet, R. (2004, June). Wedge Splitting Test: a test to measure the polysaccharide influence on adhesion of mortar on its substrate. In *Proceedings of the 11th International Congress on Polymers in Concrete, Berlin, Germany* (pp. 569-576).
- Betioli, A. M., Gleize, P. J. P., Silva, D. A., John, V. M., & Pileggi, R. G. (2009). Effect of HMEC on the consolidation of cement pastes: isothermal calorimetry versus oscillatory rheometry. *Cement and concrete Research*, 39(5), 440-445.
- Bett, E. K. (2011). Geothermal well cementing, materials and placement techniques.
- Beaupre, D. (1994). *Rheology of high performance shotcrete* (Doctoral dissertation, University of British Columbia).
- Bird, R. B., Armstrong, R. C., & Hassager, O. (1987). Dynamics of polymeric liquids. Volume 1: fluid mechanics. A Wiley-Interscience Publication, John Wiley & Sons.
- Blaine, R. L. (1949). Surface available to nitrogen in hardened Portland cements. *Journal of Research of the National Bureau of Standards Monograph*, 42(3), 257-267.
- Boluk, Y., Lahiji, R., Zhao, L., & McDermott, M. T. (2011). Suspension viscosities and shape parameter of cellulose nanocrystals (CNC). *Colloids and Surfaces A: Physicochemical and Engineering Aspects*, 377(1), 297-303.

- Bondeson, D., Mathew, A., & Oksman, K. (2006). Optimization of the isolation of nanocrystals from microcrystalline cellulose by acid hydrolysis. *Cellulose*, 13(2), 171-180.
- Bonett, A., & Pafitis, D. (1996). Getting to the root of gas migration. *Oilfield Review*, 8(1), 36-49.
- Börger, A., Supancic, P., & Danzer, R. (2002). The ball on three balls test for strength testing of brittle discs: stress distribution in the disc. *Journal of the European Ceramic Society*, 22(9), 1425-1436.
- Brice Jr, J. W., & Holmes, B. C. (1964). Engineered Casing Cementing Programs Using Turbulent Flow Techniques. *Journal of Petroleum Technology*, 16(05), 503-508.
- Broni-Bediako, E., Joel, O. F., & Ofori-Sarpong, G. (2016). Oil Well Cement Additives: A Review of the Common Types. *Oil & Gas Research*, 2, 112.
- Brumaud, C., Baumann, R., Schmitz, M., Radler, M., & Roussel, N. (2014). Cellulose ethers and yield stress of cement pastes. *Cement and concrete research*, 55, 14-21.
- Brunauer, S., Emmett, P. H., & Teller, E. (1938). Adsorption of gases in multimolecular layers. *Journal of the American chemical society*, 60(2), 309-319.
- Bülichen, D., & Plank, J. (2012). Mechanistic study on carboxymethyl hydroxyethyl cellulose as fluid loss control additive in oil well cement. *Journal of Applied Polymer Science*, 124(3), 2340-2347.
- Burkowsky, M., Ott, H. P., & Schillinger, H. (1981). Cemented pipe-in-pipe casing strings solve field problems. *World Oil;(United States)*, 193(5).

- Calvert, D.G. (2006). Preface. In: Nelson, E.B. and Guillot, D. (Ed.), *Well Cementing*, Schlumberger, Texas, pp. 1-11.
- Canadian Standards Association. (2013). CSA A3000–13 Cementitious materials compendium. *CSA Group*.
- Cao, X., Dong, H., & Li, C. M. (2007). New nanocomposite materials reinforced with flax cellulose nanocrystals in waterborne polyurethane. *Biomacromolecules*, 8(3), 899-904.
- Cao, Y., Zavatterri, P., Youngblood, J., Moon, R., & Weiss, J. (2015). The influence of cellulose nanocrystal additions on the performance of cement paste. *Cement and Concrete Composites*, 56, 73-83.
- Cao, Y., Zavattieri, P., Youngblood, J., Moon, R., & Weiss, J. (2016). The relationship between cellulose nanocrystal dispersion and strength. *Construction and Building Materials*, 119, 71-79.
- Cao, Y., Tian, N., Bahr, D., Zavattieri, P. D., Youngblood, J., Moon, R. J., & Weiss, J. (2016). The influence of cellulose nanocrystals on the microstructure of cement paste. *Cement and Concrete Composites*, 74, 164-173.
- Capadona, J. R., Shanmuganathan, K., Trittschuh, S., Seidel, S., Rowan, S. J., & Weder, C. (2009). Polymer nanocomposites with nanowhiskers isolated from microcrystalline cellulose. *Biomacromolecules*, 10(4), 712-716.
- Cappellari, M., Daubresse, A., & Chaouche, M. (2013). Influence of organic thickening admixtures on the rheological properties of mortars: Relationship with water-retention. *Construction and Building Materials*, 38, 950-961.

- Carter, L. G. (1968). *Effect of bore-hole stresses on set cement* (Doctoral dissertation, University of Oklahoma).
- Claramunt, J., Ardanuy, M., García-Hortal, J. A., & Tolêdo Filho, R. D. (2011). The hornification of vegetable fibers to improve the durability of cement mortar composites. *Cement and Concrete Composites*, 33(5), 586-595.
- Cooke Jr, C. E., Kluck, M. P., & Medrano, R. (1983). Field measurements of annular pressure and temperature during primary cementing. *Journal of Petroleum Technology*, 35(08), 1-429.
- Copeland, L. E., & Hayes, J. C. (1953). *The determination of non-evaporable water in hardened portland cement paste* (No. 47).
- Copeland, L. E., & Bragg, R. H. (1954). The hydrates of magnesium perchlorate. *The Journal of Physical Chemistry*, 58(12), 1075-1077.
- Coussot, P., Proust, S., & Ancey, C. (1996). Rheological interpretation of deposits of yield stress fluids. *Journal of Non-Newtonian Fluid Mechanics*, 66(1), 55-70.
- Coussot, P., Bertrand, F., & Herzhaft, B. (2004). Rheological behavior of drilling muds, characterization using MRI visualization. *Oil & gas science and technology*, 59(1), 23-29.
- Cowan, K. M., & Eoff, L. (1993, January). Surfactants: additives to improve the performance properties of cements. In *SPE International Symposium on Oilfield Chemistry*. Society of Petroleum Engineers.
- Damasceni, A., Dei, L., Fratini, E., Ridi, F., Chen, S. H., & Baglioni, P. (2002). A novel approach based on differential scanning calorimetry applied to the study of

- tricalcium silicate hydration kinetics. *The Journal of Physical Chemistry B*, *106*(44), 11572-11578.
- Davis, N. I., & Tooman, C. E. (1989). New laboratory tests evaluate the effectiveness of gilsonite resin as a borehole stabilizer. *SPE drilling engineering*, *4*(01), 47-56.
- De Andrade Silva, F., Mobasher, B., & Toledo Filho, R. D. (2010). Fatigue behavior of sisal fiber reinforced cement composites. *Materials Science and Engineering: A*, *527*(21), 5507-5513.
- De Andrade Silva, F., Mobasher, B., Soranakom, C., & Toledo Filho, R. D. (2011). Effect of fiber shape and morphology on interfacial bond and cracking behaviors of sisal fiber cement based composites. *Cement and Concrete Composites*, *33*(8), 814-823.
- De Larrard, F., Hu, C., Sedran, T., Sztikar, J. C., Joly, M., Claux, F., & Derkx, F. (1997). A new rheometer for soft-to-fluid fresh concrete. *Materials Journal*, *94*(3), 234-243.
- De Souza Lima, M. M., Wong, J. T., Paillet, M., Borsali, R., & Pecora, R. (2003). Translational and rotational dynamics of rodlike cellulose whiskers. *Langmuir*, *19*(1), 24-29.
- Deshpande, A. P., Krishnan, J. M., & Kumar, S. Rheology of complex fluids. 2010.
- Dri, F. L., Hector, L. G., Moon, R. J., & Zavattieri, P. D. (2013). Anisotropy of the elastic properties of crystalline cellulose I $\beta$  from first principles density functional theory with Van der Waals interactions. *Cellulose*, *20*(6), 2703-2718.
- Dufresne, A. (2005). A special issue devoted to cellulose-based composites. *Compos Interf*, *12*, 1-2.

- Dufresne, A. (2008). Polysaccharide nano crystal reinforced nanocomposites. *Canadian Journal of Chemistry*, 86(6), 484-494.
- Dufresne, A. (2012). *Nanocellulose: from nature to high performance tailored materials*. Walter de Gruyter.
- Dufresne, A. (2013). Nanocellulose: a new ageless bionanomaterial. *Materials Today*, 16(6), 220-227.
- Eichhorn, S. J., Dufresne, A., Aranguren, M., Marcovich, N. E., Capadona, J. R., Rowan, S. J., & Gindl, W. (2010). Review: current international research into cellulose nanofibres and nanocomposites. *Journal of materials science*, 45(1), 1.
- Elazzouzi-Hafraoui, S., Nishiyama, Y., Putaux, J. L., Heux, L., Dubreuil, F., & Rochas, C. (2007). The shape and size distribution of crystalline nanoparticles prepared by acid hydrolysis of native cellulose. *Biomacromolecules*, 9(1), 57-65.
- Favier, V., Canova, G. R., Cavailé, J. Y., Chanzy, H., Dufresne, A., & Gauthier, C. (1995). Nanocomposite materials from latex and cellulose whiskers. *Polymers for Advanced Technologies*, 6(5), 351-355.
- Favier, V., Chanzy, H., & Cavaille, J. Y. (1995). Polymer nanocomposites reinforced by cellulose whiskers. *Macromolecules*, 28(18), 6365-6367.
- Favier, V., Dendievel, R., Canova, G., Cavaille, J. Y., & Gilormini, P. (1997). Simulation and modeling of three-dimensional percolating structures: case of a latex matrix reinforced by a network of cellulose fibers. *Acta Materialia*, 45(4), 1557-1565.
- Fengel, D., & Wegener, G. (Eds.). (1983). *Wood: chemistry, ultrastructure, reactions*. Walter de Gruyter.

- Ferraris, C., De Larrard, F., & Martys, N. (2001). Fresh concrete rheology: recent developments. *Materials Science of Concrete VI, Amer. Cer. Soc. Ed. S. Mindess, J. Skalny*, 215-241.
- Ferraris, C. F., & Martys, N. S. (2003). Relating fresh concrete viscosity measurements from different rheometers. *Journal of research of the National Institute of Standards and Technology*, 108(3), 229.
- Figg, J. W. (1973). Methods of measuring the air and water permeability of concrete. *Magazine of Concrete Research*, 25(85), 213-219.
- Fu, T., Montes, F., Suraneni, P., Youngblood, J., & Weiss, J. (2017). The Influence of Cellulose Nanocrystals on the Hydration and Flexural Strength of Portland Cement Pastes. *Polymers*, 9(9), 424.
- George, C., & Gerke, R. R. (1985). U.S. Patent No. 4,557,763. Washington, DC: U.S. Patent and Trademark Office.
- Ghio, V. A., Monteiro, P. J., & Demsetz, L. A. (1994). The rheology of fresh cement paste containing polysaccharide gums. *Cement and concrete research*, 24(2), 243-249.
- Goodwin, K. J., & Crook, R. J. (1992). Cement sheath stress failure. *SPE Drilling Engineering*, 7(04), 291-296.
- Goto, S., & Roy, D. M. (1981). The effect of w/c ratio and curing temperature on the permeability of hardened cement paste. *Cement and Concrete Research*, 11(4), 575-579.
- Gregg, S. J., Sing, K. S. W., & Salzberg, H. W. (1967). Adsorption surface area and porosity. *Journal of the Electrochemical Society*, 114(11), 279C-279C.

- Grim, R. E. (1955). Clay mineralogy, 1968. *Karl Jasmund, Die silicatischen Tonminerale, 2nd enlarged ed.*
- Grosseau, P., Pourchez, J., Guilhot, B., Guyonnet, R., & Ruot, B. (2007). Impact of cellulose ethers on the C3S hydration. In *International Congress on the Chemistry of Cement*.
- Habibi, Y., Lucia, L. A., & Rojas, O. J. (2010). Cellulose nanocrystals: chemistry, self-assembly, and applications. *Chemical reviews, 110(6)*, 3479-3500.
- Halamickova, P., Detwiler, R. J., Bentz, D. P., & Garboczi, E. J. (1995). Water permeability and chloride ion diffusion in Portland cement mortars: relationship to sand content and critical pore diameter. *Cement and concrete research, 25(4)*, 790-802.
- Hanehara, S., & Yamada, K. (1999). Interaction between cement and chemical admixture from the point of cement hydration, absorption behaviour of admixture, and paste rheology. *Cement and Concrete Research, 29(8)*, 1159-1165.
- Hanley, S. J., Giasson, J., Revol, J. F., & Gray, D. G. (1992). Atomic force microscopy of cellulose microfibrils: comparison with transmission electron microscopy. *Polymer, 33(21)*, 4639-4642.
- Harris, K. L., & Johnson, B. J. (1992, January). Successful remedial operations using ultrafine cement. In *SPE Mid-Continent Gas Symposium*. Society of Petroleum Engineers.
- Heinold, T., Dillenbeck, R. L., & Rogers, M. J. (2002, January). The effect of key cement additives on the mechanical properties of normal density oil and gas well cement

- systems. In *SPE Asia Pacific Oil and Gas Conference and Exhibition*. Society of Petroleum Engineers.
- Helbert, W., Cavaille, J. Y., & Dufresne, A. (1996). Thermoplastic nanocomposites filled with wheat straw cellulose whiskers. Part I: processing and mechanical behavior. *Polymer composites*, *17*(4), 604-611.
- Hoseini, M., Bindiganavile, V., & Banthia, N. (2009). The effect of mechanical stress on permeability of concrete: a review. *Cement and Concrete Composites*, *31*(4), 213-220.
- Hoseini, M. (2013). *Effect of compressive loading on transport properties of cement-based materials* (Doctoral dissertation, University of Alberta).
- Hoyos, C. G., Cristia, E., & Vázquez, A. (2013). Effect of cellulose microcrystalline particles on properties of cement based composites. *Materials & Design*, *51*, 810-818.
- Hubbe, M. A., Rojas, O. J., Lucia, L. A., & Sain, M. (2008). Cellulosic nanocomposites: a review. *BioResources*, *3*(3), 929-980.
- Jennings, H. M., Thomas, J. J., Gevrenov, J. S., Constantinides, G., & Ulm, F. J. (2007). A multi-technique investigation of the nanoporosity of cement paste. *Cement and Concrete Research*, *37*(3), 329-336.
- Joshi, R. C., & Lohita, R. P. (1997). *Fly ash in concrete: production, properties and uses* (Vol. 2). CRC Press.
- Juenger, M. C. G., & Jennings, H. M. (2001). The use of nitrogen adsorption to assess the microstructure of cement paste. *Cement and Concrete Research*, *31*(6), 883-892.

- Jupe, A. C., Wilkinson, A. P., Luke, K., & Funkhouser, G. P. (2005). Class H oil well cement hydration at elevated temperatures in the presence of retarding agents: an in situ high-energy X-ray diffraction study. *Industrial & engineering chemistry research*, 44(15), 5579-5584.
- Jupe, A. C., Wilkinson, A. P., Luke, K., & Funkhouser, G. P. (2007). Slurry Consistency and In Situ Synchrotron X-Ray Diffraction during the Early Hydration of Portland Cements with Calcium Chloride. *Journal of the American Ceramic Society*, 90(8), 2595-2602.
- Justnes, H., Skalle, P., Sveen, J., & Øye, B. A. (1995). Porosity of oil well cement slurries during setting. *Advances in Cement Research*, 7(25), 5-12.
- Justnes, H., Van Loo, D., Reyniers, B., Skalle, P., Sveen, J., & Sellevold, E. J. (1995). Chemical shrinkage of oil well cement slurries. *Advances in cement research*, 7(26), 85-90.
- Kalousek, G. L., Richard, J. O., Ziems, K. L., & Saxer, E. L. (1953, November). Relation of shrinkage to moisture content in concrete block. In *Journal Proceedings* (Vol. 50, No. 11, pp. 225-240).
- Kamal, M. R., & Khoshkava, V. (2015). Effect of cellulose nanocrystals (CNC) on rheological and mechanical properties and crystallization behavior of PLA/CNC nanocomposites. *Carbohydrate polymers*, 123, 105-114.
- Khan, B., & Baradan, B. (2002). The effect of sugar on setting-time of various types of cements. *Quarterly science vision*, 8(1), 71-78.

- Khayat, K. H., & Yahia, A. (1997). Effect of welan gum-high-range water reducer combinations on rheology of cement grout. *Materials Journal*, 94(5), 365-372.
- Khayat, K. H. (1998). Viscosity-enhancing admixtures for cement-based materials—an overview. *Cement and Concrete Composites*, 20(2-3), 171-188.
- Kinoshita, M., Yamaguchi, S., Yamamoto, T., & Tomosawa, F. (1990). Chemical structure and performance of new type high-range water-reducing AE agent. In *JCA Proceedings of Cement & Concrete* (Vol. 44, pp. 222-227).
- Klemm, D., Kramer, F., Moritz, S., Lindström, T., Ankerfors, M., Gray, D., & Dorris, A. (2011). Nanocelluloses: A new family of nature-based materials. *Angewandte Chemie International Edition*, 50(24), 5438-5466.
- Kumar, S., Singh, C. J., Singh, R. P., & Kachari, J. (2002, April). Microfine cement: special superfine Portland cement. In Proc., Seventh NCB International Seminar, New Delhi, India.
- Lachemi, M., Hossain, K. M. A., Lambros, V., Nkinamubanzi, P. C., & Bouzoubaâ, N. (2004). Self-consolidating concrete incorporating new viscosity modifying admixtures. *Cement and Concrete Research*, 34(6), 917-926.
- Lahiji, R. R., Xu, X., Reifenberger, R., Raman, A., Rudie, A., & Moon, R. J. (2010). Atomic force microscopy characterization of cellulose nanocrystals. *Langmuir*, 26(6), 4480-4488.
- Larson, R. G. (1999). *The structure and rheology of complex fluids* (Vol. 150). New York: Oxford university press.

- Laskar, A. I., & Talukdar, S. (2008). Rheological behavior of high performance concrete with mineral admixtures and their blending. *Construction and Building materials*, 22(12), 2345-2354.
- Lasseuguette, E., Roux, D., & Nishiyama, Y. (2008). Rheological properties of microfibrillar suspension of TEMPO-oxidized pulp. *Cellulose*, 15(3), 425-433.
- Lee, J. H., Park, S. E., Lee, H. J., & Lee, H. L. (2002). Thermal shock behaviour of alumina ceramics by ball-on-3-ball test. *Materials Letters*, 56(6), 1022-1029.
- Leemann, A., & Winnefeld, F. (2007). The effect of viscosity modifying agents on mortar and concrete. *Cement and Concrete Composites*, 29(5), 341-349.
- Li, M. C., Wu, Q., Song, K., Qing, Y., & Wu, Y. (2015). Cellulose nanoparticles as modifiers for rheology and fluid loss in bentonite water-based fluids. *ACS applied materials & interfaces*, 7(8), 5006-5016.
- Loosveldt, H., Lafhaj, Z., & Skoczylas, F. (2002). Experimental study of gas and liquid permeability of a mortar. *Cement and Concrete Research*, 32(9), 1357-1363.
- Lu, Y., Weng, L., & Cao, X. (2005). Biocomposites of plasticized starch reinforced with cellulose crystallites from cottonseed linter. *Macromolecular Bioscience*, 5(11), 1101-1107.
- Luckham, P. F., & Rossi, S. (1999). The colloidal and rheological properties of bentonite suspensions. *Advances in Colloid and Interface Science*, 82(1), 43-92.
- Magarini, P., Lanzetta, C., Galletta, A. (1999) Drilling Design Manual Eni-Agip Division 97-107.

- Malkin, A. Y., Askadsky, A. A., Kovriga, V. V., & Chalykh, A. E. (1983). Experimental methods of polymer physics. *Measurement of mechanical properties, viscosity and diffusion* (Mir, Moscow, 1983).
- Malkin, A. Y., & Isayev, A. I. (2017). *Rheology: concepts, methods, and applications*. Elsevier.
- Marca, C. (1990). 13 Remedial Cementing. *Developments in Petroleum Science*, 28, 13-1.
- Matsuhisa, M., Yamada, K., Ishimori, M., & Kaneda, Y. (1998). Effects of cement character on the fluidity of cement paste added with beta-naphthalene sulfonate type or polycarboxylate type superplasticizers. *Proceedings of the Japan Concrete Institute*, 20(2), 67-72.
- Mehta, P. K. (1986). Concrete. Structure, properties and materials.
- Mezger, T. G. (2006). *The rheology handbook: for users of rotational and oscillatory rheometers*. Vincentz Network GmbH & Co KG.
- Mikhail, R. S., Copeland, L. E., & Brunauer, S. (1964). Pore structures and surface areas of hardened Portland cement pastes by nitrogen adsorption. *Canadian Journal of Chemistry*, 42(2), 426-438.
- Mikhail, R. S., & Selim, S. A. (1966). Adsorption of organic vapors in relation to the pore structure of hardened Portland cement pastes. *Highway Research Board Special Report*, (90).
- Miller, A. F., & Donald, A. M. (2003). Imaging of anisotropic cellulose suspensions using environmental scanning electron microscopy. *Biomacromolecules*, 4(3), 510-517.

- Mindess, S., Young, J. F., & Darwin, D. (2003). *Concrete*. Prentice Hall.
- Mohr, B. J., Biernacki, J. J., & Kurtis, K. E. (2007). Supplementary cementitious materials for mitigating degradation of kraft pulp fiber-cement composites. *Cement and Concrete Research*, 37(11), 1531-1543.
- Moon, R. J., Martini, A., Nairn, J., Simonsen, J., & Youngblood, J. (2011). Cellulose nanomaterials review: structure, properties and nanocomposites. *Chemical Society Reviews*, 40(7), 3941-3994.
- Morton, J. H., Cooke, T., & Akers, S. A. S. (2010). Performance of slash pine fibers in fiber cement products. *Construction and building materials*, 24(2), 165-170.
- Mueller, D. T., & Bray, W. S. (1993, January). Characterization of surfactant-enhanced cement fluid-loss additives. In *SPE Production Operations Symposium*. Society of Petroleum Engineers.
- Mukherjee, S. M., & Woods, H. J. (1953). X-ray and electron microscope studies of the degradation of cellulose by sulphuric acid. *Biochimica et biophysica acta*, 10, 499-511.
- Nachbaur, L., Nonat, A., Mutin, J. C., & Choplin, L. (2000). Dynamic mode rheology of cement pastes. In *Proceedings of the 2 nd International RILEM Workshop on Hydration and Setting, RILEM publications* (pp. 281-293).
- Nachbaur, L., Mutin, J. C., Nonat, A., & Choplin, L. (2001). Dynamic mode rheology of cement and tricalcium silicate pastes from mixing to setting. *Cement and Concrete Research*, 31(2), 183-192.

- Nawa, T. (2006). Effect of chemical structure on steric stabilization of polycarboxylate-based superplasticizer. *Journal of Advanced Concrete Technology*, 4(2), 225-232.
- Nehdi, M., & Rahman, M. A. (2004). Estimating rheological properties of cement pastes using various rheological models for different test geometry, gap and surface friction. *Cement and concrete research*, 34(11), 1993-2007.
- Neithalath, N., Weiss, J., & Olek, J. (2004). Acoustic performance and damping behavior of cellulose–cement composites. *Cement and Concrete Composites*, 26(4), 359-370.
- Nelson, E. B. (Ed.). (1990). Well cementing (Vol. 28). Newnes.
- Nelson, E. B., Baret, J. F., & Michaux, M. (1990). 3 Cement Additives and Mechanisms of Action. *Developments in Petroleum Science*, 28, 3-1.
- Nickerson, R. F., & Habrle, J. A. (1947). Cellulose intercrystalline structure. *Industrial & Engineering Chemistry*, 39(11), 1507-1512.
- Niknaddaf, S., Atkinson, J. D., Shariaty, P., Lashaki, M. J., Hashisho, Z., Phillips, J. H., Anderson, J. E. & Nichols, M. (2016). Heel formation during volatile organic compound desorption from activated carbon fiber cloth. *Carbon*, 96, 131-138.
- Nilsson, J., & Sargenius, P. (2011). Effect of microfibrillar cellulose on concrete equivalent mortar fresh and hardened properties.
- Nishiyama, Y. (2009). Structure and properties of the cellulose microfibril. *Journal of Wood Science*, 55(4), 241-249.

- Nyame, B. K., & Illston, J. M. (1981). Relationships between permeability and pore structure of hardened cement paste. *Magazine of Concrete Research*, 33(116), 139-146.
- Odler, I. (2003). The BET-specific surface area of hydrated Portland cement and related materials. *Cement and Concrete Research*, 33(12), 2049-2056.
- Ohno, A., & Yamamoto, T. (1997). Fluidity of various cement pastes added polycarboxylic acid type admixture. In *JCA Proceedings of Cement & Concrete* (Vol. 51, pp. 258-263).
- Oksman, K., & Sain, M. (Eds.). (2006). *Cellulose nanocomposites: processing, characterization, and properties*. American Chemical Society.
- Orchard, D. F. (1962). *Concrete Technology, Vol. 1, Properties of Materials*. 358p.
- Orts, W. J., Godbout, L., Marchessault, R. H., & Revol, J. F. (1998). Enhanced ordering of liquid crystalline suspensions of cellulose microfibrils: A small angle neutron scattering study. *Macromolecules*, 31(17), 5717-5725.
- Page, C., Short, N. R., & El Tarras, A. (1981). Diffusion of chloride ions in hardened cement pastes. *Cement and concrete research*, 11(3), 395-406.
- Paiva, H., Silva, L. M., Labrincha, J. A., & Ferreira, V. M. (2006). Effects of a water-retaining agent on the rheological behaviour of a single-coat render mortar. *Cement and Concrete Research*, 36(7), 1257-1262.
- Papo, A., & Caufin, B. (1991). A study of the hydration process of cement pastes by means of oscillatory rheological techniques. *Cement and concrete research*, 21(6), 1111-1117.

- Parrott, L. J., Geiker, M., Gutteridge, W. A., & Killoh, D. (1990). Monitoring Portland cement hydration: comparison of methods. *Cement and Concrete Research*, 20(6), 919-926.
- Patural, L., Marchal, P., Govin, A., Grosseau, P., Ruot, B., & Deves, O. (2011). Cellulose ethers influence on water retention and consistency in cement-based mortars. *Cement and Concrete Research*, 41(1), 46-55.
- Peschard, A., Govin, A., Grosseau, P., Guilhot, B., & Guyonnet, R. (2004). Effect of polysaccharides on the hydration of cement paste at early ages. *Cement and Concrete Research*, 34(11), 2153-2158.
- Peschard, A., Govin, A., Pourchez, J. A. E., Fredon, E., Bertrand, L., Maximilien, S., & Guilhot, B. (2006). Effect of polysaccharides on the hydration of cement suspension. *Journal of the European Ceramic Society*, 26(8), 1439-1445.
- Picandet, V., Rangeard, D., Perrot, A., & Lecompte, T. (2011). Permeability measurement of fresh cement paste. *Cement and Concrete Research*, 41(3), 330-338.
- Pierre, A., Perrot, A., Picandet, V., & Guevel, Y. (2015). Cellulose ethers and cement paste permeability. *Cement and Concrete Research*, 72, 117-127.
- Pietz, L. M., & Thomas, E. A. (2014). Strengthening Construction Materials Via Incorporation of Cellulose Nanocrystals: A Sustainable Biomaterial.
- Pitkethly, M. J. (2004). Nanomaterials—the driving force. *Materials today*, 7(12), 20-29.
- Plank, J., Brandl, A., Zhai, Y., & Franke, A. (2006). Adsorption behavior and effectiveness of poly (N, N-dimethylacrylamide-co-Ca 2-acrylamido-2-methylpropanesulfonate) as cement fluid loss additive in the presence of acetone-

formaldehyde-sulfite dispersant. *Journal of applied polymer science*, 102 (5), 4341-4347.

Plank, J., Lummer, N. R., & Dugonjić-Bilić, F. (2010). Competitive adsorption between an AMPS®-based fluid loss polymer and Welan gum biopolymer in oil well cement. *Journal of applied polymer science*, 116(5), 2913-2919.

Poinot, T., Bartholin, M. C., Govin, A., & Grosseau, P. (2015). Influence of the polysaccharide addition method on the properties of fresh mortars. *Cement and Concrete Research*, 70, 50-59.

Poon, C. S., Wong, Y. L., & Lam, L. (1997). The influence of different curing conditions on the pore structure and related properties of fly-ash cement pastes and mortars. *Construction and Building Materials*, 11(7-8), 383-393.

Pourchez, J., Govin, A., Grosseau, P., Guyonnet, R., Guilhot, B., & Ruot, B. (2006). Alkaline stability of cellulose ethers and impact of their degradation products on cement hydration. *Cement and Concrete Research*, 36(7), 1252-1256.

Pourchez, J., Grosseau, P., Guyonnet, R., & Ruot, B. (2006). HEC influence on cement hydration measured by conductometry. *Cement and Concrete Research*, 36(9), 1777-1780.

Pourchez, J., Peschard, A., Grosseau, P., Guyonnet, R., Guilhot, B., & Vallée, F. (2006). HPMC and HEMC influence on cement hydration. *Cement and Concrete Research*, 36(2), 288-294.

- Powers, T. C., & Brownyard, T. L. (1946, September). Studies of the physical properties of hardened Portland cement paste. In *Journal Proceedings* (Vol. 43, No. 9, pp. 101-132).
- Powers, C. A., Holman, G. B., & Smith, R. C. (1977). U.S. Patent No. 4,036,301. Washington, DC: U.S. Patent and Trademark Office.
- Pranger, L., & Tannenbaum, R. (2008). Biobased nanocomposites prepared by in situ polymerization of furfuryl alcohol with cellulose whiskers or montmorillonite clay. *Macromolecules*, *41*(22), 8682-8687.
- Qiao, C., Chen, G., Zhang, J., & Yao, J. (2016). Structure and rheological properties of cellulose nanocrystals suspension. *Food Hydrocolloids*, *55*, 19-25.
- Rajabipour, F., Sant, G., & Weiss, J. (2008). Interactions between shrinkage reducing admixtures (SRA) and cement paste's pore solution. *Cement and Concrete Research*, *38*(5), 606-615.
- Ramachandran, V. S. (1996). *Concrete admixtures handbook: properties, science and technology*. William Andrew.
- Rarick, R. L., Bhatti, J. I., & Jennings, H. M. (1995). Surface area measurement using gas sorption: application to cement paste. *Material Science of Concrete IV*, *American Ceramic Society*, 1-41.
- Ravi, K., Bosma, M., & Gastebled, O. (2002, January). Improve the economics of oil and gas wells by reducing the risk of cement failure. In *IADC/SPE Drilling Conference*. Society of Petroleum Engineers.

- Reier, G. E., & Shangraw, R. F. (1966). Microcrystalline cellulose in tableting. *Journal of Pharmaceutical Sciences*, 55(5), 510-514.
- Ridi, F., Dei, L., Fratini, E., Chen, S. H., & Baglioni, P. (2003). Hydration kinetics of tri-calcium silicate in the presence of superplasticizers. *The Journal of Physical Chemistry B*, 107(4), 1056-1061.
- Ridi, F., Fratini, E., Mannelli, F., & Baglioni, P. (2005). Hydration process of cement in the presence of a cellulosic additive. A calorimetric investigation. *The Journal of Physical Chemistry B*, 109(30), 14727-14734.
- Rols, S., Ambroise, J., & Pera, J. (1999). Effects of different viscosity agents on the properties of self-leveling concrete. *Cement and Concrete Research*, 29(2), 261-266.
- Roohani, M., Habibi, Y., Belgacem, N. M., Ebrahim, G., Karimi, A. N., & Dufresne, A. (2008). Cellulose whiskers reinforced polyvinyl alcohol copolymers nanocomposites. *European polymer journal*, 44(8), 2489-2498.
- Roussel, N. (2005). Steady and transient flow behaviour of fresh cement pastes. *Cement and concrete research*, 35(9), 1656-1664.
- Roussel, N., Stefani, C., & Leroy, R. (2005). From mini-cone test to Abrams cone test: measurement of cement-based materials yield stress using slump tests. *Cement and Concrete Research*, 35(5), 817-822.
- Ruiz, M. M., Cavaille, J. Y., Dufresne, A., Gerard, J. F., & Graillat, C. (2000). Processing and characterization of new thermoset nanocomposites based on cellulose whiskers. *Matériaux & Techniques*, 88(7-8), 63-68.

- Ruot, B., Goto, T., & Pourchez, J. (2007). Some aspects of cellulose ethers and latexes influence on the properties of cement-based materials—examples of results obtained within the CEReM. *Proceedings of the VII SBTA (7 Simposio Brasileiro De Tecnologia Das Argamassas)*.
- Rusli, R., & Eichhorn, S. J. (2008). Determination of the stiffness of cellulose nanowhiskers and the fiber-matrix interface in a nanocomposite using Raman spectroscopy. *Applied Physics Letters*, 93(3), 033111.
- Russo, V., Ferrari, G., Salvioni, D., Valentini, L., Artioli, G., & Stefancic, M. (2017, April). Study of the effect a novel metal-silicate nanodispersion on the water permeability of concrete. Proceedings of the 39th International Cement Microscopy Association Conference, Toronto (pp. 198-206).
- Saito, T., Nishiyama, Y., Putaux, J. L., Vignon, M., & Isogai, A. (2006). Homogeneous suspensions of individualized microfibrils from TEMPO-catalyzed oxidation of native cellulose. *Biomacromolecules*, 7(6), 1687-1691.
- Salim, P., & Amani, M. (2013). Special considerations in cementing high pressure high temperature wells. *International Journal of Engineering*, 1(4), 2305-8269.
- Sant, G., Dehadrai, M., Bentz, D., Lura, P., Ferraris, C. F., Bullard, J. W., & Weiss, J. (2009). Detecting the fluid-to-solid transition in cement pastes. *Concrete international*, 31(06), 53-58.
- Savastano, H., Warden, P. G., & Coutts, R. S. P. (2003). Mechanically pulped sisal as reinforcement in cementitious matrices. *Cement and Concrete Composites*, 25(3), 311-319.

- Savastano, H., & Warden, P. G. (2005). Special theme issue: Natural fibre reinforced cement composites.
- Schultz, M. A. (1991). *Rheological studies of fresh cement pastes* (Doctoral dissertation, University of Illinois at Urbana-Champaign).
- Schultz, M. A., & Struble, L. J. (1993). Use of oscillatory shear to study flow behavior of fresh cement paste. *Cement and Concrete Research*, 23(2), 273-282.
- Shafiei Sabet, S. (2013). *Shear rheology of cellulose nanocrystal (CNC) aqueous suspensions* (Doctoral dissertation, University of British Columbia).
- Shafeiei Sabet, S., Hamad, W. Y., & Hatzikiriakos, S. G. (2013). Influence of degree of sulfation on the rheology of cellulose nanocrystal suspensions. *Rheologica Acta*, 52(8-9), 741-751.
- Shahriar, A. (2011). *Investigation on rheology of oil well cement slurries* (Doctoral dissertation, The University of Western Ontario).
- Shahriar, A., & Nehdi, M. L. (2012). Rheological properties of oil well cement slurries. *Proceedings of the ICE-Construction Materials*, 165(1), 25-44.
- Shaughnessy, R., & Clark, P. E. (1988). The rheological behavior of fresh cement pastes. *Cement and Concrete Research*, 18(3), 327-341.
- Shih, J. Y., Chang, T. P., & Hsiao, T. C. (2006). Effect of nanosilica on characterization of Portland cement composite. *Materials Science and Engineering: A*, 424(1), 266-274.
- Shuker, M. T., Memon, K. R., Tunio, S. Q., & Memon, M. K. (2014). Laboratory investigation on performance of cement using different additives schemes to

- improve early age compressive strength. *Research Journal of Applied Sciences, Engineering and Technology*, 7(11), 2298-2305.
- Siqueira, G., Bras, J., & Dufresne, A. (2010). Cellulosic bionanocomposites: a review of preparation, properties and applications. *Polymers*, 2(4), 728-765.
- Siró, I., & Plackett, D. (2010). Microfibrillated cellulose and new nanocomposite materials: a review. *Cellulose*, 17(3), 459-494.
- Slagle, K. A., & Carter, L. G. (1959, January). Gilsonite-A Unique Additive for Oil-well Cements. In *Drilling and Production Practice*. American Petroleum Institute.
- Smith, D. K. (1989). *Cementing*. SPE Monograph Series. Society of Petroleum Engineers, Richardson, Texas.
- Sonebi, M. (2006). Rheological properties of grouts with viscosity modifying agents as diutan gum and welan gum incorporating pulverised fly ash. *Cement and Concrete Research*, 36(9), 1609-1618.
- Soroushian, P., Won, J. P., & Hassan, M. (2012). Durability characteristics of CO<sub>2</sub>-cured cellulose fiber reinforced cement composites. *Construction and Building Materials*, 34, 44-53.
- Specification, A. P. I. (2010). 10A. *Cements and Materials for Well Cementing*.
- Standard, A. S. T. M. "C150/C150M-17 (2017)." *Standard specification for Portland cement* (2017).
- Šturcová, A., Davies, G. R., & Eichhorn, S. J. (2005). Elastic modulus and stress-transfer properties of tunicate cellulose whiskers. *Biomacromolecules*, 6(2), 1055-1061.

- Sun, X., Wu, Q., Ren, S., & Lei, T. (2015). Comparison of highly transparent all-cellulose nanopaper prepared using sulfuric acid and TEMPO-mediated oxidation methods. *Cellulose*, 22(2), 1123-1133.
- Sun, X., Wu, Q., Zhang, J., Qing, Y., Wu, Y., & Lee, S. (2017). Rheology, curing temperature and mechanical performance of oil well cement: Combined effect of cellulose nanofibers and graphene nano-platelets. *Materials & Design*, 114, 92-101.
- Tanaka, K., & Kurumisawa, K. (2002). Development of technique for observing pores in hardened cement paste. *Cement and Concrete Research*, 32(9), 1435-1441.
- Tattersall, G. H., & Banfill, P. F. (1983). *The rheology of fresh concrete* (Vol. 759). London: Pitman.
- Tattersall, G. H. (2003). *Workability and quality control of concrete*. CRC Press.
- Taylor, H. F. (1997). *Cement chemistry*. Thomas Telford.
- Terech, P., Chazeau, L., & Cavaille, J. Y. (1999). A small-angle scattering study of cellulose whiskers in aqueous suspensions. *Macromolecules*, 32(6), 1872-1875.
- Thomas, J. J., Jennings, H. M., & Allen, A. J. (1998). The surface area of cement paste as measured by neutron scattering: evidence for two CSH morphologies. *Cement and Concrete Research*, 28(6), 897-905.
- Thomas, J. J., Jennings, H. M., & Allen, A. J. (1999). The surface area of hardened cement paste as measured by various techniques. *Concrete Science and Engineering*, 1(1), 45-64.

- Tiab, D., & Donaldson, E. C. (2015). *Petrophysics: theory and practice of measuring reservoir rock and fluid transport properties*. Gulf professional publishing.
- Toledo Filho, R. D., Ghavami, K., England, G. L., & Scrivener, K. (2003). Development of vegetable fibre–mortar composites of improved durability. *Cement and concrete composites*, 25(2), 185-196.
- Toledo Filho, R. D., Ghavami, K., Sanjuán, M. A., & England, G. L. (2005). Free, restrained and drying shrinkage of cement mortar composites reinforced with vegetable fibres. *Cement and Concrete Composites*, 27(5), 537-546.
- Tonoli, G. H. D., Rodrigues Filho, U. P., Savastano, H., Bras, J., Belgacem, M. N., & Lahr, F. R. (2009). Cellulose modified fibres in cement based composites. *Composites Part A: Applied Science and Manufacturing*, 40(12), 2046-2053.
- Tonoli, G. H. D., Santos, S. F., Savastano, H., Delvasto, S., de Gutiérrez, R. M., & de Murphy, M. D. M. L. (2011). Effects of natural weathering on microstructure and mineral composition of cementitious roofing tiles reinforced with fique fibre. *Cement and Concrete Composites*, 33(2), 225-232.
- Uchikawa, H., Ogawa, K., & Uchida, S. (1983). Effect of admixtures on the rheology of fly ash cement. In *JCA Proceedings of Cement & Concrete* (Vol. 37, pp. 53-56).
- Uchikawa, H., Uchida, S., Ogawa, K., & Hanehara, S. (1984). Influence of  $\text{CaSO}_4 \cdot 2\text{H}_2\text{O}$ ,  $\text{CaSO}_4 \cdot 12\text{H}_2\text{O}$  and  $\text{CaSO}_4$  on the initial hydration of clinker having different burning degree. *Cement and Concrete Research*, 14(5), 645-656.

- Uchikawa, H., Sawaki, D., & Hanehara, S. (1995). Influence of kind and added timing of organic admixture on the composition, structure and property of fresh cement paste. *Cement and Concrete Research*, 25(2), 353-364.
- Ureña-Benavides, E. E., Ao, G., Davis, V. A., & Kitchens, C. L. (2011). Rheology and phase behavior of lyotropic cellulose nanocrystal suspensions. *Macromolecules*, 44(22), 8990-8998.
- Venere, E. (2013). Cellulose nanocrystals possible green wonder material. Science Daily.
- Verbeck, G. J. (1968). Structures and physical properties of cement paste, Invited Paper. In *5th International Symposium on the Chemistry of Cement, Tokyo* (pp. 1-32).
- Vidick, B., Fletcher, P., & Michaux, M. (1989). Evolution at early hydration times of the chemical composition of liquid phase of oil-well cement pastes with and without additives Part II. Cement pastes containing additives. *Cement and Concrete Research*, 19(4), 567-578.
- Vlachou, P. V., & Piau, J. M. (1997). The influence of the shear field on the microstructural and chemical evolution of an oil well cement slurry and its rheometric impact. *Cement and Concrete Research*, 27(6), 869-881.
- Wagner, R., Moon, R. J., & Raman, A. (2016). Mechanical properties of cellulose nanomaterials studied by contact resonance atomic force microscopy. *Cellulose*, 23(2), 1031-1041.
- Wang, N., Ding, E., & Cheng, R. (2007). Thermal degradation behaviors of spherical cellulose nanocrystals with sulfate groups. *Polymer*, 48(12), 3486-3493.
- Whorlow, R. (1980). Rheological techniques.

- Wilson, M. A., & Sabins, F. L. (1988). A laboratory investigation of cementing horizontal wells. *SPE drilling engineering*, 3(03), 275-280.
- With, G., & Wagemans, H. H. (1989). Ball-on-Ring Test Revisited. *Journal of the American Ceramic Society*, 72(8), 1538-1541.
- Wong, H. S., Buenfeld, N. R., & Head, M. K. (2006). Estimating transport properties of mortars using image analysis on backscattered electron images. *Cement and Concrete Research*, 36(8), 1556-1566.
- Wong, H. S., Head, M. K., & Buenfeld, N. R. (2006). Pore segmentation of cement-based materials from backscattered electron images. *Cement and Concrete Research*, 36(6), 1083-1090.
- Wu, Q., Meng, Y., Wang, S., Li, Y., Fu, S., Ma, L., & Harper, D. (2014). Rheological behavior of cellulose nanocrystal suspension: influence of concentration and aspect ratio. *Journal of Applied Polymer Science*, 131(15).
- Yahaba, N. (2010). *How Does A Decrease In Oil Production Affect The World Economy?*. Australia-Japan Research Centre.
- Yahia, A., & Khayat, K. H. (2001). Analytical models for estimating yield stress of high-performance pseudoplastic grout. *Cement and Concrete Research*, 31(5), 731-738.
- Yang, R., & Buenfeld, N. R. (2001). Binary segmentation of aggregate in SEM image analysis of concrete. *Cement and Concrete Research*, 31(3), 437-441.
- Yongliang, L., Xiangming, K., Yanrong, Z., & Peiyu, Y. (2012). Static and dynamic mechanical properties of cement-asphalt composites. *Journal of Materials in Civil Engineering*, 25(10), 1489-1497.

- Zhang, J., Xu, M., Yan, Z., & Gao, L. (2008). Hydration and hardening of Class G oilwell cement with and without silica sands under high temperatures. *J Chin Ceram Soc*, 36(7), 935-941.
- Zhang, J., Weissinger, E. A., Peethamparan, S., & Scherer, G. W. (2010). Early hydration and setting of oil well cement. *Cement and Concrete research*, 40(7), 1023-1033.
- Zhang, M. H., & Li, H. (2011). Pore structure and chloride permeability of concrete containing nano-particles for pavement. *Construction and Building Materials*, 25(2), 608-616.
- Zhang, Z., Wang, P., & Wu, J. (2012). Dynamic mechanical properties of EVA polymer-modified cement paste at early age. *Physics Procedia*, 25, 305-310.
- Zimmermann, T., Bordeanu, N., & Strub, E. (2010). Properties of nanofibrillated cellulose from different raw materials and its reinforcement potential. *Carbohydrate Polymers*, 79(4), 1086-1093.
- Živica, V. (1997). Relationship between pore structure and permeability of hardened cement mortars: on the choice of effective pore structure parameter. *Cement and Concrete Research*, 27(8), 1225-1235.
- Zomorrodian, M. A. (2014). *Wellbore integrity: Modifying and characterizing oil well cement to enhance wellbore logging and prevent perforating damages in hydraulic fractured wells*. (Master's Thesis, University of Houston).